

Immunometabolic responses of adult and umbilical cord macrophages to stimulation with *Mycobacterium tuberculosis* or Lipopolysaccharide



Trinity College Dublin
Coláiste na Tríonóide, Baile Átha Cliath
The University of Dublin

A Thesis Submitted to the University of Dublin, Trinity College,
for the Degree of Doctor of Philosophy in the Faculty of Medicine

2022

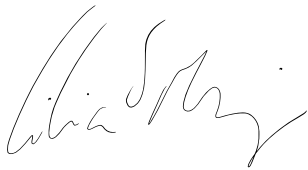
Dr. Cilian Ó Maoldomhnaigh MB BCH BAO

Supervisors: Prof Joe Keane, MD, Prof Sharee Basdeo, PhD
Tuberculosis Immunology Research Group,
Department of Clinical Medicine,
Trinity Translational Medicine Institute,
St. James's Hospital,
Trinity College,
University of Dublin.

I, Cilian Ó Maoldomhnaigh, declare that this thesis has not been submitted as an exercise for a degree at this or any other university and it is entirely my own work.

I agree to deposit this thesis in the University's open access institutional repository or allow the Library to do so on my behalf, subject to Irish Copyright Legislation and Trinity College Library conditions of use and acknowledgement.

I consent to the examiner retaining a copy of the thesis beyond the examining period, should they so wish (EU GDPR May 2018).

A handwritten signature in black ink, appearing to read 'Cilian Ó Maoldomhnaigh', written in a cursive style.

Cilian Ó Maoldomhnaigh

Date: June 30th, 2021

Acknowledgements

Firstly, I would like to thank all of the mothers who agreed to take part in this research, the donors who gave their blood through the Irish Blood Transfusion Service and the National Children's Research Centre for funding this PhD project.

Prof Joseph Keane and Prof Sharee Basdeo are owed my deepest gratitude and endless appreciation. Thank you, Joe, for the opportunity to pursue a clinical scientist career, for the welcome to your laboratory and for the constant supervision and enthusiasm over the last 4 years. It was my great fortune Sharee, to sit beside such a fantastic scientist and person on my first day. Thank you for your patience and kindness and for teaching me how to be a scientist. For your friendship I am forever grateful. To the rest of the TB lab, particularly Dónal, James, Kate, and Karl, thank you for all of the much needed help and for the comradery.

Thank you to my Paediatric Infectious Disease families. Prof Karina Butler, Dr Patrick Gavin and Dr Ronan Leahy have encouraged me from my first steps in my PID career and have been a constant source of inspiration and support. To my new NYU PID family, particularly Dr Adam Ratner and Dr Rebecca Madan, and Stephanie and Michal, thank you for the unfaltering kindness in looking after me and my family and helping me to achieve the next steps.

My wonderful parents, Michael and Triona, have been unwavering in their encouragement, advice, love and support and I hope you know how much I appreciate everything you do for me. To Fiachra and Ailbhe and our new family members, Arya, Rincy, and Cian, thank you for the tireless belief and motivation. To my darling wife Chloe and wonderful daughter Fiadh, you both mean the world to me, I love you so. Thank you for everything.

Table of Contents

Chapter 1 Introduction.....	1
1.1.1 Tuberculosis.....	1
1.1.2 TB in children.....	3
1.1.3 The immune response to tuberculosis	6
1.1.4 The adaptive immune response to TB.....	10
1.1.5 Infant immune susceptibility to TB.....	11
1.1.6 Macrophages	12
1.1.7 Macrophage Polarisation.....	13
1.1.8 Markers of Macrophage differentiation.....	16
1.1.9 Macrophage Metabolism	19
1.1.10 Immunometabolism	21
1.1.11 Host directed therapy.....	26
1.1.12 Hypothesis.....	28
1.1.13 Aims.....	28
Chapter 2 Methods	29
2.1 Monocyte derived macrophages from adult and umbilical cord donors	29
2.1.1 Isolation of adult PBMC.....	29
2.1.2 Isolation of umbilical cord mononuclear cells	29
2.1.3 Cell Counting	30
2.1.4 Monocyte derived macrophage differentiation	31
2.1.5 The phenotype of adult and cord blood monocyte derived macrophages	31
2.2 Mycobacterial Infection and Stimulation of MDM.....	35
2.2.1 Culture and preparation of attenuated live Mtb, H37Ra	35
2.2.2 Preparation of irradiated Mtb H37Rv	35
2.2.3 Determination of multiplicity of Infection.....	36
2.2.4 Phagocytosis of Mtb in adult MDM compared with cord blood MDM	37
2.2.5 Mtb infection of MDM.....	38
2.2.6 Assessing mycobacterial growth	38
2.3 Flow cytometry.....	43
2.4 Metabolic flux analysis	46
2.4.1 Seahorse XFe24 Analyzer.....	46
2.4.2 Mitochondrial Stress Test.....	47
2.4.3 Mitochondrial Stress Test Protocol	48
2.5 MDM stimulation with LPS and polarisation with IFN-γ or IL-4.....	52
2.5.1 Lipopolysaccharide stimulation	52
2.5.2 Polarisation of MDM with IFN- γ or IL-4	52
2.6 Analysis of Cytokine production.....	53

2.6.1 Measurement of cytokine production by Enzyme Linked Immuno Sorbant Assay (ELISA)	53
2.6.2 Measurement of cytokine production by Mesoscale Discovery System.....	54
2.7 Western Blotting.....	54
2.8 Optimisation of the use of exogenous sodium-lactate on human MDM	55
2.8.1 The effect of exogenous lactate on cell viability	55
2.8.2 The effect of sodium-lactate on pH.....	56
2.8.3 The effect of sodium-lactate on the phagocytic capacity of human MDM.....	57
2.8.4 Determining the effects of sodium-lactate on human MDM.....	57
2.9 Statistical analysis.....	63
Chapter 3	64
3.1 The Warburg effect occurs early in adult but not cord blood macrophages	64
3.1.1 Introduction	64
3.1.2 Hypothesis and Aims.....	66
3.2 Results.....	67
3.2.1 The Warburg effect occurs early in response to stimulation with Mtb or LPS in human adult MDM.....	67
3.2.1a Mtb and LPS cause a rapid increase in glycolysis in adult and cord blood MDM	68
3.2.1b OCR significantly decreases in adult but not cord blood MDM following Mtb or LPS stimulation.....	69
3.2.1c ECAR/OCR ratio increases in both adult and cord blood MDM after stimulation with Mtb or LPS.....	70
3.2.1d Comparison of metabolic changes in adult and cord blood MDM 2.5 hours after stimulation with Mtb or LPS.....	70
3.2.2 Human MDM show persistent metabolic changes 24 hours after stimulation. .	78
3.2.2a The increased ECAR observed 2.5 hours after stimulation with Mtb or LPS persists at 24 hours.....	78
3.2.2b OCR 24 hours following Mtb or LPS stimulation in adult and cord blood MDM.	79
3.2.2c Basal ECAR/OCR ratio in adult and cord blood MDM 24 hours post stimulation with Mtb or LPS.....	80
3.2.2d Comparison of adult and cord blood MDM metabolism 24 hours after Mtb or LPS stimulation.....	80
3.2.2e Mitochondrial stress test analysis for adult and cord blood MDM 24 hours following LPS or Mtb stimulation.....	81
3.2.3 Comparison between metabolic responses at 2.5 hours and 24 hours following Mtb or LPS stimulation.....	89
3.2.4 Cord blood MDM have similar cell surface marker expression compared with adult MDM.	94
3.2.5 Cord blood MDM produce less TNF in response to Mtb and more IL-6 in response to LPS stimulation compared with adult MDM.	104

3.3 Discussion.....	108
3.4 Conclusions.....	112
Chapter 4 Polarisation with IFN-γ or IL-4 alters human macrophage immunometabolism.....	113
4.1 Introduction.....	113
4.1.1 Hypothesis and Aims	114
4.2 Results.....	115
4.2.1 The effect of IFN- γ or IL-4 on the phenotype of adult and cord blood MDM....	115
4.2.1a Adult and cord blood MDM morphology after polarisation.....	116
4.2.1b The effect of IFN- γ or IL-4 on cell surface marker expression in adult and cord blood MDM	117
4.2.2 The effect of IFN- γ or IL-4 on metabolism in adult and cord blood MDM.....	129
4.2.2a IFN- γ increases OCR in adult, but not cord blood MDM.....	129
4.2.2b IFN- γ increases and IL-4 decreases ECAR in both adult and cord blood MDM	130
4.2.2c Comparison between adult and cord blood MDM metabolism 24 hours after treatment with IFN- γ or IL-4.....	131
4.2.2d ECAR/OCR ratio of adult and cord blood MDM 24 hours after treatment with IFN- γ or IL-4	132
4.2.3 The effect of IFN- γ or IL-4 on adult and cord blood MDM metabolic responses to Mtb and LPS.....	139
4.2.3a IL-4 inhibits the drop in OCR seen after Mtb stimulation in adult MDM.....	140
4.2.3b IFN- γ increases ECAR in adult MDM while IL-4 decreases ECAR in both adult and cord MDM after Mtb stimulation	141
4.2.3c IL-4 decreases the ECAR/OCR ratio in both adult and cord blood MDM after Mtb stimulation.....	143
4.2.3d IFN- γ augments glycolysis in adult MDM but not in cord blood MDM in response to stimulation with Mtb.....	144
4.2.3e IL-4 abrogates the decreased OCR observed in response to LPS stimulation in adult MDM	145
4.2.3f IL-4 decreases ECAR in adult MDM after LPS stimulation	146
4.2.3g IL-4 decreases the ECAR/OCR ratio in both adult and cord blood MDM after LPS stimulation	148
4.2.3h Direct comparison of LPS responses between adult and cord blood MDM after IFN- γ or IL-4	148
4.2.4 Expression of cell surface markers in IFN- γ or IL-4 treated adult and cord blood MDM after Mtb or LPS stimulation	162
4.2.5 The effect of pretreatment with IFN- γ or IL-4 on subsequent cytokine responses to Mtb or LPS.....	172
4.3 Discussion.....	179
4.4 Conclusions.....	182

Chapter 5 Lactate alters metabolism in human macrophages and improves their ability to kill <i>Mycobacterium tuberculosis</i>	184
5.1 Introduction	184
5.1.1 Hypothesis and Aims.....	185
5.2 Results	186
5.2.1 Lactate alters human adult and cord blood MDM metabolism.....	186
5.2.1a Lactate immediately decreases ECAR and increases OCR in both adult and cord blood MDM.....	187
5.2.1b NaCl has no effect on metabolism of adult MDM.....	188
5.2.2 Lactate pretreatment alters MDM metabolic responses to Mtb or LPS.....	194
5.2.2a Pre-treatment with lactate decreases ECAR after Mtb or LPS stimulation.....	194
5.2.2b Pre-treatment with lactate increases OCR after Mtb or LPS stimulation.....	196
5.2.3 The metabolic effect of pre-treatment with lactate 24 hours after Mtb or LPS stimulation.....	206
5.2.4 Pre-treatment with lactate does not alter the expression of cell surface markers on adult and cord blood MDM after Mtb or LPS stimulation.....	212
5.2.5 The effect of pre-treatment with lactate on cytokine secretion from adult and cord blood MDM after stimulation with Mtb or LPS.....	222
5.2.6 Lactate improved ability of adult MDM to kill Mtb.....	228
5.3 Discussion	235
5.4 Conclusions	239
Chapter 6 General Discussion and Future Work	240
6.1 General Discussion	240
6.2 Study limitations and newly identified research gaps	249
6.3 Conclusions	252

Table of Figures

Figure 1.1 Possible fates in the natural history of tuberculosis infection.	5
Figure 1.2 Glycolytic pathway and TCA cycle.	20
Figure 1.3 Summary of immunometabolic changes in macrophages in published literature.....	25
Figure 2.1 Isolation of PBMC from blood.	32
Figure 2.2 Umbilical cord blood sampling from the placental umbilical cord.	33
Figure 2.3. Adult and cord blood MDM morphology	34
Figure 2.4 Multiplicity of infection for adult and cord blood MDM.	40
Figure 2.5 Increasing MOI produced a corresponding increase in TNF production in cord blood MDM.	41
Figure 2.6 Phagocytosis of Mtb by adult and cord blood MDM.	42
Figure 2.7 Adult and cord blood MDM viability and purity following differentiation. ...	45
Figure 2.8 Calculation of Mitochondrial Stress Test parameters.	51
Figure 2.9 MDM viability after the addition of lactate.....	59
Figure 2.10 MDM viability after the addition of NaCl.	60
Figure 2.11 Sodium lactate does not alter pH.	61
Figure 2.12 Lactate does not alter MDM phagocytic ability.....	62
Figure 3.1 ECAR rises rapidly in adult and cord blood MDM after Mtb or LPS stimulation.	72
Figure 3.2 Analysis of ECAR in adult and cord blood MDM after Mtb or LPS stimulation.	73
Figure 3.3 OCR falls rapidly in adult but not cord blood MDM after Mtb or LPS stimulation.	74
Figure 3.4 Analysis of OCR in adult and cord blood MDM after Mtb or LPS stimulation.	75
Figure 3.5 ECAR/OCR ratio for adult and cord blood MDM after Mtb or LPS stimulation.	76
Figure 3.6 Comparison between adult and cord blood MDM responses after Mtb or LPS stimulation.	77
Figure 3.7 Analysis of Baseline ECAR in adult and cord blood MDM 24 hours after Mtb or LPS stimulation.....	83

Figure 3.8 Analysis of Baseline OCR in adult and cord blood MDM 24 hours after Mtb or LPS stimulation.	84
Figure 3.9 ECAR/OCR ratio for adult and cord blood MDM 24 hours after Mtb or LPS stimulation.	85
Figure 3.10 Comparison between adult and cord blood MDM responses 24 hours after Mtb or LPS stimulation.....	86
Figure 3.11 Mitochondrial stress test in adult and cord blood MDM 24 hours after stimulation with Mtb or LPS.....	87
Figure 3.12 Cord blood MDM have a similar mitochondrial stress test profile to adult MDM.	88
Figure 3.13 Phenogram of adult MDM 2.5 and 24 hours following Mtb or LPS stimulation.	91
Figure 3.14 Phenogram of cord blood MDM 2.5 and 24 hours following Mtb or LPS stimulation.	92
Figure 3.15 Comparison of metabolic responses to Mtb or LPS stimulation at 2.5 and 24 hours post stimulation with Mtb or LPS for adult and cord blood MDM.....	93
Figure 3.16 Adult and cord blood MDM expression of CD40 24 hours after Mtb or LPS stimulation.	98
Figure 3.17 Adult and cord blood MDM expression of HLA-DR 24 hours after Mtb or LPS stimulation.....	99
Figure 3.18 Adult and cord blood MDM expression of CD83 24 hours after Mtb or LPS stimulation.	100
Figure 3.19 Adult and cord blood MDM expression of CD80 24 hours after Mtb or LPS stimulation.	101
Figure 3.20 Adult and cord blood MDM expression of CD86 24 hours after Mtb or LPS stimulation.	102
Figure 3.21 Adult and cord blood MDM expression of MMR 24 hours after Mtb or LPS stimulation.	103
Figure 3.22 Cytokine production of adult and cord blood MDM 24 hours after Mtb or LPS stimulation.....	107
Figure 4.1 Morphology of adult and cord blood MDM 24 hours after treatment with IFN- γ or IL-4.....	122

Figure 4.2 Expression of CD40 on adult and cord blood MDM 24 hours after IFN- γ or IL-4 treatment.	123
Figure 4.3 Expression of HLA-DR on adult and cord blood MDM 24 hours after IFN- γ or IL-4 treatment.	124
Figure 4.4 Expression of CD86 on adult and cord blood MDM 24 hours after IFN- γ or IL-4 treatment.	125
Figure 4.5 Expression of MMR on adult and cord blood MDM 24 hours after IFN- γ or IL-4 treatment.	126
Figure 4.6 Expression of CD83 on adult and cord blood MDM 24 hours after IFN- γ or IL-4 treatment.	127
Figure 4.7 Expression of CD80 on adult and cord blood MDM 24 hours after IFN- γ or IL-4 treatment.	128
Figure 4.8 IFN- γ increases OCR in adult, but not cord blood MDM.....	133
Figure 4.9 Analysis of OCR in adult and cord blood MDM after IFN- γ or IL-4.	134
Figure 4.10 IFN- γ increases, and IL-4 decreases ECAR in both adult and cord blood MDM	135
Figure 4.11 Analysis of ECAR in adult and cord blood MDM after IFN- γ or IL-4.....	136
Figure 4.12 Comparison between adult and cord blood MDM metabolic responses 24 hours after IFN- γ or IL-4.	137
Figure 4.13 ECAR/OCR ratio of adult and cord blood MDM 24 hours after IFN- γ or IL-4 treatment	138
Figure 4.14 IL-4 inhibits the drop in OCR seen after Mtb stimulation in adult MDM..	150
Figure 4.15 Analysis of OCR in IFN- γ and IL-4 treated adult and cord blood MDM after Mtb stimulation.....	151
Figure 4.16 IFN- γ increases ECAR in adult MDM while IL-4 decreases ECAR in both adult and cord MDM after Mtb stimulation.....	152
Figure 4.17 Analysis of ECAR in IFN- γ and IL-4 treated adult and cord blood MDM after Mtb stimulation.....	153
Figure 4.18 IL-4 decreases the ECAR/OCR ratio in both adult and cord blood MDM..	154
Figure 4.19 Comparison between adult and cord blood MDM metabolic responses after Mtb stimulation, 24 hours after IFN- γ or IL-4 treatment.....	155

Figure 4.20 IL-4 inhibits the decrease in OCR seen after LPS stimulation in adult MDM.	156
Figure 4.21 Analysis of OCR in IFN- γ and IL-4 treated adult and cord blood MDM after LPS stimulation.....	157
Figure 4.22 IL-4 decreases ECAR in adult MDM after LPS stimulation.....	158
Figure 4.23 Analysis of ECAR in IFN- γ and IL-4 treated adult and cord blood MDM after LPS stimulation.....	159
Figure 4.24 IL-4 decreases the ECAR/OCR ratio in both adult and cord blood MDM after LPS stimulation.....	160
Figure 4.25 Comparison between adult and cord blood MDM metabolic responses after LPS stimulation, 24 hours after IFN- γ or IL-4 treatment.....	161
Figure 4.26 Expression of HLA-DR on adult and cord blood MDM 48 hours after IFN- γ or IL-4 treatment and 24 hours after Mtb or LPS stimulation.	166
Figure 4.27 Expression of MMR on adult and cord blood MDM 48 hours after IFN- γ or IL-4 treatment and 24 hours after Mtb or LPS stimulation.....	167
Figure 4.28 Expression of CD40 on adult and cord blood MDM 48 hours after IFN- γ or IL-4 treatment and 24 hours after Mtb or LPS stimulation.....	168
Figure 4.29 Expression of CD83 on adult and cord blood MDM 48 hours after IFN- γ or IL-4 treatment and 24 hours after Mtb or LPS stimulation.....	169
Figure 4.30 Expression of CD80 on adult and cord blood MDM 48 hours after IFN- γ or IL-4 treatment and 24 hours after Mtb or LPS stimulation.....	170
Figure 4.31 Expression of CD86 on adult and cord blood MDM 48 hours after IFN- γ or IL-4 treatment and 24 hours after Mtb or LPS stimulation.....	171
Figure 4.32 Mtb or LPS induced IL-1 β production after pre-treatment with IFN- γ or IL- 4.	175
Figure 4.33 Mtb or LPS induced TNF production after pre-treatment with IFN- γ or IL-4.	176
Figure 4.34 Mtb or LPS induced IL-6 production after pre-treatment with IFN- γ or IL-4.	177
Figure 4.35 Mtb or LPS induced IL-10 production after pre-treatment with IFN- γ or IL- 4.	178
Figure 5.1 Lactate decreases ECAR in adult and cord blood MDM.	190

Figure 5.2 Lactate increases OCR in adult and cord blood MDM.	191
Figure 5.3 Analysis of the changes in ECAR and OCR in adult and cord blood MDM after lactate administration.	192
Figure 5.4 NaCl does induce metabolic changes in adult MDM.	193
Figure 5.5 ECAR in adult and cord blood MDM pretreated with lactate after Mtb stimulation.	199
Figure 5.6 ECAR in adult and cord blood MDM pretreated with lactate after LPS stimulation.	200
Figure 5.7 Analysis of the ECAR in adult and cord blood MDM pretreated with lactate after Mtb or LPS stimulation.	201
Figure 5.8 OCR in adult and cord blood MDM pretreated with lactate after Mtb stimulation.	202
Figure 5.9 OCR in adult and cord blood MDM pretreated with lactate after LPS stimulation.	203
Figure 5.10 Analysis of the OCR and ECAR/OCR ratio in adult and cord blood MDM pretreated with lactate after Mtb or LPS stimulation.	204
Figure 5.11 Phenogram of lactate treated adult MDM following Mtb or LPS stimulation.	205
Figure 5.12 Mitochondrial stress test of lactate treated MDM 24 hours after Mtb or LPS stimulation.	209
Figure 5.13 Analysis of the baseline OCR, ECAR and ECAR/OCR ratio of MDM pre-treated with lactate, 24 hours after stimulation with Mtb or LPS.	210
Figure 5.14 Mitochondrial stress test profile of MDM pre-treated with lactate 24 hours after Mtb or LPS stimulation.	211
Figure 5.15 Expression of CD40 in lactate pre-treated adult and cord blood MDM 24 hours after Mtb or LPS stimulation.	216
Figure 5.16 Expression of HLA-DR in lactate pre-treated adult and cord blood MDM 24 hours after Mtb or LPS stimulation.	217
Figure 5.17 Expression of CD83 in lactate pre-treated adult and cord blood MDM 24 hours after Mtb or LPS stimulation.	218
Figure 5.18 Expression of CD80 in lactate pre-treated adult and cord blood MDM 24 hours after Mtb or LPS stimulation.	219

Figure 5.19 Expression of CD86 in lactate pre-treated adult and cord blood MDM 24 hours after Mtb or LPS stimulation.	220
Figure 5.20 Expression of MMR in lactate pre-treated adult and cord blood MDM 24 hours after Mtb or LPS stimulation.	221
Figure 5.21 Cytokine production in adult MDM pre-treated with lactate 24 hours after Mtb stimulation.	224
Figure 5.22 Cytokine production in cord blood MDM pre-treated with lactate 24 hours after Mtb stimulation.	225
Figure 5.23 Cytokine production in adult MDM pre-treated with lactate 24 hours after LPS stimulation.	226
Figure 5.24 Cytokine production in cord blood MDM pre-treated with lactate 24 hours after LPS stimulation.	227
Figure 5.25 Lactate improved ability of adult MDM to kill Mtb.	232
Figure 5.26 Lactate does not affect Mtb growth in axenic conditions.	233
Figure 5.27 Lactate overcomes the autophagic block caused by Mtb.	234
Figure 6.1 Macrophage activation states in human MDM.	248

List of Abbreviations

2DG	2-deoxy glucose
3MA	3-methyladenine
ADP	Adenosine Di-Phosphate
AM	Alveolar Macrophage
ANOVA	Analysis of Variance
ATP	Adenosine Tri-Phosphate
BCG	Bacille Calmette-Guérin
BMDM	Bone Marrow Derived Macrophages
BSL	Bio Safety Level
CD	Cluster of Differentiation
CFU	Colony Forming Units
Cl	Chloride
CLR	C-type Lectin Receptor
cRPMI	Complete Roswell Park Memorial Institute-1640
D	Day
DC	Dendritic Cell
ECAR	Extracellular Acidification Rate
ETC	Electron Transport Chain
FADH ₂	flavin adenine dinucleotide
FCCP	Carbonyl cyanide-4- (trifluoromethoxy) phenylhydrazone
FCS	Fetal Calf Serum
FMO	Fluorescence Minus One

FSc	Forward Scatter
GMCSF	Granulocyte Macrophage Colony Stimulating Factor
HLA	Human Leucocyte Antigen
HIF	Hypoxia induction factor
IFN	Interferon
IGRA	Interferon Gamma Release Assay
IL	Interleukin
LPS	Lipopolysaccharide
MAIT	Mucosal Associated Invariant T cell
MCSF	Macrophage Colony Stimulating Factor
MDM	Monocyte Derived Macrophage
MDR	Multi Drug Resistant
MFI	Median Fluorescent Intensity
MHC	Major Histocompatibility
MMR	Macrophage Mannose Receptor
MOI	Multiplicity of Infection
MSD	Mesocale discovery
Mtb	Mycobacterium tuberculosis
Na	Sodium
NADH	Nicotinamide adenine dinucleotide
NK	Natural Killer
NLR	NOD Like Receptor
NOD	Nucleotide-binding oligomerization domain

NMOC	Non-mitochondrial oxygen consumption
NF- κ B	Nuclear transcription factor- κ B
OADC	Oleic Albumin Dextrose Catalase
OCR	Oxygen Consumption Rate
OXPPOS	Oxidative Phosphorylation
PBS	Phosphate Buffered Saline
PFA	Paraformaldehyde
PPD	Purified Protein Derivative
PPP	Pentose Phosphate Pathway
PRR	Pattern Recognition Receptor
RNA	Ribonucleic Acid
RNA-Seq	Ribonucleic Acid Sequencing
RPMI	Roswell Park Memorial Institute-1640
PBMC	Peripheral Blood Mononuclear Cell
STAT3	Signal transducer and activator of transcription 3
SD	Standard Deviation
SDS	Sodium dodecyl sulfate
SEM	Standard Error of the Mean
SRC	Spare Respiratory Capacity
SSc	Side Scatter
T cell	Thymically-derived CD3-expressing lymphocyte
TB	Tuberculosis
Th	T helper cell

TLR	Toll Like Receptor
TNF	Tumour Necrosis Factor
TCA	Tricarboxylic acid
TBST	Tris-Buffered saline Tween
WHO	World Health Organisation

Abstract

Tuberculosis (TB) has been the biggest infectious killer in the world in the last decade and young children are among the most vulnerable groups. *Mycobacterium tuberculosis* (Mtb), the bacteria that causes TB, is phagocytosed by macrophages. Macrophages can mount an effective immune response and kill the intracellular bacteria, or, in certain circumstances, the macrophage response is suboptimal and allows intracellular bacterial growth, causing active TB disease. The Warburg effect, defined as increased glycolysis and decreased oxidative phosphorylation (OXPHOS), occurs in murine macrophages following lipopolysaccharide (LPS) stimulation and is required for activation. It was hypothesised that immunometabolic responses in human macrophages are different to murine responses and that umbilical cord derived macrophages have an altered immunometabolic response compared with adult macrophages, which may make infants and children particularly vulnerable to TB.

The Warburg effect was demonstrated in adult monocyte derived macrophages (MDM) immediately in response to stimulation with LPS or Mtb. Cord blood MDM however did not decrease OXPHOS. At 24 hours post stimulation, glycolysis remains elevated in both adult and cord blood MDM, however LPS stimulated adult MDM have increased OXPHOS. Cord blood MDM secreted less TNF following Mtb stimulation and more IL-6 following LPS stimulation compared with adult MDM.

The effects of IFN- γ or IL-4 on human macrophage immunometabolic phenotype and function were investigated. IFN- γ increased glycolysis and OXPHOS and IL-4 resulted in a marked decline in glycolysis. IFN- γ equalised cord and adult TNF production in response to Mtb. IL-4 caused a decrease in IL-1 β production in both adult and cord MDM stimulated with Mtb. A consequence of increased glycolysis is an increase in extracellular lactate. The addition of exogenous lactate was found to have an immediate effect on metabolism, causing a decrease in glycolysis and an increase in OXPHOS. Lactate significantly reduced the concentrations of TNF and IL-1 β produced by human macrophages in response to Mtb. In addition, lactate significantly improved bacillary clearance in human macrophages infected with Mtb.

These data indicate that key differences exist in the kinetics of the immunometabolic response to stimulation in human macrophages compared with that which is established in the literature in mice. Furthermore, adult and cord blood macrophages exhibit distinct immunometabolic function upon stimulation which may underlie their differential ability to respond to infection. These data may help to inform therapeutic strategies for host-directed therapies for TB.

Lay Abstract

Tuberculosis (TB) is one of the biggest infectious killers in the world. There is a far higher chance of a baby getting TB disease following exposure to the bug than an adult. Babies tend to get more severe disease, often spreading outside the lungs. This research aims to figure out the reasons behind these differences. Blood samples from adults and from the placental umbilical cord immediately following birth were collected and the immune cells that fight TB infection, called macrophages, were examined.

New research has shown the importance of metabolism, or the way that cells use energy, in generating an appropriate immune response in order to fight infection. Previous research was mostly done in mouse cells and the human responses are poorly understood. The research presented here sheds new light on how metabolism in human macrophages alters during an immune response. Human cells change their metabolism very rapidly after TB exposure. Some of these changes are reversed 24 hours later; the time point at which much of the previous mouse studies were performed. Baby immune cells respond differently to adult cells in how they use oxygen for metabolism. They also make less pro-inflammatory messenger molecules after exposure to TB.

Another aspect of this research was to examine how metabolism of human macrophages is altered by signals from priming messenger molecules that are increased in infection. Macrophages increase their use of oxygen and glucose in response to an activating signal and decrease their glucose use in response to an anti-inflammatory signal. By understanding how these processes occur, therapies that manipulate these changes can be developed. Finally, the effect of lactate, a product generated in the body when macrophages are activated, was found to have an immunosuppressive effect on macrophages and to increase their ability to kill tuberculosis. This indicates that lactate may have potential as a medical therapy.

Hypothesis

It was hypothesised herein that the difference in clinical phenotype seen between adults and newborns following exposure to Mtb is a result of underlying differences in macrophage metabolic and functional responses. Polarisation with IFN- γ or IL-4 has been shown to produce a distinct metabolic pattern in murine bone marrow derived macrophages (BMDM) and it was hypothesised that the immunometabolic pattern in human MDM in response to polarisation with IFN- γ or IL-4 would be distinct from the murine model. The glycolytic shift that is induced by macrophage activation results in increased lactate secretion and it was hypothesised that this molecule would have a direct immunometabolic effect on surrounding MDM.

Aims

- Directly compare the immunometabolic profile of adult and cord blood macrophages in response to stimulation with Mtb or LPS.
- Examine the phenotypic differences of macrophages differentiated from adult and cord blood after IFN- γ or IL-4 polarisation.
- Examine the effect of exogenous lactate on the immunometabolic profile of adult and cord blood macrophages and the effect on the ability of adult macrophages to kill Mtb.

Value of Research

This research presents a number of novel findings that help explain the differences in murine and human macrophage models of immunometabolism and is the first to show kinetic differences in immunometabolic responses in humans in response to *Mycobacterium tuberculosis* (Mtb) or lipopolysaccharide (LPS). In order to develop host directed therapies targeting metabolism a clear understanding of the basic science in human systems is required. Macrophages from umbilical cord blood have a different metabolic response to Mtb or LPS stimulation compared to adults and this may explain the fundamental vulnerability of infants to TB or other infections. The data presented in Chapter 3 has been published in an Open Access journal, ensuring that these discoveries can influence the scientific community at large and are accessible to the lay community who have supported this research through the National Children's Research Centre.

Macrophage polarisation occurs in multiple disease states, from atherosclerosis to cancer and the research in Chapter 4 reveals the profound changes that occur in human macrophage metabolism following exposure to IFN- γ or IL-4. The methods described in this work result in distinct immunophenotypes between Mtb, LPS, IFN- γ or IL-4 treated human macrophages and could be the framework to standardise methodology in this complex and overlapping field and to identify new targets for metabolic manipulation in these disease states.

The research on the effect of lactate on macrophage metabolism adds value to the immense potential of host directed therapy for TB. In active TB disease the mycobacteria are replicating and the inflammatory response damages the lungs, both of which were improved in this experimental model.

Outputs

Publications

Ó Maoldomhnaigh C, Cox D, Phelan J, Malone F, Keane J and Basdeo S. **The Warburg Effect Occurs Rapidly in Stimulated Human Adult but Not Umbilical Cord Blood Derived Macrophages** Front. Immunol., 13 April 2021 doi.org/10.3389/fimmu.2021.657261

Cox DJ, Coleman AM, Gogan KM, Phelan JJ, Ó Maoldomhnaigh C, Dunne PJ, Basdeo SA, Keane J. **Inhibiting Histone Deacetylases in Human Macrophages Promotes Glycolysis, IL-1 β , and T Helper Cell Responses to Mycobacterium tuberculosis.** Front Immunol. 2020 Jul 23;11:1609.

Phelan J, McQuaid K, Kenny C, Gogan K, Cox D, Basdeo S, O'Leary S, Tazoll S, Ó Maoldomhnaigh C, O'Sullivan M, O'Neill L, O'Sullivan MJ, Keane J. **Desferrioxamine supports metabolic function in primary human macrophages infected with Mycobacterium tuberculosis** Front. Immunol. May 2020 11:836.

Ó Maoldomhnaigh C, Cox D, Phelan J, Gogan K, McQuaid K, Coleman A, Basdeo S, Keane J. **Lactate Alters Metabolism in Human Macrophages and Improves their Ability to Kill Mycobacterium tuberculosis** Front Immunology – Under review

Cox D, Ó Maoldomhnaigh C, Gogan K, Phelan J, Keane J and Basdeo S. **IFN-gamma priming human macrophages promotes energetic activation in response to Mtb.** To be submitted to the Journal of Redox Biology in August 2021.

Presentations

C Ó Maoldomhnaigh, Donal Cox, James Phelan, Sharee Basdeo, Joseph Keane **Lactate Alters Metabolism in Human Macrophages and Improves their Ability to Kill Mycobacterium tuberculosis** Infectious Disease Society of New York Annual Meeting, May 2021

C Ó Maoldomhnaigh, S Basdeo, J Keane **Immunometabolism of adult and neonatal macrophages infected with Mycobacterium tuberculosis** Immunometabolism Forum, Trinity College Dublin, June 2021

C Ó Maoldomhnaigh, S Basdeo, J Keane **Paediatric Tuberculosis - "Your kiss of affection, the germ of infection"** Trinity Translational Medicine Institute Blitz Presentation, November 2018, TCD, Ireland

Posters

C Ó Maoldomhnaigh, D Cox, A Coleman, K Gogan, K McQuaid, S Basdeo, J Keane **Lactate improves killing of Mycobacterium tuberculosis in human macrophages by driving autophagy** British Society of Immunology Congress December 2019, Liverpool, UK
Cilian Ó Maoldomhnaigh, Donal Cox, Amy Coleman, Sharee Basdeo, Joseph Keane **Lactate improves killing of Mycobacterium Tuberculosis in human macrophages** Irish Society of Immunology, September 2019, Dublin, Ireland

C Ó Maoldomhnaigh, S Basdeo, J Keane **The immunomodulatory effect of dimethylfumarate during Mycobacterium tuberculosis infection** British Society of Immunology Immunometabolism Meeting 2019, Newcastle, United Kingdom

C Ó Maoldomhnaigh, S Basdeo, J Keane **Defining the neonatal immune response to Mycobacterium tuberculosis infection** St Judes/PIDS Symposium 2019, Memphis, TN, USA

C Ó Maoldomhnaigh, S Basdeo, J Keane **Neonatal macrophage immune response to tuberculosis infection** National Children's Research Centre Annual Research Centre Symposium, December 2018, Dublin, Ireland

C Ó Maoldomhnaigh, S Basdeo, J Keane **The effect of exogenous lactate on human macrophages infected with Mycobacterium tuberculosis** British Society of Immunology Congress December 2017, Brighton, UK

Chapter 1 Introduction

1.1.1 Tuberculosis

Tuberculosis (TB) has plagued humankind for millennia¹. Prior to the Sars-CoV-2 pandemic, TB was the single biggest infectious killer in the world, killing 1.4 million people in 2019². The coronavirus pandemic has restricted access to healthcare, interrupted treatment regimens and placed untold burdens on struggling healthcare systems. The impact of this on the incidence of TB has yet to be fully borne out, but emerging evidence indicates that less cases are being diagnosed and appropriately treated, which the World Health Organisation (WHO) estimate will result in an extra 400,000 TB deaths annually²⁻⁶. Although progress has been made over the last number of decades, the decrease in the incidence of TB was just 9% between 2015 and 2020 which fell far short of the WHO's End TB Strategy that aimed to achieve a 20% reduction in the same timeframe⁷.

Tuberculosis in adults is primarily a pulmonary disease, with the classical symptoms of cough, haemoptysis, weight loss, fever and night sweats⁸ occurring as the immune response damages pulmonary tissue in its efforts to control the bacterial growth⁹⁻¹¹. TB can disseminate from the lung and cause disease in any organ system, known as extra-pulmonary TB, and this occurs in ~15% of cases^{2,12}. TB is caused by *Mycobacterium tuberculosis* (Mtb), a small, slow growing, acid fast bacilli, first described by Koch in 1882¹³. It is primarily spread through respiratory contact, with infected people coughing bacilli in to their surrounding environment where they are then inhaled by the next potential host¹⁴. The mycobacteria then must traverse the physical barriers of the host

to infection, such as the mucosal airway barrier and secretory IgA, until it reaches the alveolus¹⁵. There the bacilli encounters the innate immune system and it is ingested by the alveolar macrophage. The disease process at this stage can take one of three potential avenues (Figure 1.1). The macrophage can clear the mycobacteria and the threat is immediately removed. Alternatively, the macrophage can ingest the bacilli but fail to kill the Mtb as the micro-organism subverts the immune response. This can either lead to uncontrolled infection which will lead to active disease within months of exposure or result in a further immune response which will halt the growth of Mtb¹⁶. This immune response and the cellular network that surrounds the macrophages infected with mycobacteria is called a granuloma, which keeps the mycobacteria in stasis^{17,18}. This is the most common outcome after exposure to tuberculosis and it is known as latent TB infection. A disastrous example of these three potential outcomes occurred in 1926 in Lübeck, Germany, when 251 newborns were administered live Mtb erroneously instead of the avirulent *Bacillus Calmette-Guérin* (BCG) vaccine strain. 77 died, 127 had radiographic evidence of disease and 47 showed no evidence of tuberculosis¹⁹.

Approximately 1.7 billion people, about a quarter of the world's population, are estimated to have latent TB^{20,21}. The risk of the mycobacteria reactivating and causing TB disease is about 5-10% over a lifetime but that risk is increased by a number of factors such as HIV infection^{22,23}, smoking²⁴⁻²⁶, diabetes^{27,28}, immunosuppression from biologic agents such as TNF blockers^{29,30} and older age³¹.

Breakthroughs in TB disease management in the 1950s, with widespread access to radiological screening³², the development of new drugs and the realisation that resistance quickly emerged on single drug regimens^{33,34}, allowed successful campaigns to reduce TB incidence. Little has changed in the first line treatment for TB since then, with a 4 drug regimen transitioning to a 2 drug regimen for many months being the standard of care³⁵. The widespread use of the BCG vaccine, which is 100 years old in 2021, also played a role in the reduction of disease, particularly in preventing TB meningitis and disseminated disease in children³⁶⁻³⁸. The emergence of resistance to multiple drugs and the increase in TB seen in people living with HIV has raised the profile of a disease that had fallen from the public consciousness.

Multi-drug resistance (MDR) TB is defined as Mtb that is resistant to at least Rifampicin and Isoniazid, the two most potent anti-TB drugs, and it is considered a global health emergency³⁹. It is estimated that there were over 200,000 cases of MDR TB diagnosed worldwide in 2019, a 10% increase from the previous year². Infections with these resistant strains result in increased morbidity and mortality and may require years of treatment with numerous, toxic and costly medications⁴⁰⁻⁴².

1.1.2 TB in children

TB in children is underdiagnosed and undertreated⁴³. In 2019, an estimated 12% of total TB cases occurred in children under 15 years of age but this group accounted for 16% of mortality, suggesting problems with accessing appropriate medical care². TB is in the top 10 causes of death for children under 5 years of age⁴⁴. Part of this reason is that children are less likely to have the classical symptoms that would prompt appropriate

investigations and they are more difficult to diagnose as they rarely produce sputum, the sample on which diagnosis is often made⁴⁵. Children also have a fundamental susceptibility to TB infection, particularly those under the age of 2 years. In the pre-treatment era, children under the age of 5 had a mortality of ~45% while those aged 5-14 had a mortality rate of 15%, similar to adults^{44,46}. Following exposure, a child is more likely to get active disease than an adult (~50% versus ~10%) and is more likely to have disseminated disease, particularly TB meningitis⁴⁷⁻⁴⁹. The time of highest vulnerability is in the neonatal period, as evidenced by outbreaks in nursery settings and data from the pre-treatment era^{50,51}.

In order for the admirable goals of the WHO's End TB campaign to be met, understanding of the fundamental disease processes which result in the death of over 1 million people every year need to be improved. The majority of adults and about half of children do not develop active disease when exposed to this ancient pathogen. If the differences in immune response are better appreciated, this could pave the way to improved treatment and adjunctive host directed therapies in the effort against TB⁵²⁻

54.

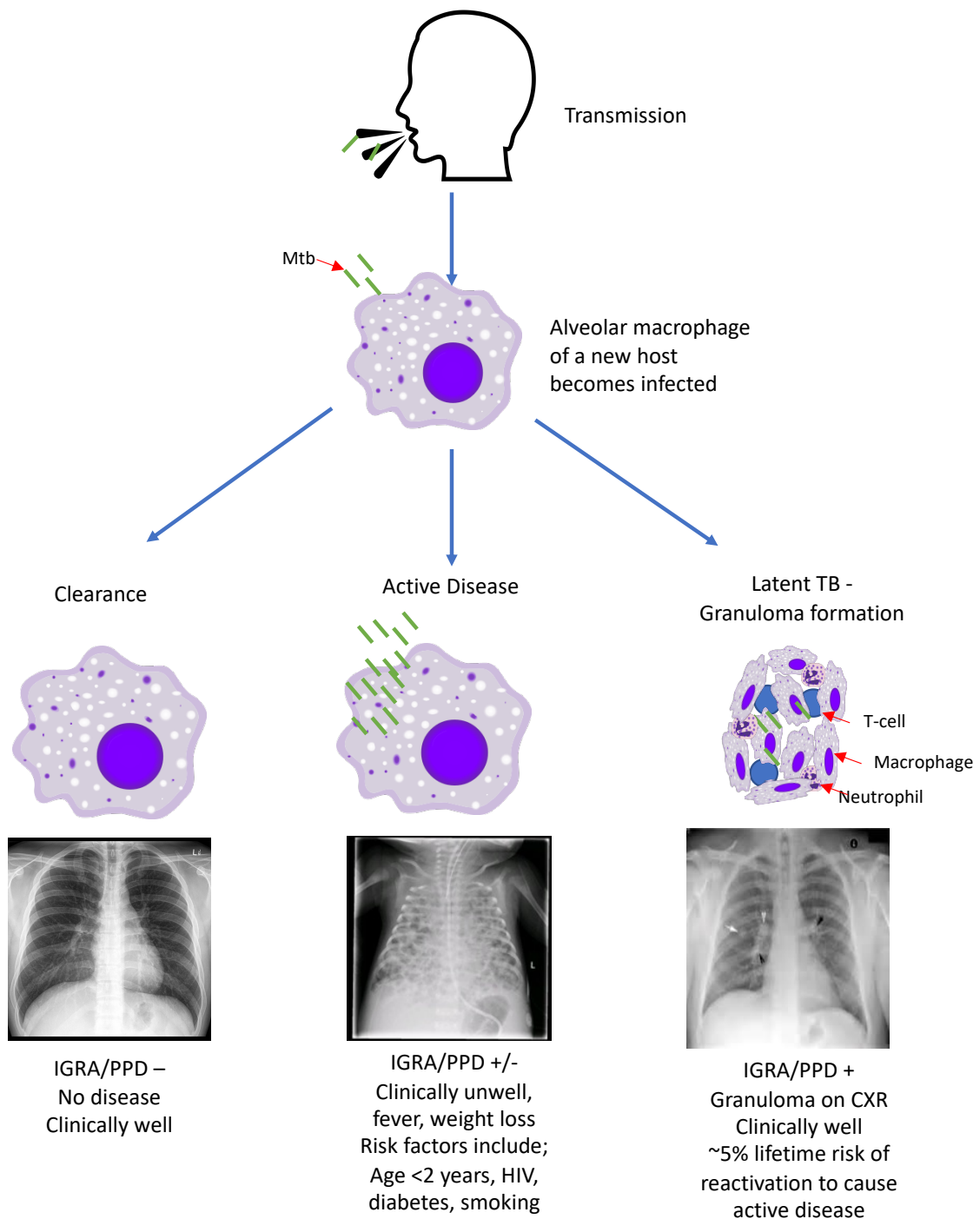


Figure 1.1 Possible fates in the natural history of tuberculosis infection.

This schematic represents the 3 potential outcomes following exposure to *Mycobacterium tuberculosis*. From left; Mycobacterial clearance where the innate immune system is able to clear the infection with no evidence of illness, persistent infection or adaptive immune responses; active disease which occurs 4-6 weeks after exposure resulting in clinical disease and possible disseminated disease as shown in the chest x-ray; latent infection where a granuloma is formed and the patient may test positive on interferon gamma release assay (IGRA) or purified protein derivative (PPD) or show signs of granuloma on chest x-ray (CXR).

1.1.3 The immune response to tuberculosis

The immune response to Mtb is multi-faceted, involving many aspects of the innate and adaptive arms of the immune system. A variety of pathogen recognition receptors (PRR) such as Toll-like receptors (TLRs), C-type lectin receptors (CLRs) such as the mannose receptor, and Nucleotide-binding oligomerization domain (NOD) -like receptors (NLRs) play a role in the recognition of Mtb by the host⁵⁵ and are present on airway epithelial cells⁵⁶ and alveolar macrophages. Lipoarabinomannan, which is an integral part of the cell wall of Mtb and is involved in intracellular survival, is recognised by TLR2. TLR2 also recognises a Mtb lipoprotein as a heterodimer with TLR6⁵⁵. These TLR signals are transduced through MyD88 and nuclear transcription factor- κ B (NF- κ B) transcription, promoting tumour necrosis factor (TNF) amongst other inflammatory cytokines⁵⁷⁻⁵⁹. Heat shock protein, which is secreted by a number of Mtb species, activates TLR4 inducing IL-1 β production⁶⁰. Stimulation of the endosomally located TLR8 and TLR9, which are able to detect intraphagosomal Mtb, causes NF- κ B activation and production of type 1 interferons⁶¹. Polymorphisms in TLR signaling have been shown to increase susceptibility to TB, highlighting their importance in immune responses to Mtb⁶²⁻⁶⁵.

C-type lectin receptors are a family of PRRs that recognise various ligands of Mtb. Of note for this work is the macrophage mannose receptor (MMR), which binds mannose-capped lipoarabinomannan on the Mtb cell wall and induces phagocytosis. Activation of MMR may be beneficial to Mtb as it has been shown to decrease phagosome maturation and increases production of anti-inflammatory cytokines such as IL-10 and IL-1R antagonist^{55,66}. In keeping with this, MMR expression is associated with an alternatively activated "M2"-like phenotype.

NOD2 is an intracellular PRR that recognises bacterial peptidoglycan and muramyl dipeptide in the mycobacteria cell wall⁶⁷. It has been found to mediate induction of IL-1 β , TNF and IL-6 and to induce the accumulation of autophagy proteins⁶⁷. NOD2 activation also synergizes with specific TLR pathways, increasing TNF production⁶⁸. The stimulation of cytokine production by Mtb is significantly impaired in individuals with NOD2 mutations⁶⁹. A consequence of PRR engagement by the host macrophages is the myriad of cytokines produced. TNF, IL-1 β , IL-6 and IL-10 are amongst the most studied cytokines in TB infection in humans⁷⁰⁻⁷⁴ and are examined in this project.

TNF was found to be produced from endotoxin stimulated murine macrophages which, unsurprisingly, caused necrosis of tumour cell lines⁷⁵. TNF- α and TNF- β were found to be homologous cytokines in the 1980s⁷⁶, and are now part of a TNF superfamily containing at least 18 different members⁷⁷. TNF is made in abundance by monocytes and macrophages and amplifies activation in an autocrine manner⁷⁷. TNF is part of the systemic acute phase response seen in sepsis⁷⁸. TNF is considered a double-edged sword in TB, as it is vital for control of the infection but also implicated in the damage caused by an excessive immune response⁷⁹⁻⁸¹. TNF induces apoptosis and necroptosis in Mtb infected macrophages⁸²⁻⁸⁴ vital for control of Mtb infection. TNF is also necessary for granuloma formation and maintenance^{17,85} and the use of anti-TNF blockers in autoimmune inflammatory disease significantly increases the risk of developing active TB disease in those with latent TB infection²⁹.

The importance of IL-1 β production in host defence in TB was confirmed by studies of knockout mice targeting MyD88, IL-1 receptor and IL-1 β pathways^{86–89}. IL-1 β is a potent pyrogenic cytokine and its production is tightly regulated by complex control of release and through antagonism of its receptor site. Briefly, the release of IL-1 β requires 2 signals. The first, priming signal upregulates the immature precursor cytokine pro-IL-1 β . The second signal cleaves this inactive form, producing mature IL-1 β . This is carried out through the inflammasome, a group of cytosolic protein complexes whose assembly triggers proteolytic cleavage of dormant procaspase-1 into active caspase-1, which in turn cleaves the pro-IL-1 β into the biologically active IL-1 β ^{69,90–92}. This second signal is required in human macrophages but not monocytes, explaining why lipopolysaccharide (LPS), a component of gram negative bacterial cell and the archetype ligand for TLR4, does not induce IL-1 β in human macrophages⁹³. Caspase independent signaling pathways have also been proposed⁸⁶. Upon its release, IL-1 β acts as a pyrogen, causing local and systemic inflammation and promotes the release of IFN- γ by T-cells which increases mycobacterial killing by macrophages^{15,94,95}.

When the human IL-6 molecule was successfully identified in 1986⁹⁶ it had already been ascribed different names based on its identification in a variety of physiological processes⁹⁷. It induces hepatocytes to produce acute phase reactants such as C reactive protein⁹⁸. It acts on B and T cells, promoting differentiation and was found to be indispensable in Th17 differentiation from naive CD4⁺ T cells⁹⁹. IL-6 has also been implicated in chronic immune activation states, prompting reabsorption of bone through osteoclast activity¹⁰⁰ and angiogenesis in diseases such as rheumatoid arthritis¹⁰¹. Its role in TB has yet to be fully elucidated. IL-6 deficient mice succumbed to

TB infection when infected with high mycobacterial loads¹⁰², however in a lower dose aerosolised model IL-6 was found to stimulate early IFN- γ but was not essential for protection from Mtb¹⁰³. IL-6 has also been found to inhibit IFN- γ induced autophagy in *ex vivo* human macrophages and may be a target for manipulation by Mtb¹⁰⁴.

IL-10 has been found at elevated levels in patients with pulmonary TB^{105–107}. It was first described in mouse T cells as a factor that inhibits the production of proinflammatory cytokines¹⁰⁸. It is now known to be a vital part of the process of immune deactivation in order to prevent pathology from an over-activated immune system. However, multiple pathogens, including Mtb, have evolved mechanisms of exploiting IL-10, leading to chronic disease states^{109,110}. In human macrophages, IL-10 was found to block phagosomal maturation in Mtb infection, through a signal transducer and activator of transcription 3 (STAT3) dependent manner, enhancing Mtb survival and growth¹¹¹.

The cytokine that is invariably associated with active disease and dominates transcriptomic profiling of active TB disease is IFN- γ ^{112,113}. IFN- γ was once thought to only be produced by adaptive immune cells such as recruited CD4⁺ T cells, however it is now recognised that Mucosal Associated Invariant T (MAIT) cells, Natural Killer (NK) cells and $\gamma\delta$ T cells also produce IFN- γ ^{114,115}. The importance of IFN- γ in control of Mtb infection is seen in murine knock out models^{116,117} and in individuals who have defects in their IFN- γ circuit and who are vulnerable to mycobacterial infection^{118,119}. The role of IFN- γ in activation of human adult or cord blood derived macrophages will be addressed herein.

The balance of these cytokines in different stages of tuberculosis disease is vital in determining outcome. For example, while blocking TNF increases the risk of progression to active disease following exposure to the pathogen, its production in later disease states perpetuates an excessive, damaging immune response resulting in lung necrosis⁹.

1.1.4 The adaptive immune response to TB

If the early innate response fails to rapidly clear Mtb infection, the adaptive immune response is activated. Dendritic cells are the main antigen presenting cells in the initiation of T cell responses following migration from the lung to the regional lymph nodes¹¹³. The magnitude of this response can be subverted by different strains of Mtb resulting in a deficient immune response¹²⁰. The importance of T cells in TB is demonstrated by the susceptibility of patients with HIV induced CD4+ lymphopenia to Mtb²², a finding replicated in CD4+ T cell-deficient mice¹²¹.

This protection is garnered from IFN- γ production by CD4+ Th1 cells which are dependent on IL-12 production from activated DC¹²². A number of other immune cells, including natural killer (NK) cells and $\gamma\delta$ T cells also produce IFN- γ but they are unable to compensate for the absence of CD4+ T cells in knock out murine models¹²³.

Macrophages play a key linking role in innate and adaptive immune responses, potentially resulting in early clearance of Mtb and if it fails to do so, subsequent activation of the adaptive system by functioning as an APC in the tissue. Mtb has evolved numerous strategies to subvert this important aspect of the host response,

which include inhibition of MHC maturation and attenuating antigen presentation of macrophages to CD4+ T cells¹²⁴.

1.1.5 Infant immune susceptibility to TB

There are numerous reviews postulating the reasons that neonates are vulnerable to Mtb infection, however much of the rationale is inferred from work in other disease states^{49,51,125}. There is minimal published data on umbilical cord blood monocyte derived macrophage (MDM) function, with multiple studies utilising whole blood assays or monocyte responses. Neonatal monocytes have been shown to produce less TNF and more IL-6 when stimulated with TLR agonists compared to adult controls in a number of studies¹²⁶⁻¹²⁹. In a study examining the changing innate response to mycobacteria over the first 9 months of life, newborn monocytes produced less TNF and IL-6 compared to 9 month old infants after BCG infection¹³⁰. Macrophages from newborns have been shown to produce less IFN- γ ¹³¹ and were found to have a deficiency in IFN- γ signaling when infected with candida^{132,133}.

A recent study examining lung resident alveolar macrophages (AM) from infants (median age 11 months) showed that they are less able to restrict Mtb growth compared with adult AM¹³⁴. The phagocytic capacity and function, including TNF and IL-1 β production, were similar between the adult and infant AM but RNA-Seq analysis revealed lower expression of IFN- γ -induced pathways.

Studies in cord blood are complicated by the presence of a number of inhibitory plasma factors^{135,136}. For example, adenosine is present at higher concentrations in umbilical

cord than adult plasma and was found to cause a reduction in TLR signaling^{137,138}. Immature CD71⁺ erythrocytes are found in abundance in umbilical cord blood compared to adult blood and have immunosuppressive properties^{139,140}. The methods of macrophage differentiation in this study, explained in Chapter 2, ensure that these factors do not influence the experiments presented in this thesis.

1.1.6 Macrophages

Ilya Mentchikoff shared the Nobel Prize for Physiology or Medicine with Paul Ehrlich in 1908 for his work in the discovery of macrophages¹⁴¹. He recognised the diversity in macrophage function, noting the role of phagocytosis not only in defence against invading organism but also in wound healing and sterile inflammation¹⁴². The true nature of this diversity is still being elucidated over a century later.

Research from the 1960s enshrined the dogma that tissue resident macrophages originated from blood derived monocytes¹⁴³. However, it is now recognised that a subpopulation of tissue resident macrophages appear to have embryological origin and may replicate in their specific organ for years^{144,145}. In early TB infection, the AM, which is the dominant phagocyte in healthy lung, recruits neutrophils and monocytes which differentiate into macrophages¹⁴⁶. In an *in vivo* mouse model, AM are found to be permissive of Mtb growth and the interstitial macrophages, which are recruited from circulating monocytes, were found to be vital for the control of mycobacterial replication¹⁴⁷. The focus of the work presented herein is on the early innate immune response to Mtb infection by MDM, formed by monocytes that are recruited to the

tissue from the blood and differentiate in situ into MDM, and are therefore akin to interstitial macrophages.

Monocytes are released into the circulation from the bone marrow and they are attracted into the tissue by a variety of chemokine and cytokines, with different combinations of cytokines resulting in the differentiation of various macrophage phenotypes¹⁴⁸. The term macrophage activation was coined in the 1960s when Mackaness described the increased microbicidal activity of macrophages upon secondary exposure to pathogens¹⁴⁹. IFN- γ was later linked to this activation state¹⁵⁰. An alternative activation state was described by Stein et al in the early 1990s when it was recognised that IL-4 caused an increase in MMR and reduced proinflammatory cytokine secretion¹⁵¹. Further recognition of the links between these 2 activation states and the Th1 and Th2 cytokine profiles in knock out mice models led to the terminology of M1 and M2 macrophages for the pro-inflammatory and anti-inflammatory phenotypes respectively¹⁵².

1.1.7 Macrophage Polarisation

The term macrophage polarisation was used to describe these two opposite macrophage phenotypes. While this dichotomous description is useful in highlighting the differential potential of macrophages, there has been increasing realisation that there are numerous possible activation states of macrophages, representing a spectrum of functions. At least 6 distinct activation states have been recognised, with multiple influencing factors in both maturation from monocytes and in activation status^{153,154}.

These pathways do not result in terminal differentiation as macrophages exhibit plasticity, being able to change their phenotype and function¹⁵⁵.

The importance of macrophage polarisation in tuberculosis infection is evidenced by the finding that proinflammatory M1 macrophages promote the formation of granulomas and have higher bactericidal activity compared with that of M2 macrophages, however, M2 macrophages predominate once the granuloma has been formed¹⁵⁶.

Differentiation into the M1 phenotype for in vivo experiments was initially achieved by the use of IFN- γ , however TLR agonists such as LPS were also used in combination with IFN- γ to achieve the pro-inflammatory M1 state¹⁵⁷. This was in part due to the variation in methodology in examining macrophage activation states, whether in murine, human cell line or primary human cell work. Human MDM have different gene signatures whether stimulated with LPS, IFN- γ or both¹⁵⁸. It is important to recognise that much of the seminal work in macrophage activation states or polarisation, was performed in murine bone marrow derived macrophages and peritoneal macrophages and that there are many differences between the mouse and human macrophage phenotype^{159,160}. Efforts have been made in recent years to address these differences but there are still a large number of methodologies and interchangeable nomenclature in use¹⁵⁷.

MDM from blood in humans are commonly generated from adherence purification of peripheral blood mononuclear cells (PBMC) in the presence of growth and survival factors¹⁶¹. This method utilises the innate ability of MDM to adhere to plastic material.

In order to further stimulate macrophage differentiation, growth factors such as granulocyte-macrophage colony-stimulating factor (GM-CSF) and macrophage colony-stimulating factor (M-CSF) have previously been utilised. However, maturation with M-CSF polarises macrophages toward an M2, anti-inflammatory phenotype and GM-CSF maturation toward a M1 pro-inflammatory phenotype^{162,163}. Use of normal human serum in macrophage differentiation has been shown to produce a more neutral macrophage phenotype and that is the method undertaken for the work in this thesis¹⁶².

1.1.8 Markers of Macrophage differentiation

The original markers of macrophage polarisation in murine macrophages have not been reliably reproducible in human systems^{153,160}. Markers of activation states in human macrophages remain poorly defined but recent research has sought to establish specific phenotype markers for different activation states^{164,165}. Based on these studies the following markers were used in this body of work to characterise macrophage phenotype and activation; CD68, CD14, CD40, CD80, CD86, Human Leucocyte Antigen (HLA)-DR (an MHC-II receptor), CD83 and CD206. There is little published data on cord blood MDM, with a limited number of studies examining monocytes from umbilical cord blood.

In the late 1980s, CD68 was recognised as a marker of human macrophages¹⁶⁶ and it is used in this study in combination with CD14 to identify macrophage populations. CD14 is a pattern PRR and acts as a TLR co-receptor. It has long been used as a marker of cells in the monocyte-macrophage lineage¹⁶⁷. A study comparing monocytes from adults and umbilical cord blood showed no difference in basal CD14 expression but did show relatively lower CD14 expression after LPS stimulation¹²⁷.

The ligation of human macrophage CD40 by T cells via CD154 induces a pro-inflammatory phenotype and it is a critical co-stimulatory molecule for immune activation¹⁶⁸. The expression of CD40 has previously been shown to be increased in M1 activation¹⁶² and in patients with TB¹⁶⁹. Upregulation of CD40 in cord blood monocytes was found to be reduced compared to adult monocytes following LPS stimulation¹⁷⁰.

CD80 and CD86 are both co-stimulatory markers that are required for T-cell activation in conjunction with T cell receptor conjugation to the macrophage antigen/ Major Histocompatibility (MHC) complex^{171,172}. They are both constitutively expressed by human macrophages. In a previous study, CD80 expression on human macrophages was shown to be increased by IFN- γ stimulation but CD86 expression was increased by both IL-4 and IFN- γ ¹⁶⁴. In a contradictory study examining macrophage differentiated in HS, CD86 was only found to be increased with IFN- γ +LPS and not IL-4¹⁵⁶. CD80 and CD86 upregulation after stimulation with IFN- γ have been shown to be lower in cord blood monocytes compared to adult monocytes¹⁷³.

HLA-DR is an antigen presenting MHC class II molecule which has been shown to be increased in both M1 and M2 activation states^{156,164}. Certain HLA-DR subtypes are associated with greater risk of developing TB¹⁷⁴. In one study comparing adult and cord blood monocytes, HLA-DR expression was found to be lower in cord blood and, furthermore, there was less of an increase in HLA-DR expression after LPS stimulation in cord blood compared with adult monocytes¹⁷⁰.

CD83 is a member of the immunoglobulin superfamily and has traditionally been studied in human dendritic cells (DC) but has now been recognised as an activation marker in numerous immune cell types, including macrophages. CD83 is important for differentiation of T and B lymphocytes and in immune response resolution^{175,176}. CD83 expression on newborn DC was found to be significantly upregulated after BCG infection, a finding not seen in adult DC¹⁷⁷.

CD206 is also known as MMR and recent work in human macrophages has confirmed the original murine observation of increases in CD206 upon M2 like activation^{151,162,164}. It is a C-type lectin important in endocytosis and phagocytosis, scavenging glycoproteins as part of immune homeostasis¹⁷⁸. Expression of CD206 in one study was similar between adult and cord blood monocytes, however it also showed that GM-CSF induced M1 phenotype had increased MMR compared with M-CSF induced M2 macrophages¹⁷⁹.

1.1.9 Macrophage Metabolism

In order for the macrophage to perform its various functions, from scavenging of cellular debris and maintaining homeostasis, to pathogen ingestion, antigen presentation and immune activation, it requires energy and substrates¹⁸⁰. Multiple metabolic pathways are utilised by human macrophages to perform these tasks and to alter the cell phenotype, including fatty acid oxidation and synthesis, amino acid metabolism, the pentose phosphate pathway (PPP), glycolysis and oxidative phosphorylation (OXPHOS)¹⁸¹. The work presented in this thesis focuses on the reprogramming of glycolysis and OXPHOS in macrophage immune responses.

Glycolysis is the pathway by which extracellular glucose is transported to the cytoplasm and converted into pyruvate. This process results in the production of 2 adenosine triphosphate (ATP) molecules along with a variety of other products which can fuel other metabolic pathways such as glucose-6-phosphate into the PPP for the synthesis of ribose, and amino acid production via the serine biosynthetic pathway. Increased flux through glycolysis, therefore, provides immune cells with the necessary building blocks they require for activation, proliferation and effector function. The tricarboxylic acid (TCA) cycle, also known as the Krebs' cycle, occurs in mitochondria and is a far more efficient process to generate ATP. It produces the reducing equivalents nicotinamide adenine dinucleotide (NADH) and flavin adenine dinucleotide (FADH₂), which support OXPHOS via the electron transport chain. These processes are linked when pyruvate is converted into acetyl-CoA, which enters the TCA cycle. This process, in the presence of sufficient oxygen, is the source of basal energy requirements in most cell types. A schematic of the glycolytic pathway and TCA cycle is shown in Figure 1.2.

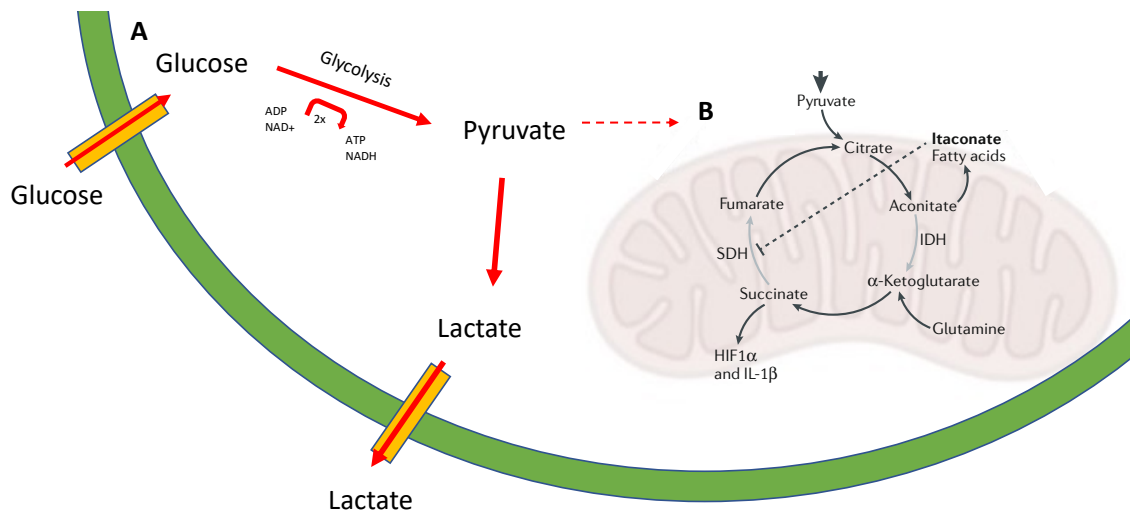


Figure 1.2 Glycolytic pathway and TCA cycle.

Activation of macrophages increases glucose uptake and aerobic glycolysis leads to the rapid production of ATP and other building blocks to facilitate immune activation, with an increase in lactate secretion (A). The Krebs's cycle is disrupted with an accumulation of citrate and succinate and increased itaconate production (B). Adapted from O'Neill and Artyomov 2019¹⁸²

1.1.10 Immunometabolism

In the absence of oxygen, pyruvate is converted into lactate – an observation made over a century ago in studies of muscle metabolism¹⁸³. The reverse of this however, that hypoxia is required for lactate production, is not true. Increased flux through glycolysis can result in lactate production and accumulation even in oxygen replete conditions. It was these such observations made by Otto Warburg in the 1920s from which the burgeoning field of immunometabolism stems¹⁸⁴. He noted that cancer cells, despite having adequate oxygenation, preferentially used aerobic glycolysis. The Warburg effect in immunometabolism describes the phenomenon of increased glycolysis and decreased oxidative phosphorylation after immune cell activation.

Changes in the metabolism of activated macrophages, with increased utilisation of glycolysis has been recognised for decades^{185,186}. Improvements in the understanding of immunological processes of macrophage activation and in the technologies allowing measurement in the changes of metabolites have led to an exponential increase in immunometabolic research in the last 15 years^{180,187}. 2-deoxyglucose (2-DG), a glucose molecule with an alteration to a hydroxyl group which prevents it from undergoing glycolysis has been shown to inhibit macrophage and other immune cell activation. Previous research in the Keane laboratory has shown that 2-DG reduces glycolysis in human macrophages and limits their ability to control Mtb growth¹⁸⁸. Inhibition of glycolysis has also been found to reduce IL-1 β production in both murine and human macrophages^{188,189}.

In murine BMDM, TLR stimulation with LPS leads not only to increased glycolysis but also to a decrease in OXPHOS 24 hours post stimulation¹⁹⁰. This break in the TCA cycle leads to the accumulation of citrate and succinate. Citrate is used for itaconate production and fatty acid synthesis, and succinate has a number of pro-inflammatory effects including the stabilisation of hypoxia induction factor (HIF) 1 α with subsequent increases in IL-1 β ^{182,187,191}.

Similar to the glycolytic switch seen after LPS stimulation, IFN- γ was shown to increase glycolysis and decrease in OXPHOS in murine BMDM 24 hours after treatment. This study also showed that 2-DG inhibited the M1 polarisation induced by IFN- γ in both murine and human macrophages¹⁹². Alternative activation with IL-4 in murine macrophages has been shown to increase OXPHOS two fold but to have only a small increase or no effect in the level of glycolysis^{193,194}. Fatty acid oxidation has been shown to be necessary for M2 activation in murine BMDM but to be dispensable in human MDM¹⁹⁵. The changes seen in macrophage metabolism after activation are summarised in Figure 1.3, although these data are mostly derived from studies in mice.

Data on macrophage immunometabolism in human MDM is lacking, with a number of differences between human and murine models evident¹⁹⁶. A study directly comparing murine BMDM and human MDM replicated the established increase in murine glycolysis, and decrease OXPHOS in response to LPS¹⁹⁷. In contrast, human MDM had reduced glycolysis and no change in OXPHOS 16 hours after LPS stimulation. Differential arginine metabolism between M1 and M2 BMDM is not seen in polarised human MDM¹⁹⁸. Analysis of the proteome of human macrophage polarised to M1 showed

upregulation of glycolytic enzymes¹⁹⁹ and genome wide ribosome profiling of human macrophages revealed that IFN- γ modulates the transcriptome to promote inflammation and to reprogram metabolic pathways²⁰⁰. In a study of human monocytes, LPS was found to have no impact on glycolysis or basal OXPHOS at 24 hours²⁰¹.

The knowledge gap in human macrophage polarisation is even more pronounced with regard to umbilical cord MDM. Two recent papers have shown contradictory results. Similar phenotypic profiles in adult and cord blood monocytes were seen after polarisation, however, a distinct immune response was seen in neonatal monocytes producing less TNF than adult monocytes¹⁷⁹. A different study in MDM showed marked differences between adult and cord blood phenotype, including a complete abrogation of oxidative phosphorylation after polarisation with IFN- γ and an inability to upregulate glycolysis²⁰². This is a common theme when examining the published literature in human MDM, in part due to the variety in methodologies used to differentiate macrophages, including the impact of growth factor on activation status¹⁶².

These immunometabolic switches have been shown to be important in TB granulomas in a number of tuberculosis models²⁰³. In a murine model, infection with Mtb induced the Warburg effect in mouse lungs as seen by transcription profiling and immunofluorescence microscopy²⁰⁴. Lactate also increases in mice infected with Mtb, with a decrease in glucose, suggestive of the glycolytic shift seen in immune cell activation²⁰⁵. In an *in vivo* rabbit model of Mtb infection, an upregulation of gene networks involved in immune response and of genes encoding the Warburg effect were seen²⁰⁶. Disease states that have been associated with altered metabolism such as

diabetes, smoking, and HIV are all associated with increased risk of developing TB^{27,28,203}. In order to realise the untapped potential of host directed therapy targeting metabolic pathways in TB and other disease states, understanding of the fundamental immunometabolic shifts in human macrophages is required.

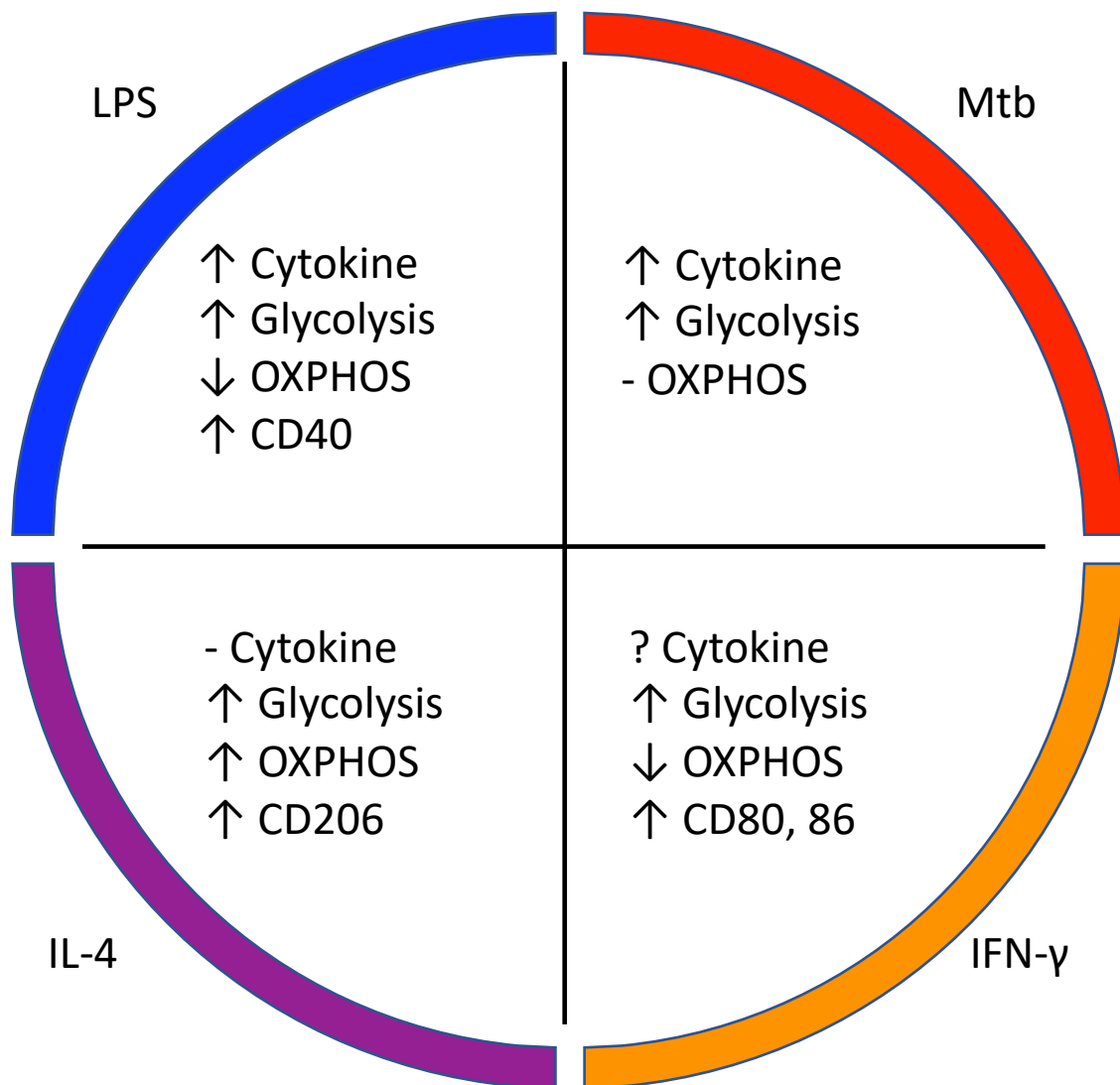


Figure 1.3 Summary of immunometabolic changes in macrophages in published literature.

This schematic summarises the various changes in macrophages documented in the literature after exposure to LPS, Mtb, IL-4 or IFN- γ . These data are primarily from studies of murine BMDM and pertain to events that occur 24 hours post the activation stimulus.

1.1.11 Host directed therapy

Traditional treatment of infectious diseases has focused on anti-microbials that target the invading pathogen, however, with the emergence of antimicrobial resistance, there is increasing recognition of the potential of host directed therapies. As highlighted in the overview above, TB infection activates numerous immune pathways, many of which are subverted or evaded by Mtb evolutionary strategies. Greater understanding of the mechanisms by which Mtb disrupts the immune response or how susceptible individuals differ from those who are immune is necessary to identify pathways that can be therapeutically manipulated to improve clinical outcomes.

Many host-directed therapies have already been added to the arsenal of anti-TB therapies that are currently in use. For example, corticosteroids have been utilised in TB infection to modulate the immune response, particularly in TB meningitis⁵⁴. Monoclonal antibodies designed to treat auto-immune conditions such as TNF blockers have been found to increase the risk of TB re-activation but they can also play a role in dampening the over active, destructive, immune response seen in late disease⁵³. Metformin, used in the treatment of type 2 diabetes, has been shown to reduce the risk of TB by increasing anti-mycobacterial activity of CD8 T cells^{207,208}. Although these therapies are effective under certain circumstances, an immuno-supportive host-directed therapy that can be used adjunctive to anti-microbials to promote early clearance remains elusive.

The recent focus on the interplay between metabolism and immune cell activation has raised the possibility of metabolic therapies to manipulate the immune response.

Targeting of glucose, lipid and arginine metabolism have all been postulated as possible host-directed therapies^{209,210}. Defining the ideal immune response at various time points during Mtb infection and TB disease is vital to ensure that immunometabolic function is appropriately targeted. For example, increased glycolysis and greater immune activation in early disease to achieve early clearance of Mtb.

1.1.12 Hypothesis

It was hypothesised that the difference in clinical phenotype seen between adults and newborns following exposure to Mtb is a result of underlying differences in macrophage metabolic and functional responses. Polarisation with IFN- γ or IL-4 has been shown to produce a distinct metabolic pattern in murine bone marrow derived macrophages (BMDM) and it was hypothesised herein that the immunometabolic pattern in human MDM in response to polarisation with IFN- γ or IL-4 would be distinct from the established murine model. The glycolytic shift that is induced by macrophage activation results in increased lactate secretion; therefore, it was hypothesised that this molecule would have a direct immunometabolic effect on surrounding MDM.

1.1.13 Aims

- Directly compare the immunometabolic profile of adult and cord blood macrophages in response to stimulation with Mtb or LPS.
- Examine the phenotypic differences of macrophages differentiated from adult and cord blood after IFN- γ or IL-4 polarisation.
- Examine the effect of exogenous lactate on the immunometabolic profile of adult and cord blood macrophages and the effect on the ability of adult macrophages to kill Mtb.

Chapter 2 Methods

2.1 Monocyte derived macrophages from adult and umbilical cord donors

2.1.1 Isolation of adult PBMC

Peripheral blood mononuclear cells (PBMC) were isolated from buffy coats from anonymous healthy adult donors, obtained with consent from the Irish Blood Transfusion Service. The buffy coats were mixed 1:1 with phosphate buffered saline (PBS; Sigma Aldrich) and centrifuged at 800 g for 10 minutes with no brake, resulting in separation of the blood into red blood cells, a white cell layer and a plasma/platelet layer (Figure 2.1 A). The white cell layer was removed and mixed with PBS to a final volume of 150 ml. 25 ml of this mixture was then layered onto 20 ml of Lymphoprep (Figure 2.1 B, Stemcell) a total of 6 times and then centrifuged at 800 g for 20 minutes with no brake. The PBMC layer was removed (Figure 2.1 C), washed in PBS and cells were pelleted by centrifugation at 600 g for 10 minutes with the brake on. This step was repeated prior to counting. To remove excess platelets if contaminating, cells were washed in PBS and pelleted by centrifugation at 250 g for 7 minutes.

2.1.2 Isolation of umbilical cord mononuclear cells

Umbilical cord blood samples were drawn from the placental umbilical cord immediately following delivery of the placenta. All babies were healthy term infants of normal birthweight who were delivered by elective Caesarean section. All mothers were well throughout pregnancy and had no co-morbidities. Informed consent was obtained from the mother prior to delivery (Appendix). Ethical approval was granted by the Rotunda Ethics Committee (Appendix). Standard practice for Caesarean section involves

the placement of two clamps on the umbilical cord after delivery of the neonate. The cord is then cut and the baby removed from the operating field prior to the delivery of the placenta. In order to facilitate sample collection, the obstetrician placed another clamp on to the umbilical cord close to the placenta prior to delivery of the placenta. This ensured that blood remained in the umbilical cord after placental delivery. Immediately following delivery, the placenta was taken out of the operating field and sampled. A blunt Sterican (B. Braun) 18 gauge needle was inserted into the umbilical vessels between the “double clamp” (Figure 2.2 A) and the sample was transferred to lithium heparin bottles (Vacutest Kima). In order to increase the sample volume the umbilical vessels proximal to the proximal clamp were also sampled if the blood volume within the placenta was intact (Figure 2.2 B). The UCB samples were processed within 4 hours of collection. The blood samples were mixed 1:1 with PBS before layering up to 30 ml of diluted blood onto 20 ml of Lymphoprep and then centrifuged at 800 g for 20 minutes with no brake. The umbilical blood mononuclear (UBMC) layer was removed and washed twice in PBS.

2.1.3 Cell Counting

PBMC and UBMC were resuspended in Roswell Park Memorial Institute-1640 medium (RPMI; Gibco) completed with 10% type AB male human serum (Sigma-Aldrich; cRPMI) and diluted in trypan blue (Sigma Aldrich). Viable mononuclear cells were counted on a light microscope (Leica) using a haemocytometer (Improved Neubauer, Hawksley England). The formula below was used to calculate the total number of cells:

Average cell number (in one quadrant) x 10^4 x trypan blue dilution factor x volume (ml)
= total cell number

2.1.4 Monocyte derived macrophage differentiation

Monocyte derived macrophages (MDM) were adherence purified from PBMC from adult or umbilical cord blood for 6-8 days. PBMC were plated at a density of 2.5×10^6 /ml on non-treated plastic tissue culture plates (Costar Corning). For experiments involving infection of MDM with Mtb, cells were concurrently plated on an 8 well Lab-Tek chamber slide (Nunc) at the same seeding density. Cells were maintained in humidified incubators at 37°C and 5% CO₂. Non-adherent cells were removed by washing every 2 to 3 days (three times) over 6-8 days with replacement of cRPMI to allow macrophage differentiation.

2.1.5 The phenotype of adult and cord blood monocyte derived macrophages

In order to ensure that this method resulted in similar macrophage differentiation from adult or cord blood, the morphology was assessed using light microscopy. PBMC were isolated from adult buffy coats or from umbilical cord blood which was collected immediately following delivery. MDM were adherence purified for 7 days in RPMI with 10% human serum and non-adherent cells were washed off on day (D) 2 and D5. Similar morphology was seen under light microscopy for both adult (Figure 2.3 A) and cord blood (Figure 2.3 B) MDM after 7 days of differentiation.

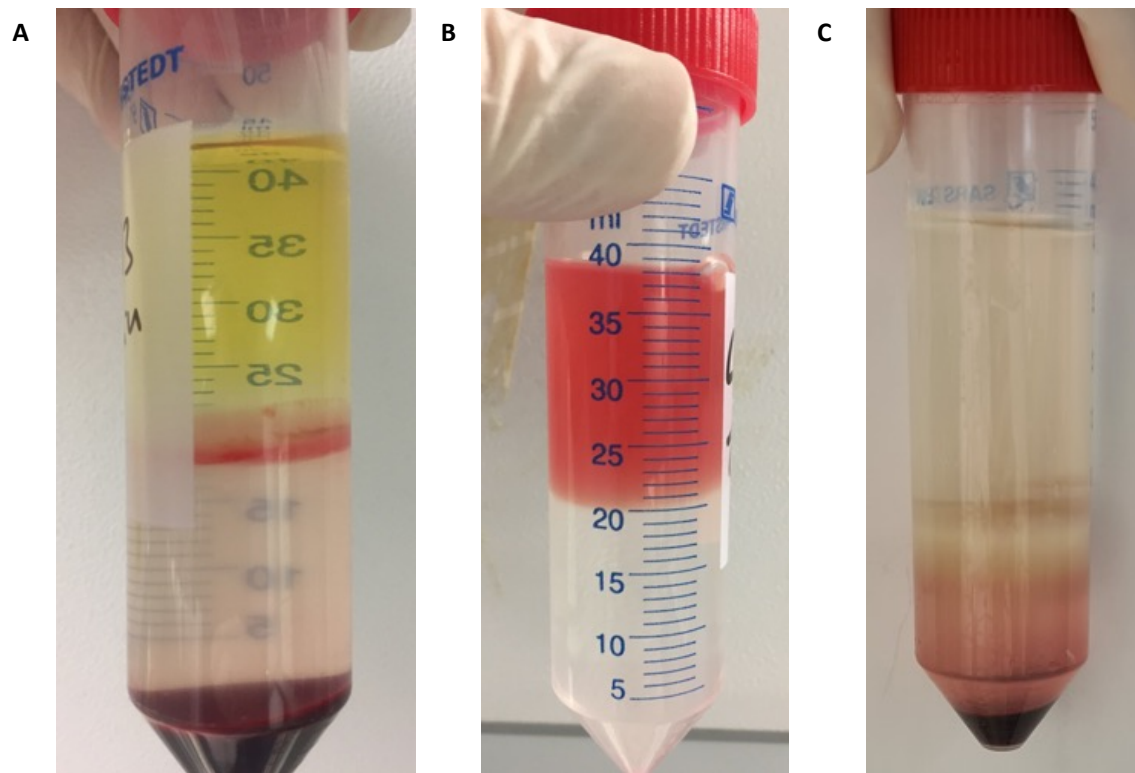


Figure 2.1 Isolation of PBMC from blood.

Blood from Buffy coats donated by the Irish Blood Transfusion Service was diluted 1:1 with sterile PBS and centrifuged at 800g for 10 minutes with the brake off. The blood separates into its constituent parts (A). The buffy coat layer containing leukocytes was removed, diluted in sterile PBS and layered over Lymphoprep™ (B). This was then centrifuged at 800 g for 20 minutes with the brake off and the desired mononucleocyte-enriched layer removed. The PBMC layer (C) was removed washed in PBS and cells were pelleted by centrifugation at 600 g for 10 minutes with the brake on.

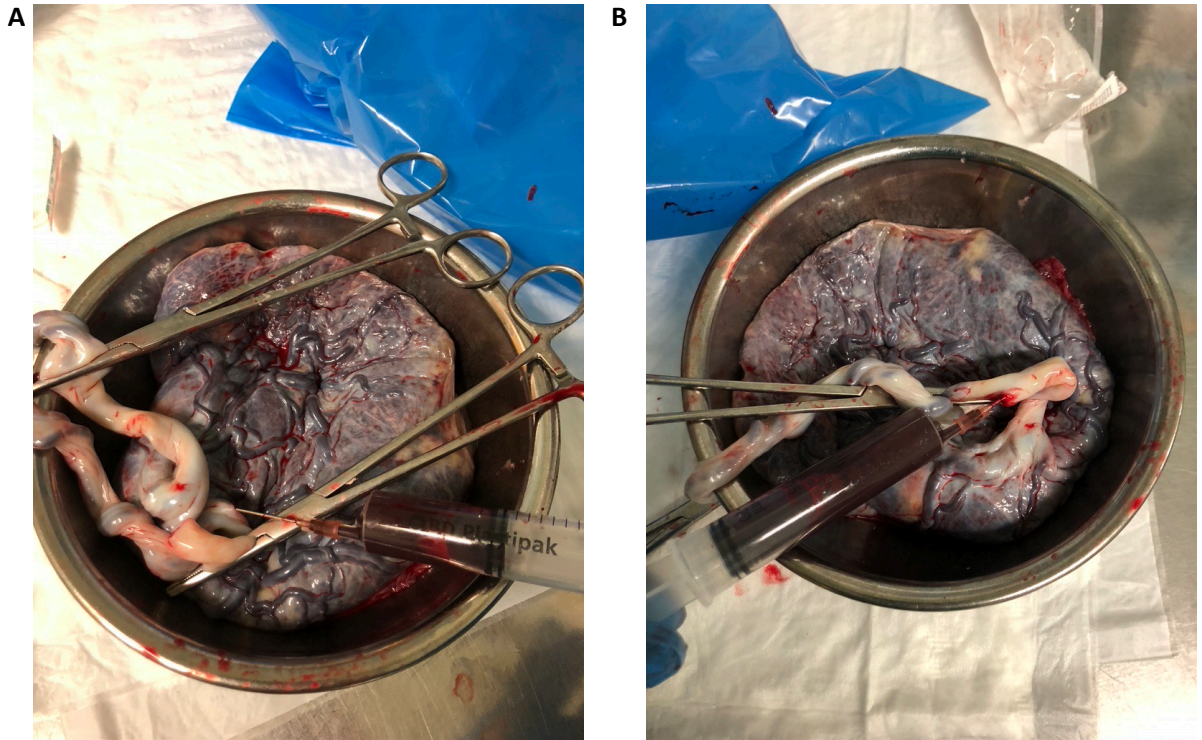


Figure 2.2 Umbilical cord blood sampling from the placental umbilical cord.

The placental umbilical cord was “double clamped” at delivery and the cord vessels accessed with a blunt 18-gauge needle (A). In order to increase yield, the umbilical vessels proximal to the proximal clamp were also accessed if there was adequate blood volume (B).

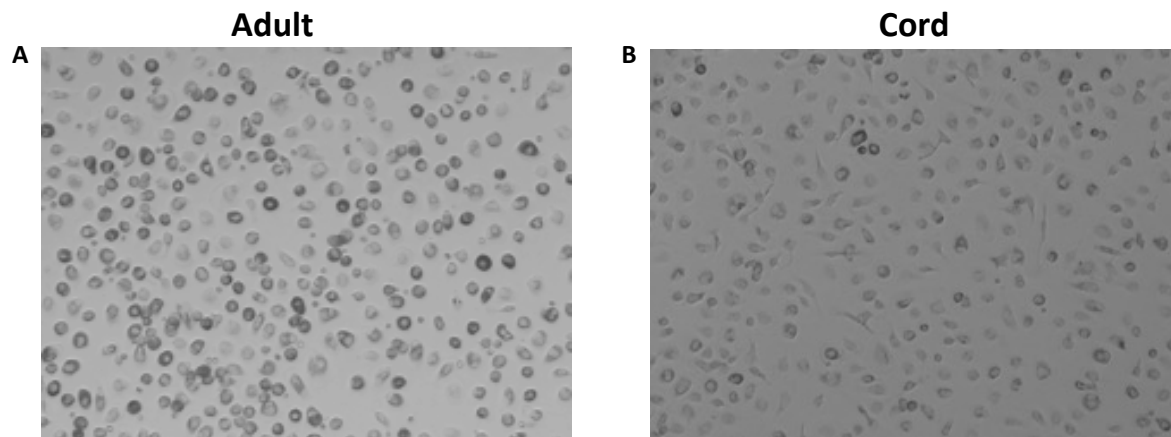


Figure 2.3. Adult and cord blood MDM morphology

PBMC were isolated from buffy coats or from umbilical cord blood samples taken immediately following delivery. Adult or cord blood MDM were adherence purified for 7 days in 10% human serum. Light microscopy images of adult (A) and cord (B) MDM were taken.

2.2 Mycobacterial Infection and Stimulation of MDM

2.2.1 Culture and preparation of attenuated live Mtb, H37Ra

A Biosafety Level 2 (BSL2) facility was used to carry out all work using Mtb H37Ra. Mtb strain H37Ra was obtained from the American Type Culture Collection (ATCC 25177) (Manassas, VA) and aliquots stored at -80°C. Middlebrook 7H9 broth (Difco) supplemented with albumin-dextrose-catalase (ADC) (Becton Dickinson) and 0.05% Tween 80 (Difco) was made up in endotoxin-free water (Sigma-Aldrich). Aliquots were thawed prior to experimentation and propagated in Middlebrook 7H9 broth (supplemented as above) to log phase.

On the day of infection, log phase Mtb was centrifuged at 2900g for 10 minutes. A 25 gauge needle was used to resuspend and homogenise the mycobacteria by aspirating 6-8 times in RPMI. Any remaining clumps were pelleted by centrifugation at 120g for 3 minutes. The supernatant was transferred to a fresh tube and the pellet discarded. The H37Ra suspended in the supernatant was used for determination of the multiplicity of infection (MOI) and infection of MDM.

2.2.2 Preparation of irradiated Mtb H37Rv

Aliquots of γ -irradiated Mtb strain H37Rv (iH37Rv) whole cells (NR-49098; BEI Resources, NIAID, NIH) were stored at -80°C. Upon thawing, iH37Rv was diluted in endotoxin free water (20 ml; Sigma Aldrich) and sonicated in a water bath sonicator for 20 minutes. The solution was aspirated 10 times with a 21 gauge needle. Bacterial clumps were pelleted by centrifugation at 120g for 5 minutes. The supernatant was removed and then aspirated several times through a 25 gauge needle. The tubes were

sonicated again for 20 minutes and the aspiration with a 25 gauge needle was repeated. These working stocks were then kept at -80°C until the morning of the experiment at which time they were thawed, sonicated for 20 minutes and aspirated through a 25 gauge needle prior to use in determining MOI and infection of MDM.

2.2.3 Determination of multiplicity of Infection

In order to correct for donor variability in phagocytic capacity of human macrophages and variation in the concentration of Mtb used in different experiments, the multiplicity of infection (MOI) was determined for each donor prior to infection with either iH37Rv or H37Ra strain. Different volumes of the prepared Mtb (iH37Rv or H37Ra) were added to the 8 well Lab-Tek chamber slide (Nunc) containing MDM. Three hours after infection the supernatant and any extracellular mycobacteria were washed off with PBS and the cells fixed with 2% paraformaldehyde (PFA) for 5 minutes. After washing with water, the cells and mycobacteria were stained with Auramine O staining kit (Becton Dickinson) and Hoechst 33358 (10 µg/mL; Sigma-Aldrich). The 8 well Lab-Tek chamber slides were removed and cover slips were applied to the slides using Dako fluorescent embedding medium (Dakocytomation). Oil immersion fluorescent microscopy (Olympus IX51) was used to determine the percentage of infected cells and the number of bacilli per cell. The MOI calculated is based upon the number of bacilli per cell and the number of cells infected. A low MOI is considered 1-5 bacilli per cell, approximately 30% of cells infected with at least 1 bacillus and with a mode of 2-3. A medium MOI is calculated on 1-10 bacilli per cell with approximately 50% of cells infected with at least 1 bacillus and with a mode of 4-6. A high MOI reflects cells containing up to 20 bacilli per cell, with approximately 70% of cells containing at least 1 bacillus and a mode of

approximately 10 (Figure 2.4). This method of determining MOI is well established in the Keane laboratory but had not been previously used in this laboratory in umbilical cord blood MDM. In order to examine the impact of increasing MOI on umbilical cord blood MDM responses, the production of TNF following stimulation with different MOI of Mtb (iH37Rv) was examined.

PBMC were isolated from umbilical cord blood samples taken immediately following delivery. Cord blood MDM were adherence purified for 7 days in 10% human serum. MDM were infected with Mtb (iH37Rv) at different MOI. Low, medium and high MOI were based upon the number of bacilli per cell and the number of cells infected; 1-5 ~30%, 1-10 ~50% and 1-10 ~70% respectively. Cytokine production was measured by ELISA 24 hours post infection (n=4, \pm SEM). There was a significant increase in TNF production between the low and high MOI infected umbilical cord blood MDM (Figure 2.5).

2.2.4 Phagocytosis of Mtb in adult MDM compared with cord blood MDM

The phagocytosis of Mtb by adult and cord blood MDM was assessed by adding Mtb (iH37Rv) to cells (plated on 8-well labteks). After 3 hours the MDM were washed, fixed with PFA (2%) and stained with Hoechst (to stain cell nuclei) and auramine O dye (to stain the bacilli). Using fluorescent microscopy, the percentage of cells infected and the numbers of bacilli per cell were recorded. This method was used to determine the multiplicity of infection (MOI) for each donor, therefore accounting for inter-donor variation in phagocytosis. The volume of Mtb required to achieve a target MOI of 70% cells infected with 1-10 bacilli per cell was calculated for an adult donor and umbilical

cord blood donor using the same vial of Mtb on 3 separate occasions. Similar volumes of Mtb were required to achieve the same multiplicity of infection for adult and cord MDM, thus indicating that adult and cord blood MDM exhibit similar the phagocytic capacity (Figure 2.6).

2.2.5 Mtb infection of MDM

Following the determination of the MOI, MDM were infected with the appropriate volume for the target MOI of iH37Rv or H37Ra. The supernatant was removed 3 hours later and extracellular mycobacteria were washed by gently pipetting PBS on and off cells. Bacteria present in the supernatants were pelleted by centrifugation at 800 g for 10 minutes and the top 50% of the supernatant was replaced back onto cells to ensure removal of any extracellular mycobacteria but allowing any early cytokines produced to remain in the system in addition to any reagents added prior to infection, depending on the experiment. Cells were incubated for the indicated time periods in humidified incubators at 37°C and 5% CO₂.

2.2.6 Assessing mycobacterial growth

MDM were infected at an MOI of 30-40%, 1-5 mycobacteria per cell. Cells were lysed in sterile 0.1% Triton-X at 3, 48 and 120 hours post infection. 7H9 Middlebrook Broth supplemented with ADC was used to serially dilute the lysates and they were plated on 7H10 Middlebrook Agar supplemented with Oleic Albumin Dextrose Catalase (OADC) in triplicate. Agar plates were incubated at 37°C for 21 days before colony forming units (CFU) were counted.

Mycobacterial growth in axenic conditions was assessed using a BacT Analyser (Biomerieux). Mtb (H37Ra) was added to 1 ml of Middlebrook 7H9 Broth (+ADC). After three days of mycobacterial propagation, 20% dilution was added to BacT bottles. Time to positivity, as measured by the BacT Analyser, was recorded for each condition.

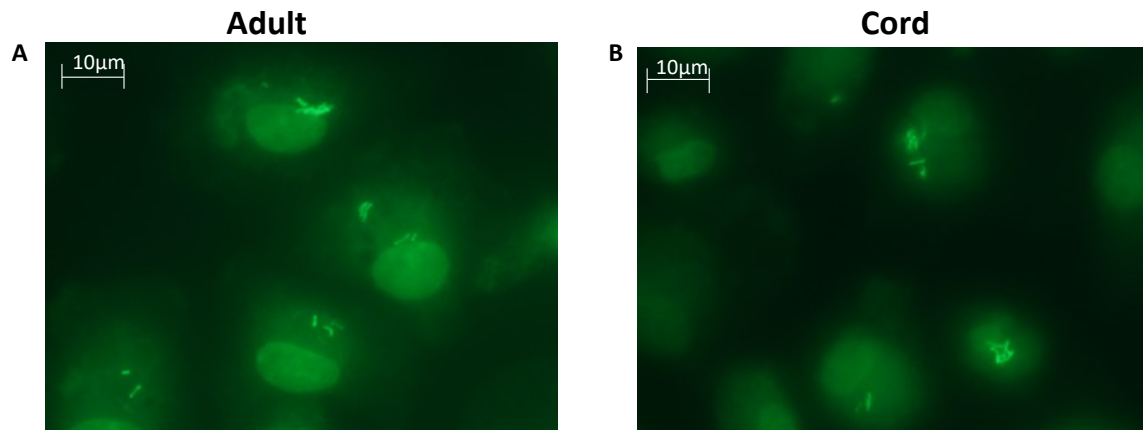


Figure 2.4 Multiplicity of infection for adult and cord blood MDM.

Prior to stimulation with Mtb a multiplicity of infection was performed for an adult and umbilical cord blood donor by adding variable amounts of Mtb to MDM on 8 well labteks. After 3 hours the MDM were washed and stained with Hoechst and Auramine O dye. Using oil immersion fluorescent microscopy (100X objective), the percentage of cells infected and the numbers of bacilli per cell were recorded and used to calculate the volume added to the experimental wells. Shown is high MOI with ~70% of MDM infected with 0-10 bacilli per cell.

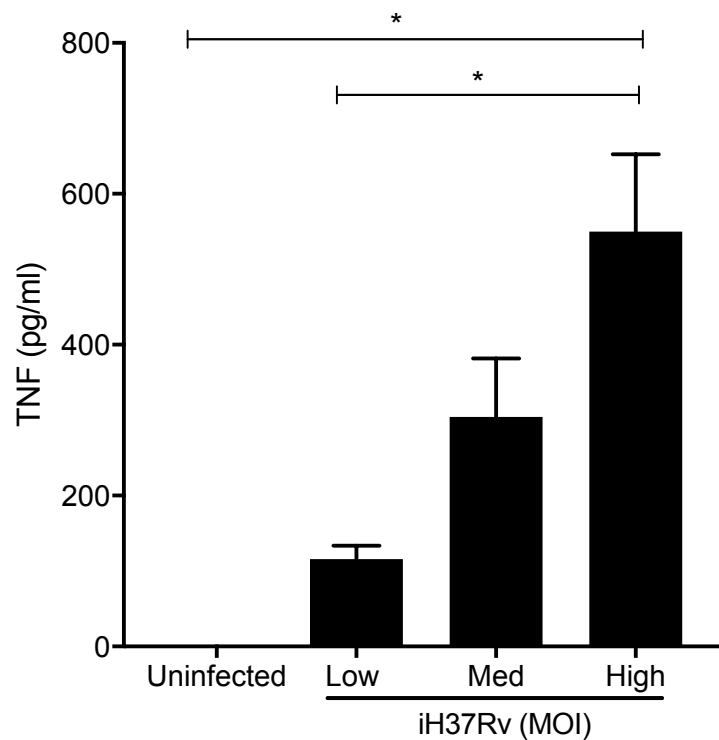


Figure 2.5 Increasing MOI produced a corresponding increase in TNF production in cord blood MDM.

PBMC were isolated from umbilical cord blood samples taken immediately following delivery. Cord blood MDM were adherence purified for 7 days in 10% human serum. MDM were infected with Mtb (iH37Rv) at different MOI. Low, medium and high MOI are based upon the number of bacilli per cell and the number of cells infected; 1-5 ~30%, 1-10 ~50% and 1-10 ~70% respectively. Cytokine production was measured by ELISA 24 hours post infection (n=4, \pm SEM). Statistical significance was determined using one-way ANOVA with Tukey's multiple comparison test; * P<0.05.

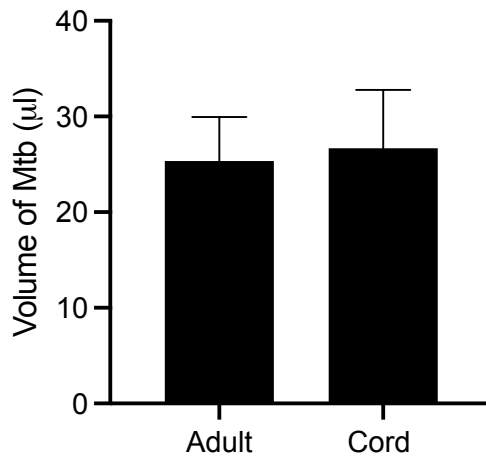


Figure 2.6 Phagocytosis of Mtb by adult and cord blood MDM.

The phagocytosis of Mtb by adult and cord blood MDM was assessed by adding Mtb (iH37Rv) to cells (plated on 8-well labteks). After 3 hours the MDM were washed, fixed with PFA (2%) and stained with Hoechst (to stain cell nuclei) and auramine O dye (to stain the bacilli). Using fluorescent microscopy, the percentage of cells infected and the numbers of bacilli per cell were recorded. The volume of Mtb required to achieve a target MOI of 70% cells infected with 1-10 bacilli per cell was calculated for the adult donor and umbilical cord blood donors (n=3). The volumes of Mtb required to obtain the desired MOI in adult and cord MDM were not statistically significantly different, as determined by a Student's t-test.

2.3 Flow cytometry

In order to determine MDM differentiation and activation status, flow cytometry was performed on FACSCanto™ II (BD Biosciences). MDM purities were determined by staining with fluorochrome conjugated antibodies specific for CD14 (FITC) and CD68 (PE; both BioLegend) on D0 and D8 of differentiation. As MDM are adherent, they were washed with cold PBS, cooled on ice for 30 minutes and then gently scraped in order to remove them from the plate. The cells were then treated with Fc block (Human TruStain FcX receptor blocking solution; BioLegend), stained with a viability dye (Zombie; BioLegend) and fluorochrome conjugated antibodies specific for CD14 (FITC), CD68 (PE), CD80 (PECy7), CD83 (PerCPCy5.5), MMR (APC), and HLA-DR (APC-Cy7). In order to adjust for spectral overlap, compensation beads, singly stained with every fluorochrome used, were acquired. Data was analysed using FlowJo software and gates were set using fluorescence minus one (FMO) and unstained controls.

In order to ensure that this method of differentiation in 10% human serum produced viable macrophages from adult and cord PBMC, the macrophage purity and viability was examined after differentiation using flow cytometry. PBMC were isolated from adult buffy coats or from umbilical cord blood which was collected immediately following delivery. MDM were adherence purified for 7 days in RPMI with 10% human serum and non-adherent cells were washed off on D2 and D5. As MDM are adherent, they were washed with cold PBS, cooled on ice for 30 minutes and then gently scraped in order to remove them from the plate. Cells were then placed in flow cytometry tubes and exposed to Zombie NIR viability dye, Fc blocked and stained with fluorochrome-conjugated antibodies specific for CD14 (FITC) and CD68 (PE) and acquired by flow

cytometry. The dot plots show the gating strategy of a representative adult and cord blood donor (Figure 2.7 A). MDM are gated on the basis of size and granularity (Forward Scatter (FSc) versus Side Scatter (SSc)), doublets were excluded (FSc-Area versus FSc-Width), dead cells were excluded (Zombie NIR negative cells were gated) and co-expression of CD14 and CD68 were analysed. The graphs illustrate collated data for n=4 cord and n= 4 adult MDM. The purity of the MDM population on D7 of differentiation (Figure 2.7 B) and viability after cold lifting and scraping (Figure 2.7 C) is shown. Both adult and cord blood MDM cultures exhibit high purity (add in number +/- SD details) based on the co-expression of CD14 and CD68 (Figure 2.7 B). Cord blood MDM were more prone to death than adult MDM after the cold scraping method of detaching MDM from plastic (Figure 2.7 C). This was carefully adjusted for throughout the experiments by counting the MDM in trypan blue and reseeding on to Seahorse plates based on live cell numbers.

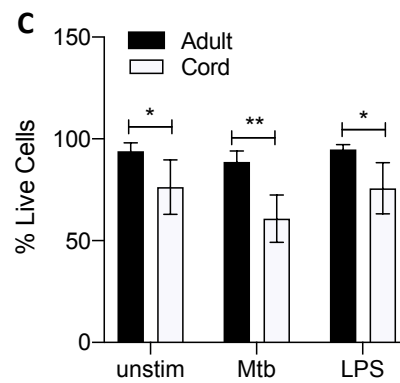
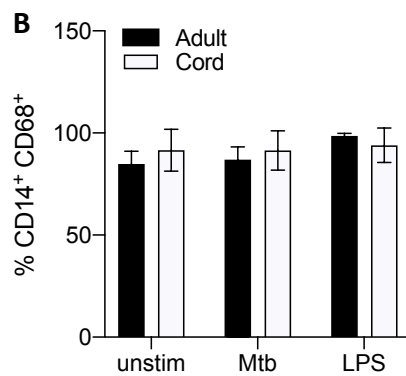
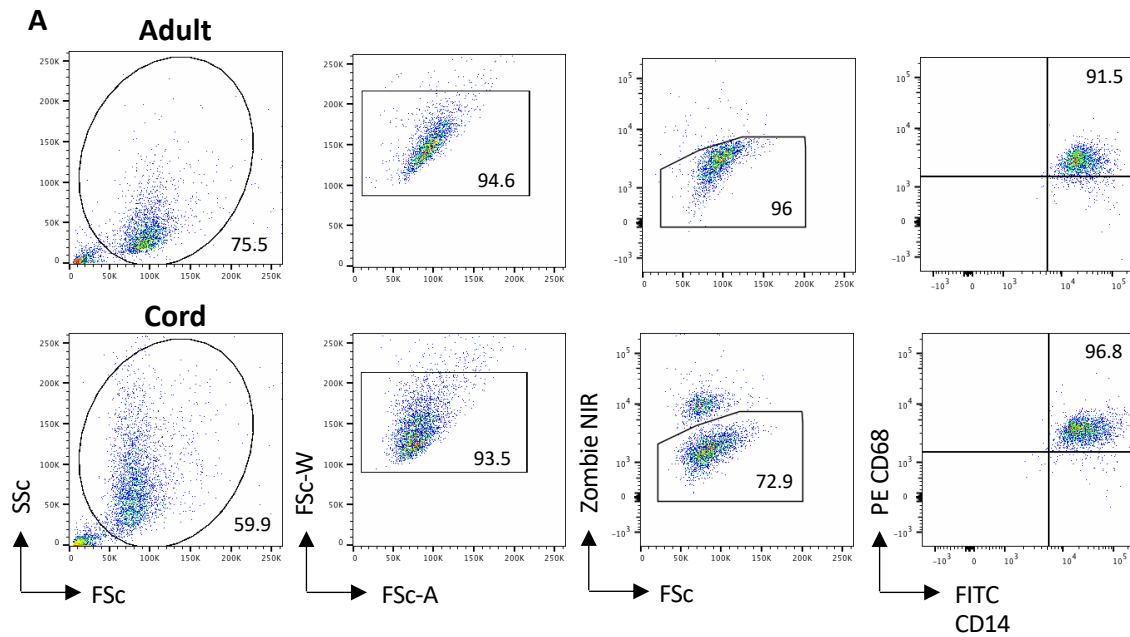


Figure 2.7 Adult and cord blood MDM viability and purity following differentiation.

PBMC were isolated from buffy coats or from umbilical cord blood samples taken immediately following delivery. Adult or cord blood MDM were adherence purified for 7 days in 10% human serum. MDM were washed with cold PBS, cooled on ice for 30 minutes and cells were then placed in flow cytometry tubes. MDM were exposed to Zombie NIR viability dye, Fc blocked and stained with fluorochrome-conjugated antibodies specific for CD14 (FITC) and CD68 (PE) and acquired by flow cytometry. The dot plots show the gating strategy of a representative adult and cord blood donor (A). The graphs illustrate collated data for n=4 cord and n=4 adult MDM. Shown is the purity of the MDM population on day 7 of differentiation (B) and viability after cold lifting and scraping (C). Statistical significance was determined using two-way ANOVA with Sidak's multiple comparison test; * P<0.05, **P<0.01.

2.4 Metabolic flux analysis

2.4.1 Seahorse XFe24 Analyzer

Extracellular flux analyses were performed using the Seahorse XFe24 Analyzer (Seahorse Biosciences, Agilent Technologies UK Ltd.) which performs real-time simultaneous measurement of extracellular acidification rate (ECAR) and oxygen consumption rate (OCR) of live cells. Sensor probes are lowered into each well to measure the concentration of dissolved oxygen and the concentration of free protons within the well for 2 – 5 minutes (until the rate of change of both measured values are linear), and the instrument then calculates the OCR and the ECAR. Probes then lift to allow mixing of medium before lowering again and repeating measurement of OCR and ECAR. OCR is a surrogate for mitochondrial oxidative phosphorylation rate and ECAR is a surrogate for glycolytic rate and lactic acid production from cells.

The Seahorse XFe24 Analyzer also incorporates an integrated drug delivery system, whereby up to four compounds can be added sequentially to all wells at pre-designated intervals. Compounds are prepared prior to experimentation and pre-loaded into ports on the Seahorse Assay Cartridge. Sequence and timing of addition of compounds can be programmed using Seahorse XF Wave Desktop Software. During metabolic interrogation, pre-loaded compounds are then added into all wells at designated intervals, gentle mixing performed, and multiple OCR and ECAR measurements made over time.

For extracellular flux analysis the adherent MDM were transferred to the Seahorse XF24 Cell Culture Microplates (Agilent) on day 6 of differentiation. MDM were washed in ice

cold PBS and left at 4°C for 30 minutes. The wells were then aspirated with ice cold PBS and pelleted by centrifugation at 300 g for 5 minutes, resuspended in cRPMI and then counted with trypan blue. 100,000 viable cells in 100 µl were placed in each Seahorse Microplate well for 2 hours prior to addition of 400 µl of cRPMI. Cells were added in a reduced volume initially in order to maximise MDM adherence to the well.

2.4.2 Mitochondrial Stress Test

The Seahorse XF Cell Mito Stress Test Kit (Seahorse Biosciences, Agilent Technologies UK Ltd.) were used in experiments where stated. The compounds added to the wells during the course of the assay are; oligomycin, Carbonyl cyanide-4- (trifluoromethoxy) phenylhydrazone (FCCP) and combined rotenone with antimycin A. These compounds target different complexes of the electron transport chain (ETC) in the mitochondria. Oligomycin inhibits ATP synthase (Complex V of the ETC). This causes a reduction in oxygen consumption by preventing ATP synthesis via oxidative phosphorylation. The difference between baseline OCR and post-oligomycin OCR is the amount of oxygen used in ATP production.

FCCP acts as a mitochondrial uncoupler, which disrupts the mitochondrial membrane potential allowing uninhibited flow of electrons through the ETC. This leads to an increase of oxygen consumption until it reaches the maximum OCR capable of the cell. The post-FCCP OCR is referred to as the maximal OCR and the difference between baseline OCR and post-FCCP OCR reflects the Spare Respiratory Capacity (SRC) of the cells which is their ability to increase mitochondrial respiration when stressed.

Finally, Rotenone and Antimycin A directly inhibit Complex I and Complex III of the ETC, respectively, effectively shutting down all ETC activity and all mitochondrial oxygen consumption. Residual oxygen consumption, therefore, reflects Non-Mitochondrial Oxygen Consumption. A hypothetical example of real-time OCR measurements at baseline and following addition of inhibitors, indicating how data can be used to calculate the baseline OCR, ATP production, SRC, non-mitochondrial oxygen consumption and proton leak, is depicted in Figure 2.8.

Alternatively, changes in ECAR and OCR in real time in response to stimulation with Mtb or LPS or treatment with lactate were analysed. Equalised volumes of LPS, iH37Rv and lactate were loaded into ports on the Seahorse Assay Cartridge and added to the wells in the order and time points as indicated. ECAR and OCR were measured in real-time post the addition of each reagent. Additions of medium only were added through the ports as controls. The third reading of ECAR or OCR was considered the baseline reading to allow calculation of the % change from baseline in order to correct for differences in cell seeding density and donor variability.

2.4.3 Mitochondrial Stress Test Protocol

PBMC were isolated from buffy coats or from umbilical cord blood samples taken immediately following delivery. Adult or cord blood MDM were adherence purified for 7 days in 10% human serum. MDM were washed and detached from the plates by cooling and gently scraped, counted and re-seeded on Seahorse culture plates at least 24 hours prior to analysis in the Seahorse XFe24 Analyzer. The Seahorse Assay Cartridge

was hydrated using Seahorse Calibrant Solution and incubated at 37°C and 0% CO₂ overnight.

On the day of analysis, Seahorse medium (bicarbonate-free DMEM; Seahorse Biosciences, Agilent Technologies UK Ltd.) was supplemented with 2 mM glutamine and 10 mM glucose, warmed to 37°C and filtered through 0.2 µm sterile syringe filters (Corning, NY). Supernatants were removed from all wells of the Seahorse microplate, 500 µl of fresh Seahorse medium was applied to each well (including blank wells) and the microplate was incubated at 37°C and 0% CO₂ prior to analysis. Supernatants removed at this point (i.e. 24 hours post-treatment / infection) were retained and stored at -30°C for subsequent cytokines analysis.

Prior to analysis, compounds from the Mito Stress Test Kit were prepared in supplemented Seahorse medium under sterile conditions and loaded into designated ports on the Seahorse Assay Cartridge as above. Mitochondrial inhibitors were added to all wells in the order oligomycin, then FCCP, then rotenone/antimycin A, with three measurements of OCR and ECAR made following the addition of each compound.

After completion of the protocol, crystal violet (CV) assay was performed to normalise for differences in cell numbers between wells. Crystal violet binds to the DNA of the MDM and the amount of CV bound in each well is used as a correlate of cell seeding density. Medium was removed and 50 µl of 1% glutaraldehyde (Sigma-Aldrich) was added to each well for 15 minutes at room temperature. Glutaraldehyde was removed and wells washed twice with PBS. 50 µl 0.1% CV (Sigma-Aldrich) was added to each well for 30 minutes. CV was removed, the microplate was inverted and left to air dry for

several hours. 40 μ l 1% Triton X solution was added to each well and the plate was placed on a shaker for 15 minutes to allow full elution to occur. Contents of each well were transferred to a 96-well plate and absorbance was read at 595 nm using an spectrophotometer. The results of ECAR and OCR from each well were divided by the OD value generated by the spectrometer to normalise for differences in cell seeding density.

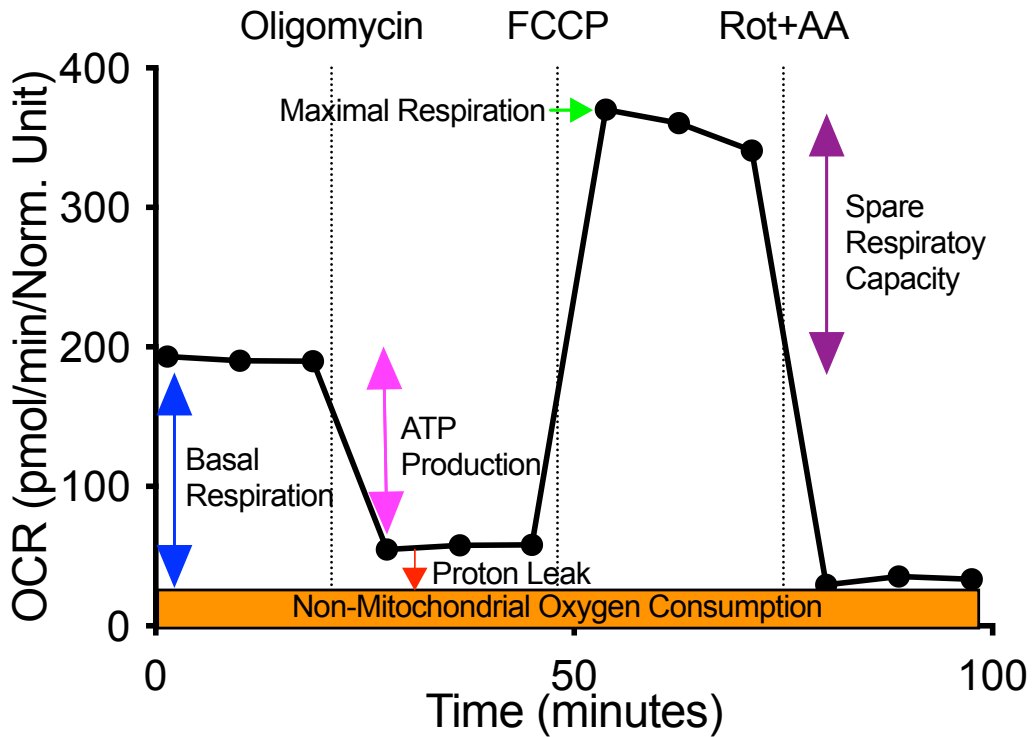


Figure 2.8 Calculation of Mitochondrial Stress Test parameters.

A hypothetical example of real-time OCR measurements at baseline and following the sequential addition of Oligomycin, FCCP and Rotenone/Actinomycin A for the Mitochondrial Stress Test. The graph indicates how data can be used to calculate the baseline OCR, ATP production, SRC, non-mitochondrial oxygen consumption and proton leak. Adapted from Agilent Seahorse XF Cell Mito Stress Test Kit User Guide.

2.5 MDM stimulation with LPS and polarisation with IFN- γ or IL-4

2.5.1 Lipopolysaccharide stimulation

The TLR4 agonist, lipopolysaccharide (LPS), is found in the outer membrane of Gram negative bacteria and was used as a positive control in all experiments. LPS (Sigma-Aldrich) was diluted in sterile PBS, aliquoted and stored at -30°C. On the day of the experiment the LPS aliquot was thawed and added to MDM at a final concentration of 100 ng/ml.

2.5.2 Polarisation of MDM with IFN- γ or IL-4

Human MDM were adherence purified from healthy adult donors for 6-8 days in the presence of human serum as described in section 2.1.4. MDM were treated with recombinant human IFN- γ (10 ng/ml; BioLegend) or IL-4 (10 ng/ml; BioLegend) for 24 hours prior to stimulation in order to induce polarisation towards the classically described M1 or M2 phenotype respectively. MDM were stimulated in the same medium containing recombinant cytokines and maintained for a further 24 hours in humidified incubators at 37°C and 5% CO₂ before analysis of surface markers by flow cytometry or cytokine production by ELISA. For IFN- γ or IL-4 experiments involving the Seahorse XFe24 Analyzer, the MDM were scraped and reseeded on Seahorse plates as described above (2.4.1). IFN- γ or IL-4 was added 24 hours prior to the live analysis of metabolic flux.

2.6 Analysis of Cytokine production

2.6.1 Measurement of cytokine production by Enzyme Linked Immuno Sorbant Assay (ELISA)

The concentrations of TNF in supernatants was quantified by ELISA (Affymetrix), as per manufacturer's instructions. Capture antibody diluted in coating buffer was applied to high-binding 96-well plates (Greiner Bio-one). Plates were incubated overnight at 4°C, capture antibody was removed and non-specific binding sites were blocked with appropriate blocking solution for 1 hour at room temperature. After blocking, plates were washed using PBS buffer supplemented with the detergent 0.5% Tween-20, dried and supernatant samples were loaded into wells in duplicates either neat or diluted 1 in 5 with assay diluent. A standard curve of serially diluted recombinant cytokine standard was also loaded onto the plates in triplicate, with the top working standard at 2000 pg/ml. Blank wells, containing assay diluents only, were included on each plate to allow the subtraction of background from each sample. Samples were incubated overnight at 4°C. After washing, biotinylated detection antibody was added to each well and incubated for 2 hours at room temperature. Plates were washed and horseradish-peroxidase conjugated to streptavidin was applied to wells for 30 minutes in the dark. The plate was thoroughly washed and the substrate tetramethylbenzidine was added. The enzyme-mediated colour reaction was protected from light while developing and stopped with the addition of 1M H₂SO₄. The optical density of the colour was determined by measuring the absorbance at 450 nm using a microtiter plate reader (BioTek, Epoch). Cytokine concentrations were calculated from the standard curve using Gen5[©] Data Analysis software (Biotek).

2.6.2 Measurement of cytokine production by Mesoscale Discovery System

Mesoscale Discovery (MSD; Meso Scale Discovery Multi-Array technology, Rockville, Maryland, United States) electrochemiluminescence detection system was also used to detect cytokine in supernatant. These are sandwich immunoassays performed on plates that are precoated with capture antibody on small spots in each well, allowing for the measurement of multiple cytokines simultaneously. Following addition of the supernatant to the wells, solution containing detection antibodies conjugated with electrochemiluminescent labels (MSD SULFO-TAG™) was added as per manufacturer's instructions. An MSD buffer that creates the appropriate chemical environment for electrochemiluminescence was added and an MSD instrument, was used to measure the intensity of emitted light following application of voltage. Variances in light intensity are used to calculate the quantitative measurement of each cytokine and was performed as per manufacturer's instructions.

2.7 Western Blotting

Western blot analyses was undertaken to characterise expression levels of LC3 and p62, proteins involved in autophagy. 24 hours post infection with Mtb (H37Ra), MDM were washed with PBS and lysed in lysis buffer (4:2:1:1 H₂O/10% SDS/glycerol/ 0.5 M Tris, pH 6.8 containing Dichlorodiphenyltrichloroethane (10%) with the addition of protease (ThermoFisher Scientific) and phosphatase inhibitor tablets (Sigma). MDM were then scraped and the protein lysate harvested and immediately heated to 95°C to inactivate proteases. Sodium dodecyl sulfate (SDS) sample buffer (100mM Tris-HCl (pH 6.8), 20% Glycerol (v/v), 4% SDS (w/v), 0.001% bromophenol blue (w/v) containing 143 mM dithiothreitol) was added to the lysates and equal volumes of the lysates (30 µl/lane)

were resolved by SDS polyacrylamide gel electrophoresis (SDS-PAGE) (10%) using the Bis-Tris Electrophoresis System (Bio-Ray). The transfer of separated proteins to polyvinylidene fluoride membrane was performed by wet blotting (Bio-Rad). The PVDF membranes were blocked with blocking buffer containing 5% milk (Marvel) in Tris-Buffered saline Tween (TBST) (0.1% (v/v) Tween-20 in TBS) at room temperature for 1 hour. Following blocking of the membrane, the immunoblot was incubated with purified mouse anti-human LC3 (1:1,000), purified rabbit anti-human p62 (1:1,000) or purified mouse anti-human Actin (1:1,000) at 4°C overnight in TBST (Nanotools). Followed by incubation with secondary goat anti-mouse or anti-rabbit IgG peroxidase conjugated antibody (Millipore) diluted in TBS for 1 hour at room temperature. The immunoblots were developed using enhanced chemiluminescence (ECL; MyBio) and visualised using a chemiluminescence imaging system (Fusion FX).

2.8 Optimisation of the use of exogenous sodium-lactate on human MDM

2.8.1 The effect of exogenous lactate on cell viability

In order to determine an appropriate concentration of sodium lactate to use *in vitro* on human MDM, optimisation experiments were carried out using a range of concentrations of lactate (from 0 to 100 mM). Cell viability was assessed to determine the optimal concentration of lactate to treat MDM with *in vitro*. Due to the limited supply of cord blood donors the following experiments were undertaken in adult MDM only. PBMC were isolated from buffy coats and MDM were adherence purified for 7 days in 10% human serum. The cells were treated with 0, 6.25, 12.5, 25, 50 and 100 mM of lactate three hours prior to infection with Mtb (iH37Rv or H37Ra), at an at an MOI of ~70% infectivity, 1-10 mycobacteria per cell, or stimulation with LPS (100 ng/ml). Cell

viability was assessed using a Propidium Iodide (PI) based cell exclusion assay. Cells were concomitantly stained with 5 µg/ml PI, 20 µg/ml Hoechst 33342 and 50 µg/ml Hoechst 33258 (all Sigma Aldrich) for 30 minutes at room temperature. Total cell numbers were detected via Hoechst staining of nuclei (461 nm) and dying/dead cells were identified via positivity for PI staining (617 nm), using the Cytell Cell Imaging System and software (GE Healthcare). At 24 hours (Figure 2.9 A), 48 hours (Figure 2.9 B) and 120 hours (Figure 2.9 C) post stimulation, the total number of live cells was determined using the Cytell Cell Imaging System.

Lactate at 25 mM was the highest concentration that did not induce statistically significant cell death at any time point or with any stimulation and, as this concentration was physiologically relevant, it was used in subsequent experiments. To control for potential osmotic stress and any potential metabolic effects caused by the presence of the sodium ion, sodium chloride was used at an equimolar concentration as a control and measured viability at 24 hours (Figure 2.10 A), 48 hours (Figure 2.10 B) and 120 hours (Figure 2.10 C) post stimulation.

2.8.2 The effect of sodium-lactate on pH

There has been contradictory evidence over the requirement for lactate to be acidified into its conjugate acid, lactic acid, in order for it to alter immune function^{211–214}. Sodium-L-lactate did not affect the pH of the medium at any concentration between 6.25 and 100 mM when tested using a pH meter (Figure 2.11).

2.8.3 The effect of sodium-lactate on the phagocytic capacity of human MDM

In order to ascertain if lactate altered the uptake of Mtb by human MDM, a phagocytosis assay was undertaken. Adult MDM were adherence purified with cRPMI for 6-8 days in an 8 well labtek. The cells were treated with 0, 6.25, 12.5 and 25 mM of lactate three hours prior to infection with Mtb, iH37Rv (Figure 2.12 A) or H37Ra (Figure 2.12 B), at an MOI of approximately 80% infectivity, 1-20 mycobacteria per cell. 3 hours after infection the cells were washed to remove extracellular mycobacteria and then fixed with 2% PFA. Fixed MDM were stained with Hoechst and Auramine O stain. Fluorescent microscopy was used to count the number of infected cells and the number of mycobacteria per cell for 3 separate donors. Representative graphs show the number of bacteria per cell (Figure 2.12). No significant differences in uptake of Mtb with any of the concentrations of lactate were observed.

2.8.4 Determining the effects of sodium-lactate on human MDM

In order to determine the effect of lactate on MDM responses, 25mM of lactate was added 3 hours prior to stimulation with Mtb (iH37Rv MOI~70%) or LPS (100ng/ml). Analysis of cell surface markers and of cytokine production were performed at 24 hours as described above (2.3, 2.6.2).

CFU experiments were carried out as described above (2.2.6) with 0, 6.25, 12.5 and 25 mM of lactate added to the MDM 3 hours prior to infection with Mtb (H37Ra) at an MOI of 30-40%, 1-5 mycobacteria per cell. Cells were lysed in sterile 0.1% Triton-X at 3, 48 and 120 hours post infection. 7H9 Middlebrook Broth supplemented with ADC was used to serially dilute the lysates and they were plated on 7H10 Middlebrook Agar

supplemented with OADC in triplicate. Agar plates were incubated at 37°C for 21 days before CFU were counted.

Mycobacterial growth in axenic conditions was assessed using a BacT Analyser (Biomérieux). Mtb (H37Ra) was added to 1 ml of Middlebrook 7H9 Broth (+ADC) with 0, 6.25, 12.5 and 25 mM of lactate. 20% dilution with 0 mM lactate was added immediately to a BacT Mycobacterial Culture bottle and placed in the BacT Analyser to act as a control. After three days of mycobacterial propagation, 20% dilution of the remaining wells were added to BacT bottles. Time to positivity, as measured by the BacT Analyser, was recorded for each condition.

Analysis of metabolic flux induced by lactate was measured in the Seahorse Xfe24 Analyzer as described above (**2.4.1**). Lactate (25mM) was added via the Seahorse ports to observe the impact on ECAR and OCR.

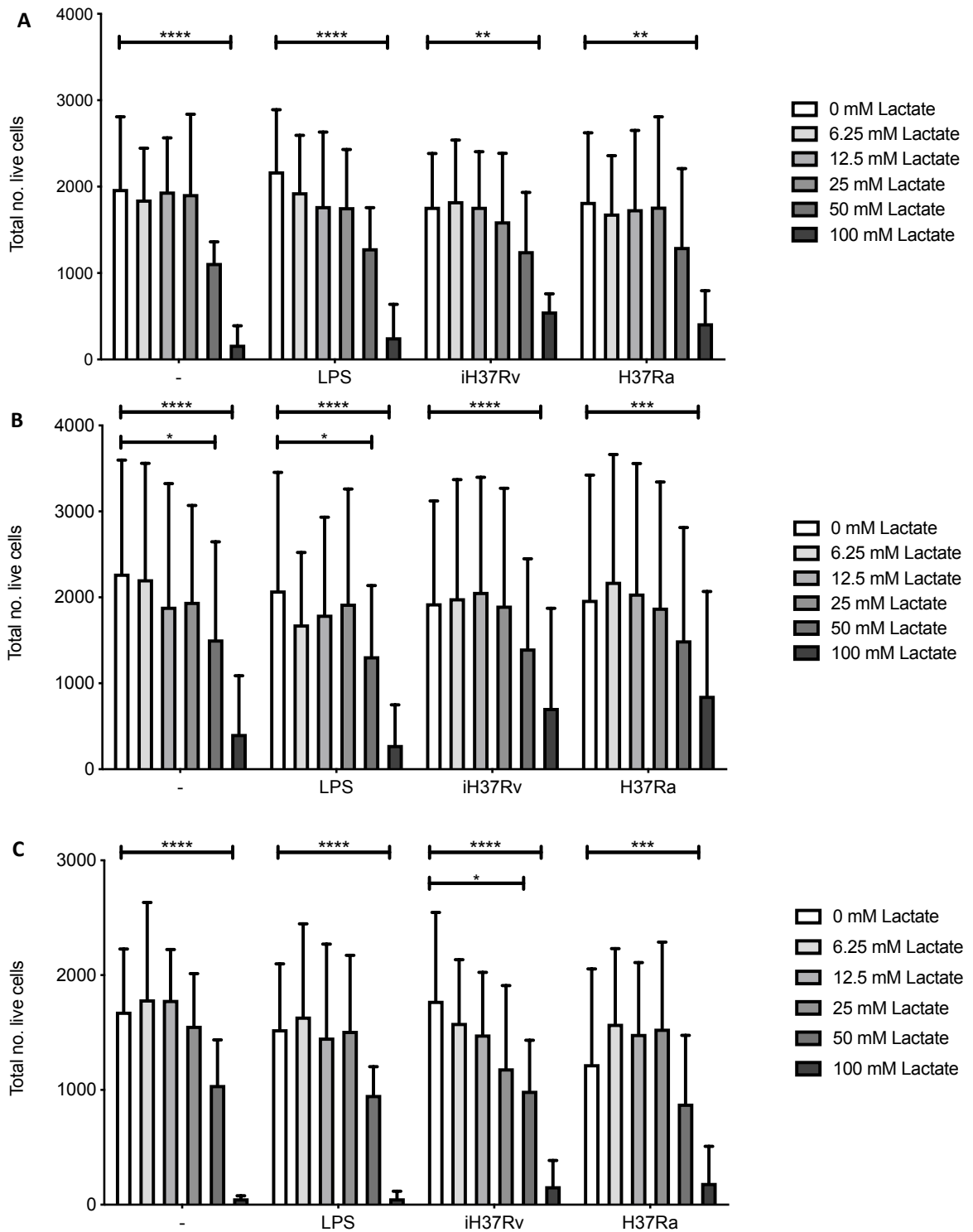


Figure 2.9 MDM viability after the addition of lactate.

PBMC were isolated from buffy coats and MDM were adherence purified for 7 days in 10% human serum. The cells were treated with 0, 6.25, 12.5, 25, 50 and 100 mM of lactate three hours prior to infection with Mtb (iH37Rv or H37Ra), at an MOI of approximately 70% infectivity, 1-10 mycobacteria per cell, or stimulation with LPS (100 ng/ml). At 24 hours (A), 48 hours (B) and 120 hours (C) cells were stained with Hoechst and PI and total number of live cells was determined using the Cytell Cell Imaging System ($n=3 \pm SD$). Statistical significance was determined using two-way ANOVA with Tukey multiple comparisons test; **** $P < 0.0001$, *** $P < 0.001$, ** $P < 0.01$, * $P < 0.05$.

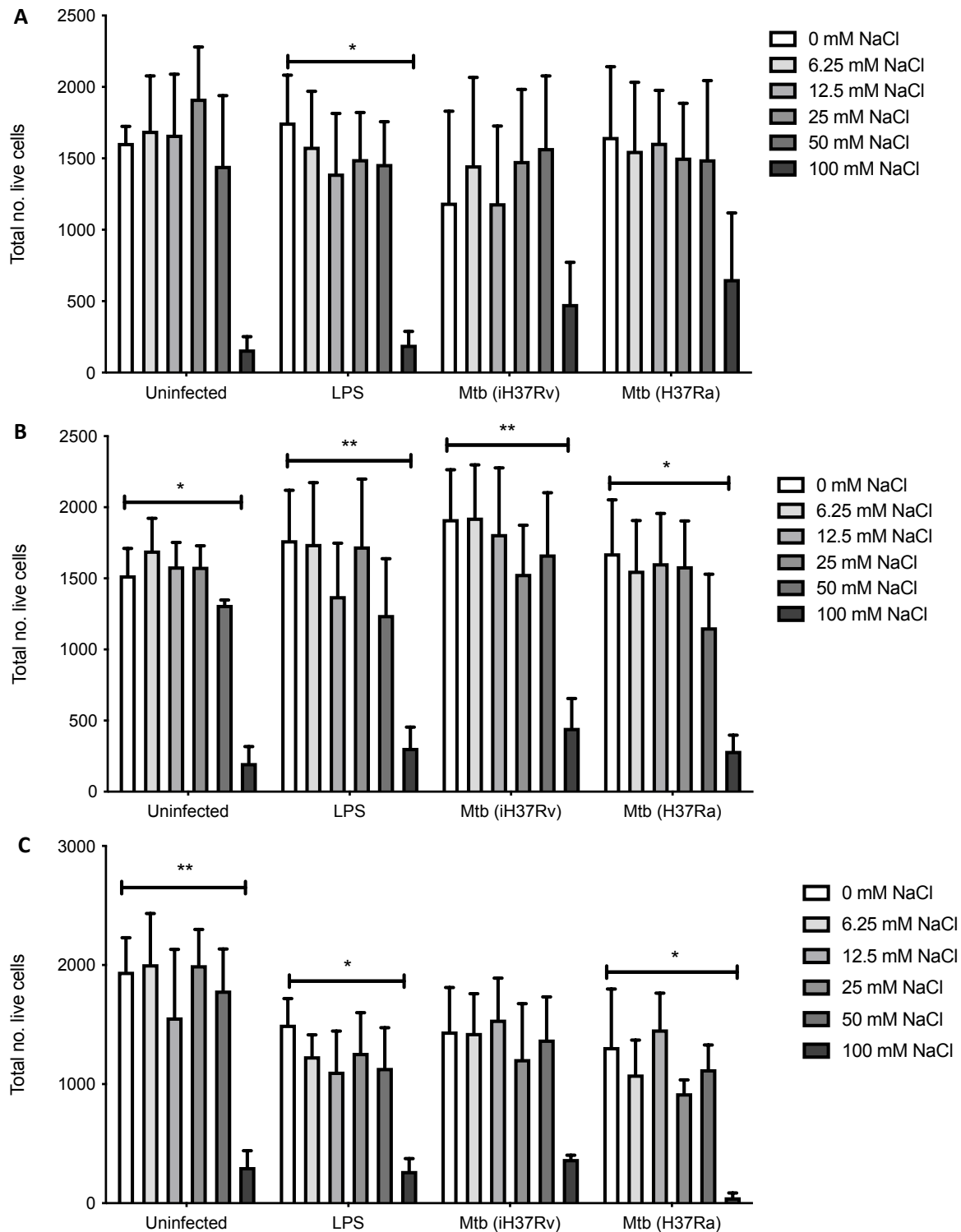


Figure 2.10 MDM viability after the addition of NaCl.

PBMC were isolated from buffy coats and MDM were adherence purified for 7 days in 10% human serum. The cells were treated with 0, 6.25, 12.5, 25, 50 and 100 mM of NaCl three hours prior to infection with Mtb (iH37Rv or H37Ra), at an MOI of approximately 70% infectivity, 1-10 mycobacteria per cell, or stimulation with LPS (100 ng/ml). At 24 hours (A), 48 hours (B) and 120 hours (C) cells were stained with Hoechst and PI and total number of live cells was determined using the Cytell Cell Imaging System ($n=3 \pm SD$). Statistical significance was determined using two-way ANOVA with Tukey multiple comparisons test; **** $P < 0.0001$, *** $P < 0.001$, ** $P < 0.01$, * $P < 0.05$.

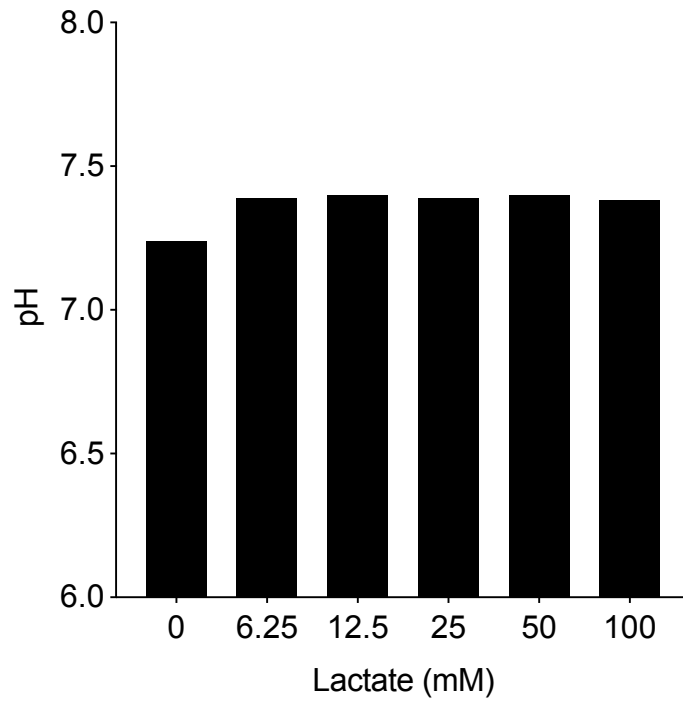


Figure 2.11 Sodium lactate does not alter pH.

Sodium-L-lactate was dissolved in RPMI and serially diluted to the following range of concentrations; 0, 6.25, 12.5, 25, 50 and 100 mM of Na-L-lactate. The pH was measured using a pH meter.

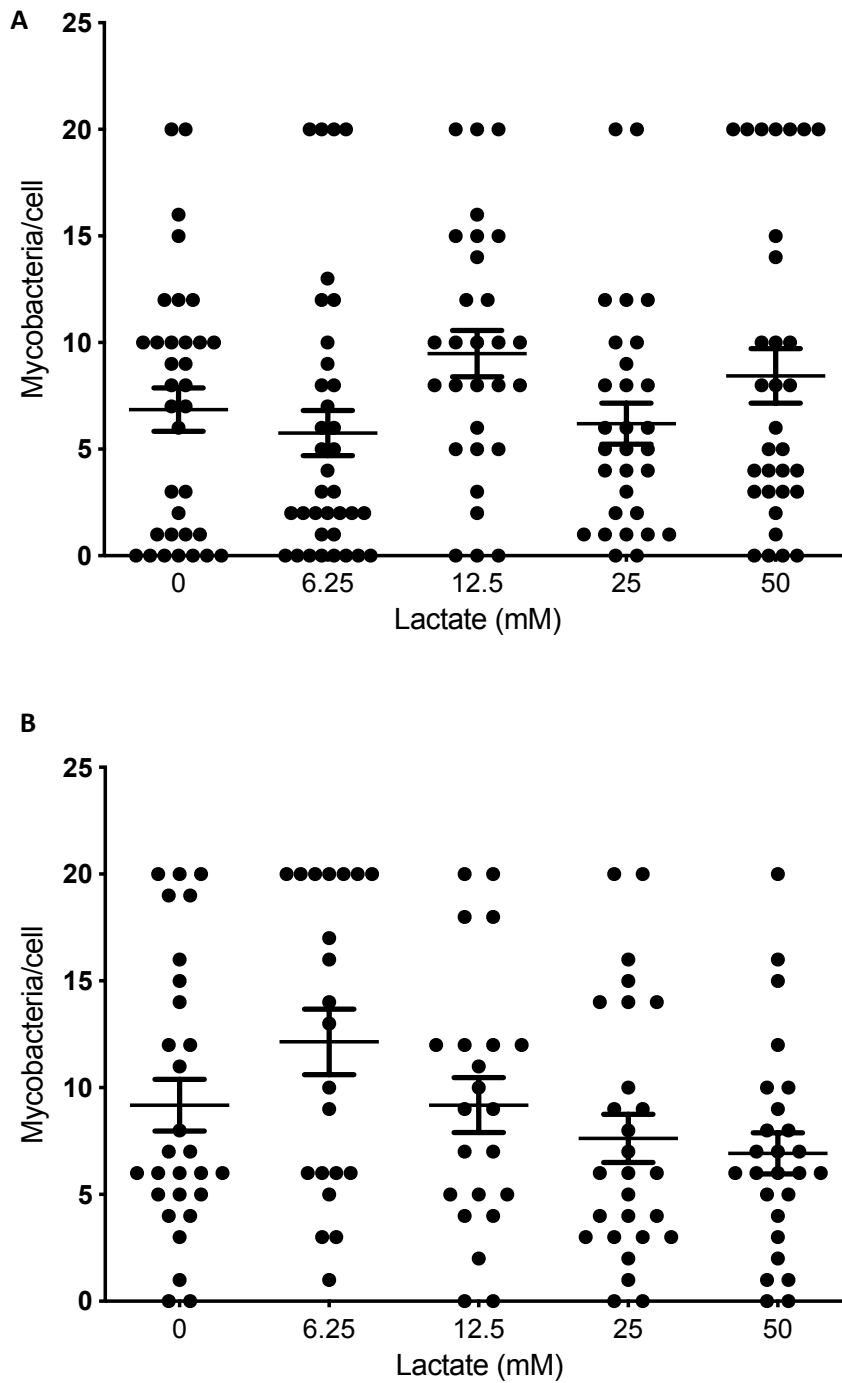


Figure 2.12 Lactate does not alter MDM phagocytic ability.

PBMC were isolated from buffy coats and MDM were adherence purified for 7 days in 10% human serum in an 8 well labtek. MDM were treated with 0, 6.25, 12.5 and 25 mM of lactate three hours prior to infection with Mtb, **A** iH37Rv and **B** H37Ra, at an MOI of 70%, 1-20 mycobacteria per cell. 3 hours after infection the cells were washed to removed extracellular mycobacteria and then fixed with 2% PFA. Fixed MDM were stained with Hoescht and auramine O stain. Fluorescent microscopy was used to count the number of infected cells and the number of mycobacteria per cell. Data shown is one representative donor. Each dot represents one cell, horizontal lines represent the mean and error bars indicate \pm SEM. Statistical significance was determined using one-way ANOVA, Bonferroni's multiple comparison test.

2.9 Statistical analysis

Statistically significant differences between two groups were determined by paired and unpaired Student's two-tailed t-tests, as appropriate. Statistically significant differences between 3 or more groups were determined by 1-way ANOVA (with Bonferroni/Sidak/Tukey post-tests, as appropriate). Statistically significant differences between 2 or more groups, each containing more than 1 variable were determined by 2-way ANOVA (with Bonferroni/Sidak/Tukey post-tests, as appropriate). All graphs were generated and statistical analyses were performed using GraphPad Prism software v 9.1.0 (GraphPad Inc) and values of $P < 0.05$ were considered significant and denoted with an asterisk. When both Student's t-test and ANOVA was undertaken and illustrated on the same graph the t-test was denoted with a #.

Chapter 3

3.1 The Warburg effect occurs early in adult but not cord blood macrophages

3.1.1 Introduction

Murine macrophages increase glycolysis and decrease oxidative phosphorylation 24 hours post lipopolysaccharide (LPS) stimulation^{187,215}. This altered metabolism in activated murine macrophages is akin to the altered metabolic function first observed in tumour cells by Otto van Warburg¹⁸⁴ and is thus, termed the 'Warburg effect'. More recent findings linking changes in the metabolic function of immune cells to their ability to mount an effective immune response^{181,216,217}, has led to development of a field of research known as immunometabolism. The majority of work published to date in macrophages has been carried out in murine BMDM, which have been crucial to the detailed mechanistic understanding of these biochemical processes. However, there is a paucity of immunometabolic data generated in primary human macrophages¹⁹⁶. Furthermore, there are seemingly contradictory findings between human and murine macrophage research, with more research required to fully establish the metabolic features of activated human immune cells^{196,197}.

A study directly comparing murine BMDM and human MDM replicated the established increase in murine extracellular acidification rate (ECAR) and decrease in oxygen consumption rate (OCR) in response to LPS¹⁹⁷. In contrast, human MDM had reduced ECAR and no change in OCR 16 hours after LPS stimulation¹⁹⁷. It is difficult to draw accurate conclusions from these findings that illustrate stark differences in human and mouse immunometabolism; however, these differences are not unexpected given the

striking disparities between human and murine susceptibility to LPS toxicity²¹⁸. Other studies examining itaconate, an immunomodulatory derivative of a tricarboxylic acid cycle intermediate, which increases after macrophage activation, found that the peak in human MDM occurred earlier than in murine BMDM^{219,220}. Thus, the kinetics of metabolic flux may occur early in human macrophages responding to stimulation.

These disparities may hamper efforts to translate this knowledge into effective therapeutic drugs. Adding further to this complexity, is the changing function of human immune responses over a lifetime. The role of metabolism in immune defects seen at the extremes of age is an area of ongoing investigation^{221,222,223}. Newborn babies are more susceptible than adults to a variety of bacterial infections, including from gram negative organisms (containing LPS) and from intracellular pathogens such as Mtb^{224,225}, the causative agent of TB. The Keane laboratory has previously shown that adult human macrophages shift their metabolic function toward aerobic glycolysis 24 hours after Mtb infection^{188,226,227}, a finding replicated in other centres^{228,229}. Furthermore, research examining monocytes or MDM from umbilical cord blood have shown them to produce less pro-inflammatory TNF in relation to adult comparators following stimulation with LPS.^{179,230,231} There is a lack of published data on metabolic activation in cord blood MDM, with only one study showing diminished glycolysis in polarised MDM²⁰². In order to exploit the therapeutic potential of manipulating metabolic pathways, basic human cellular research is required to build on the growing literature generated from murine studies in immunometabolism.

Differences in adult and cord blood MDM have not been inconsistently reproduced, in part because of the numerous methods used to differentiate human macrophages from

monocytes^{173,232,233}. In this thesis the experimental model used monocytes that were differentiated with adherence purification in 10% human serum which is a well-established method in adult monocytes, but has rarely been used in cord blood^{26,188,226,227,234,235}. In order to ensure that this method resulted in similar macrophage differentiation from adult or cord blood, the morphology and purity were assessed using light microscopy and flow cytometry, respectively (**2.1.5, 2.3**). Having established the validity of this model of macrophage differentiation in adult and cord blood MDM, the knowledge gap in human immunometabolic response to stimulation with Mtb or LPS was explored.

3.1.2 Hypothesis and Aims

Hypothesis:

It was hypothesised that the difference in clinical phenotype seen between adults and newborns following exposure to Mtb is a result of underlying differences in macrophage metabolic and functional responses and that the kinetics of human macrophage immunometabolic responses to stimulation differ from the well-established murine pattern, occurring at an earlier timepoint.

Aims:

Directly compare the immunometabolic profile of adult and cord blood macrophages in response to stimulation with Mtb or LPS using the Seahorse XFe Analyzer technology.

- Elucidate the differential kinetics of immunometabolic changes in activated human macrophages by examining the response to stimulation in real time and 24 hours post activation .

- Examine the phenotypic differences of macrophages differentiated from adult and cord blood and stimulated with Mtb or LPS using flow cytometry.
- Examine the differential ability of adult or cord blood macrophages to produce key cytokines following stimulation with Mtb or LPS, using ultra-sensitive electrochemiluminescence MescoScaleDiscovery (MSD) Multi array analysis.

3.2 Results

3.2.1 The Warburg effect occurs early in response to stimulation with Mtb or LPS in human adult MDM

In order to examine if the Warburg effect (i.e., increased glycolysis and decreased oxidative phosphorylation) occurs in activated human macrophages, the kinetics of the metabolic response of human MDM to stimulation with LPS or Mtb in real time were analysed. Since Mtb has been shown to subvert macrophage metabolism^{235,236}, irradiated H37Rv (iH37Rv) strain of Mtb was used to elucidate the host response. This ensures that the host metabolic response is unperturbed by interference from live, growing Mtb. PBMC were isolated from buffy coats or from umbilical cord blood samples taken immediately following delivery. Adult or cord blood MDM were adherence purified for 7 days in 10% human serum. MDM were washed and detached from the plates by cooling and gently scraped, counted and re-seeded on Seahorse culture plates prior to analysis. Using the injection ports of the Seahorse XFe24 Analyzer, either Mtb (iH37Rv; MOI 1-10) or LPS (100 ng/ml) was added to wells containing differentiated human adult or cord blood MDM and the extracellular

acidification rate (ECAR) and the oxygen consumption rate (OCR), surrogates for glycolysis and oxidative phosphorylation, respectively, were evaluated.

3.2.1a Mtb and LPS cause a rapid increase in glycolysis in adult and cord blood MDM

Baseline measurements of ECAR were recorded for 30 minutes prior to the injection of medium (unstimulated, denoted as “unstim”), Mtb or LPS via the Seahorse Analyzer ports. The data are expressed as both the raw values and the % change from the third baseline reading in order to normalise for differences in human variability and for technical variability in cell seeding density on the Seahorse culture plate. For both the adult (Figure 3.1 A) and cord blood MDM (Figure 3.1 B), the time course graphs show a rapid increase in ECAR following stimulation with Mtb or LPS compared with the unstimulated control. The elevated ECAR plateaus and persists for the duration of the analysed time period. The % change in ECAR follows the same pattern, with a rapid increase following stimulation with Mtb or LPS in both adult (Figure 3.1 C) and cord blood MDM (Figure 3.1 D).

Analysis of the data for n=7 independent adult and n=6 cord blood MDM independent experiments was undertaken at the indicated timepoint on the time-course graph, approximately 150 minutes (2.5 hours) post stimulation (Figure 3.2). This timepoint was when the ECAR and OCR were consistently furthest from baseline. A statistically significant increase in ECAR in both the raw value and % change from baseline was seen in the adult MDM stimulated with Mtb (Figure 3.2 A, $P < 0.01$) or LPS (Figure 3.2 B, $P < 0.01$). Cord blood MDM stimulated with Mtb had a significant increase in the ECAR (Figure 3.2 C, left, $P < 0.01$) and the % change in ECAR (Figure 3.2 C, right, $P < 0.05$). LPS

stimulation also induced a significant increase in the ECAR (Figure 3.2 D, left, $P < 0.05$) and % change in ECAR (Figure 3.2 D, right, $P < 0.01$) in cord blood MDM.

3.2.1b OCR significantly decreases in adult but not cord blood MDM following Mtb or LPS stimulation.

Baseline measurements of OCR were also recorded for 30 minutes prior to the injection of medium (unstimulated, denoted as “unstim”), Mtb or LPS. The data are expressed as both the raw values and the % change from the third baseline reading in order to normalise for differences in human variability and for technical variability in cell seeding density on the Seahorse culture plate. For the adult MDM, the time course graphs show a rapid decrease in OCR stimulation with Mtb or LPS compared with the unstimulated control (Figure 3.3 A). The OCR returns to the baseline rate at approximately 300 minutes. In contrast to the adult MDM however, there is only a minor flux in the OCR in the cord blood MDM after stimulation with Mtb or LPS (Figure 3.3 B). These findings are replicated in the % change in OCR from baseline for the adult (Figure 3.3 C) and cord blood (Figure 3.3 D) MDM after Mtb or LPS stimulation.

Data was extracted at the analysis timepoint indicated on the time-course graph, approximately 150 minutes (2.5 hours) post stimulation (Figure 3.4). For the adult MDM ($n=7$), the OCR (Figure 3.4 A, left $P < 0.05$) and % change in OCR (Figure 3.4 A, right $P < 0.01$) were significantly decreased by stimulation with Mtb. The decline in OCR seen in adult MDM after LPS stimulation (Figure 3.4 B, left) was not statistically significant, however, when the values were normalised to % change in OCR this decrease was statistically significantly different compared with baseline (Figure 3.4 B, right $P < 0.01$).

No statistically significant changes were seen in the OCR or the % change in OCR for cord blood MDM (n=6) stimulated with Mtb (Figure 3.4 C, left) or LPS (Figure 3.4 D, right).

3.2.1c ECAR/OCR ratio increases in both adult and cord blood MDM after stimulation with Mtb or LPS.

The ECAR/OCR ratio is a measure of cellular energetics which indicates cellular preference for glycolysis versus oxidative phosphorylation and it was calculated at the analysis time point, 2.5 hours post stimulation. In keeping with the above findings of a marked increase in glycolysis in both adult and cord blood MDM following Mtb or LPS stimulation, a statistically significant increase in the ECAR/OCR ratio was observed at the analysed timepoint for both Mtb and LPS stimulated adult (Figure 3.5 A, $P < 0.01$ for both Mtb and LPS) and cord blood (Figure 3.5 B, $P < 0.01$ for both Mtb and LPS).

3.2.1d Comparison of metabolic changes in adult and cord blood MDM 2.5 hours after stimulation with Mtb or LPS.

In order to determine the differential ability of adult and cord blood MDM to undergo early metabolic alterations in response to stimulation, the % change in ECAR or OCR or the ECAR/OCR ratios were directly compared. The data indicates that adult and cord blood MDM exhibit similar changes in ECAR upon stimulation with Mtb (Figure 3.6 A, left) or LPS (Figure 3.6 B, left). However, adult MDM have significantly lower OCR compared with cord blood MDM stimulated with Mtb (Figure 3.6 A middle; $P < 0.05$) or LPS (Figure 3.6 B middle; $P < 0.05$).

Directly comparing the ECAR/OCR ratios, cord blood MDM stimulated with Mtb exhibit a significantly reduced ECAR/OCR ratio compared with adult MDM at this early timepoint (Figure 3.6 A, right $P < 0.05$). The ECAR/OCR ratios for MDM stimulated with LPS are not significantly different between the adult and cord blood MDM (Figure 3.6 B, right).

Taken together, these data demonstrate that the Warburg effect occurs in human adult MDM but not in cord blood MDM, and that this change occurs early in response to stimulation and is short lived. Cord blood MDM undergo a shift towards glycolysis but do not concomitantly reduce oxidative phosphorylation, in the way that their adult counterparts do. Although cord blood MDM exhibit significantly increased ECAR/OCR ratios in response to Mtb or LPS, the ECAR/OCR ratio is significantly reduced in the cord blood MDM compared with the adult MDM in response to Mtb.

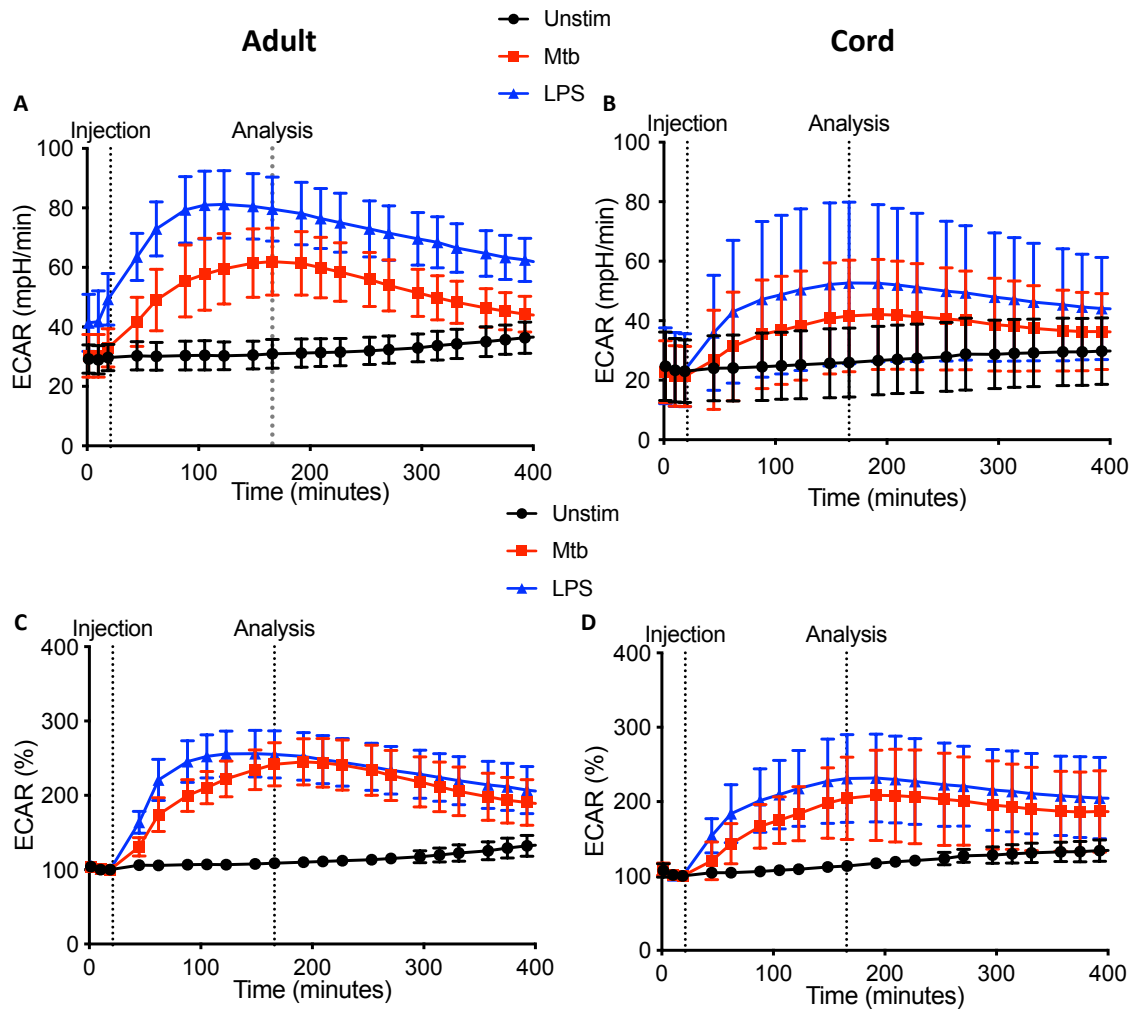


Figure 3.1 ECAR rises rapidly in adult and cord blood MDM after Mtb or LPS stimulation.

PBMC were isolated from buffy coats or from umbilical cord blood samples taken immediately following delivery. Adult or cord blood MDM were adherence purified for 7 days in 10% human serum. MDM were washed and detached from the plates by cooling and gently scraped, counted and re-seeded on Seahorse culture plates prior to analysis in the Seahorse XFe24 Analyzer. Mtb (iH37Rv; MOI 1-10) or LPS (100 ng/ml) were added to the cells in the Seahorse Analyzer. The Extracellular Acidification Rates (ECAR) was recorded approximately every 20 minutes. Correction for small variations in cell density was achieved by % comparison to the basal ECAR. After 30 minutes, the Seahorse Analyzer injected medium (unstim), Mtb or LPS into assigned wells at the point on the graph labelled 'injection'. The ECAR readings were then continually sampled in real time. The time-course graphs illustrate the ECAR and % change in ECAR from baseline of adult MDM (n=7 A,C) or cord blood MDM (n=6 B, D) in real time in response to stimulation with Mtb or LPS.

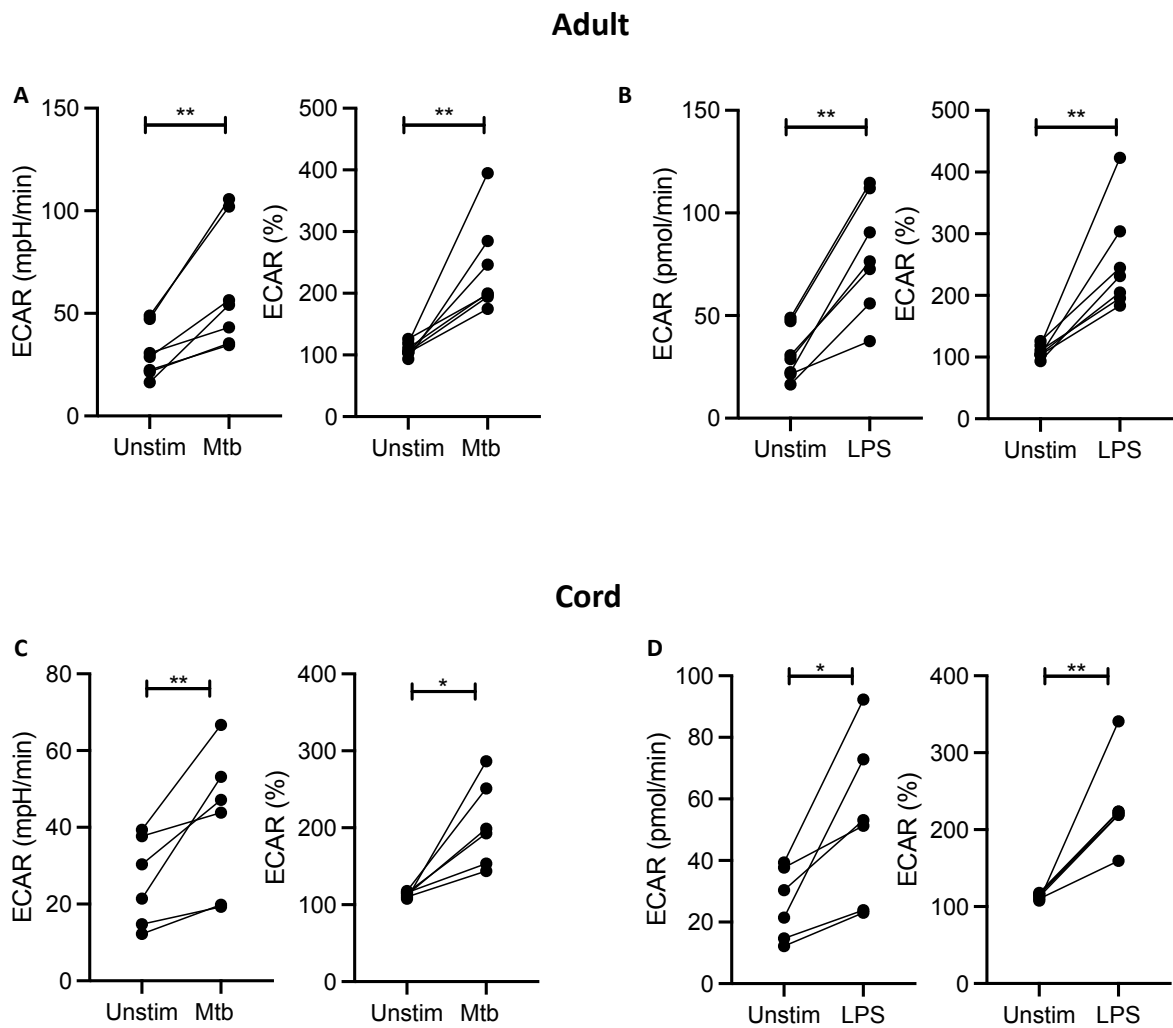


Figure 3.2 Analysis of ECAR in adult and cord blood MDM after Mtb or LPS stimulation. PBMC were isolated from buffy coats or from umbilical cord blood samples taken immediately following delivery. Adult or cord blood MDM were adherence purified for 7 days in 10% human serum. MDM were washed and detached from the plates by cooling and gently scraped, counted and re-seeded on Seahorse culture plates prior to analysis in the Seahorse XFe24 Analyzer. Mtb (iH37Rv; MOI 1-10) or LPS (100 ng/ml) were added to the cells in the Seahorse Analyzer. Correction for small variations in cell density was achieved by % comparison to the basal ECAR. After 30 minutes, the Seahorse Analyzer injected medium (unstim), Mtb or LPS into assigned wells. At the time point indicated in Figure 3.1, 150 minutes after stimulation, the ECAR and % change in ECAR from baseline was analysed for Mtb and LPS stimulated cells for the adult (n=7 A,B) and cord blood MDM (n=6 C,D). Statistically significant differences were determined using a paired Student's t test; * P<0.05, ** P< 0.01.

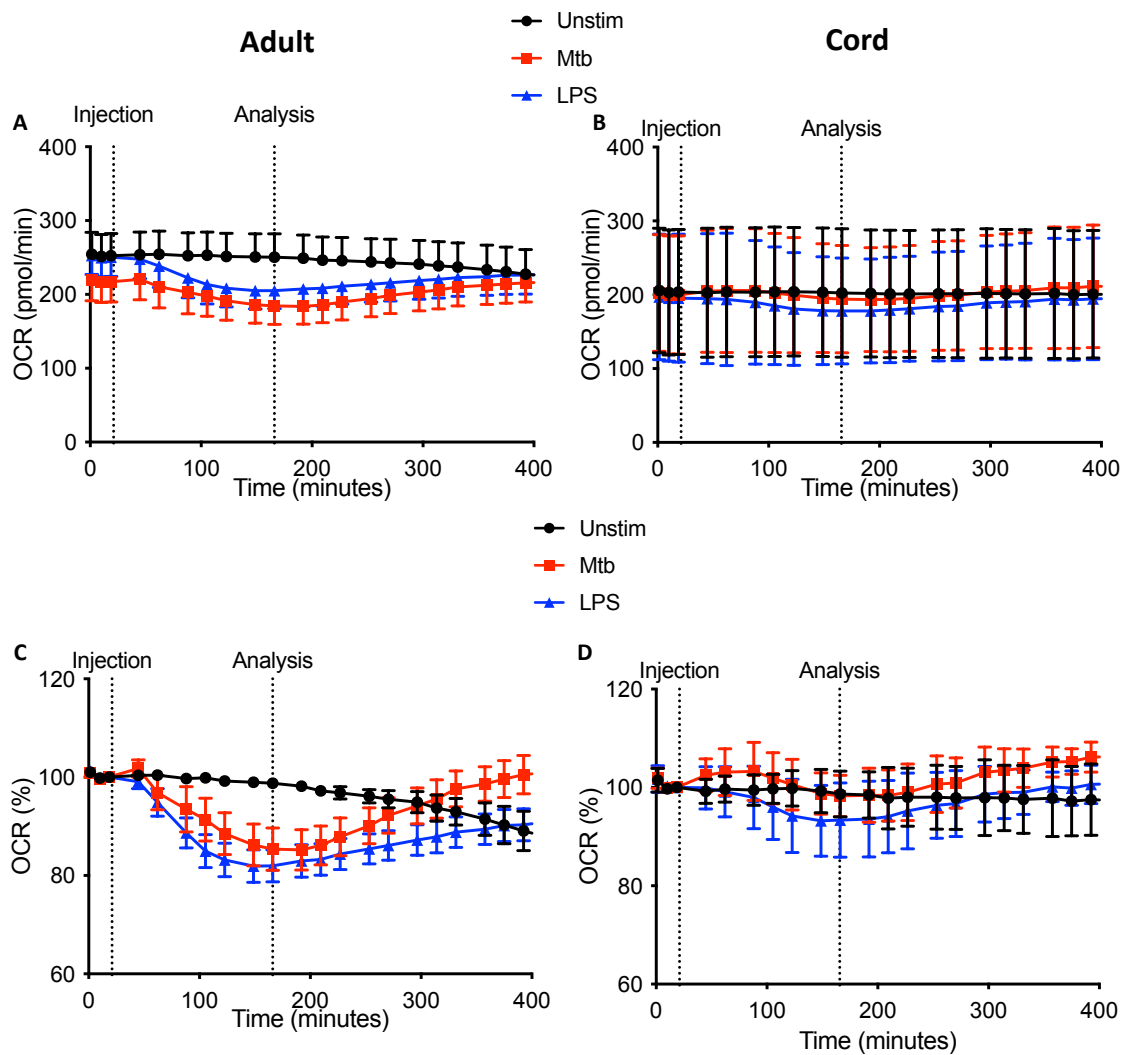


Figure 3.3 OCR falls rapidly in adult but not cord blood MDM after Mtb or LPS stimulation.

PBMC were isolated from buffy coats or from umbilical cord blood samples taken immediately following delivery. Adult or cord blood MDM were adherence purified for 7 days in 10% human serum. MDM were washed and detached from the plates by cooling and gently scraped, counted and re-seeded on Seahorse culture plates prior to analysis in the Seahorse XFe24 Analyzer. Mtb (iH37Rv; MOI 1-10) or LPS (100 ng/ml) were added to the cells in the Seahorse Analyzer. The Oxygen Consumption Rate (OCR) was recorded approximately every 20 minutes. Correction for small variations in cell density was achieved by % comparison to the basal ECAR. After 30 minutes, the Seahorse Analyzer injected medium (unstim), Mtb or LPS into assigned wells. The OCR readings were then continually sampled in real time. The time-course graphs illustrate the OCR and the % change in OCR from baseline of adult MDM (n=7 A,C) or cord blood MDM (n=6 B,D) in real time in response to stimulation with Mtb or LPS.

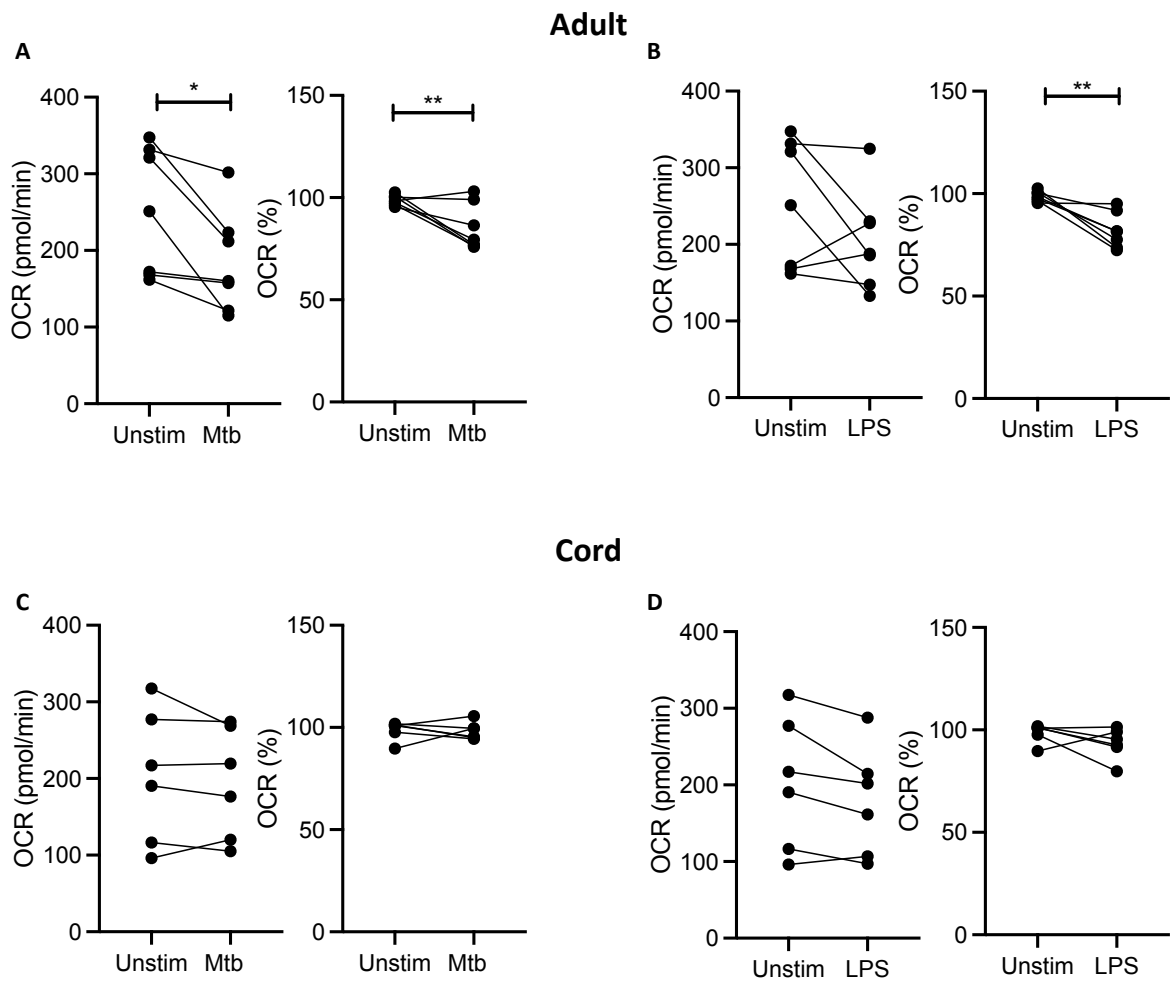


Figure 3.4 Analysis of OCR in adult and cord blood MDM after Mtb or LPS stimulation. PBMC were isolated from buffy coats or from umbilical cord blood samples taken immediately following delivery. Adult or cord blood MDM were adherence purified for 7 days in 10% human serum. MDM were washed and detached from the plates by cooling and gently scraped, counted and re-seeded on Seahorse culture plates prior to analysis in the Seahorse XFe24 Analyzer. Mtb (iH37Rv; MOI 1-10) or LPS (100 ng/ml) were added to the cells in the Seahorse Analyzer. Correction for small variations in cell density was achieved by % comparison to the basal OCR. After 30 minutes, the Seahorse Analyzer injected medium (unstim), Mtb or LPS into assigned wells. At the time point indicated in Figure 3.3, 150 minutes after stimulation, the OCR was analysed for Mtb and LPS stimulated cells for the adult (n=7 A,C) and cord blood MDM (n=6 B,D). Statistically significant differences were determined using a paired Student's t test; * P<0.05, ** P< 0.01.

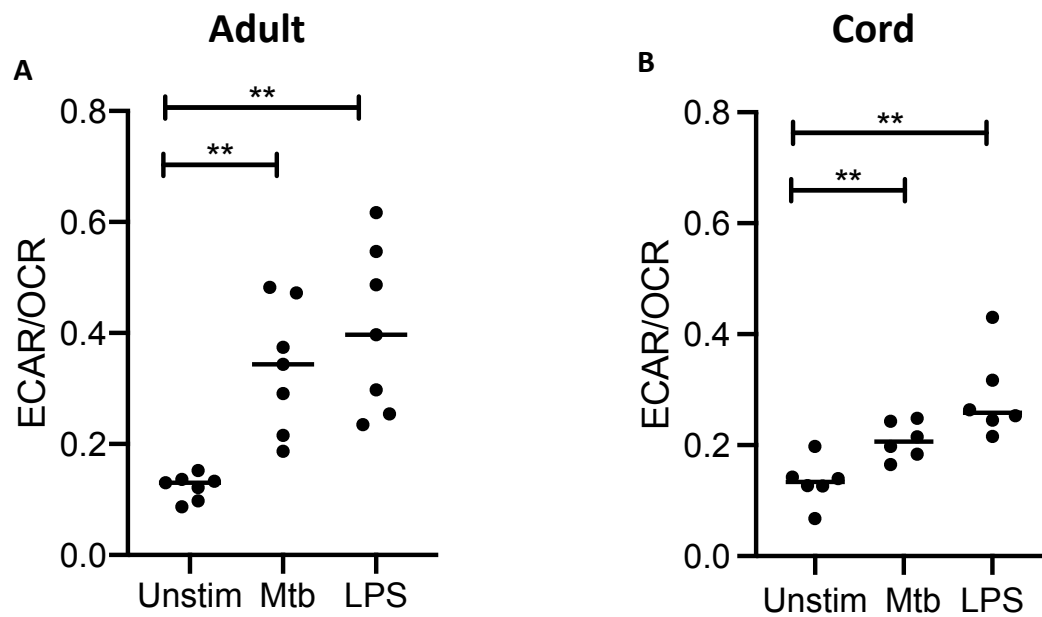


Figure 3.5 ECAR/OCR ratio for adult and cord blood MDM after Mtb or LPS stimulation.

PBMC were isolated from buffy coats or from umbilical cord blood samples taken immediately following delivery. Adult or cord blood MDM were adherence purified for 7 days in 10% human serum. MDM were washed and detached from the plates by cooling and gently scraped, counted and re-seeded on Seahorse culture plates prior to analysis in the Seahorse XFe24 Analyzer. Mtb (iH37Rv; MOI 1-10) or LPS (100 ng/ml) were added to the cells in the Seahorse Analyzer. After 30 minutes, the Seahorse Analyzer injected medium (unstim), Mtb or LPS into assigned wells. At the time point indicated in Figure 3.1, 150 minutes after stimulation, the ECAR/OCR ratio was calculated for Mtb or LPS stimulated cells for the adult (A, n=7) and cord blood MDM (B, n=6). Statistically significant differences were determined using a paired Student's t test; * P<0.05, ** P< 0.01.

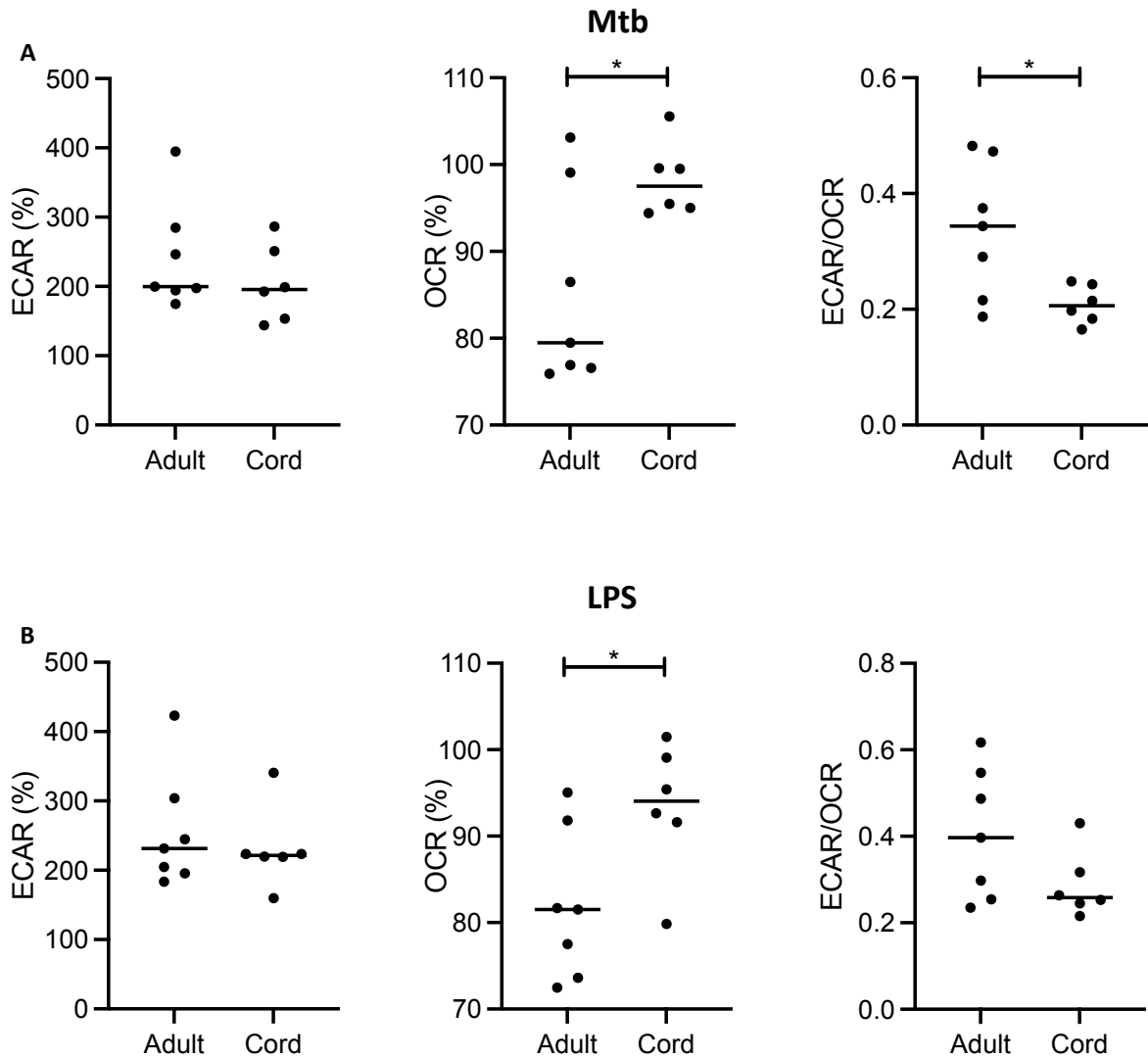


Figure 3.6 Comparison between adult and cord blood MDM responses after Mtb or LPS stimulation.

PBMC were isolated from buffy coats or from umbilical cord blood samples taken immediately following delivery. Adult or cord blood MDM were adherence purified for 7 days in 10% human serum. MDM were washed and detached from the plates by cooling and gently scraped, counted and re-seeded on Seahorse culture plates prior to analysis in the Seahorse XFe24 Analyzer. Mtb (iH37Rv; MOI 1-10) or LPS (100 ng/ml) were added to the cells in the Seahorse Analyzer. After 30 minutes, the Seahorse Analyzer injected medium (unstim), Mtb or LPS into assigned wells. At the time point indicated, 150 minutes after stimulation, the % change in ECAR and OCR and ECAR/OCR ratio was calculated for Mtb (A) and LPS (B) stimulated cells for the adult (n=7) and cord blood MDM (n=6) and the differences between adult and cord responses were compared. Statistically significant differences were determined using an unpaired Student's t test; * P<0.05.

3.2.2 Human MDM show persistent metabolic changes 24 hours after stimulation.

Previous studies have shown the Warburg effect in murine macrophages at 16-24 hours post activation with LPS but the data at this time point in human MDM is inconsistent^{188,196,197}. In order to examine the metabolism of adult and cord blood MDM at this later time point, the Seahorse XFe24 Analyzer was used to examine the ECAR and OCR of both adult and cord blood MDM 24 hours after stimulation with Mtb or LPS.

PBMC were isolated from buffy coats or from umbilical cord blood samples taken immediately following delivery. Adult or cord blood MDM were adherence purified for 7 days in 10% human serum. MDM were washed and detached from the plates by cooling and gently scraped, counted and re-seeded on Seahorse culture plates prior to analysis in the Seahorse XFe24 Analyzer. Mtb (iH37Rv; MOI 1-10) or LPS (100 ng/ml) were added 24 hours prior to mitochondrial stress test analysis for adult and cord blood MDM. Differences in cell density was corrected for by crystal violet normalisation. The ECAR and OCR were recorded approximately every 9 minutes.

3.2.2a The increased ECAR observed 2.5 hours after stimulation with Mtb or LPS persists at 24 hours

The ECAR of adult and cord blood MDM were recorded 24 hours after stimulation with Mtb or LPS. The third reading of the unstimulated MDM was used as the comparison to calculate the % change from baseline. The ECAR raw values and the % change in ECAR from baseline are both statistically significantly raised in adult MDM (n=7) 24 hours after stimulation with Mtb (Figure 3.7 A, $P < 0.01$) or LPS (Figure 3.7 B, $P < 0.01$). Cord blood MDM exhibit a similar phenotype to adult MDM. 24 hours after stimulation with Mtb,

the ECAR and the % change in ECAR are both significantly raised (Figure 3.7 C, $P < 0.05$ for both). LPS induced a significant increase in ECAR (Figure 3.7 D, left, $P < 0.01$) and % change in ECAR (Figure 3.7 D, right $P < 0.05$) in cord blood MDM.

3.2.2b OCR 24 hours following Mtb or LPS stimulation in adult and cord blood MDM.

The OCR was concurrently recorded for adult and cord blood MDM 24 hours after stimulation with Mtb or LPS. The third reading of the unstimulated MDM was used as the comparison to calculate the % change from baseline. Adult MDM stimulated with Mtb show no change in OCR or % change in OCR (Figure 3.8 A) from baseline 24 hours after stimulation. 24 hours after stimulation with LPS, adult MDM had a statistically significant increase in OCR and % change in OCR from baseline (Figure 3.8 B, $P < 0.001$ for both). The cord blood MDM showed no change in OCR or % change in OCR for either Mtb (Figure 3.8 C) or LPS (Figure 3.8 D) stimulation.

These data indicate that after 24 hours, adult MDM stimulated with LPS exhibit enhanced cellular energetics, with both ECAR and OCR elevated. Whereas adult MDM stimulated with Mtb for 24 hours exhibit increased ECAR, but stable OCR compared with control, indicating glycolytic metabolism but not a bona fide Warburg effect. The cord blood MDM showed increased glycolysis but no change in OCR for both Mtb and LPS at this time point.

3.2.2c Basal ECAR/OCR ratio in adult and cord blood MDM 24 hours post stimulation with Mtb or LPS.

Having established the ECAR and OCR at 24 hours post stimulation, the ECAR/OCR ratio for adult and cord blood MDM was then calculated to indicate the cellular preference for glycolysis versus oxidative phosphorylation (Figure 3.9). The ECAR/OCR ratio in adult MDM (n=7) is significantly increased in cells stimulated with Mtb compared with controls (Figure 3.9 A, middle, $P < 0.05$ paired t test), however, the ECAR/OCR ratio in cord blood MDM (n=4, middle, Figure 3.9 B) was not statistically significant in cells stimulated with Mtb compared with controls. Both adult (Figure 3.9 A, right) and cord blood MDM (Figure 3.9 B, right) had a statistically significant increase in the ECAR/OCR ratio 24 hours post LPS stimulation ($P < 0.05$).

3.2.2d Comparison of adult and cord blood MDM metabolism 24 hours after Mtb or LPS stimulation

Next, the metabolic outputs of adult MDM were directly compared with that of the cord blood MDM. The % change from unstimulated controls for ECAR or OCR are not statistically significant between adult and cord blood MDM stimulated with either Mtb (Figure 3.10 A, left, middle) or LPS (Figure 3.10 B, left, middle). In keeping with this finding, no difference is seen in the ECAR/OCR ratio between adult and cord blood MDM after Mtb stimulation (Figure 3.10 A, right), however, the ECAR/OCR ratio for the cord blood MDM is significantly increased compared with the adult MDM 24 hours following LPS stimulation (Figure 3.10, B, right; $P < 0.05$).

These data indicate that by 24 hours post stimulation with Mtb, adult and cord blood MDM exhibit similar cellular energetics. In contrast, when MDM are stimulated with LPS for 24 hours, adult MDM exhibit enhanced cellular energetics whereas cord blood MDM exhibit enhanced glycolysis only. This results in cord blood MDM displaying a significantly increased ECAR/OCR ratio compared with adults, 24 hours post LPS stimulation.

3.2.2e Mitochondrial stress test analysis for adult and cord blood MDM 24 hours following LPS or Mtb stimulation

24 hours after Mtb or LPS stimulation adult and cord blood MDM were placed in the Seahorse XFe24 Analyzer and a Mitochondrial Stress test was performed with the sequential administration of oligomycin (1 μ M), FCCP (1 μ M) and antimycin-A/rotenone (0.5 μ M). Three baseline OCR and ECAR measurements were obtained prior to the administration of the reagents. Three subsequent OCR and ECAR measurements were also obtained over 15 min following injection with each of oligomycin, FCCP and antimycin-A/rotenone. The ECAR and OCR time course graphs of the mitochondrial stress test are shown for the adult (Figure 3.11 A, B) and cord blood (Figure 3.11 C, D) MDM.

Maximal respiration, spare respiratory capacity, proton leak, ATP respiration and non-mitochondrial oxygen consumption was calculated as per Figure 2.8. Although adult and cord blood MDM responses to the Mito Stress Test were similar, the adult MDM exhibited significant changes in proton leak after both Mtb and LPS stimulation ($P < 0.05$; Figure 3.12) whereas the cord blood MDM did not. Since increased proton leak is

associated with augmented mitochondrial activity, such as increased oxidative phosphorylation, this observation is in keeping with the previously observed inability of cord blood MDM to increase OCR in response to Mtb or LPS 24 hours post stimulation. Non-mitochondrial oxygen consumption was significantly increased in adult but not cord blood MDM in response to LPS stimulation ($P < 0.01$; Figure 3.12).

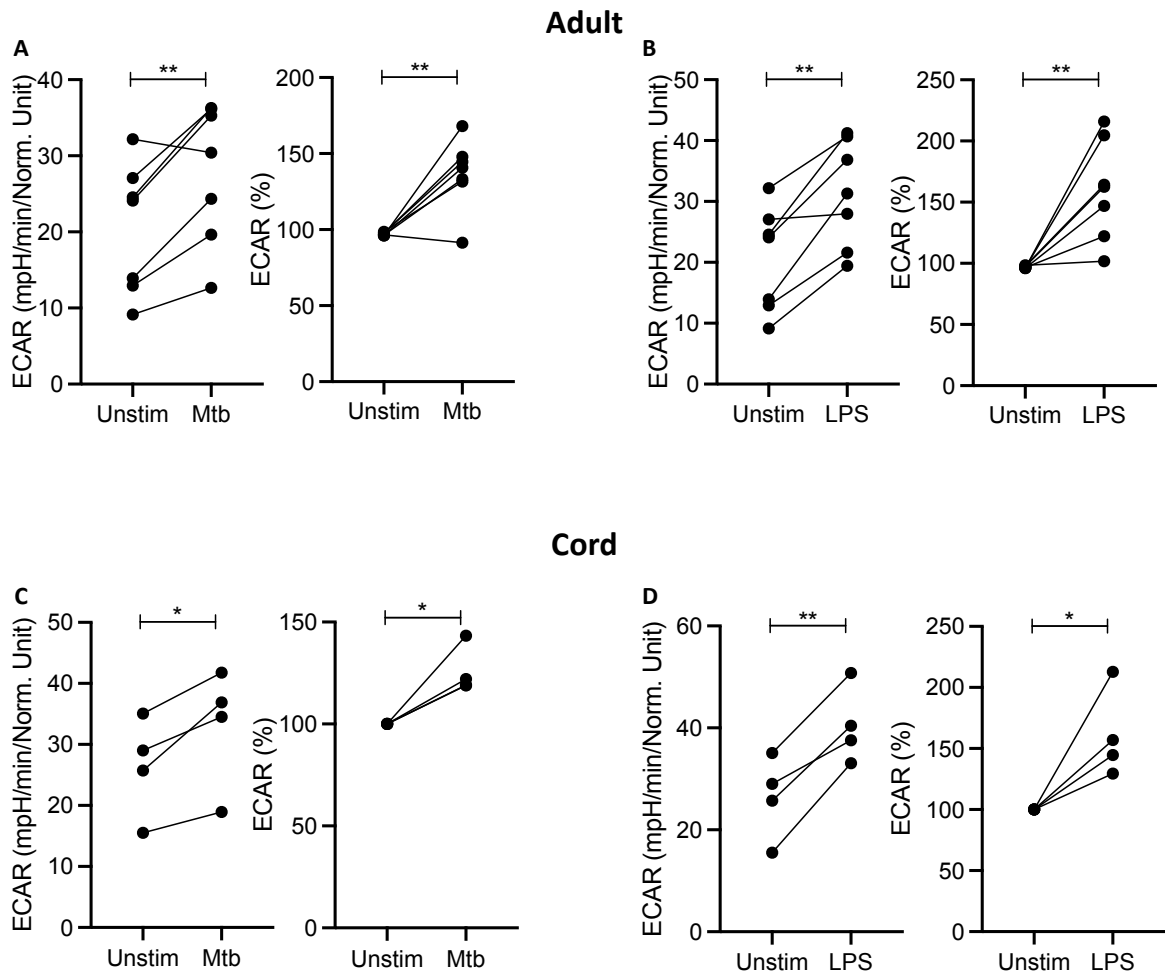


Figure 3.7 Analysis of Baseline ECAR in adult and cord blood MDM 24 hours after Mtb or LPS stimulation.

PBMC were isolated from buffy coats or from umbilical cord blood samples taken immediately following delivery. Adult or cord blood MDM were adherence purified for 7 days in 10% human serum. MDM were washed and detached from the plates by cooling and gently scraped, counted and re-seeded on Seahorse culture plates prior to analysis in the Seahorse XFe24 Analyzer. Mtb (iH37Rv; MOI 1-10) or LPS (100 ng/ml) were added 24 hours prior to analysis. Differences in cell density was corrected for by crystal violet normalisation. The ECAR was recorded approximately every 9 minutes. Shown is the baseline ECAR and the % change from unstimulated MDM for Mtb or LPS stimulated adult (n=7, A, B) and cord blood MDM (n=4, C, D). Statistically significant differences were determined using a paired Student's t test * P<0.05, ** P< 0.01.

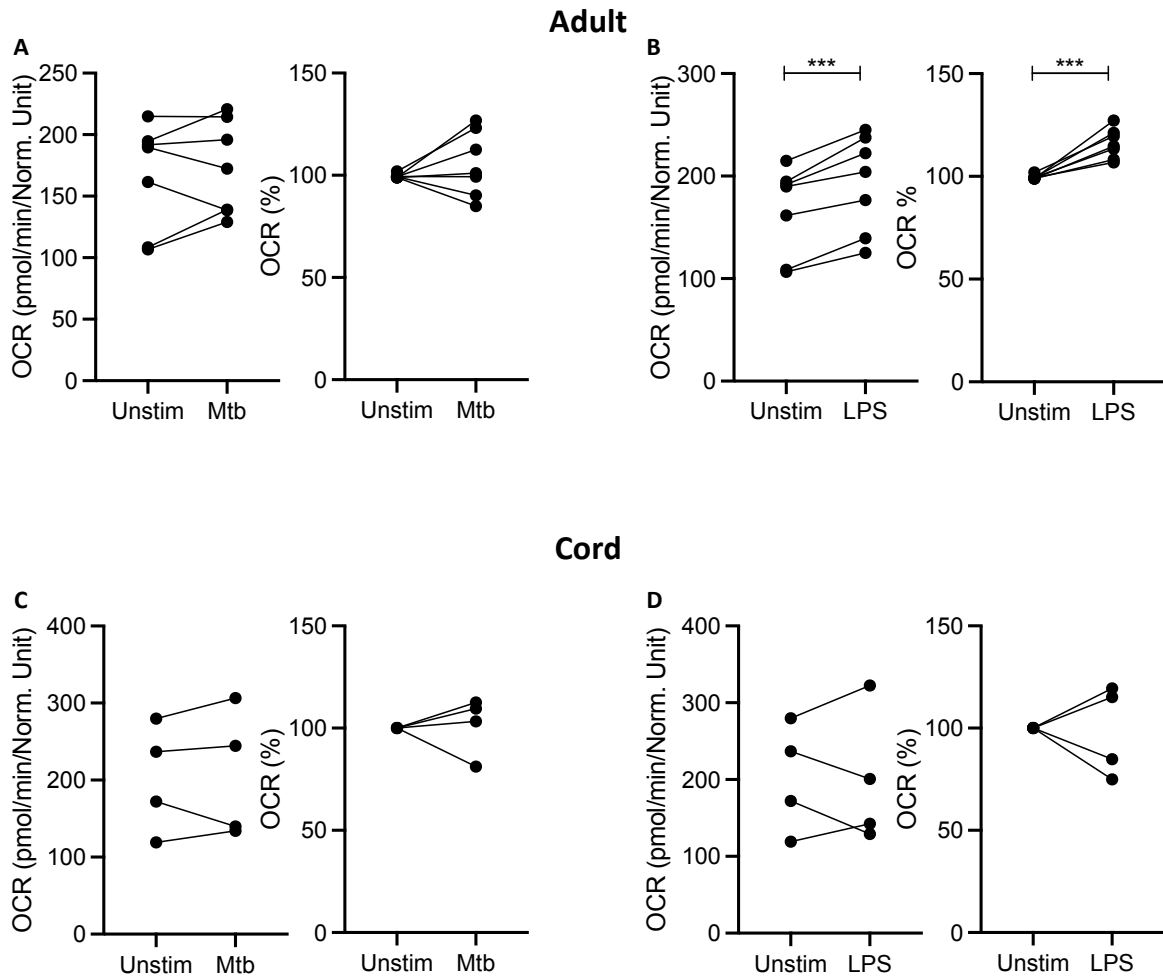


Figure 3.8 Analysis of Baseline OCR in adult and cord blood MDM 24 hours after Mtb or LPS stimulation.

PBMC were isolated from buffy coats or from umbilical cord blood samples taken immediately following delivery. Adult or cord blood MDM were adherence purified for 7 days in 10% human serum. MDM were washed and detached from the plates by cooling and gently scraped, counted and re-seeded on Seahorse culture plates prior to analysis in the Seahorse XFe24 Analyzer. Mtb (iH37Rv; MOI 1-10) or LPS (100 ng/ml) were added 24 hours prior to mitochondrial stress test analysis for adult and cord blood MDM. Differences in cell density was corrected for by crystal violet normalisation. The OCR was recorded approximately every 9 minutes. Shown is the baseline OCR and the % change from unstimulated MDM for Mtb or LPS stimulated adult (n=7, A, B) and cord blood MDM (n=4, C, D). Statistically significant differences were determined using a paired Student's t test *** P< 0.001.

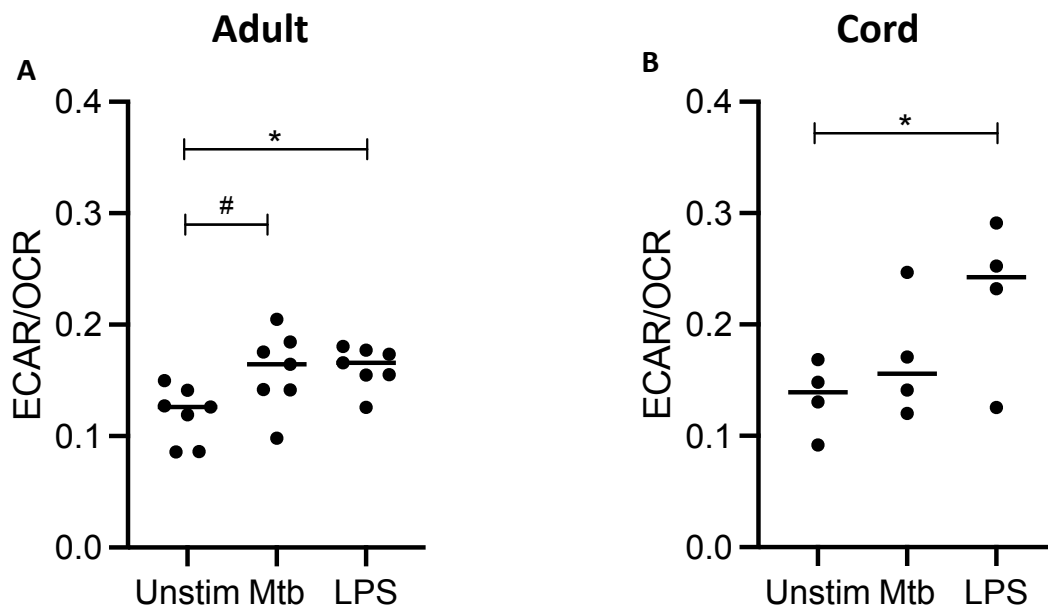


Figure 3.9 ECAR/OCR ratio for adult and cord blood MDM 24 hours after Mtb or LPS stimulation.

PBMC were isolated from buffy coats or from umbilical cord blood samples taken immediately following delivery. Adult or cord blood MDM were adherence purified for 7 days in 10% human serum. MDM were washed and detached from the plates by cooling and gently scraped, counted and re-seeded on Seahorse culture plates prior to analysis in the Seahorse XFe24 Analyzer. Mtb (iH37Rv; MOI 1-10) or LPS (100 ng/ml) were added 24 hours prior to mitochondrial stress test analysis for adult and cord blood MDM. Differences in cell density was corrected for by crystal violet normalisation. The ECAR/OCR ratio was calculated and is shown for adult (A) and cord blood (B) MDM. Statistically significant differences were determined using a one-way ANOVA; * $P < 0.05$, $P < 0.01$, or paired Student's t test; # $P < 0.05$.

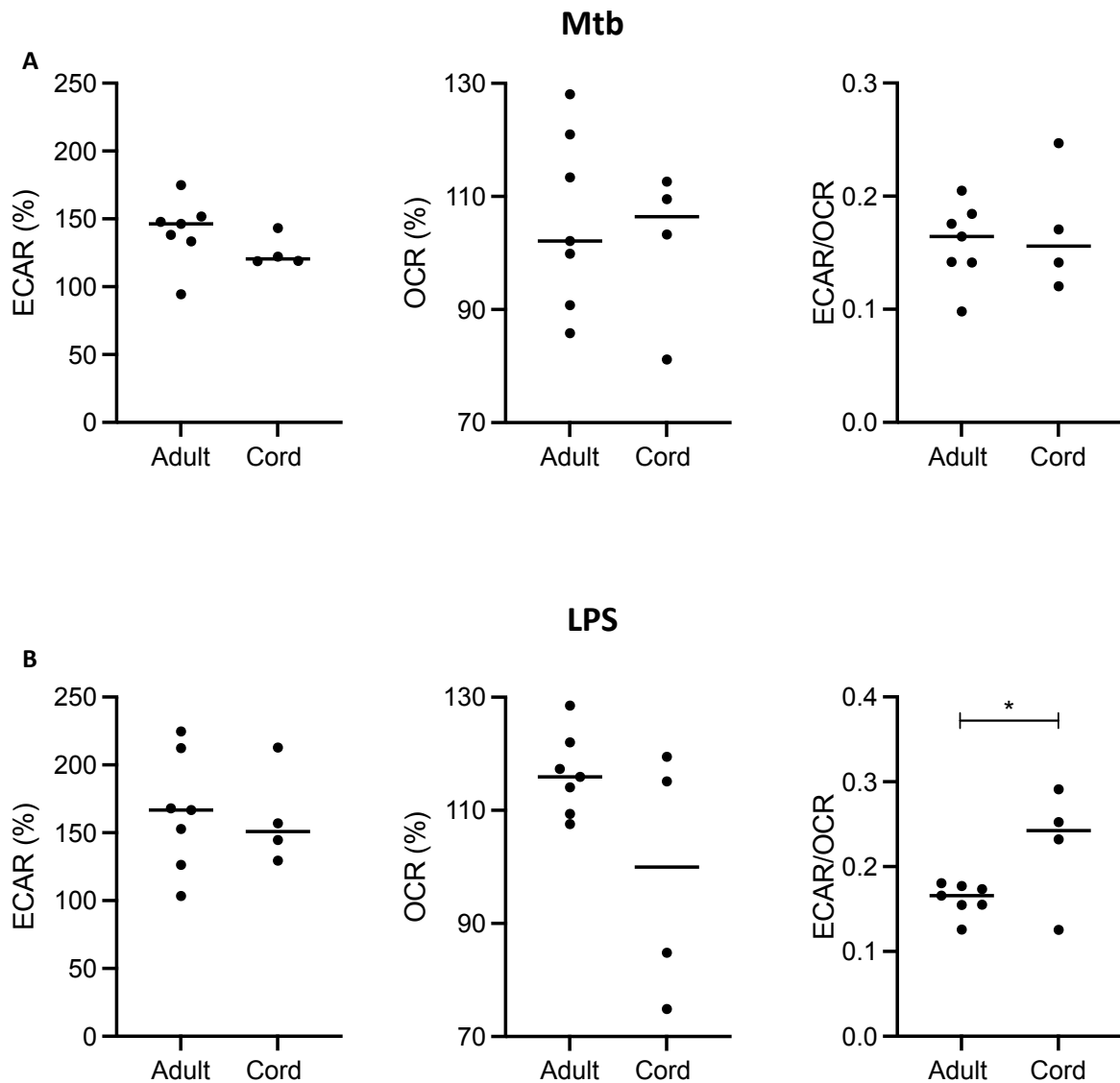


Figure 3.10 Comparison between adult and cord blood MDM responses 24 hours after Mtb or LPS stimulation.

PBMC were isolated from buffy coats or from umbilical cord blood samples taken immediately following delivery. Adult or cord blood MDM were adherence purified for 7 days in 10% human serum. MDM were washed and detached from the plates by cooling and gently scraped, counted and re-seeded on Seahorse culture plates prior to analysis in the Seahorse XFe24 Analyzer. Mtb (iH37Rv; MOI 1-10) or LPS (100 ng/ml) were added 24 hours prior to mitochondrial stress test analysis for adult and cord blood MDM. Differences in cell density was corrected for by crystal violet normalisation. The % change in ECAR and OCR and ECAR/OCR ratio was calculated for Mtb (A) and LPS (B) stimulated cells for the adult (n=7) and cord blood MDM (n=4) and the differences between adult and cord responses were compared. Statistically significant differences were determined using an unpaired Student's t test; * P<0.05.

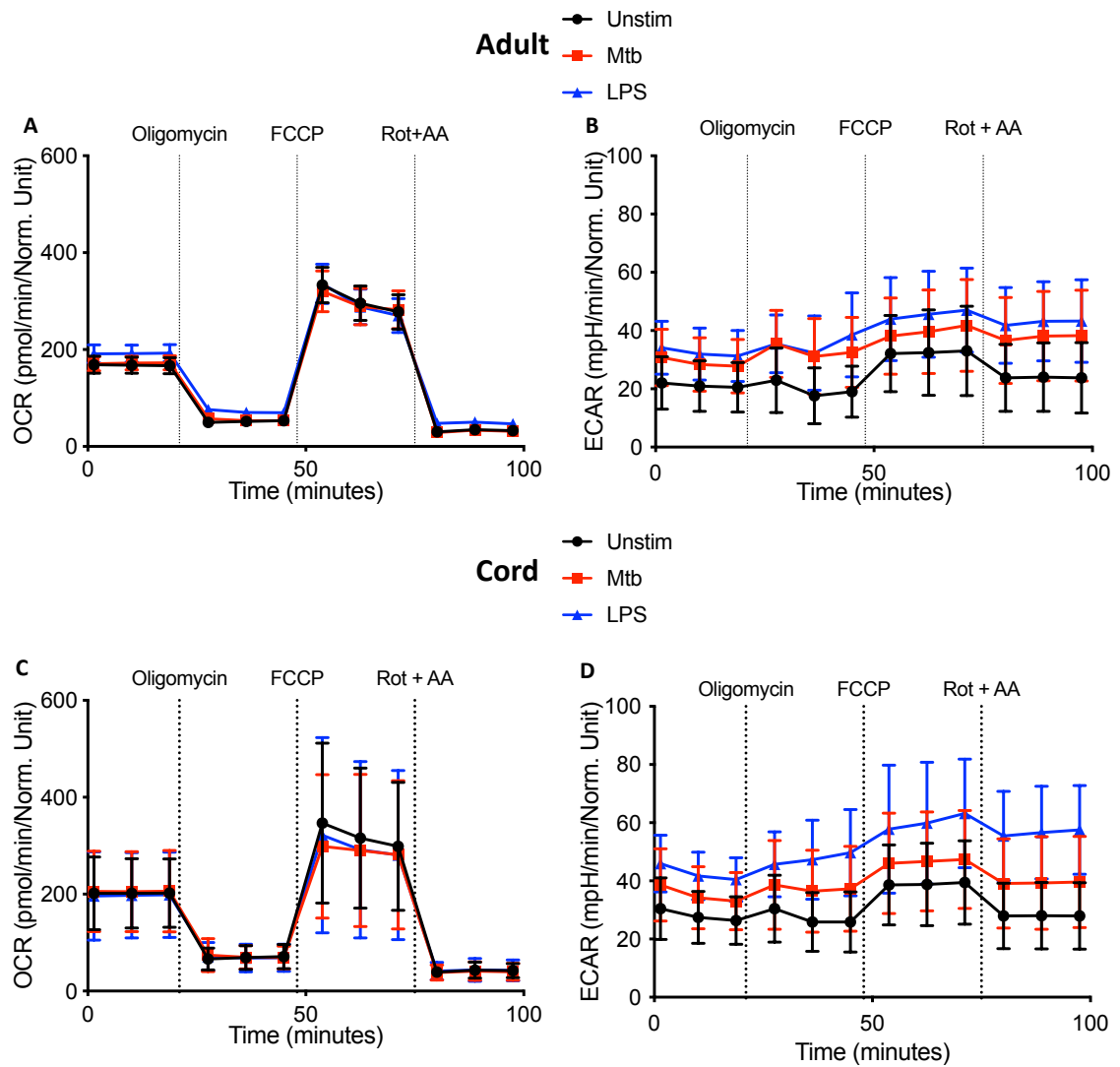


Figure 3.11 Mitochondrial stress test in adult and cord blood MDM 24 hours after stimulation with Mtb or LPS.

PBMC were isolated from buffy coats or from umbilical cord blood samples taken immediately following delivery. Adult or cord blood MDM were adherence purified for 7 days in 10% human serum. MDM were washed and detached from the plates by cooling and gently scraped, counted and re-seeded on Seahorse culture plates prior to analysis in the Seahorse XFe24 Analyzer. Mtb (iH37Rv; MOI 1-10) or LPS (100 ng/ml) were added 24 hours prior to mitochondrial stress test analysis for adult and cord blood MDM. Sequential administration of oligomycin (1 μ M), FCCP (1 μ M) and antimycin-A/rotenone (0.5 μ M) was undertaken through the Seahorse ports. Differences in cell density was corrected for by crystal violet normalisation. The OCR and ECAR was recorded approximately every 9 minutes for the adult (n=7 A,B) and cord blood MDM (n=4 C,D).

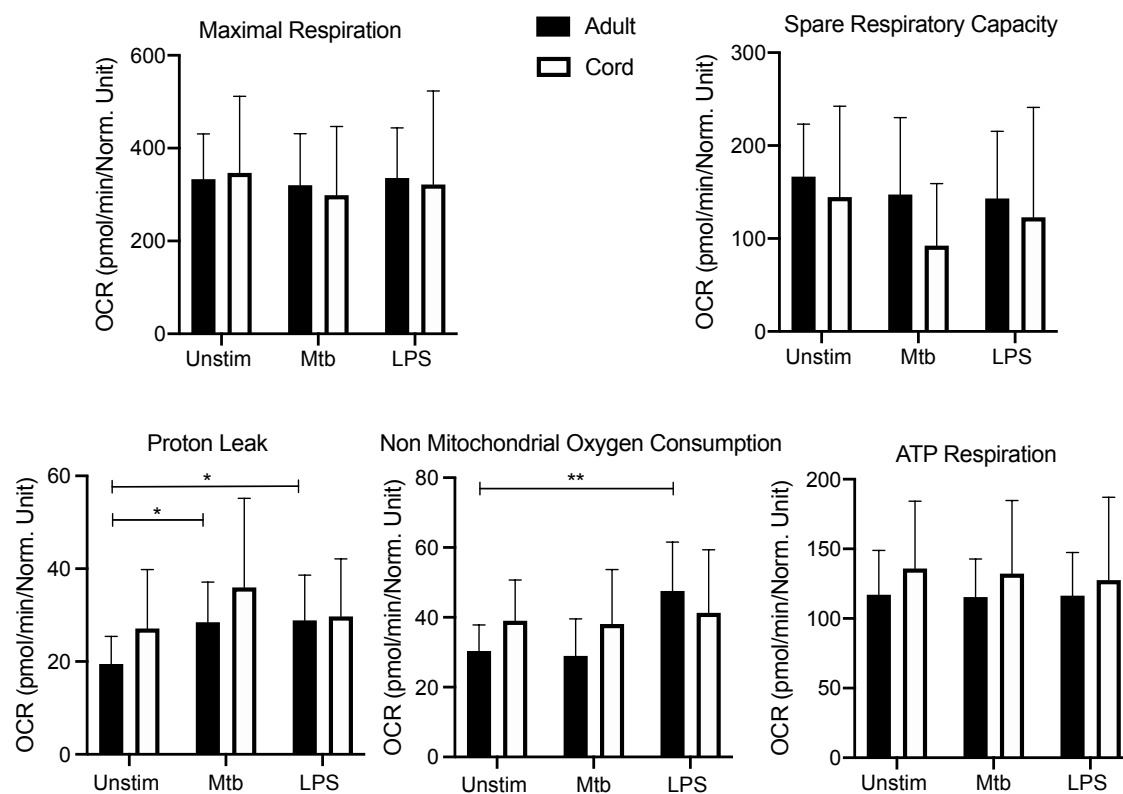


Figure 3.12 Cord blood MDM have a similar mitochondrial stress test profile to adult MDM.

PBMC were isolated from buffy coats or from umbilical cord blood samples taken immediately following delivery. Adult or cord blood MDM were adherence purified for 7 days in 10% human serum. MDM were washed with cold PBS, cooled on ice for 30 minutes and then gently scraped, counted and re-seeded on Seahorse culture plates prior to analysis in the Seahorse XFe24 Analyzer. Mtb (iH37Rv; MOI 1-10) or LPS (100 ng/ml) were added in real time in the Seahorse XFe24 Analyzer or 24 hours prior to mitochondrial stress test analysis for adult and cord blood MDM. Drugs that modulate mitochondrial function were introduced to the cells sequentially. Differences in cell densities were corrected for by crystal violet normalisation. The extracellular OCR was recorded approximately every 9 minutes. The mitochondrial stress test allows the calculation of the Spare Respiratory Capacity, ATP respiration, Proton Leak, Maximal respiration and Non-Mitochondrial Oxygen Consumption which are illustrated in the graphs for both adult (n=7) and cord blood MDM (n=4 ±SD). Statistical significance was determined using two-way ANOVA with Sidak's multiple comparison test * P<0.05, **P<0.01

3.2.3 Comparison between metabolic responses at 2.5 hours and 24 hours following Mtb or LPS stimulation.

The experimental data in this chapter illustrate the importance of timing when determining immunometabolic responses in human MDM. In order to illustrate the differences in the energetic profiles at the different time points, phenograms were created for adult (Figure 3.13) and cord blood MDM (Figure 3.14). The phenogram plots ECAR (x-axis) against OCR (y-axis). Cells that have low levels of both ECAR and OCR are considered “Quiescent”, located in the lower left quadrant and cells with high levels of both are considered “Energetic”, in the right upper quadrant. When cells have a high ECAR and low OCR, they are considered “Glycolytic”, in the right lower quadrant. A high OCR and low ECAR is considered an “Oxidative” state, located in the left upper quadrant.

Adult MDM move towards a glycolytic state 150 minutes after stimulation with Mtb or LPS (Figure 3.13 A). At 24 hours Mtb or LPS stimulation has a less marked effect and now shifts the adult MDM metabolism towards an energetic state (Figure 3.13 B), particularly for the LPS treated MDM. This illustrates the increases in both ECAR and OCR seen at 24 hours in the LPS treated adult MDM. The fact that these changes are not seen in Mtb stimulated adult cells highlight the differential metabolic response to different stimuli.

The phenogram for the cord blood MDM illustrate the fact that there is less metabolic shift in cord blood MDM than adult MDM after stimulation with either Mtb or LPS.

There is little change in the OCR at either 150 minutes (Figure 3.14 A) or 24 hours (Figure 3.14 B) with a reduction in the glycolytic shift between the two time points.

Comparison was also made between the ECAR/OCR ratios at 2.5 hours with those 24 hours post stimulation for both the adult and cord MDM (Figure 3.15). These data illustrate that adult MDM have significantly reduced ECAR/OCR ratios at 24 hours post stimulation with Mtb (Figure 3.15 A, middle, $P < 0.05$) or LPS (Figure 3.15 A, middle, $P < 0.05$) compared with the earlier timepoint. In contrast, cord blood MDM do not have significantly different ECAR/OCR ratios at 2.5 hours compared with those at 24 hours post stimulation with Mtb or LPS (Figure 3.15 B).

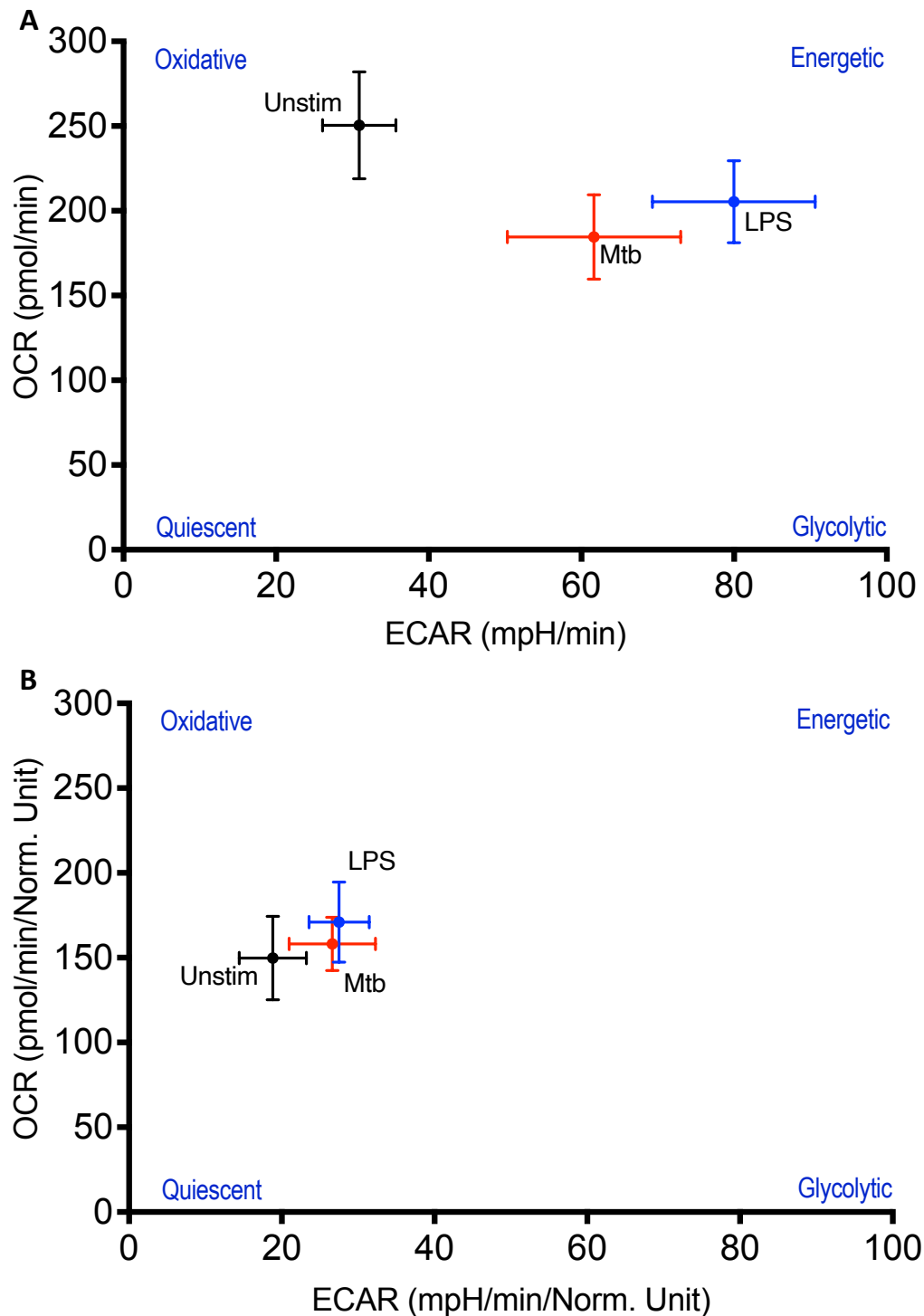


Figure 3.13 Phenogram of adult MDM 2.5 and 24 hours following Mtb or LPS stimulation.

PBMC were isolated from buffy coats and adult MDM were adherence purified for 7 days in 10% human serum. MDM were washed with cold PBS, cooled on ice for 30 minutes and then gently scraped, counted and re-seeded on Seahorse culture plates prior to analysis in the Seahorse XFe24 Analyzer. Mtb (iH37Rv; MOI 1-10) or LPS (100 ng/ml) were added in real time in the Seahorse XFe24 Analyzer or 24 hours prior to mitochondrial stress test analysis. The phenograms illustrates the energetic profile of adult MDM by plotting ECAR versus OCR, as determined by Seahorse at 2.5 hours (A) and 24 hours (B) ($n=7 \pm$ SEM) after Mtb or LPS stimulation.

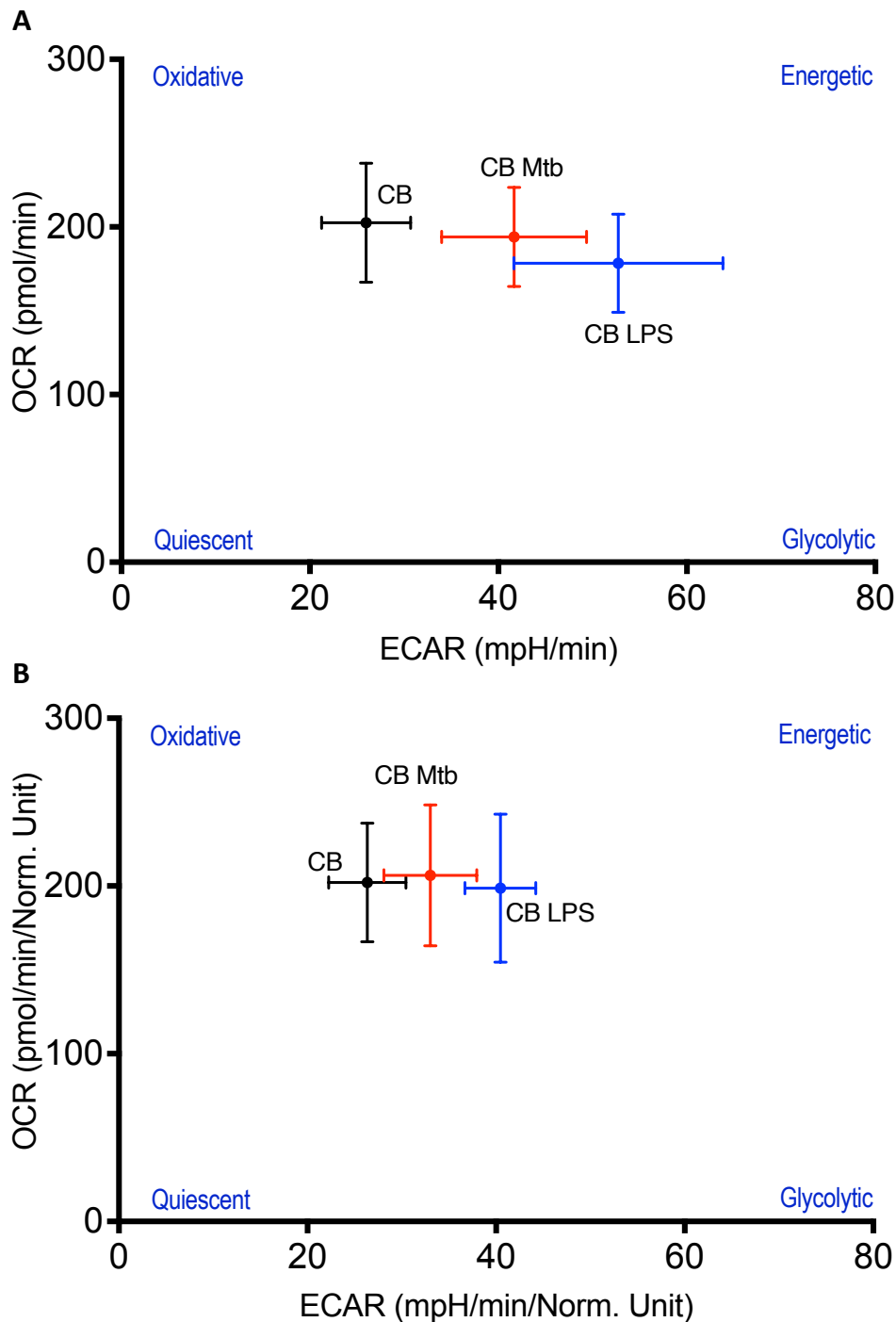


Figure 3.14 Phenogram of cord blood MDM 2.5 and 24 hours following Mtb or LPS stimulation.

PBMC were isolated from umbilical cord blood samples taken immediately following delivery. Cord blood MDM were adherence purified for 7 days in 10% human serum. MDM were washed with cold PBS, cooled on ice for 30 minutes and then gently scraped, counted and re-seeded on Seahorse culture plates prior to analysis in the Seahorse XFe24 Analyzer. Mtb (iH37Rv; MOI 1-10) or LPS (100 ng/ml) were added in real time in the Seahorse XFe24 Analyzer or 24 hours prior to mitochondrial stress test analysis. The phenograms illustrates the energetic profile of cord blood MDM by plotting ECAR versus OCR, as determined by Seahorse at 2.5 hours (A) and 24 hours (B) ($n=4-6 \pm \text{SEM}$) after Mtb or LPS stimulation.

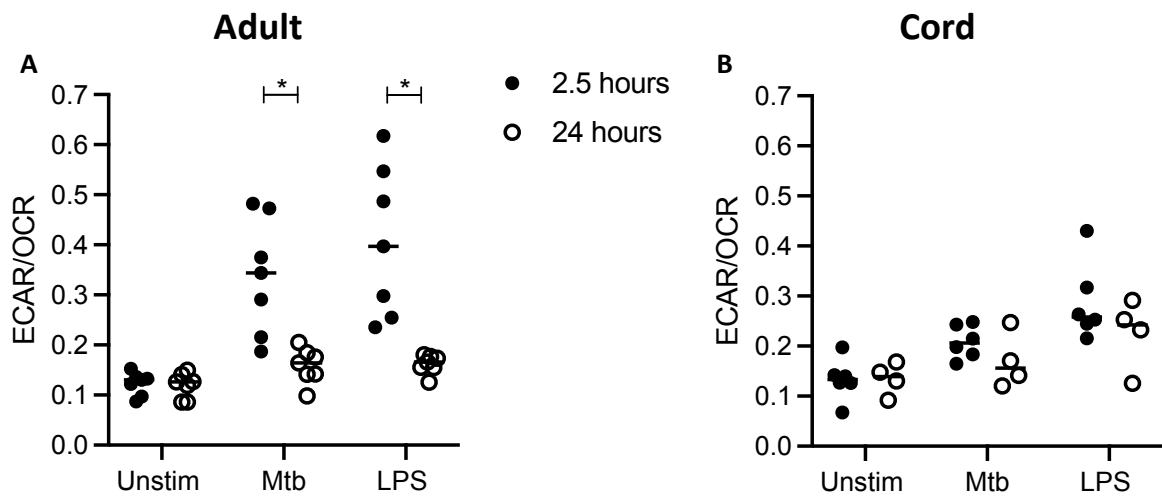


Figure 3.15 Comparison of metabolic responses to Mtb or LPS stimulation at 2.5 and 24 hours post stimulation with Mtb or LPS for adult and cord blood MDM.

PBMC were isolated from buffy coats or from umbilical cord blood samples taken immediately following delivery. Adult or cord blood MDM were adherence purified for 7 days in 10% human serum. MDM were washed with cold PBS, cooled on ice for 30 minutes and then gently scraped, counted and re-seeded on Seahorse culture plates prior to analysis in the Seahorse XFe24 Analyzer. Mtb (iH37Rv; MOI 1-10) or LPS (100 ng/ml) were added in real time in the Seahorse XFe24 Analyzer or 24 hours prior to mitochondrial stress test analysis for adult and cord blood MDM. Graphs show the differences in the ECAR/OCR ratios at 2.5 hours versus 24 hours post stimulation for the adult (A n=7) and cord blood MDM (B n=4-6). Statistical significance was determined using two-way ANOVA with Sidak's multiple comparison test * P<0.05.

3.2.4 Cord blood MDM have similar cell surface marker expression compared with adult MDM.

Since metabolic function is known to underpin macrophage phenotype^{237,238}, we examined the expression of cell surface markers of activation, some of which are associated with pro-inflammatory “M1” or anti-inflammatory “M2” type phenotypes as described in the introduction (1.1.8). We performed flow cytometry 24 hours after stimulation with Mtb or LPS on adult and cord blood MDM. MDM were harvested by placing in ice-cold PBS at 4°C for 30 minutes prior to gentle scraping. Cells were Fc blocked and stained with Zombie NIR viability dye and fluorochrome-conjugated antibodies specific for CD68, CD14, CD40, CD80, CD86, HLA-DR, CD83 and CD206 (MMR) prior to acquisition by flow cytometry as described in the methods (Chapter 2.3) and shown in the gating strategy (Figure 2.7).

CD40 is a critical costimulatory molecule and the representative histogram (Figure 3.16 A) illustrates the increased expression of CD40 in adult MDM upon stimulation with Mtb or LPS. Collated Median Fluorescent Intensity (MFI) values indicate that the increased CD40 expression is statistically significant in adult MDM after Mtb (Figure 3.16 B, $P < 0.05$) or LPS stimulation (Figure 3.16 B, $P < 0.01$) compared with unstimulated controls. Similarly, cord blood MDM exhibit increased expression for CD40 upon stimulation, as shown in the representative histogram (Figure 3.16 C). Bar graphs of collated MFI data show that the increased expression of CD40 was statistically significant in cord blood MDM in response to Mtb (Figure 3.16 D, $P < 0.05$) but not LPS stimulation (Figure 3.16 D). No significant differences between the adult and cord blood responses were observed (Figure 3.16 E).

The expression of HLA-DR, an antigen presenting molecule, was also upregulated in adult MDM in response to stimulation, as seen in the representative histogram (Figure 3.17 A). Bar graphs of collated MFI data show that adult MDM significantly increased expression of HLA-DR in response to Mtb (Figure 3.17 B, $P < 0.05$) or LPS (Figure 3.17 B, $P < 0.01$) compared with controls. Similarly, in cord blood MDM, the representative histogram shows increased expression of HLA-DR in cells stimulated with Mtb or LPS compared with controls (Figure 3.17 C). The increase observed upon stimulation with Mtb was not statistically significant compared with the control (Figure 3.17D) however, a statistically significant increase in HLA-DR expression following LPS stimulation (Figure 3.17 D, $P < 0.01$) was observed compared with unstimulated controls. Expression of HLA-DR was reduced overall in cord blood MDM compared with adult MDM, and this was statistically significant after stimulation with LPS (Figure 3.17 E, $P < 0.05$).

The expression of the activation marker CD83 was upregulated in adult MDM upon stimulation, as illustrated in the representative histogram (Figure 3.18 A). Bar graphs showing collated MFI data demonstrate that CD83 is significantly increased after both Mtb (Figure 3.18 B, $P < 0.05$) and LPS (Figure 3.18 B, $P < 0.01$) stimulation compared with the control. A representative histogram for the cord blood MDM expression of CD83 is also shown (Figure 3.18 C). Bar graphs showing collated MFI data for cord blood MDM expression of CD83 demonstrate that the changes seen after Mtb or LPS stimulation did not reach statistical significance (Figure 3.18 D). No significant differences between the adult and cord blood responses were observed (Figure 3.18 E).

A histogram from one representative adult donor is shown for the costimulatory molecule CD80 (Figure 3.19 A). CD80 was significantly increased in adult MDM in response to LPS (Figure 3.19 B, $P < 0.05$) but not in response to Mtb (Figure 3.19 B). The effect of stimulation on the expression of CD80 in cord blood MDM is illustrated in the representative histogram (Figure 3.19 C). Neither Mtb or LPS stimulation (Figure 3.19 D) resulted in significant changes in CD80 expression in cord blood MDM. There was no significant difference between adult and cord blood CD80 expression (Figure 3.19 E).

The effect on CD86 expression in adult MDM after Mtb or LPS stimulation are shown in a histogram from one representative donor (Figure 3.20 A). No significant changes were observed in CD86 expression after Mtb or LPS stimulation (Figure 3.20 B). Cord blood MDM expression of CD86 is illustrated in the representative histogram (Figure 3.20 C) and analysis is shown in Figure 3.20 D in which showed no significant changes. No differences were seen between the adult and cord blood responses (Figure 3.20 E).

MMR (CD206) is associated with an M2 phenotype. MMR expression after stimulation with Mtb or LPS on adult MDM is illustrated in the histogram (Figure 3.21 A) and no significant changes were seen with either stimuli (Figure 3.21 B). Similar findings were seen in the cord blood histogram (Figure 3.21 C) and analysis of MMR expression after Mtb or LPS stimulation, with no significant changes seen (Figure 3.21 D). No differences were seen between the adult and cord blood responses (Figure 3.21 E).

These data indicate that adult and cord blood MDM display similar expression of cell surface markers of antigen presentation, maturation and M1/M2 phenotypes at

baseline and after stimulation with Mtb or LPS with the only significant difference seen in HLA-DR after LPS stimulation, where cord blood MDM express significantly less than adult.

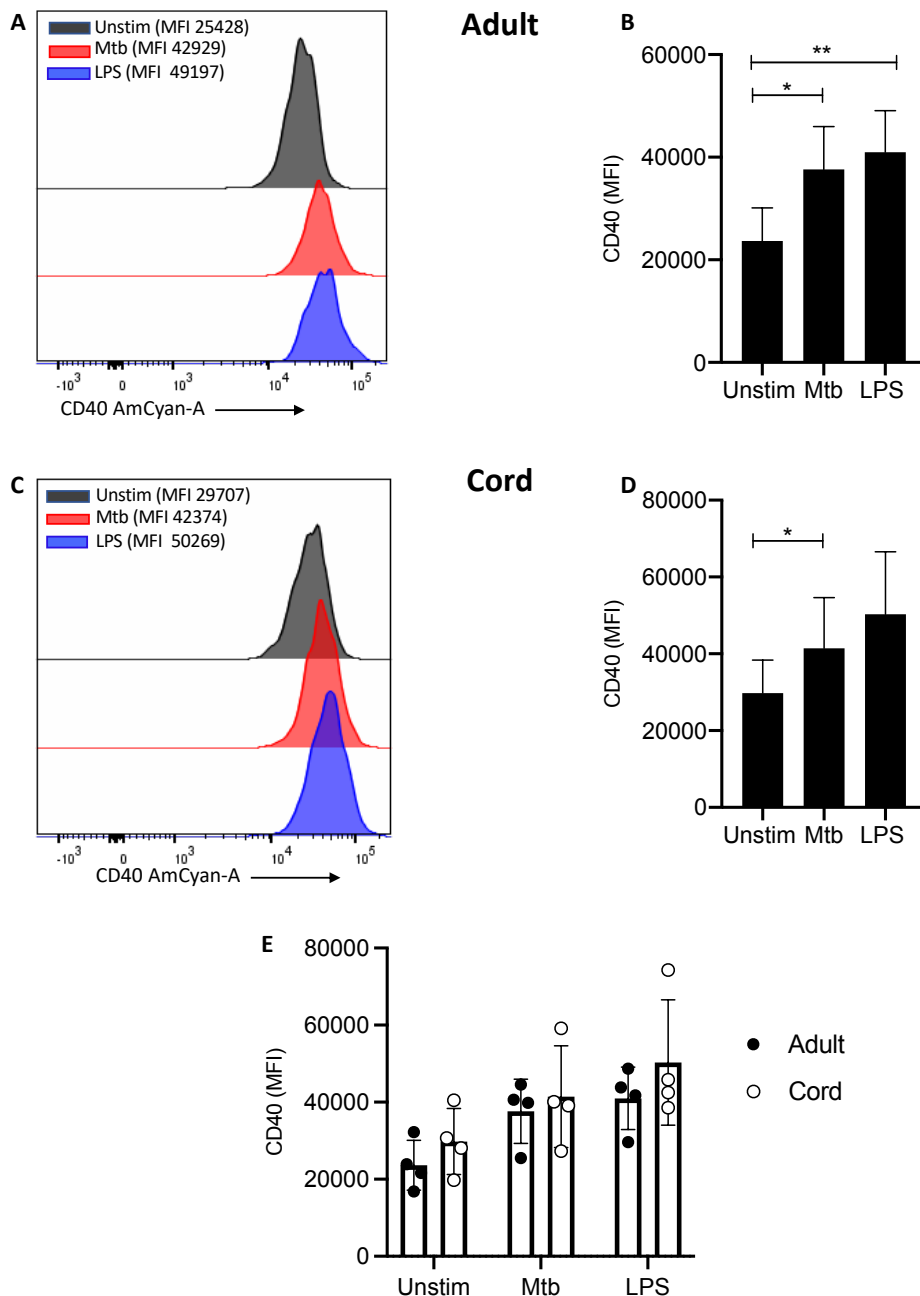


Figure 3.16 Adult and cord blood MDM expression of CD40 24 hours after Mtb or LPS stimulation.

PBMC were isolated from buffy coats or from umbilical cord blood samples taken immediately following delivery. Adult or cord blood MDM were adherence purified for 7 days in 10% human serum. 24 hours after stimulation with Mtb (iH37Rv; MOI 1-10) or LPS (100 ng/ml) MDM were washed and detached from the plates by cooling and gently scraped and placed in flow cytometry tubes. Cells were Fc blocked and stained with fluorochrome-conjugated antibodies specific for CD14, CD68 and CD40. Cells were analysed by flow cytometry. A histogram of a representative donor and the mean fluorescent intensity (MFI) of the phenotypic markers for the adult (A,B; $n=4 \pm SD$) and cord (C,D; $n=4 \pm SD$) MDM are shown. Comparison was made between the adult and cord blood responses (E). Statistical significance was determined using one-way ANOVA with Dunnett's multiple comparison test and two-way ANOVA using Sidak's multiple comparison test; * $P < 0.05$, ** $P < 0.01$.

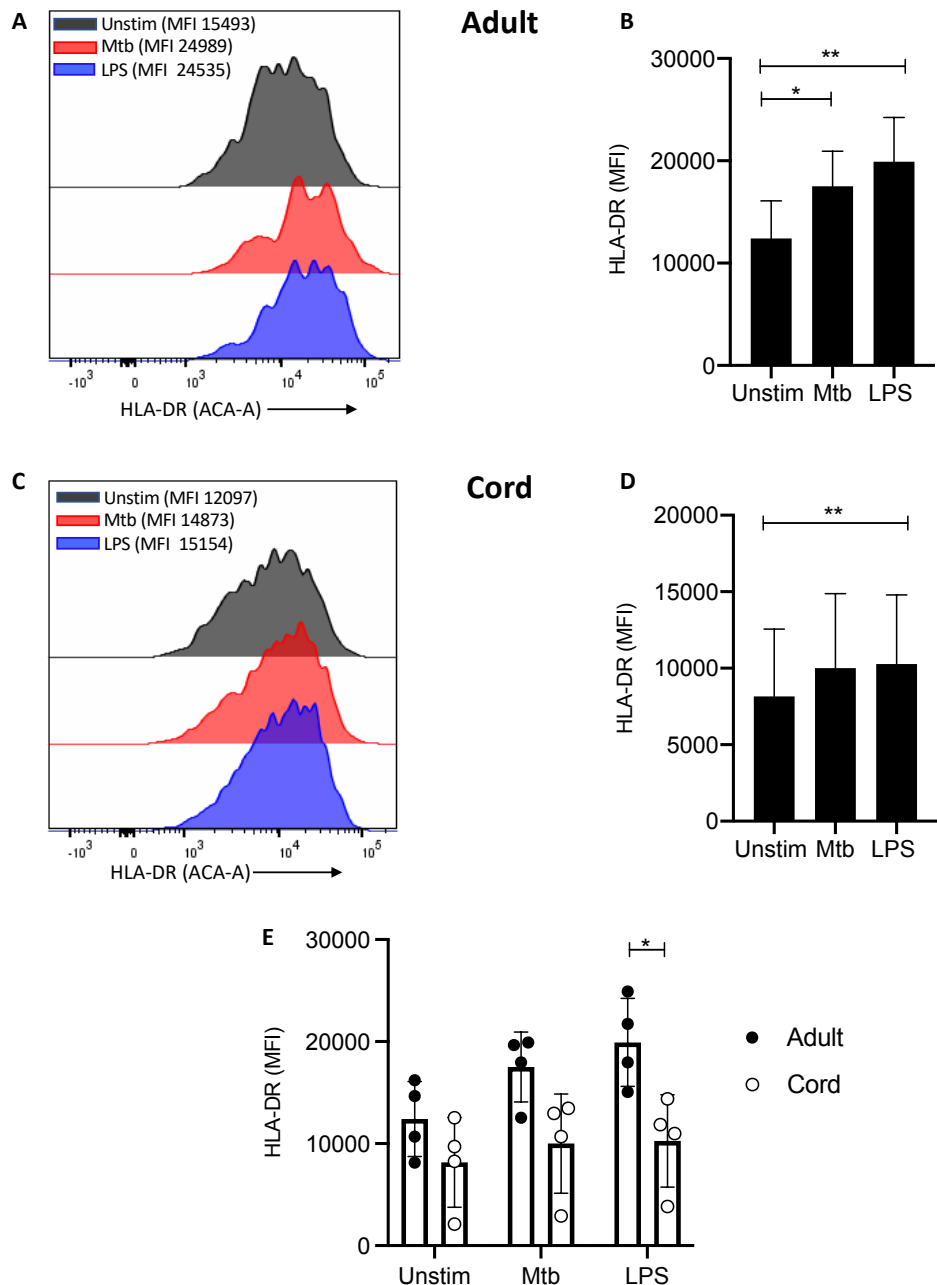


Figure 3.17 Adult and cord blood MDM expression of HLA-DR 24 hours after Mtb or LPS stimulation.

PBMC were isolated from buffy coats or from umbilical cord blood samples taken immediately following delivery. Adult or cord blood MDM were adherence purified for 7 days in 10% human serum. 24 hours after stimulation with Mtb (iH37Rv; MOI 1-10) or LPS (100 ng/ml) MDM were washed and detached from the plates by cooling and gently scraped and placed in flow cytometry tubes. Cells were Fc blocked and stained with fluorochrome-conjugated antibodies specific for CD14, CD68 and HLA-DR. Cells were analysed by flow cytometry. A histogram of a representative donor and the mean fluorescent intensity (MFI) of the phenotypic markers for the adult (A,B; n=4 \pm SD) and cord (C,D; n=4 \pm SD) MDM are shown. Comparison was made between the adult and cord blood responses (E). Statistical significance was determined using one-way ANOVA with Dunnett's multiple comparison test and two-way ANOVA using Sidak's multiple comparison test; * P<0.05, **P<0.01.

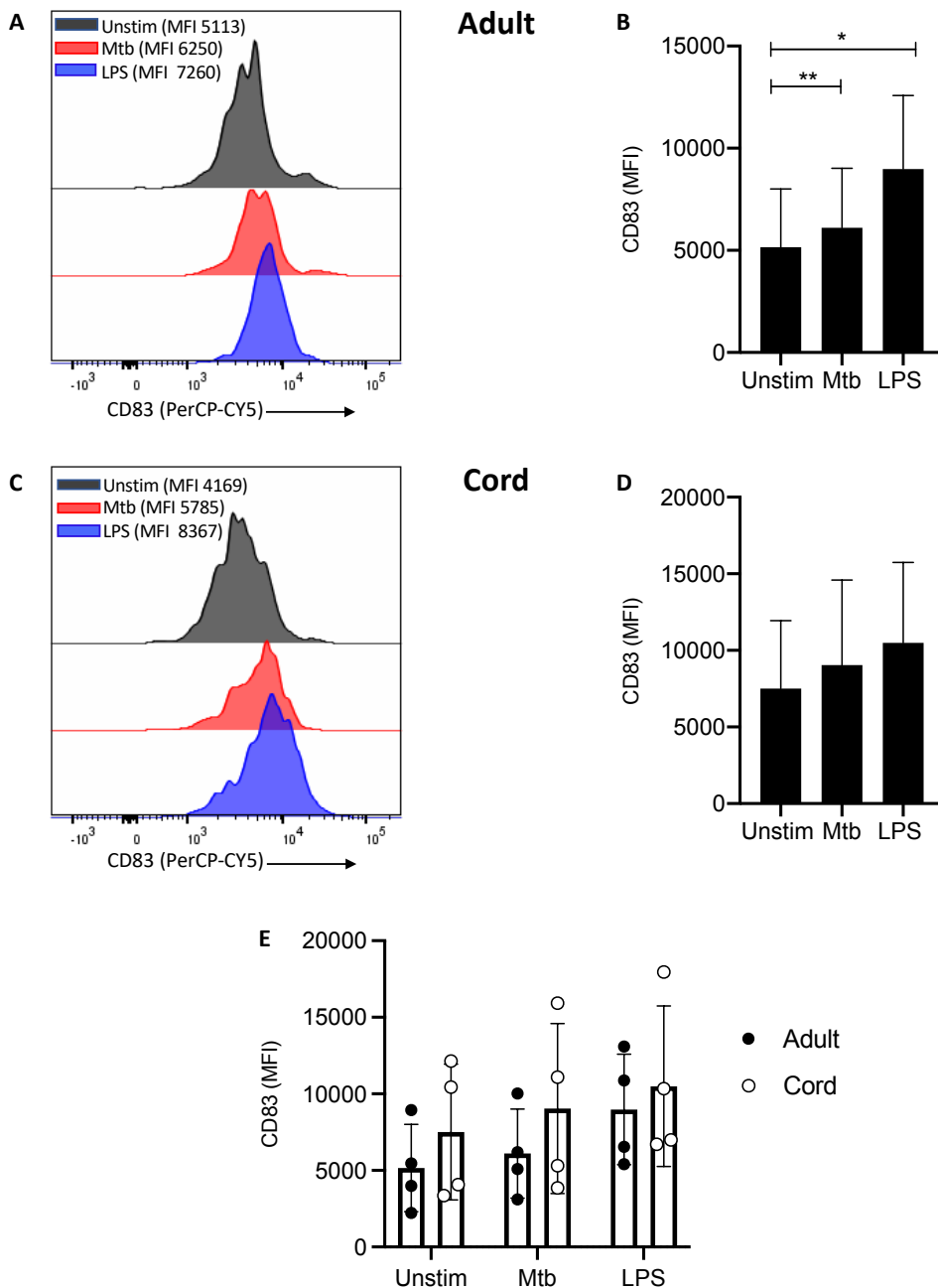


Figure 3.18 Adult and cord blood MDM expression of CD83 24 hours after Mtb or LPS stimulation.

PBMC were isolated from buffy coats or from umbilical cord blood samples taken immediately following delivery. Adult or cord blood MDM were adherence purified for 7 days in 10% human serum. 24 hours after stimulation with Mtb (iH37Rv; MOI 1-10) or LPS (100 ng/ml) MDM were washed and detached from the plates by cooling and gently scraped and placed in flow cytometry tubes. Cells were Fc blocked and stained with fluorochrome-conjugated antibodies specific for CD14, CD68 and CD83. Cells were analysed by flow cytometry. A histogram of a representative donor and the mean fluorescent intensity (MFI) of the phenotypic markers for the adult (A,B; n=4 ±SD) and cord (C,D; n=4 ±SD) MDM is shown. Comparison was made between the adult and cord blood responses (E). Statistical significance was determined using one-way ANOVA with Dunnett's multiple comparison test and two-way ANOVA using Sidak's multiple comparison test; * P<0.05, **P<0.01.

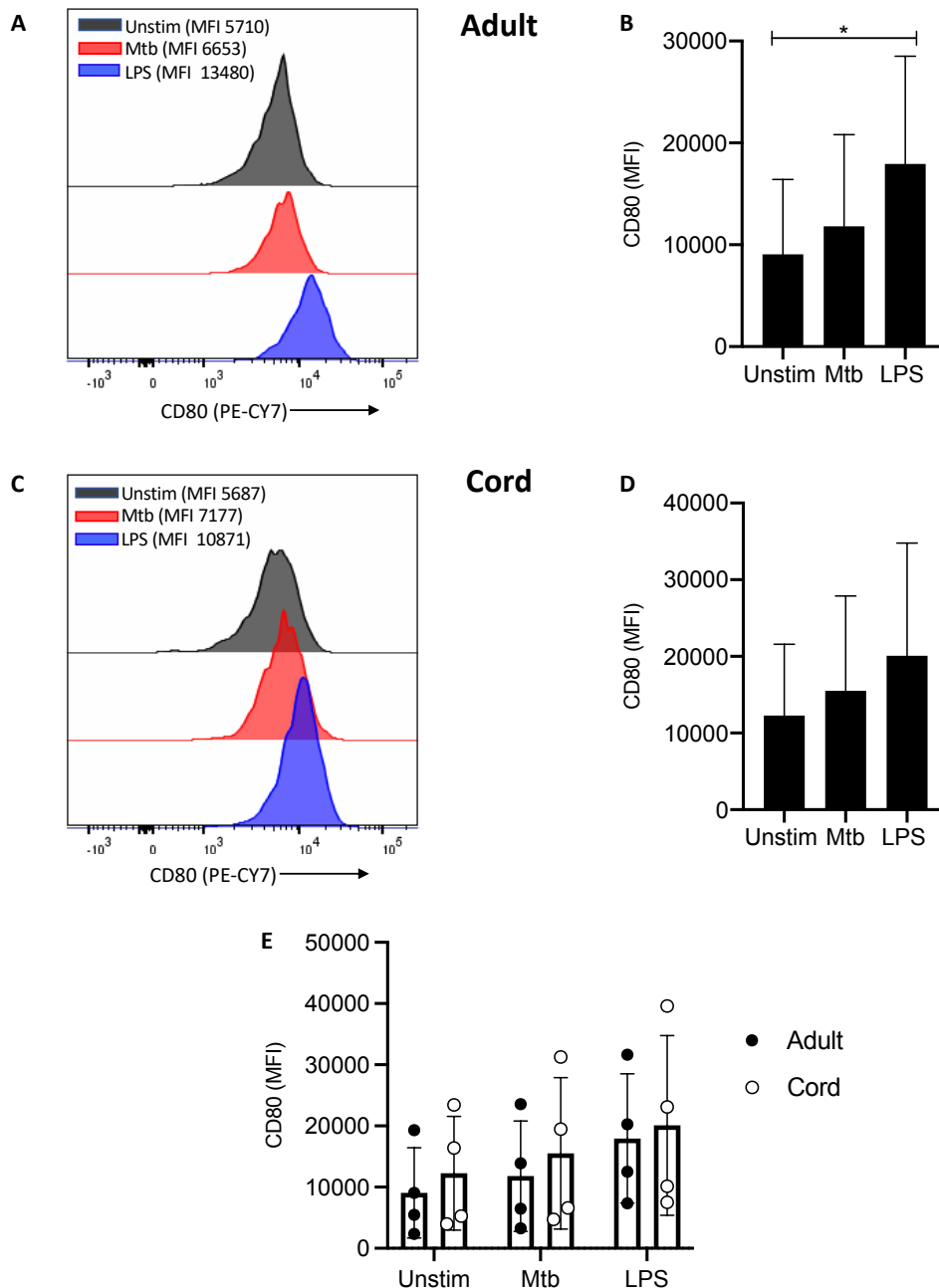


Figure 3.19 Adult and cord blood MDM expression of CD80 24 hours after Mtb or LPS stimulation.

PBMC were isolated from buffy coats or from umbilical cord blood samples taken immediately following delivery. Adult or cord blood MDM were adherence purified for 7 days in 10% human serum. 24 hours after stimulation with Mtb (iH37Rv; MOI 1-10) or LPS (100 ng/ml) MDM were washed and detached from the plates by cooling and gently scraped and placed in flow cytometry tubes. Cells were Fc blocked and stained with fluorochrome-conjugated antibodies specific for CD14, CD68 and CD80. Cells were analysed by flow cytometry. A histogram of a representative donor and the mean fluorescent intensity (MFI) of the phenotypic markers for the adult (A,B; n=4 \pm SD) and cord (C,D; n=4 \pm SD) MDM is shown. Comparison was made between the adult and cord blood responses (E). Statistical significance was determined using one-way ANOVA with Dunnett's multiple comparison test and two-way ANOVA using Sidak's multiple comparison test; * P<0.05.

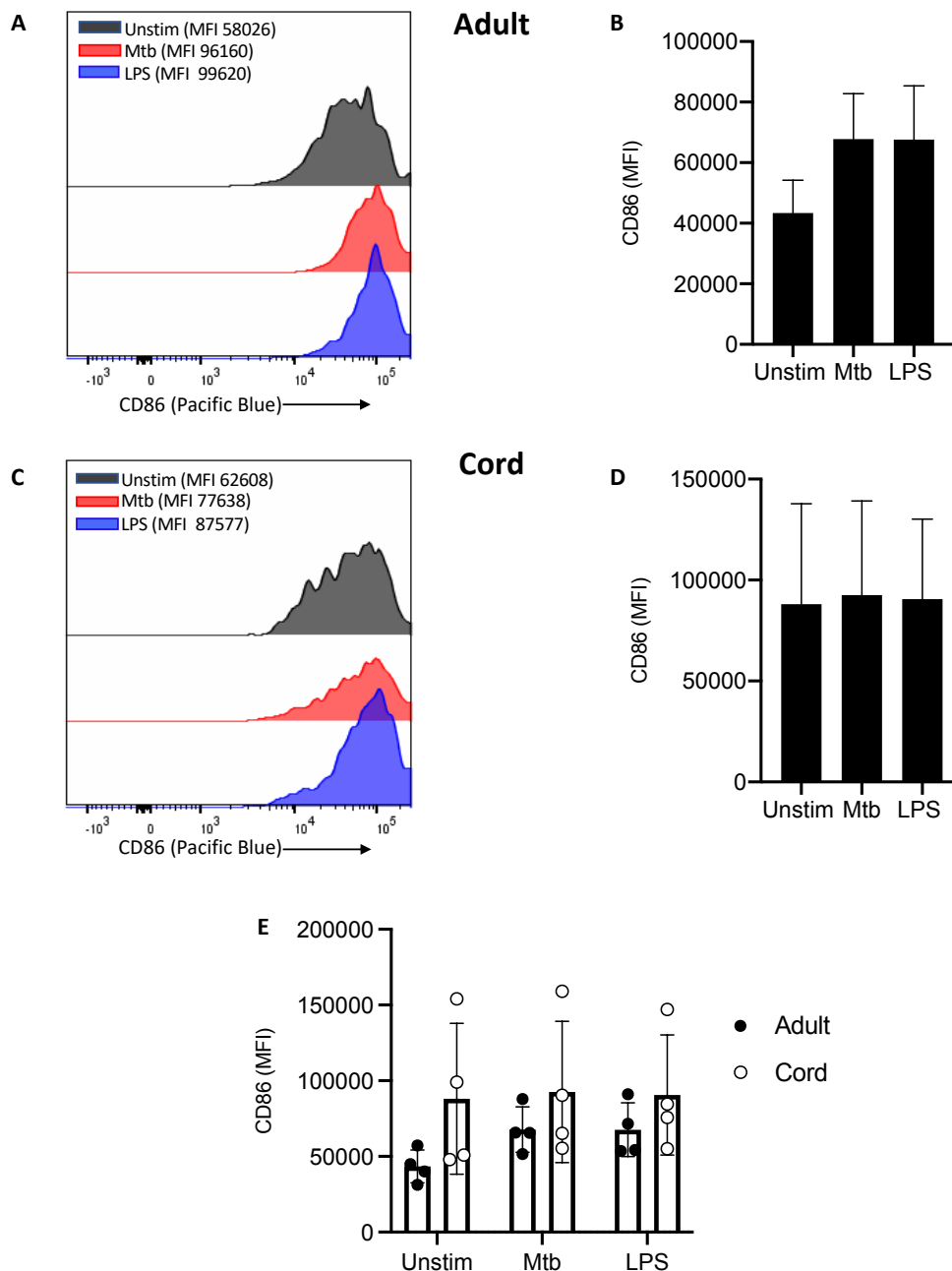


Figure 3.20 Adult and cord blood MDM expression of CD86 24 hours after Mtb or LPS stimulation.

PBMC were isolated from buffy coats or from umbilical cord blood samples taken immediately following delivery. Adult or cord blood MDM were adherence purified for 7 days in 10% human serum. 24 hours after stimulation with Mtb (iH37Rv; MOI 1-10) or LPS (100 ng/ml) MDM were washed and detached from the plates by cooling and gently scraped and placed in flow cytometry tubes. Cells were Fc blocked and stained with fluorochrome-conjugated antibodies specific for CD14, CD68 and CD86. Cells were analysed by flow cytometry. A histogram of a representative donor and the mean fluorescent intensity (MFI) of the phenotypic markers for the adult (A,B; n=4 \pm SD) and cord (C,D; n=4 \pm SD) MDM is shown. Comparison was made between the adult and cord blood responses (E). Statistical significance was determined using one-way ANOVA with Dunnett's multiple comparison test and two-way ANOVA using Sidak's multiple comparison test.

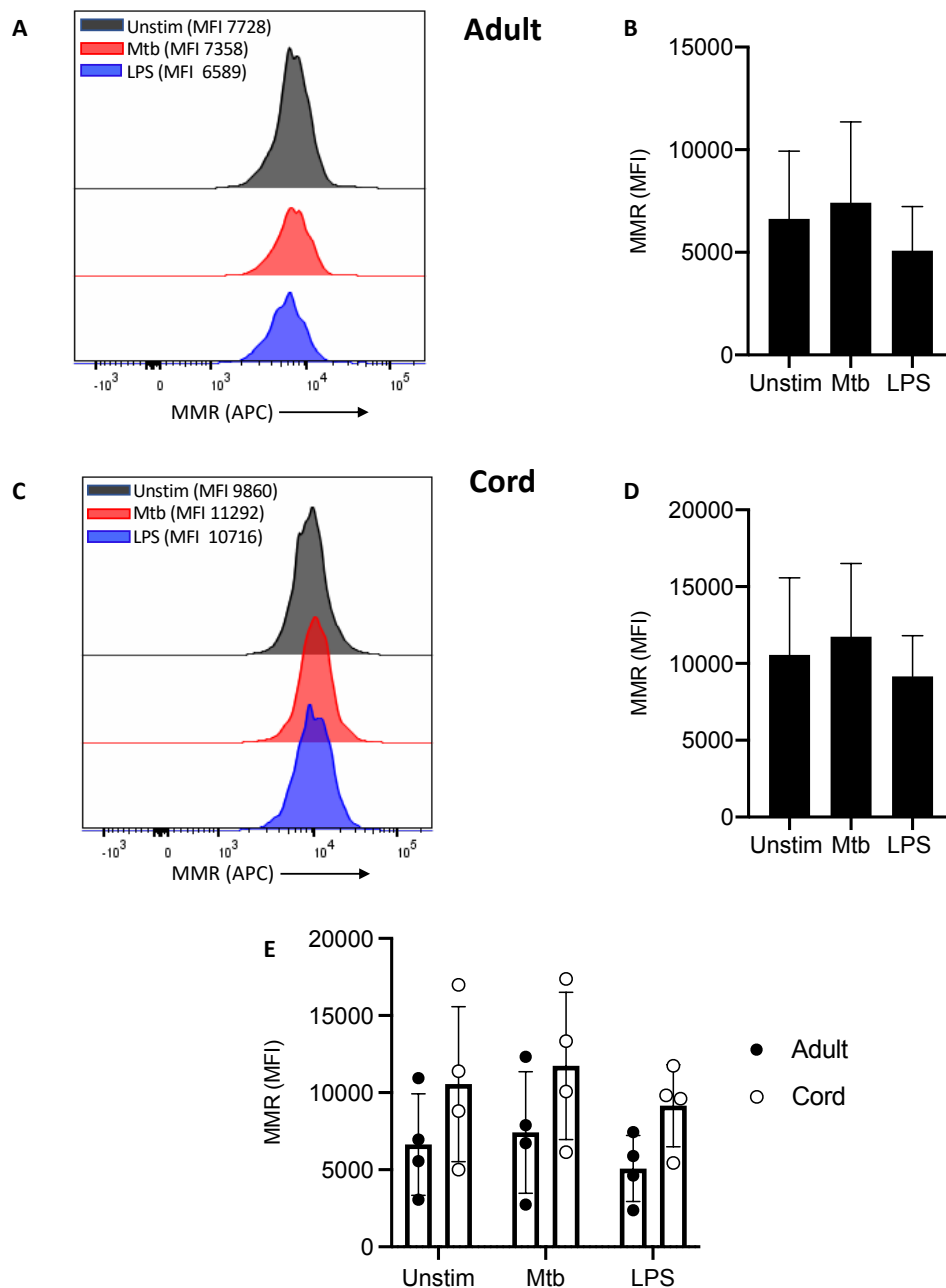


Figure 3.21 Adult and cord blood MDM expression of MMR 24 hours after Mtb or LPS stimulation.

PBMC were isolated from buffy coats or from umbilical cord blood samples taken immediately following delivery. Adult or cord blood MDM were adherence purified for 7 days in 10% human serum. 24 hours after stimulation with Mtb (iH37Rv; MOI 1-10) or LPS (100 ng/ml) MDM were washed and detached from the plates by cooling and gently scraped and placed in flow cytometry tubes. Cells were Fc blocked and stained with fluorochrome-conjugated antibodies specific for CD14, CD68 and MMR. Cells were analysed by flow cytometry. A histogram of a representative donor and the mean fluorescent intensity (MFI) of the phenotypic markers for the adult (A,B; n=4 ±SD) and cord (C,D; n=4 ±SD) MDM is shown. Comparison was made between the adult and cord blood responses (E). Statistical significance was determined using one-way ANOVA with Dunnett's multiple comparison test and two-way ANOVA using Sidak's multiple comparison test.

3.2.5 Cord blood MDM produce less TNF in response to Mtb and more IL-6 in response to LPS stimulation compared with adult MDM.

Functional impairment of cytokine production in cord blood mononuclear cells is well established^{239,240,241} although there are fewer published data on umbilical cord blood MDM, with contradictory results^{179,230}. In addition, inhibition of glycolysis in human macrophages infected with Mtb resulted in decreased IL-1 β and increased IL-10 production¹⁸⁸. Having established that the Warburg effect is not observed in cord blood MDM early in the response to stimulation, the ability of umbilical cord blood MDM to produce cytokine was next determined. Since neonates are highly susceptible to TB and moreover, have increased risk of disseminated disease and increased mortality, it was hypothesised that cord blood and adult MDM may have differential capacity to produce key pro-inflammatory cytokines in response to stimulation with Mtb. Therefore, the concentrations of cytokines including TNF, IL-1 β , IL-10 and IL-6, present in the supernatants of MDM from adult or cord blood 24 hours post stimulation with Mtb or LPS (Figure 3.22) were examined.

TNF is a critical host defence cytokine produced by macrophages in response to stimulation with a wide range of immune stimuli. Previous studies on cytokine production in CBMC cells report a decrease in TNF production compared with adult PBMC^{242,243}. In the context of TB, TNF plays a crucial role in host defence as evidenced by the reactivation of latent TB in people on anti-TNF therapy²⁹. One study examining cord blood monocytes using LPS and lipoarabinomannan, a component of the mycobacterial cell wall, showed a decrease in TNF production 6 hours after stimulation²⁴⁴. However, there is no published data to the author's knowledge

examining the ability of cord blood MDM to produce TNF in response to stimulation with Mtb. Cord blood MDM secreted significantly less TNF than adult MDM in response to stimulation with Mtb (Figure 3.22 A, $P < 0.01$);). No significant differences were observed between adult and cord blood MDM secretion of TNF in response to LPS stimulation (Figure 3.22 B).

A critical role for IL-1 β in mediating bacterial killing in the context of Mtb infection¹⁸⁸ has previously been reported by the Keane laboratory. This production of IL-1 β in response to Mtb infection is associated with increased flux through glycolysis^{188,226,227}. More broadly, the Warburg effect observed in murine macrophages has been reported to be intrinsically linked to the production of IL-1 β ¹⁸⁷. Adult and cord blood MDM have similar capacities to secrete IL-1 β 24 hours post stimulation with Mtb (Figure 3.22 C), although donor-to-donor variability is high in both cord blood and in adults. Unsurprisingly, LPS alone does not significantly induce mature IL-1 β secretion in either adult or cord blood MDM (Figure 3.22 D).

IL-6 is a key pyrogenic cytokine with pleiotropic effects including inducing acute phase proteins and the production of neutrophils in the bone marrow. Adult and cord blood MDM produce comparable concentrations of IL-6 in response to Mtb (Figure 3.22 E), but cord blood MDM produce significantly more IL-6 in response to LPS stimulation compared with adult MDM (Figure 3.22 F, $P < 0.05$).

Finally, IL-10 is a potent anti-inflammatory cytokine, which promotes immune regulation and is associated with an “M2” phenotype. In the context of TB, induction of

IL-10 by Mtb is thought to play a key role in immune evasion^{111,245}. Both adult and cord blood MDM secrete similar concentrations of IL-10 in response to stimulation with Mtb or LPS (Figure 3.22 G,H).

Taken together, these data indicate that cord blood MDM are not generally hyporesponsive in terms of their ability to produce cytokines. Interestingly, cord blood MDM have reduced capacity to produce TNF specifically in response to Mtb but increased ability to produce IL-6 in response to LPS.

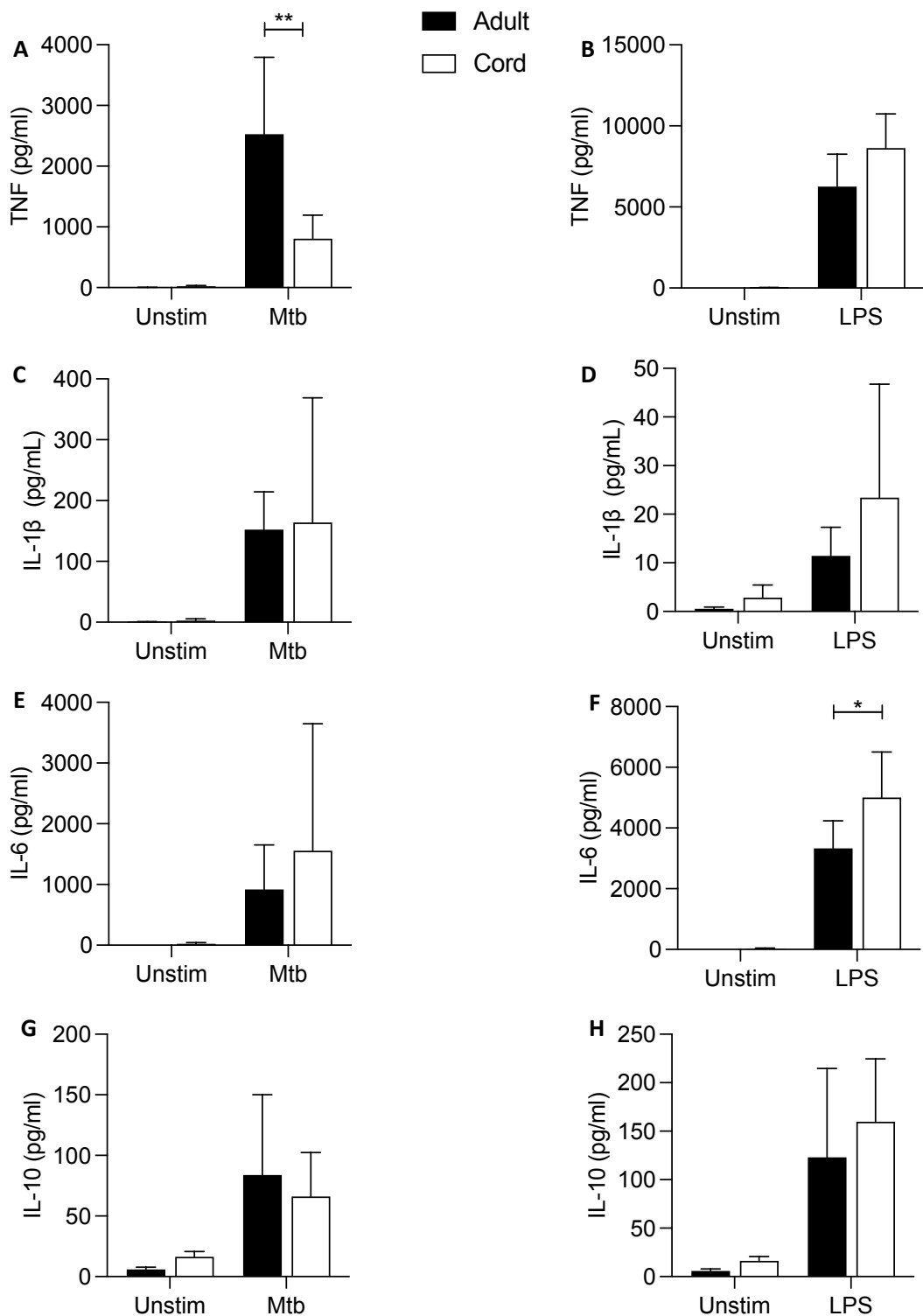


Figure 3.22 Cytokine production of adult and cord blood MDM 24 hours after Mtb or LPS stimulation.

PBMC were isolated from buffy coats or from umbilical cord blood samples taken immediately following delivery. MDM were adherence purified for 7 days in 10% human serum. The concentrations of TNF (A,B), IL-1 β (C,D), IL-6 (E,F) and IL-6 (G,H) in supernatant were measured by Mesoscale Discovery assay 24 hours after stimulation with Mtb (iH37Rv; MOI 1-10) or LPS (100 ng/ml). Graphs illustrate collated data from n=4 adult and n=4 cord MDM \pm SD. Statistical significance was determined using two-way ANOVA with Sidak's multiple comparison test; * P<0.05, ** P<0.01.

3.3 Discussion

The data in this chapter shows for the first time that the Warburg effect occurs in human adult primary macrophages within the first hours after stimulation and then resolves. Twenty-four hours after stimulation, adult MDM stimulated with Mtb or LPS have an increased rate in glycolysis compared to unstimulated control but the reduction in oxygen consumption has returned to baseline in Mtb and is unexpectedly increased after LPS. These data also demonstrate, for the first time, that cord blood MDM do not shift to Warburg metabolism early in the response to stimulation but display similar energetic profiles compared with adults by 24 hours post stimulation.

This early change in glycolysis following stimulation with Mtb or LPS occurs too rapidly to be the result of changes in gene expression for glycolytic enzymes, although this has been seen at the later time point of 24 hours in human and murine macrophages^{203,236}. Various TLRs have been implicated in the glycolytic shift following immune activation though the exact mechanism is unknown²⁴⁶. Glucose transport through monocarboxylate transporters have the potential to be rapidly switched on^{247,248} and may upregulate glycolysis. Alternatively, enzymatic control of glycolysis may be rapidly manipulated causing an influx of glucose.

Macrophage effector function is vital for Mtb control²⁵⁰. Neonates are 5-10 fold more likely to develop TB infection^{51,251} following exposure to mycobacteria and alveolar macrophages from newborns are unable to control Mtb¹³⁴. This work reveals that in contrast to adult MDM, MDM from cord blood fail to reduce OXPHOS upon stimulation.

This reduction in OXPHOS is thought to be as a result of a break in the Krebs's cycle resulting accumulation of a number of metabolic intermediaries such as succinate and citrate which have roles in HIF-1 α stabilisation and fatty acid synthesis respectively¹⁹¹. The quantification of these metabolites in adult and cord blood macrophages at these early time points is an area of future study.

Deficiencies in immune cells from umbilical cord blood have been attributed to the altered immune environment required for foetal growth, in particular high levels of migratory inhibitory factor and adenosine in cord blood serum¹³⁶. In this system, the adult and cord blood MDM have been differentiated in the same manner, in the presence of pooled adult human serum. This process also requires multiple washings of non-adherent cells and media changes which results in experiments being performed free from any persisting environmental factors. This method also does not polarise the cells, which may explain the differences between our data and another study which showed that IFN- γ or IL-10 polarised cord blood MDM failed to increase glycolysis during a glycolysis stress test²⁰². In this project, cord blood MDM significantly increased glycolysis after both Mtb and LPS stimulation. Since the ability to shift to glycolysis is intrinsically linked with IL-1 β secretion¹⁸⁸, the finding that cord blood MDM can undergo a shift to glycolysis is consistent with these data, and with previously published data^{252,253}, showing that cord blood and adult MDM make similar amounts of IL-1 β .

During the optimisation work for this chapter, outlined in the methods, a similar morphology and phagocytic ability were observed in cord and adult MDM, as previously described^{230,254,255}. Cord blood MDM were more prone to death following exposure to

cold and then gentle scraping. This was adjusted for in these experiments to ensure numbers were equal, however, it is plausible that cord blood MDM may exhibit increased susceptibility to death following stress than adult MDM.

Flow cytometry based phenotypic analysis of adult and cord blood MDM showed similar expression of cell surface markers 24 hours after stimulation, supporting the results of previous studies indicating that monocytes or macrophages from cord blood are phenotypically similar to adults and are able to respond appropriately to stimulation in certain contexts^{179,231,239}. At this timepoint, adult and cord MDM metabolic function are very similar and since metabolic function is associated with 'M1/M2' phenotypes, it is therefore unsurprising that 'M1/M2' markers are broadly similar in adult and cord MDM. Although cord blood MDM stimulated with LPS have a higher ECAR/OCR ratio at 24 hours than their adult counterparts, this is not reflected in differences in their cell surface expression of key activation markers and is rather a consequence of the raised OCR seen in adult MDM at this time point. Cord blood MDM displayed reduced expression of HLA-DR and were significantly less able to upregulate HLA-DR expression upon stimulation with LPS compared with their adult counterparts. Reduced HLA-DR expression on monocytes has been associated with increased mortality during sepsis in both adults^{256,257} and neonates²⁵⁸ and has been recognised previously as a potential contributor to the increased susceptibility of neonates to bacterial infection^{259,260}.

This difference in metabolic response to different stimuli has been explored previously in human monocytes²⁰¹. Mtb lysate but not LPS was found to increase the basal ECAR 24 hours after stimulation, though the amount of lactate in the supernatant was

significantly raised after LPS²⁰¹. These findings may be, at least in part, explained by the observations herein whereby an earlier glycolytic shift occurs in human macrophages in response to stimulation. Of note, human monocytes produce mature IL-1 β but differentiated human macrophages require a second signal to activate the NLRP3 inflammasome and caspase-1^{93,261}. Despite this checkpoint to IL-1 β secretion, the glycolytic shift in MDM remains intact after LPS stimulation. Recent research examining the metabolomic profile of differentiated human macrophages showed distinct metabolomic profiles between LPS and Mtb though the mechanism of these differing response have yet to be elucidated²⁶².

Significant reduction in TNF from cord blood MDM stimulated with Mtb compared with adults was observed; this novel finding may, at least in part, account for increased susceptibility to Mtb infection in neonates and warrants further exploration in clinical settings. Production of TNF is not thought to be metabolically mediated, as evidence from mice suggests that TNF remains stable when glycolysis (and therefore IL-1 β production) is being modulated¹⁸⁷. Whilst this phenomenon may be distinct and unrelated from the altered metabolic profile, previously published data from the Keane lab^{226,227} suggested that TNF may be linked to metabolic function in humans and therefore warrants further study. Timing and the kinetics of metabolic flux versus cytokine production may be imperative to understanding how these processes are connected in humans. Since these data examined the concentrations of cytokines present and accumulated over a 24-hour period, it cannot be ruled out that differences may exist in the early production of cytokines. Since the bona fide Warburg effect does not occur in cord blood MDM in the immediate aftermath of stimulation, this indicates

that production of IL-1 β may be affected; however, by 24 hours, the metabolic response to Mtb is similar in both adults and cord blood MDM as is their ability to produce mature IL-1 β . Interestingly, the data indicates that cord blood MDM have enhanced ability to produce IL-6 in response to LPS compared with adults. This is in keeping with published work showing increased IL-6/TNF ratios in cord blood versus adult PBMC²⁴³.

3.4 Conclusions

Adult human macrophages exhibit the Warburg effect rapidly post stimulation and an elevated ECAR (but normalised or increased OCR) 24 hours later. This is in contrast to the metabolic flux described in murine models, which exhibits Warburg metabolism 24 hours post stimulation with LPS. The data presented herein highlights the importance of assessing immunometabolic kinetics in primary human immune cells. These data illustrate that there is a fundamental metabolic difference in MDM from umbilical cord blood and adult blood, despite using the same method of differentiation from monocytes. Furthermore, cord blood MDM produce significantly less TNF in response to Mtb compared with adult MDM. These key differences in early metabolic flux and cytokine production may help to determine why certain populations are more vulnerable to infection than others and may lead to the development of specific immuno-supportive therapies for susceptible people.

Chapter 4 Polarisation with IFN- γ or IL-4 alters human macrophage immunometabolism

4.1 Introduction

The data from chapter 3 illustrate that LPS or Mtb stimulation activate human macrophages resulting in alterations in cell surface markers, pro-inflammatory cytokine production and metabolic reprogramming. The novel findings of inflammatory Warburg early in response to stimulation and increased oxidative phosphorylation 24 hours after LPS stimulation are also described. This activation state marked by increased glycolysis and raised expression of co-stimulatory markers such as HLA-DR and CD40 is in keeping with classically activated macrophages as described in Chapter 1.

Monocytes recruited from the circulation are influenced by a variety of factors in the tissue microenvironment as they are attracted into the site of inflammation and begin differentiating into macrophages²⁶³, including cytokines such as IL10, IL4, IFN- γ , and GM-CSF and M-CSF, as detailed in chapter 1.

Stimulating differentiated macrophages with IFN- γ (usually in the presence of LPS) or IL-4 is a well-established method of polarising macrophages to the classically activated, pro-inflammatory “M1” or alternatively activated, anti-inflammatory “M2” phenotype in mice^{153,160}. There are fewer studies in humans, with a variety of methodologies in use which makes interpretation of standard changes in macrophage challenging¹⁶².

There is growing murine research supporting the importance of metabolic shifts in macrophage cytokine polarisation. *In vitro* murine models have shown that IFN- γ causes a rapid glycolytic shift in BMDM that persists at 24 hours and that BMDM activation is blocked by 2-DG²⁶⁴. Data in human MDM is lacking but there is some evidence that metabolism plays a role in polarisation in proteomic analysis¹⁹⁹ and genome wide ribosome profiling.²⁰⁰

The knowledge gap in human macrophage polarisation is even more pronounced with regard to umbilical cord MDM. Two recent papers have shown contradictory results, one showing similar cellular profiles in adult and cord blood MDM after polarisation¹⁷⁹ and the other showing marked differences, including a complete abrogation of oxidative phosphorylation and an inability to upregulate glycolysis during a glycolysis stress test²⁰². The data shown in chapter 3 contradicts these findings as cord blood MDM undergo a glycolytic shift following Mtb or LPS stimulation, but do not undergo early inflammatory Warburg, as seen in human adult cells.

4.1.1 Hypothesis and Aims

Hypothesis:

Polarisation with IFN- γ or IL-4 has been shown to produce a distinct metabolic pattern in murine bone marrow derived macrophages (BMDM) and it was hypothesised herein that the immunometabolic phenotype in human MDM in response to polarisation with IFN- γ or IL-4 would be distinct from the murine model. It was also hypothesised that IFN- γ may support and abrogate the defects observed in cord blood MDM responses compared with adults.

Aims:

- Examine the phenotypic differences of macrophages differentiated from adult and cord blood after IFN- γ or IL-4 polarisation using flow cytometry to analyse the expression of cell surface markers.
- Directly compare the immunometabolic profile of adult and cord blood macrophages in response to stimulation with Mtb or LPS 24 hours after IFN- γ or IL-4 polarisation using the Seahorse XFe Analyzer technology.
- Elucidate the differential kinetics of immunometabolic changes in activated human macrophages treated with IFN- γ or IL-4 by examining the response to stimulation in real time.
- Examine the differential ability of adult or cord blood macrophages which have been pre-treated with IFN- γ or IL-4 to produce key cytokines 24 hours after stimulation with Mtb or LPS.

4.2 Results

4.2.1 The effect of IFN- γ or IL-4 on the phenotype of adult and cord blood MDM

In murine models, IFN- γ and IL-4 are well-established methods of post differentiation macrophage polarisation, to either a pro or anti-inflammatory state respectively^{153,160}.

Both of these cytokines are relevant in TB infection. IFN- γ has long been known to increase macrophage ability to kill Mtb²⁶⁵ and has been used as host directed therapy to improve macrophage function in patients with MDR TB^{266,267}. T cell memory responses to Mtb produce IFN- γ and this forms the basis of modern diagnostic

technologies for the diagnosis of Mtb²⁶⁸. IFN- γ production has also been shown to be deficient in umbilical cord blood PBMC compared to adults following stimulation with phytohemagglutinin^{131,269}. IL-4 promotes an anti-inflammatory macrophage phenotype^{151,162}, and is found in increased levels in TB disease. It has been postulated that mycobacteria may induce IL-4 production as a strategy to promote an anti-inflammatory phenotype and to subvert the immune response²⁷⁰. Due to their biological relevance in TB infection IFN- γ and IL-4 were chosen as the cytokines to induce macrophage polarisation.

At the outset of this project, the effects of IFN- γ and IL-4 on the phenotype of human MDM differentiated with 10% human serum was established by the examination of their morphology under light microscopy and the expression of cell surface markers by flow cytometry.

4.2.1a Adult and cord blood MDM morphology after polarisation

Polarisation with IFN- γ or IL-4 has previously been shown to alter macrophage morphology in adult MDM¹⁶², with IFN- γ causing an increase in elongated, spindle shaped MDM and IL-4 causing a more rounded shape. There is little data in cord blood MDM with one study showing similar morphology between adult and umbilical cord blood MDM when polarised with GM-CSF or M-CSF¹⁷⁹. PBMC were isolated from adult buffy coats or from umbilical cord blood which was collected immediately following delivery. MDM were adherence purified for 7 days in RPMI with 10% human serum and non-adherent cells were washed off on days 2 and 5. IFN- γ (10ng/ml) or IL-4 (10ng/ml) were added to differentiated MDM 24 hours prior to examination under light

microscopy. Qualitatively, IFN- γ increased the number of elongated, spindly MDM in both adult and cord blood MDM though this was more noticeable in the adult MDM (Figure 4.1). IL-4 treated adult MDM were rounded and had reduced numbers of elongated, spindly MDM to untreated controls. In general, cord blood MDM were more rounded than their adult MDM counterparts. Although IFN- γ treated cord blood MDM displayed some features of elongation, this was markedly reduced compared with adult MDM treated with IFN- γ . Very few elongated, spindly MDM were observed in the untreated or IL-4 treated cord blood MDM. These data indicate that treating adult MDM with IFN- γ results in elongation and a spindly appearance. This effect of IFN- γ on MDM morphology is qualitatively reduced in cord blood MDM. Conversely, IL-4 promotes rounded MDM morphology in human MDM.

4.2.1b The effect of IFN- γ or IL-4 on cell surface marker expression in adult and cord blood MDM

The expression of cell surface markers associated with macrophage activation in humans is inconsistently described in the literature. There is less consensus regarding the markers that accurately reflect classical pro-inflammatory “M1”-like activation of macrophages and alternatively activated anti-inflammatory “M2”-like macrophages in humans compared with the robust and reproducible markers described in mice^{153,160,162,165,196}. This may in part be due to disparate methods of macrophage differentiation and polarisation in human MDM.

This project sought to determine the phenotypic profile of human adult and cord blood MDM, differentiated using human serum and adherence purification, followed by

treatment with IFN- γ or IL-4. Briefly, PBMC were isolated from adult buffy coats or from umbilical cord blood which was collected immediately following delivery. MDM were adherence purified for 7 days in RPMI with 10% human serum and non-adherent cells were washed off on days 2 and 5. MDM were treated with IFN- γ or IL-4 on day 7 for 24 hours. MDM were harvested by placing in ice-cold PBS at 4°C for 30 minutes prior to gentle scraping. Cells were Fc blocked and stained with Zombie NIR viability dye and fluorochrome-conjugated antibodies specific for CD68, CD14, CD40, CD80, HLA-DR, CD83 and CD206 (mannose receptor; MMR) prior to acquisition by flow cytometry. MDM were gated on the basis of forward and side scatter, doublets and dead cells were excluded, and macrophages were identified as CD68⁺ CD14⁺ as described in the methods section **2.3** and as shown in the gating strategy (Figure 2.7).

CD40 is a key co-stimulatory molecule associated with “M1”-like proinflammatory activation of macrophages. CD40 cell surface expression was determined by median fluorescence intensity (MFI). A representative histogram for an adult donor shows the MFI for CD40 expression in untreated (black), IFN- γ (gold) or IL-4 (purple) treated MDM (Figure 4.2 A). Collated data from n=4 adult donors illustrate that CD40 was significantly upregulated in response to both IFN- γ (P<0.05) or IL-4 (P<0.05; Figure 4.2 B) and that IFN- γ significantly increased CD40 expression compared to IL-4 (P<0.05). A cord blood donor representative histogram illustrating the CD40 expression after treatment with IFN- γ (gold) or IL-4 (purple) or without treatment (black) is also shown (Figure 4.2 C). Similar to adult MDM, significant increases in CD40 expression were seen in cord blood MDM (n=4) after the addition of either IFN- γ (P<0.05) or IL-4 (P<0.05; Figure 4.2 D), however, the difference between IFN- γ and IL-4 did not reach statistical significance.

When the expression levels of CD40 were directly compared in adult and cord blood MDM, the data indicated that the increase in CD40 in response to IFN- γ treatment was significantly higher in the cord blood MDM compared with adult MDM ($P < 0.05$; Figure 4.2 E).

The expression of HLA-DR, an antigen presenting molecule, was determined by MFI and a representative adult donor histogram is shown in Figure 4.3 A. Treatment with IFN- γ significantly increased HLA-DR MFI in adult MDM ($P < 0.05$, Student's t-test, $n=4$) but no significant changes were seen with IL-4 treatment (Figure 4.3 B). Expression of HLA-DR was also examined in cord blood MDM ($n=4$) after IFN- γ or IL-4 treatment and a representative histogram is shown (Figure 4.3 C). There was a significant increase in HLA-DR seen in the cord blood MDM after both IFN- γ ($P < 0.01$) or IL-4 ($P < 0.01$) and the increase seen after IFN- γ was significantly higher than IL-4 ($P < 0.05$) (Figure 4.3 D). No significant difference in HLA-DR MFI was seen between the adult and cord blood MDM in response to IFN- γ or IL-4 (Figure 4.3 E).

CD86 is a co-stimulatory marker that has been described to increase following IL-4 exposure and to be associated with Th2 responses^{271,272}. A representative histogram for CD86 expression on MDM in an adult donor is shown (Figure 4.4 A). IFN- γ made no significant difference to CD86 but IL-4 significantly increased its expression compared with untreated controls (Figure 4.4 B, $n=4$, $P < 0.01$) and compared with IFN- γ treatment ($P < 0.05$). A cord blood MDM representative histogram is illustrated in Figure 4.4 C. Similarly to the adult response, IL-4 treatment significantly increased CD86 expression compared with untreated controls ($n=4$, $P < 0.05$, Student's t-test) and compared with

IFN- γ treatment ($P < 0.05$) (Figure 4.4 D). No significant difference in CD86 MFI was seen between the adult and cord blood MDM in response to IFN- γ or IL-4 (Figure 4.4 E).

MMR (CD206) was the first marker of the alternative activation pathway (analogous to 'M2' macrophages) to be described in murine macrophages¹⁵¹. A representative histogram of MMR expression in MDM from an adult donor is shown in Figure 4.5 A. MMR expression was not altered by IFN- γ but was statistically significantly increased after IL-4 treatment in adult MDM (Figure 4.5 B, $n=4$ $P < 0.05$, Student's t-test). Cord blood MDM were also analysed for MMR expression after IFN- γ or IL-4 treatment and a representative histogram is shown (Figure 4.5 C). IL-4 increased MMR expression compared with controls ($P < 0.05$, student's t-test) but no difference was seen with IFN- γ treatment (Figure 4.5 D). When the adult and cord blood MMR responses were compared, no significant differences were seen (Figure 4.5 E).

The expression of the activation marker CD83 in adult MDM is represented in a histogram from one donor (Figure 4.6 A). No significant difference is seen in CD83 expression after IFN- γ or IL-4 treatment (Figure 4.6 B). A representative histogram of CD83 expression in MDM from a cord blood donor is shown in Figure 4.6 C. IFN- γ or IL-4 treatment did not alter CD83 expression in cord blood MDM (Figure 4.6 D, $n=4$) and there was no significant difference between adult and cord blood MDM responses (Figure 4.6 E).

Similarly, no differences were seen in adult or cord blood MDM expression of CD80 after IFN- γ or IL-4 treatment. A representative adult donor (Figure 4.7 A) and the graph of the adult data for CD80 expression in MDM after IFN- γ or IL-4 treatment is shown (Figure

4.7 B, n=4). A representative histogram of CD80 expression in MDM from a cord blood donor is also shown (Figure 4.7 C). IFN- γ or IL-4 treatment did not alter CD83 expression in cord blood MDM (Figure 4.7 D, n=4) and there was no significant difference between adult and cord blood MDM responses (Figure 4.7 E).

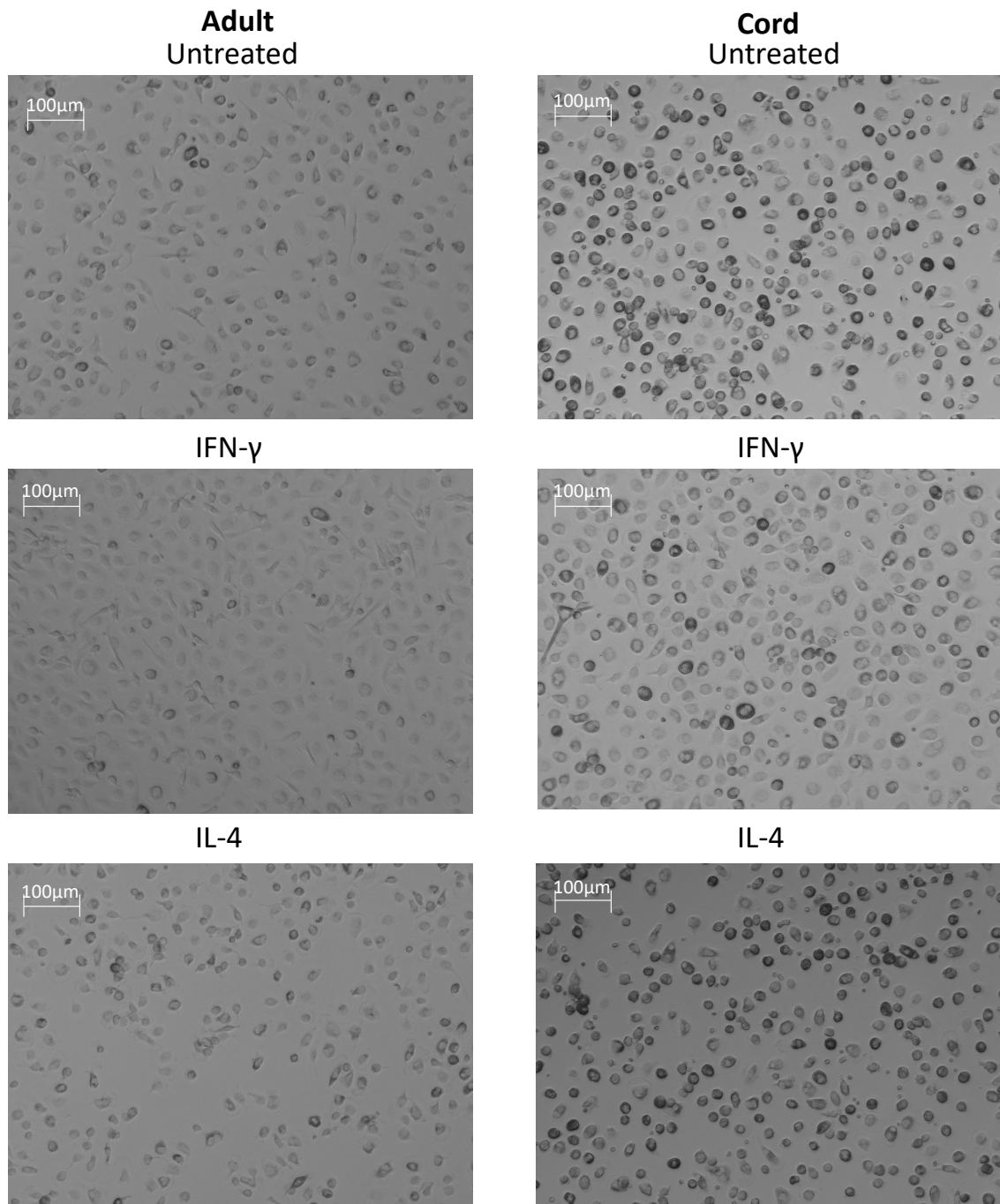


Figure 4.1 Morphology of adult and cord blood MDM 24 hours after treatment with IFN- γ or IL-4.

PBMC were isolated from buffy coats or from umbilical cord blood samples taken immediately following delivery. Adult or cord blood MDM were adherence purified for 7 days in 10% human serum. 24 hours after treatment with IFN- γ (10ng/ml) or IL-4 (10ng/ml) light microscopy (using a 10X objective) images of adult and cord MDM were taken.

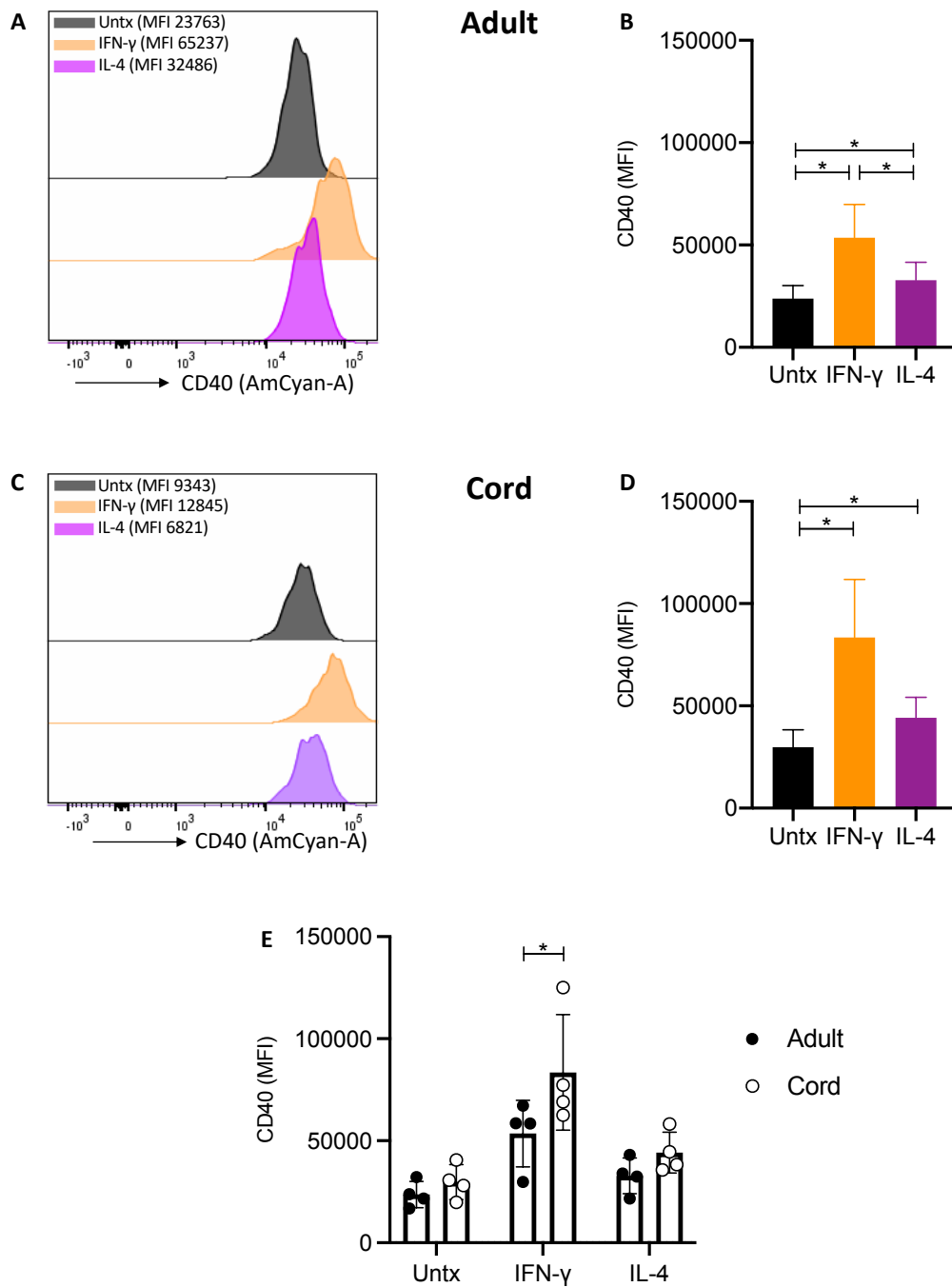


Figure 4.2 Expression of CD40 on adult and cord blood MDM 24 hours after IFN-γ or IL-4 treatment.

PBMC were isolated from buffy coats or from umbilical cord blood samples taken immediately following delivery. Adult or cord blood MDM were adherence purified for 7 days in 10% human serum. 24 hours after treatment with IFN-γ (10ng/ml) or IL-4 (10ng/ml), MDM were washed and detached from the plates by cooling and gentle scraping. Cells were Fc blocked, exposed to viability dye Zombie NIR and stained with fluorochrome-conjugated antibodies specific for CD14, CD68 and CD40. Cells were analysed by flow cytometry. The mean fluorescent intensity (MFI) of CD40 for the adult (A,B; n=4 ±SD) and cord (C,D; n=4 ±SD) MDM is shown. Comparison between the adult and cord blood values are show (E). Statistical significance was determined using one-way ANOVA with Dunnett's multiple comparison test and two-way ANOVA using Sidak's multiple comparison test; * P<0.05. Paired student t-tests were also performed.

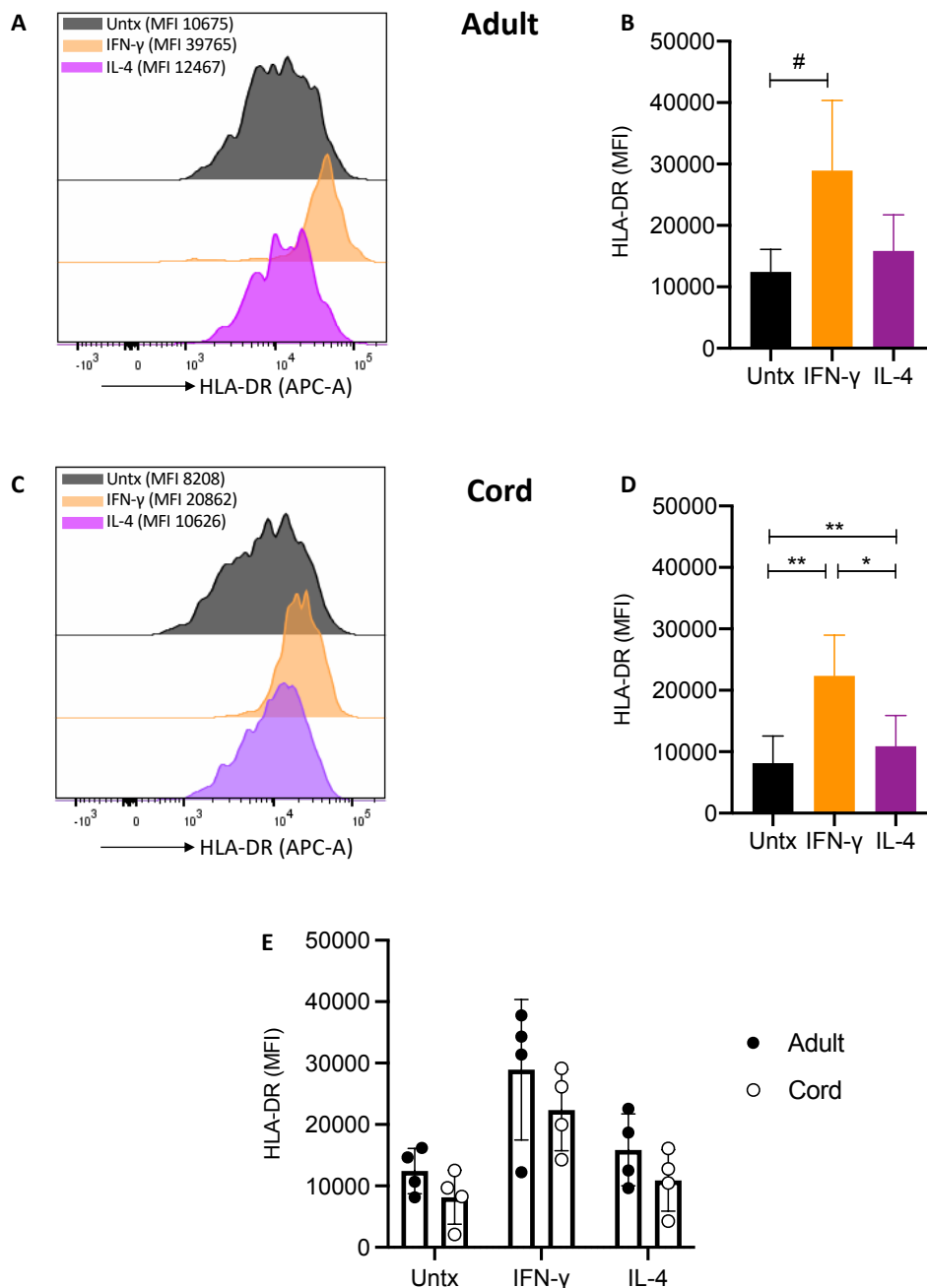


Figure 4.3 Expression of HLA-DR on adult and cord blood MDM 24 hours after IFN- γ or IL-4 treatment.

PBMC were isolated from buffy coats or from umbilical cord blood samples taken immediately following delivery. Adult or cord blood MDM were adherence purified for 7 days in 10% human serum. 24 hours after treatment with IFN- γ (10ng/ml) or IL-4 (10ng/ml), MDM were washed and detached from the plates by cooling and gentle scraping. Cells were Fc blocked, exposed to viability dye Zombie NIR and stained with fluorochrome-conjugated antibodies specific for CD14, CD68 and HLA-DR. Cells were analysed by flow cytometry. The mean fluorescent intensity (MFI) of HLA-DR for the adult (A,B; $n=4 \pm SD$) and cord (C,D; $n=4 \pm SD$) MDM is shown. Comparison between the adult and cord blood values are shown (E). Statistical significance was determined using one-way ANOVA with Dunnett's multiple comparison test and two-way ANOVA using Sidak's multiple comparison test; * $P<0.05$, ** $P<0.01$. Paired student t-tests were also performed; # $P<0.05$.

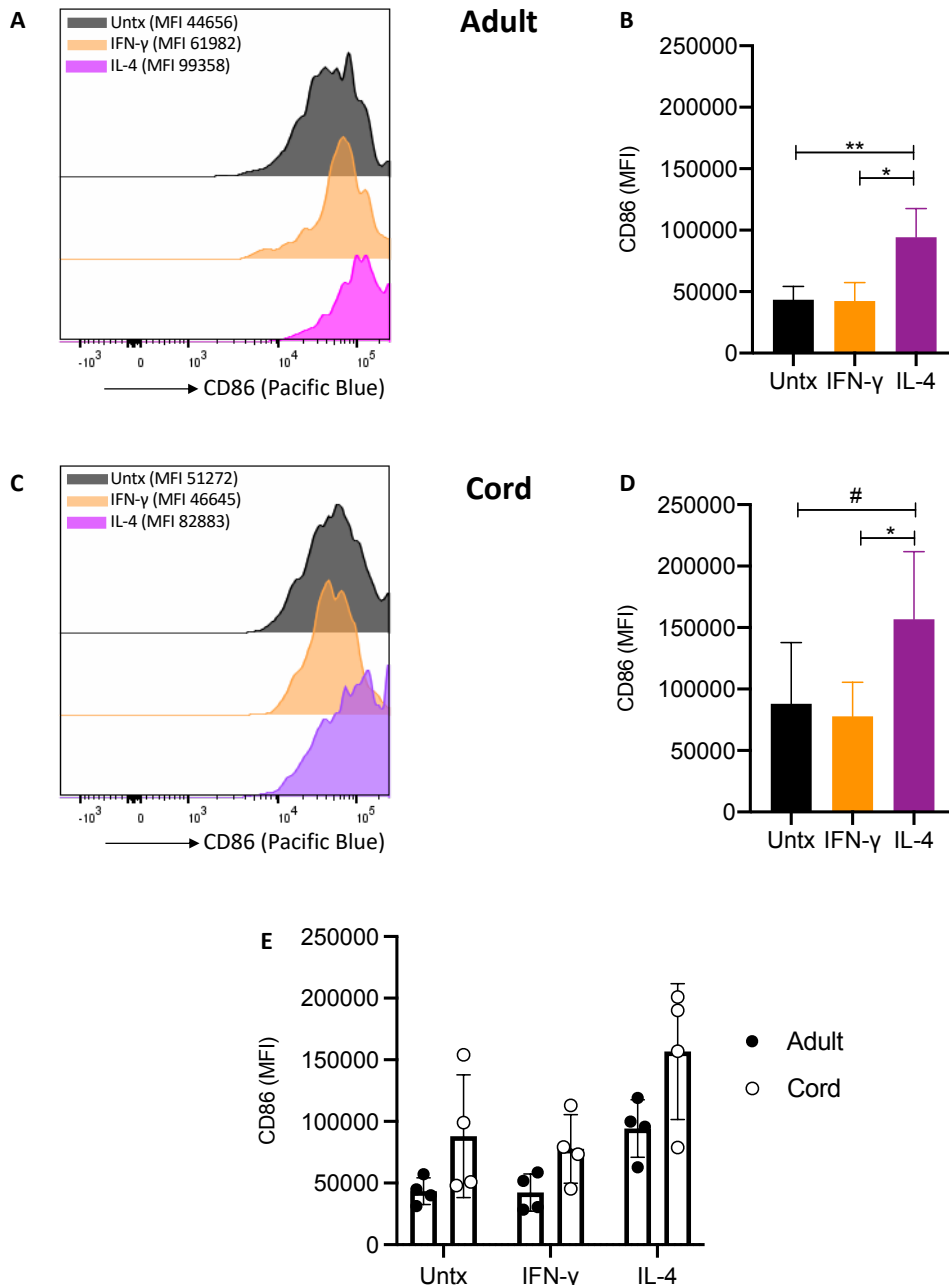


Figure 4.4 Expression of CD86 on adult and cord blood MDM 24 hours after IFN- γ or IL-4 treatment.

PBMC were isolated from buffy coats or from umbilical cord blood samples taken immediately following delivery. Adult or cord blood MDM were adherence purified for 7 days in 10% human serum. 24 hours after treatment with IFN- γ (10ng/ml) or IL-4 (10ng/ml), MDM were washed and detached from the plates by cooling and gentle scraping. Cells were Fc blocked, exposed to viability dye Zombie NIR and stained with fluorochrome-conjugated antibodies specific for CD14, CD68 and CD86. Cells were analysed by flow cytometry. The mean fluorescent intensity (MFI) of CD86 for the adult (A,B; $n=4 \pm SD$) and cord (C,D; $n=4 \pm SD$) MDM is shown. Comparison between the adult and cord blood values are shown (E). Statistical significance was determined using one-way ANOVA with Dunnett's multiple comparison test and two-way ANOVA using Sidak's multiple comparison test; * $P<0.05$, ** $P<0.01$. Paired student t-tests were also performed; # $P<0.05$.

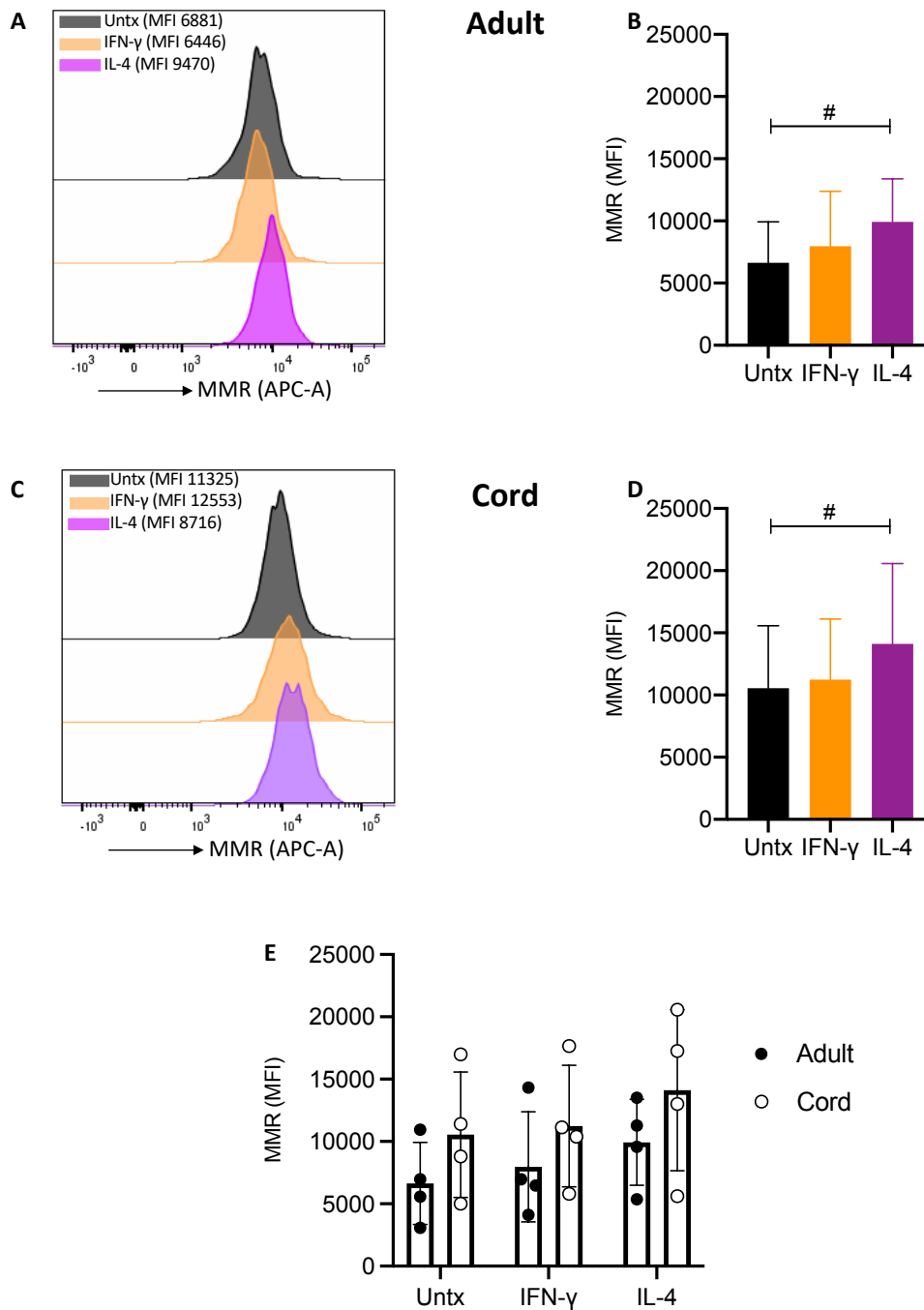


Figure 4.5 Expression of MMR on adult and cord blood MDM 24 hours after IFN- γ or IL-4 treatment.

PBMC were isolated from buffy coats or from umbilical cord blood samples taken immediately following delivery. Adult or cord blood MDM were adherence purified for 7 days in 10% human serum. 24 hours after treatment with IFN- γ (10ng/ml) or IL-4 (10ng/ml), MDM were washed and detached from the plates by cooling and gentle scraping. Cells were Fc blocked, exposed to viability dye Zombie NIR and stained with fluorochrome-conjugated antibodies specific for CD14, CD68 and MMR. Cells were analysed by flow cytometry. The mean fluorescent intensity (MFI) of MMR for the adult (A,B; $n=4 \pm SD$) and cord (C,D; $n=4 \pm SD$) MDM is shown. Comparison between the adult and cord blood values are shown (E). Statistical significance was determined using one-way ANOVA with Dunnett's multiple comparison test and two-way ANOVA using Sidak's multiple comparison test. Paired student t-tests were also performed; # $P < 0.05$.

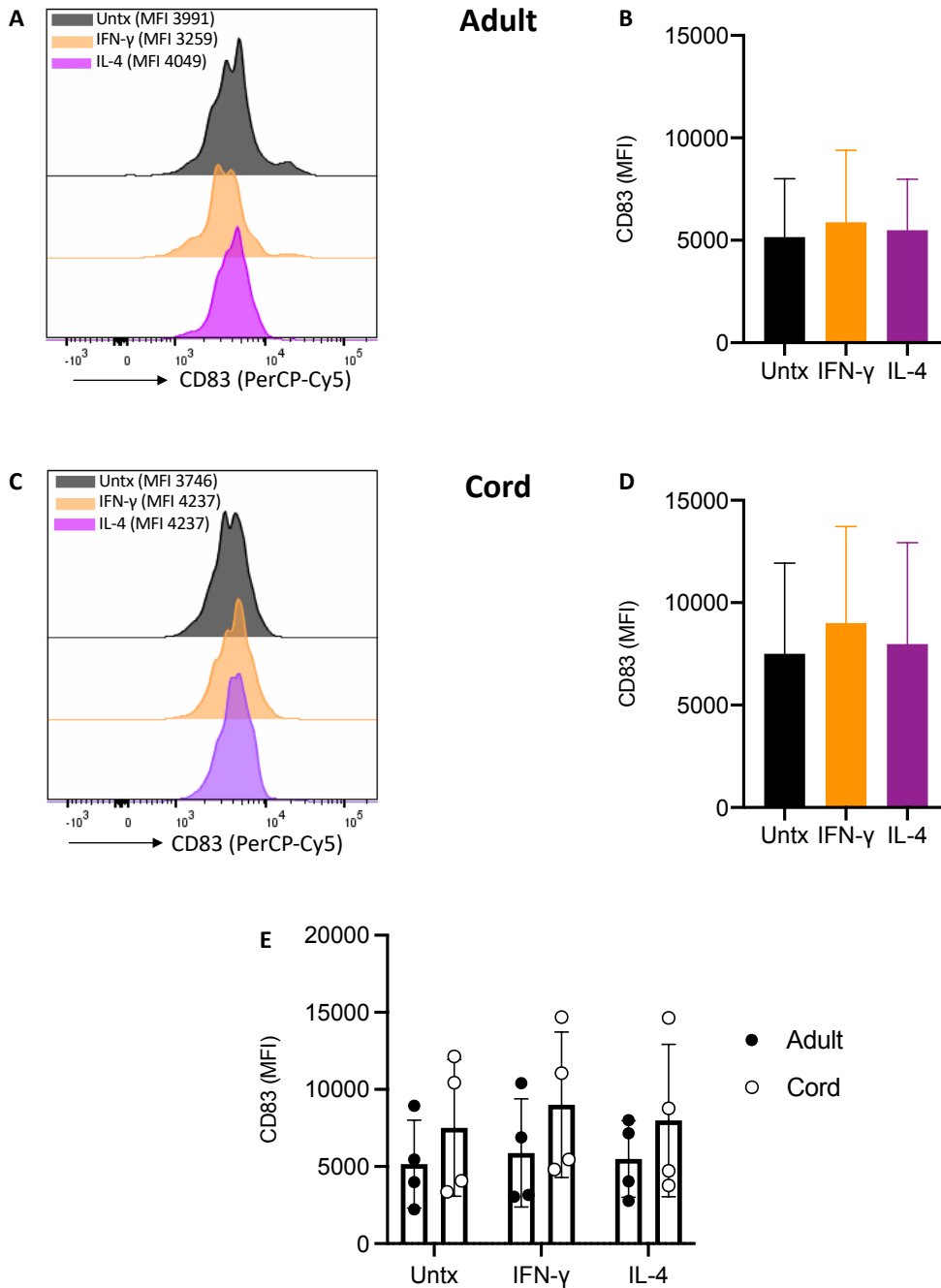


Figure 4.6 Expression of CD83 on adult and cord blood MDM 24 hours after IFN- γ or IL-4 treatment.

PBMC were isolated from buffy coats or from umbilical cord blood samples taken immediately following delivery. Adult or cord blood MDM were adherence purified for 7 days in 10% human serum. 24 hours after treatment with IFN- γ (10ng/ml) or IL-4 (10ng/ml), MDM were washed and detached from the plates by cooling and gentle scraping. Cells were Fc blocked, exposed to viability dye Zombie NIR and stained with fluorochrome-conjugated antibodies specific for CD14, CD68 and CD83. Cells were analysed by flow cytometry. The mean fluorescent intensity (MFI) of CD83 for the adult (A,B; $n=4 \pm SD$) and cord (C,D; $n=4 \pm SD$) MDM is shown. Comparison between the adult and cord blood values are shown (E). Statistical significance was determined using one-way ANOVA with Dunnett's multiple comparison test and two-way ANOVA using Sidak's multiple comparison test. Paired student t-tests were also performed.

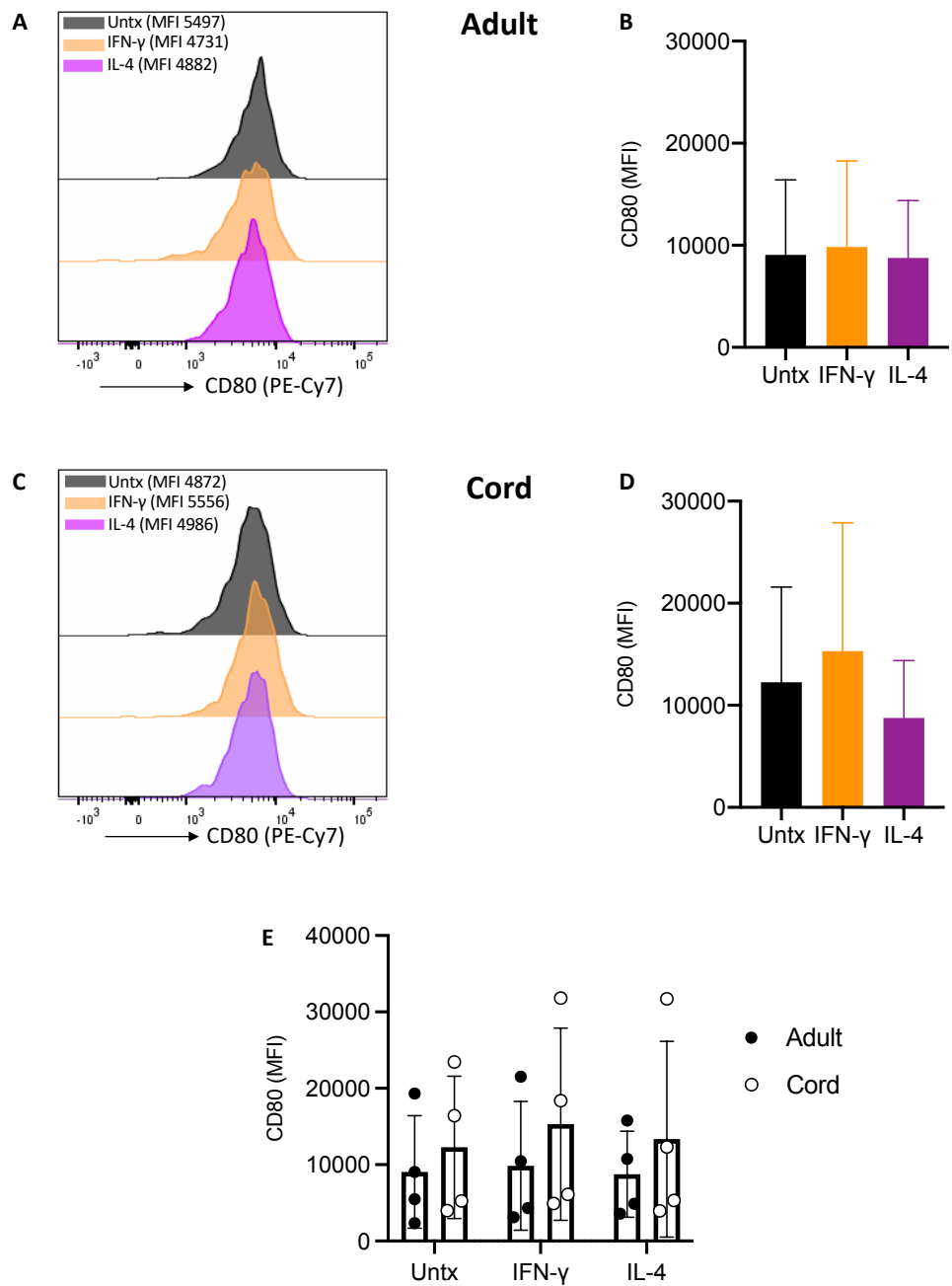


Figure 4.7 Expression of CD80 on adult and cord blood MDM 24 hours after IFN- γ or IL-4 treatment.

PBMC were isolated from buffy coats or from umbilical cord blood samples taken immediately following delivery. Adult or cord blood MDM were adherence purified for 7 days in 10% human serum. 24 hours after treatment with IFN- γ (10ng/ml) or IL-4 (10ng/ml), MDM were washed and detached from the plates by cooling and gentle scraping. Cells were Fc blocked, exposed to viability dye Zombie NIR and stained with fluorochrome-conjugated antibodies specific for CD14, CD68 and CD80. Cells were analysed by flow cytometry. The mean fluorescent intensity (MFI) of CD80 for the adult (A,B; n=4 \pm SD) and cord (C,D; n=4 \pm SD) MDM is shown. Comparison between the adult and cord blood values are shown (E). Statistical significance was determined using one-way ANOVA with Dunnett's multiple comparison test and two-way ANOVA using Sidak's multiple comparison test. Paired student t-tests were also performed.

4.2.2 The effect of IFN- γ or IL-4 on metabolism in adult and cord blood MDM

There is a paucity of data on changes in metabolism in human MDM following polarisation with cytokines. IFN- γ polarisation in murine models has previously been demonstrated to depend on glycolysis but most murine studies show minimal change in glycolysis in IL-4 polarised MDM^{273–275}. However, the data generated in chapter 3 highlights the differences in reported murine BMDM metabolism and those found in human MDM²⁷⁶. In a model of polarised macrophages from umbilical cord blood, IFN- γ was shown to abrogate glycolysis during a stress test but the changes to the baseline glycolytic rate was not reported²³⁰.

In order to examine the metabolic impact of IFN- γ or IL-4 in human macrophages, the metabolic response of human MDM to stimulation with IFN- γ or IL-4 was analysed 24 hours after treatment. PBMC were isolated from buffy coats or from umbilical cord blood samples taken immediately following delivery. Adult or cord blood MDM were adherence purified for 7 days in 10% human serum. MDM were washed and detached from the plates by cooling and gently scraped, counted and re-seeded on Seahorse culture plates prior to analysis. IFN- γ (10ng/ml) or IL-4 (10ng/ml) was added 24 hours prior to analysis of the baseline ECAR and OCR, which was taken as the third reading on the Seahorse XFe Analyzer.

4.2.2a IFN- γ increases OCR in adult, but not cord blood MDM

24 hours after treatment with IFN- γ or IL-4 the OCR of both adult and cord blood MDM were recorded (Figure 4.8). Time course graphs for collated data of adult and cord blood MDM are expressed as both the raw values (Figure 4.8 A and B respectively) and the %

change (Figure 4.8 C and D respectively) from the third baseline reading of the untreated MDM in order to normalise for differences in human variability and for technical variability in cell seeding density on the Seahorse culture plate. This reading was chosen as it allows time for the machine to reach a steady state of measurement after calibration. An increase is seen in the OCR in adult MDM (Figure 4.8 A) but not cord MDM (Figure 4.8 B) after IFN- γ treatment. The % change in OCR from the untreated MDM show an increase in OCR after IFN- γ and a slight decrease after IL-4 in adult MDM (Figure 4.8 C) but no obvious changes in cord blood responses (Figure 4.8 D).

In order to analyse the effect of cytokine treatment on the OCR, the third reading taken on the Seahorse Analyzer for the MDM treated with IFN- γ or IL-4 was used to compare with the third reading for the untreated MDM (Figure 4.9). In adult MDM the raw values in OCR after IFN- γ treatment were not significantly altered (Figure 4.9 A, left) but the % change from the untreated MDM was significantly increased (Figure 4.9 A, right, $P < 0.05$). IL-4 did not significantly alter the OCR or the % change in OCR from untreated MDM in adult donors (Figure 4.9 B). In cord blood MDM no significant difference in OCR or % change in OCR was observed after either IFN- γ (Figure 4.9 C) or IL-4 (Figure 4.9 D).

4.2.2b IFN- γ increases and IL-4 decreases ECAR in both adult and cord blood MDM

The ECAR of both adult and cord blood MDM was recorded 24 hours after treatment with IFN- γ or IL-4. Time course graphs for collated data of adult and cord blood MDM are expressed as both the raw values (Figure 4.10 A and B respectively) and the % change (Figure 4.10 C and D respectively) from the third baseline reading of the untreated MDM in order to normalise for differences in human variability and for

technical variability in cell seeding density on the Seahorse culture plate. On the time course graphs, IFN- γ increased the raw values and % change in ECAR in adult and cord blood MDM and IL-4 caused a decrease in the raw ECAR and % change in ECAR. Analysis was undertaken at the third reading. In the adult MDM, IFN- γ caused a significant increase in the ECAR ($P < 0.05$) and the % difference in ECAR from baseline (Figure 4.11 A, $P < 0.01$). IL-4 significantly reduced the ECAR ($P < 0.05$) and the % difference in ECAR from baseline (Figure 4.11 B, $P < 0.01$). A similar pattern was seen in the cord blood MDM with an increase in ECAR ($P < 0.05$) after IFN- γ treatment, however the % difference in ECAR was not statistically significant (Figure 4.11 C). IL-4 also caused a trend downward in cord blood MDM ECAR and % change in ECAR ($P = 0.06$) though the differences did not reach statistical significance.

4.2.2c Comparison between adult and cord blood MDM metabolism 24 hours after treatment with IFN- γ or IL-4

In order to determine the differential metabolic effect of IFN- γ or IL-4 in adult and cord blood MDM, a direct comparison between the ECAR or OCR values from adult and cord MDM was made. Data points from the third reading as described above for the ECAR and OCR absolute raw values and % changes from unstimulated controls were analysed. No statistically significant differences between the adult and cord blood responses to IFN- γ or IL-4 were seen in OCR (Figure 4.12 A), ECAR (Figure 4.12 B), % change in OCR (Figure 4.12 C), or % change in ECAR (Figure 4.12 D). Although not statistically significant, these data highlights the similar patterns seen in ECAR in both adult and cord blood MDM after IFN- γ or IL-4 treatment. However, adult MDM alter OCR in response to IFN- γ but cord blood MDM do not alter their oxygen consumption.

4.2.2d ECAR/OCR ratio of adult and cord blood MDM 24 hours after treatment with IFN- γ or IL-4

The ECAR/OCR ratio was calculated for both adult and cord blood MDM 24 hours after treatment with IFN- γ or IL-4. For the adult MDM, a significant increase was seen in the ECAR/OCR ratio after IFN- γ treatment ($P < 0.05$, Student's t-test) and a decrease was seen after IL-4 treatment (Figure 4.13 A, $P < 0.05$). The difference in ECAR/OCR ratio between IFN- γ and IL-4 was also significant (Figure 4.13 A). For the cord blood MDM, the ECAR/OCR ratio changes after IFN- γ or IL-4 were not significantly different compared with untreated MDM, although the difference in the ECAR/OCR ratio between IFN- γ and IL-4 reached statistical significance (Figure 4.13 B, $P < 0.05$). Comparison was made between the ECAR/OCR ratios of the adult and cord blood MDM (Figure 4.13 C) and no significant differences were seen. The ECAR/OCR ratio in cord blood MDM treated with IFN- γ trends toward an increase compared with the adult MDM, which is consistent with the stable OCR in cord blood MDM treated with IFN- γ compared with the increased OCR in IFN- γ treated adult MDM.

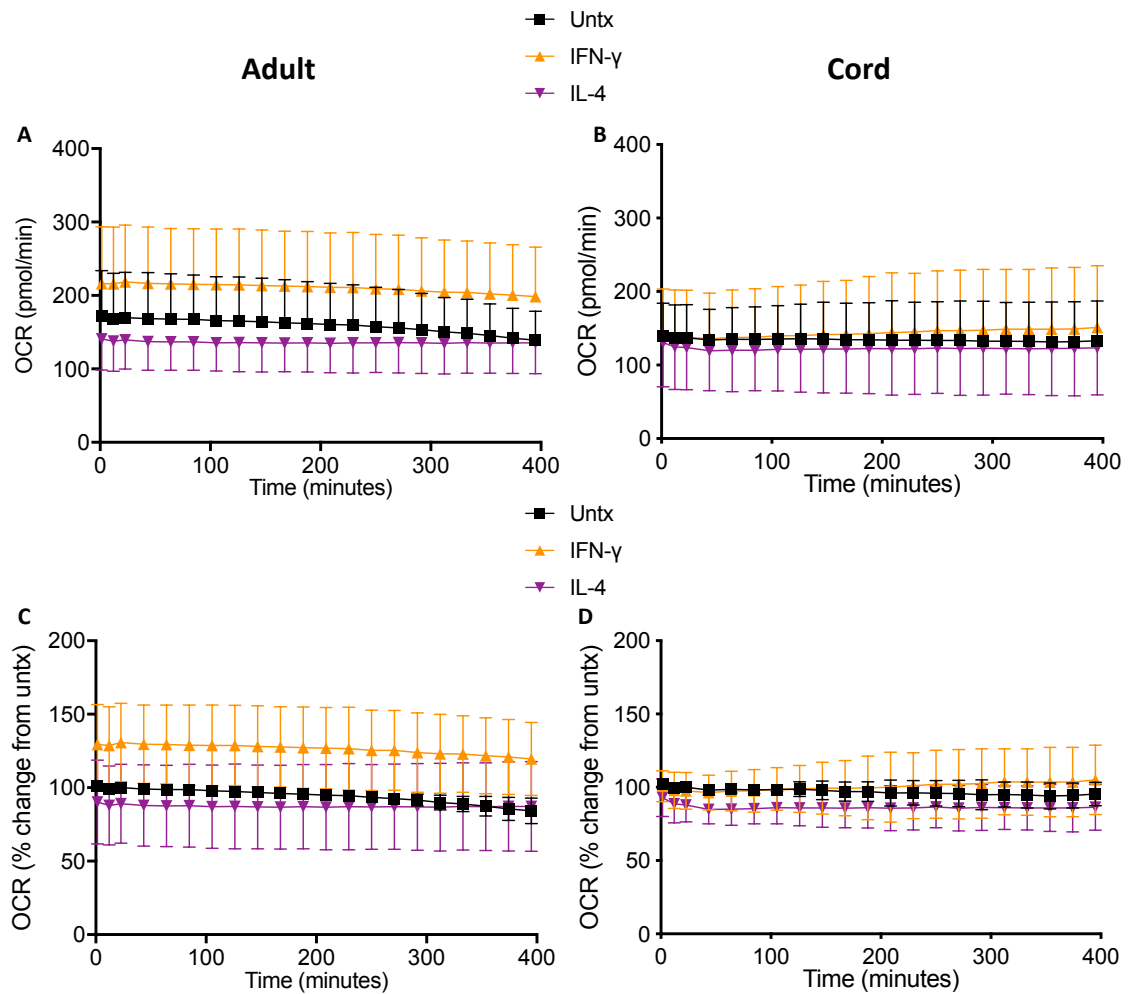
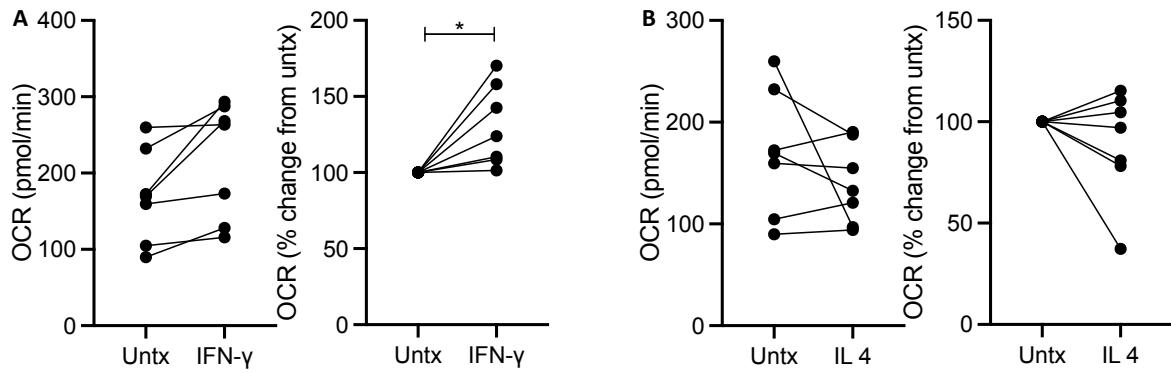


Figure 4.8 IFN- γ increases OCR in adult, but not cord blood MDM.

PBMC were isolated from buffy coats or from umbilical cord blood samples taken immediately following delivery. Adult or cord blood MDM were adherence purified for 7 days in 10% human serum. MDM were washed and detached from the plates by cooling and gently scraped, counted and re-seeded on Seahorse culture plates prior to analysis in the Seahorse XFe24 Analyzer. IFN- γ (10ng/ml) or IL-4 (10ng/ml) was added 24 hours prior to analysis in the Seahorse Analyzer. The OCR was recorded approximately every 9 minutes. Correction for small variations in cell density was achieved by % comparison to the OCR of the untreated (untx) MDM. The time-course graphs illustrate the OCR of adult MDM (A,C n=7) or cord blood MDM (n=3) in real time 24 hours after treatment with IFN- γ or IL-4.

Adult



Cord

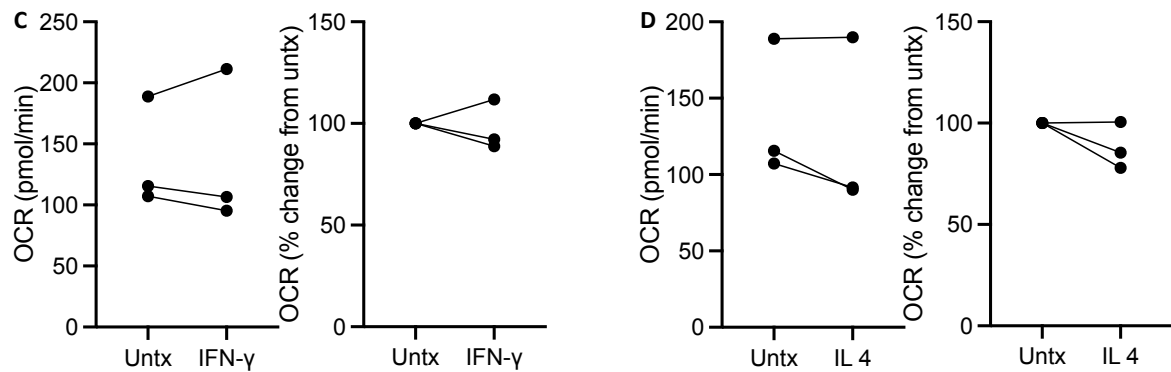


Figure 4.9 Analysis of OCR in adult and cord blood MDM after IFN- γ or IL-4.

PBMC were isolated from buffy coats or from umbilical cord blood samples taken immediately following delivery. Adult or cord blood MDM were adherence purified for 7 days in 10% human serum. MDM were washed and detached from the plates by cooling and gently scraped, counted, and re-seeded on Seahorse culture plates prior to analysis in the Seahorse XFe24 Analyzer. IFN- γ (10ng/ml) or IL-4 (10ng/ml) was added 24 hours prior to analysis in the Seahorse Analyzer. The OCR was recorded approximately every 9 minutes. Correction for small variations in cell density was achieved by % comparison to the OCR of the untreated (untx) MDM. The third reading of OCR in Figure 4.8 was analysed for the adult (n=7) and cord blood MDM (n=3). Statistically significant differences were determined using a paired Student's t test; * P<0.05.

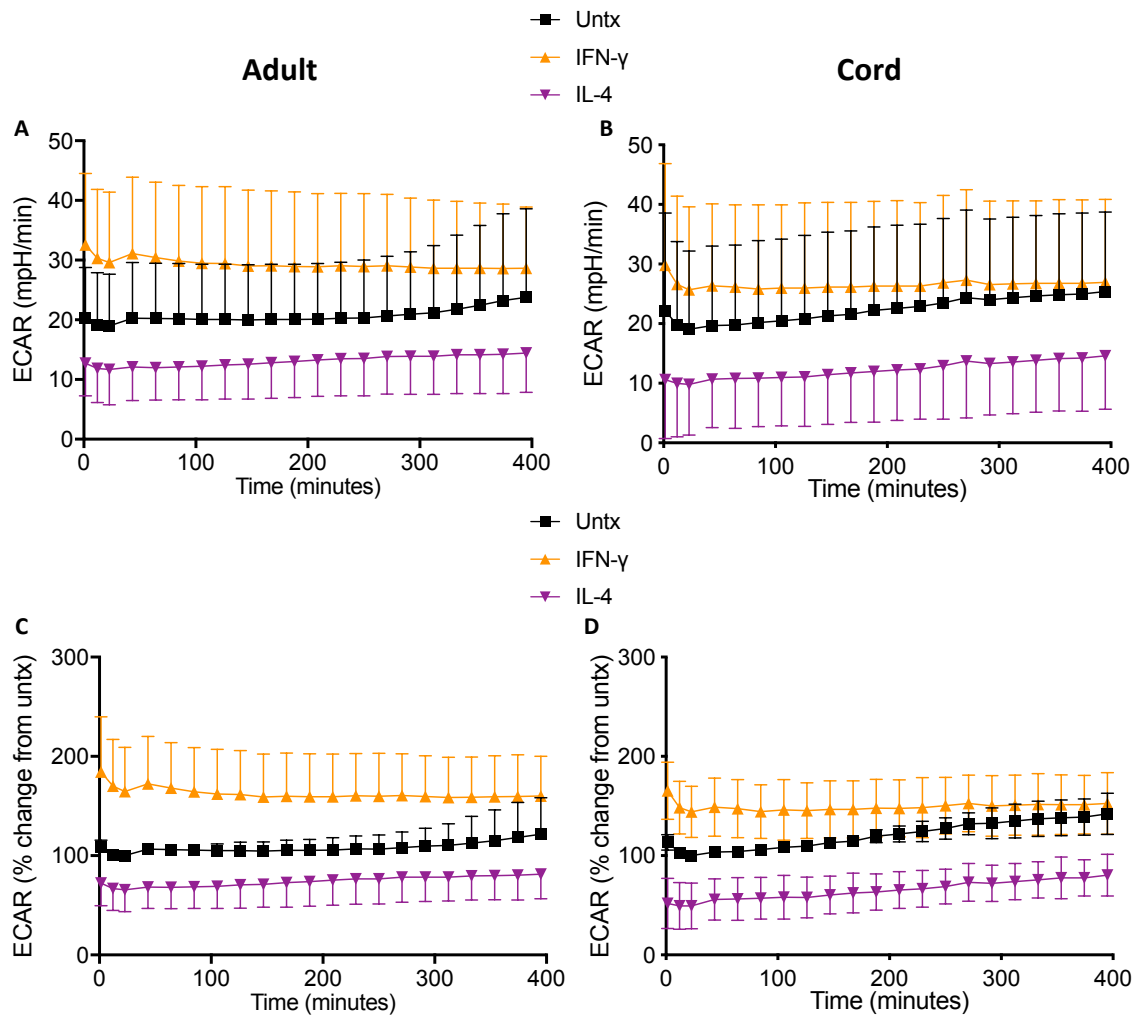


Figure 4.10 IFN- γ increases, and IL-4 decreases ECAR in both adult and cord blood MDM

PBMC were isolated from buffy coats or from umbilical cord blood samples taken immediately following delivery. Adult or cord blood MDM were adherence purified for 7 days in 10% human serum. MDM were washed and detached from the plates by cooling and gently scraped, counted and re-seeded on Seahorse culture plates prior to analysis in the Seahorse XFe24 Analyzer. IFN- γ (10ng/ml) or IL-4 (10ng/ml) was added 24 hours prior to analysis in the Seahorse Analyzer. The ECAR was recorded approximately every 9 minutes. Correction for small variations in cell density was achieved by % comparison to the ECAR of the untreated (untx) MDM. The time-course graphs illustrate the ECAR of adult MDM (A,C n=7) or cord blood MDM (B,D n=3) in real time 24 hours after treatment with IFN- γ or IL-4.

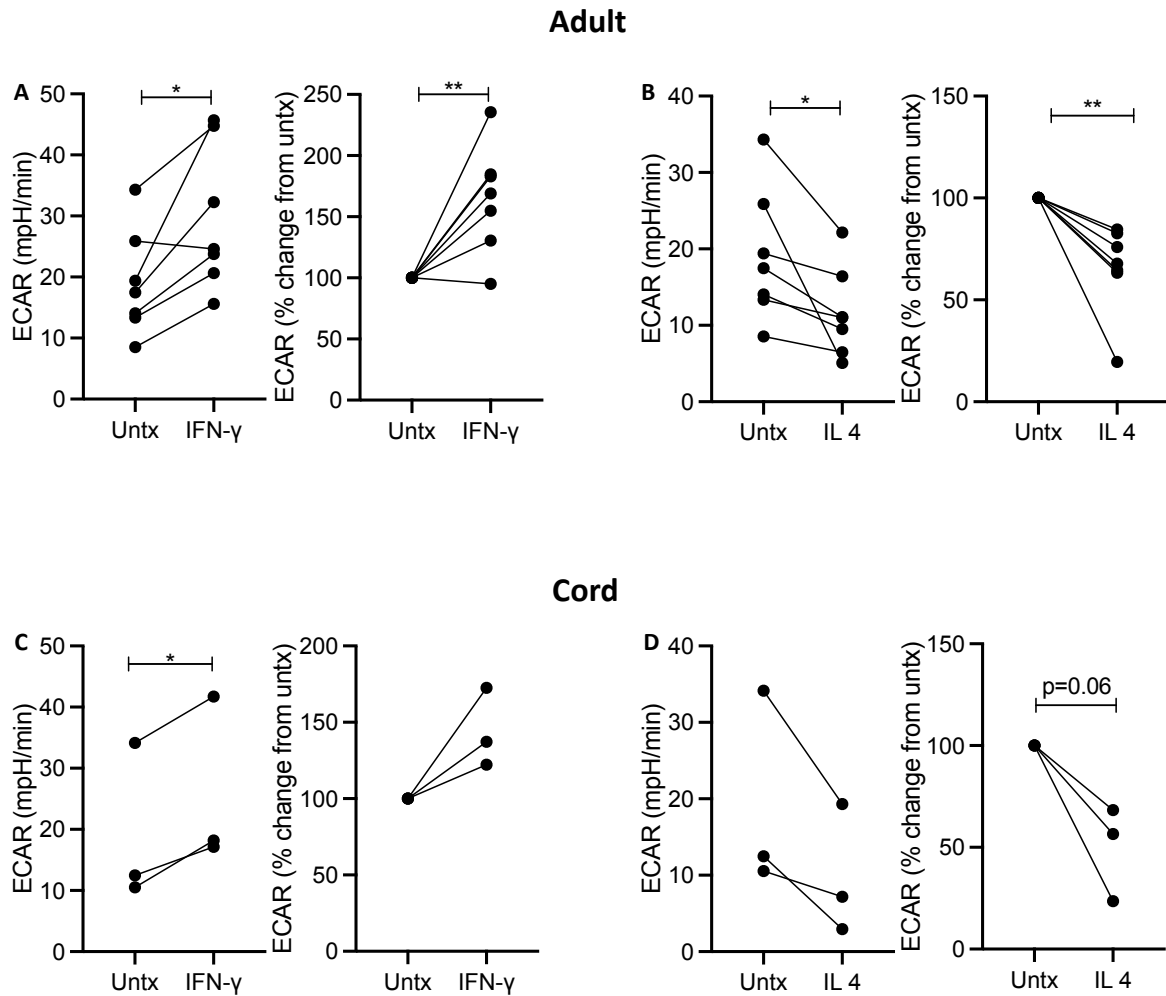


Figure 4.11 Analysis of ECAR in adult and cord blood MDM after IFN- γ or IL-4.

PBMC were isolated from buffy coats or from umbilical cord blood samples taken immediately following delivery. Adult or cord blood MDM were adherence purified for 7 days in 10% human serum. MDM were washed and detached from the plates by cooling and gently scraped, counted and re-seeded on Seahorse culture plates prior to analysis in the Seahorse XFe24 Analyzer. IFN- γ (10ng/ml) or IL-4 (10ng/ml) was added 24 hours prior to analysis in the Seahorse Analyzer. The ECAR was recorded approximately every 9 minutes. Correction for small variations in cell density was achieved by % comparison to the OCR of the untreated (untx) MDM. The third reading of ECAR in Figure 4.10 was analysed for the adult (n=7) and cord blood MDM (n=3). Statistically significant differences were determined using a paired Student's t test; * P<0.05, ** P<0.01.

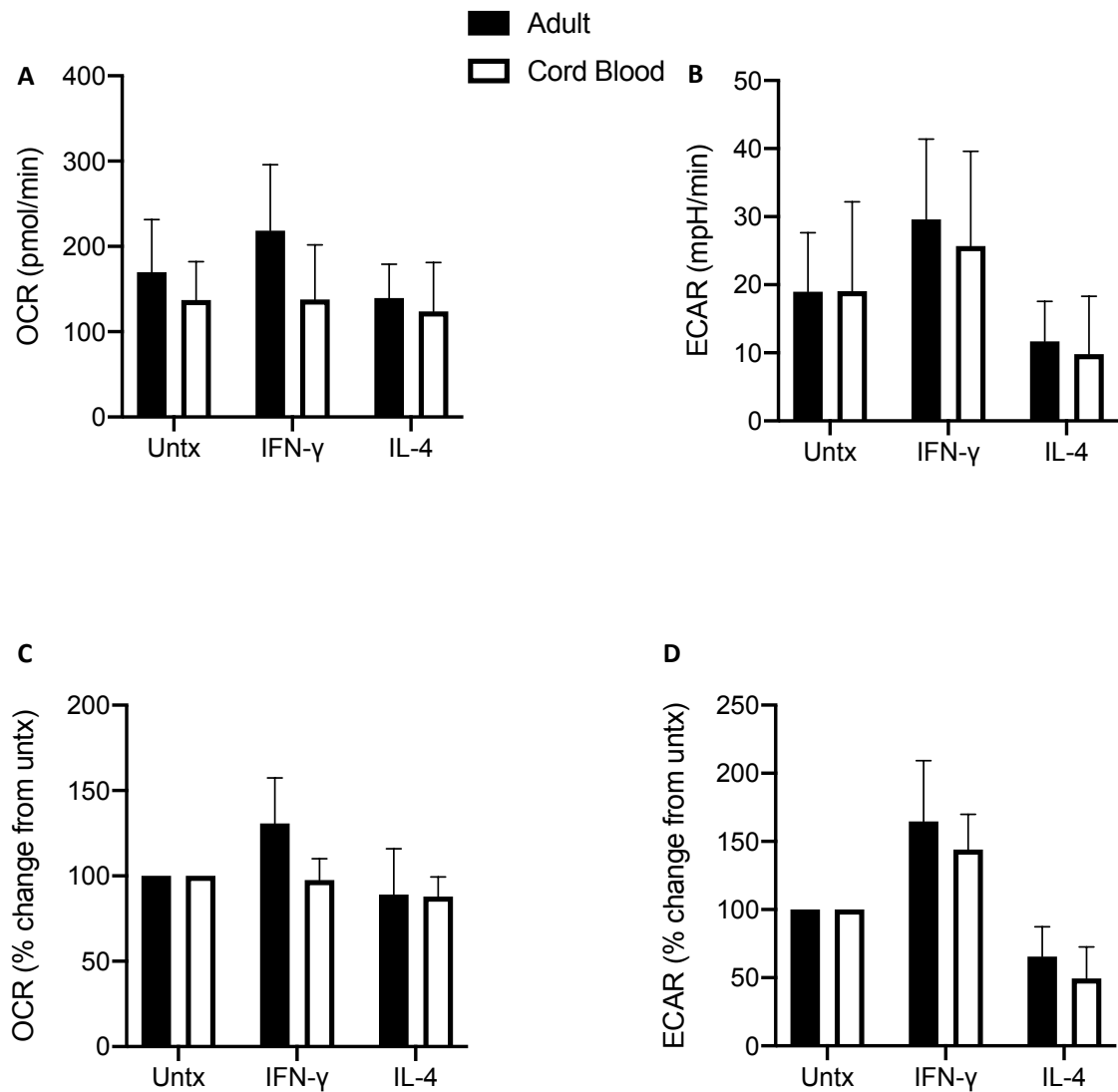


Figure 4.12 Comparison between adult and cord blood MDM metabolic responses 24 hours after IFN- γ or IL-4.

PBMC were isolated from buffy coats or from umbilical cord blood samples taken immediately following delivery. Adult or cord blood MDM were adherence purified for 7 days in 10% human serum. MDM were washed and detached from the plates by cooling and gently scraped, counted and re-seeded on Seahorse culture plates prior to analysis in the Seahorse XFe24 Analyzer. IFN- γ (10ng/ml) or IL-4 (10ng/ml) was added 24 hours prior to analysis in the Seahorse Analyzer. The ECAR and OCR was recorded approximately every 9 minutes. Correction for small variations in cell density was achieved by % comparison to the untreated (untx) MDM. Comparative analysis of the adult (n=7) and cord blood MDM (n=3) is shown. Statistically significant differences were determined using one-way ANOVA.

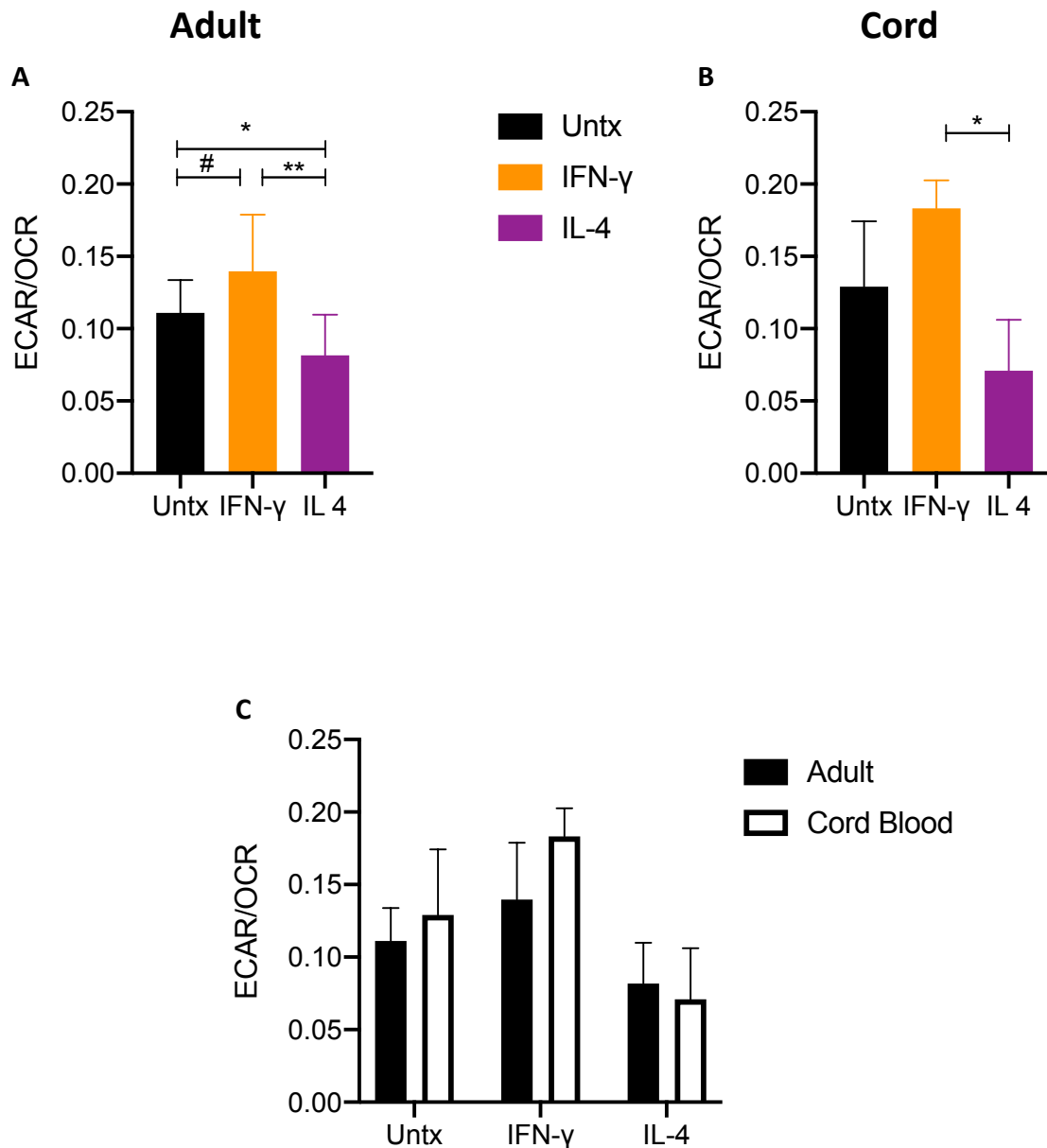


Figure 4.13 ECAR/OCR ratio of adult and cord blood MDM 24 hours after IFN- γ or IL-4 treatment

PBMC were isolated from buffy coats or from umbilical cord blood samples taken immediately following delivery. Adult or cord blood MDM were adherence purified for 7 days in 10% human serum. MDM were washed and detached from the plates by cooling and gently scraped, counted and re-seeded on Seahorse culture plates prior to analysis in the Seahorse XFe24 Analyzer. IFN- γ (10ng/ml) or IL-4 (10ng/ml) was added 24 hours prior to analysis in the Seahorse Analyzer. The ECAR and OCR was recorded approximately every 9 minutes. The baseline OCR and ECAR was taken as the third reading and the ECAR/OCR ratio calculated from these values for the adult (A, n=7) and cord blood MDM (B, n=3). Comparative analysis between the adult and cord blood ECAR/OCR ratio is shown (C). Statistical significance was determined using one-way ANOVA with Tukey's multiple comparison test and two-way ANOVA using Sidak's multiple comparison test; * P<0.05, **P<0.01. Paired student t-tests were also performed; # P<0.05.

4.2.3 The effect of IFN- γ or IL-4 on adult and cord blood MDM metabolic responses to Mtb and LPS

Having established that IFN- γ and IL-4 impact MDM metabolism and phenotype in both adult and cord blood MDM, the effect of exposure to these cytokines on subsequent immunometabolic responses to Mtb and LPS was established. Novel findings of early inflammatory Warburg were described in Chapter 3 and the impact of pretreatment for 24 hours with IFN- γ and IL-4 on subsequent metabolic shifts in adult and cord blood MDM following Mtb or LPS stimulation was examined in the Seahorse XFe24 Analyzer.

PBMC were isolated from buffy coats or from umbilical cord blood samples taken immediately following delivery. Adult or cord blood MDM were adherence purified for 7 days in 10% human serum. MDM were washed and detached from the plates by cooling and gently scraped, counted, and re-seeded on Seahorse culture plates prior to analysis in the Seahorse XFe24 Analyzer. IFN- γ (10ng/ml) or IL-4 (10ng/ml) were added 24 hours prior to live analysis of ECAR and OCR in the Seahorse XFe24 Analyzer. Mtb (iH37Rv; MOI 1-10) or LPS (100 ng/ml) were added to wells containing differentiated human adult or cord blood MDM using the injection ports of the Seahorse XFe24 Analyzer. The ECAR and OCR were recorded approximately every 9 minutes for the first 3 readings and then every 20 minutes thereafter. The third Seahorse reading was taken as the baseline to calculate the % change from baseline in order to normalise for differences in human variability and for technical variability in cell seeding density on the Seahorse culture plate. This value highlights the effect of the pretreatment of IFN- γ and IL-4 on the subsequent metabolic shift after Mtb or LPS stimulation. The untreated MDM, immediately prior to Mtb stimulation, which is the third reading on the Seahorse

XFe Analyzer, was used as the comparison for the % change from unstimulated MDM. This value illustrates the cumulative impact of both the cytokine and the antigen stimulation on the levels of ECAR and OCR. Analysis of the metabolic shifts was undertaken at the same time point in Chapter 3, 150 minutes after stimulation. This timepoint was when the ECAR and OCR were furthest from baseline.

4.2.3a IL-4 inhibits the drop in OCR seen after Mtb stimulation in adult MDM

The time course graph of the OCR response of both adult and cord blood MDM to Mtb stimulation after IFN- γ and IL-4 is illustrated in Figure 4.14. The time course for the collated adult raw values (n=6) show that the OCR for the IFN- γ treated MDM is higher than the untreated MDM and that there is a drop in the OCR after Mtb stimulation (Figure 4.14 A). The cord blood MDM (n=3) have little difference in OCR between the untreated, IFN- γ and IL-4 both before and after Mtb stimulation (Figure 4.14 B). The % change in OCR from the untreated adult MDM highlights the greater OCR of the IFN- γ treated MDM prior to and after Mtb stimulation (Figure 4.14 C). The cord blood % change from baseline OCR shows that IFN- γ does increase the OCR and IL-4 decrease the OCR when compared to the untreated MDM (Figure 4.14 D). The % change from baseline, which shows the change in OCR after Mtb stimulation, shows that the untreated and IFN- γ treated MDM both decrease OCR after Mtb stimulation, as seen in Chapter 3, but that the IL-4 treated MDM do not decrease OCR (Figure 4.14 E). The IL-4 treated cord blood MDM appear to have a minimal increase in the OCR as expressed by % change from baseline but little effect is seen in the IFN- γ treated or untreated MDM (Figure 4.14 F).

Analysis of the changes in OCR at 150 minutes post stimulation in the adult MDM show that pre-treatment with IFN- γ significantly increases the OCR when compared with the untreated ($P < 0.01$) or to the IL-4 treated MDM (Figure 4.15 A, $P < 0.01$). No significant change is seen in the cord blood MDM OCR response to Mtb with IFN- γ or IL-4 (Figure 4.15 B). The % change from the untreated MDM show a similar pattern with IFN- γ significantly increasing the OCR when compared with the untreated ($P < 0.01$) or to the IL-4 treated MDM (Figure 4.15 C, $P < 0.01$). The % change from untreated in cord blood MDM does not show any significant difference after IFN- γ or IL-4 treatment (Figure 4.15 D). The % change from baseline, which is a reflection of the shift in metabolism after Mtb stimulation, shows that IL-4 treatment significantly increases the OCR % change from baseline in response to Mtb (Figure 4.15 E, $P < 0.05$). Both the untreated and IFN- γ treated MDM drop the OCR to approximately 88% of the baseline upon Mtb stimulation, while the IL-4 treated MDM remain at 100% of baseline. This shows that IL-4 prevents the decrease seen in OCR after Mtb stimulation. In the cord blood MDM, IL-4 treated MDM also show a significant increase in OCR % change from baseline ($P < 0.05$) when compared to untreated MDM (Figure 4.15 F). However, this reflects the increase in OCR that IL-4 alone caused as the untreated cord blood MDM are unchanged from baseline, as demonstrated in Chapter 3.

4.2.3b IFN- γ increases ECAR in adult MDM while IL-4 decreases ECAR in both adult and cord MDM after Mtb stimulation

The shift in glycolysis after Mtb stimulation of the untreated, IFN- γ and IL-4 treated adult and cord blood MDM is shown in the time course graphs in Figure 4.16. The increase in ECAR of the adult MDM after IFN- γ and the decrease in IL-4 is clearly shown

(Figure 4.16 A). The response to Mtb stimulation appears to follow a similar pattern in all 3 conditions, as the differences in ECAR prior to stimulation persist at the peak of glycolysis. In the cord blood MDM the effect of pre-treatment with IFN- γ and IL-4 prior to Mtb treatment is also apparent (Figure 4.16 B); with IFN- γ eliciting a higher ECAR and IL-4 eliciting a lower ECAR. After Mtb stimulation, the ECAR of the untreated cord blood MDM almost matches the ECAR of the IFN- γ treated MDM whereas the IL-4 treated MDM remain well below the untreated MDM despite showing an increased ECAR after Mtb stimulation (Figure 4.16 B). The % change in ECAR from the untreated adult MDM illustrate similar findings to the raw values, with IFN- γ causing an increase in ECAR pre Mtb stimulation that persists at peak glycolysis and IL-4 causing a decrease in the pre-stimulation ECAR that results in a lower peak (Figure 4.16 C). The cord blood MDM % change in ECAR from untreated also highlights the different starting points with IFN- γ or IL-4 treatment. The peak glycolysis in the untreated cord blood MDM matches the peak of the IFN- γ (Figure 4.16 D). The % change from baseline in the adult MDM shows that untreated and IFN- γ or IL-4 treated MDM all have a similar response to Mtb stimulation (Figure 4.16 E). The cord blood MDM % change from baseline illustrate that the IFN- γ treated cord blood MDM have a reduced glycolytic shift compare with IL-4 and untreated MDM, both of which show similar patterns of increase (Figure 4.16 F). This may represent a maximal point of glycolysis reached by the combination of IFN- γ and Mtb.

Analysis of the differences in ECAR at the time point indicated, 150 minutes after stimulation with Mtb, shows the significant increase in ECAR in adult MDM by pre-treatment with IFN- γ ($P < 0.05$) and the decrease in ECAR by pre-treatment with IL-4

(Figure 4.17 A, $P < 0.05$). In the cord blood MDM, IFN- γ did significantly increase the ECAR at 150 minutes post stimulation but IL-4 caused a statistically significant decrease in ECAR ($P < 0.05$, Student's t-test) (Figure 4.17 B). The % change from untreated show a similar pattern to the raw values. In the adult MDM stimulated with Mtb, the % change in ECAR from untreated MDM is significantly increased by IFN- γ ($P < 0.01$) and decreased by IL-4 (Figure 4.17 C, $P < 0.05$). The difference between the ECAR in MDM treated with IFN- γ or IL-4 responses is also significantly different ($P < 0.001$). In the cord blood MDM, the ECAR % change from unstimulated is significantly decreased by IL-4 compared with untreated cells (Figure 4.17 D, $P < 0.05$, Student's t-test). There is no significant difference in the % change from baseline in adult MDM with either IFN- γ or IL-4 suggesting that the MDM are able to shift glycolysis to a similar degree despite the underlying differences in ECAR caused by the pre-treatment with cytokine (Figure 4.17 E). In cord blood MDM the % change from baseline by pre-treatment with IFN- γ was not statistically significant from untreated MDM (Figure 4.17 F), although the mean change in ECAR from baseline was 201% in the untreated and 127% in the IFN- γ treated MDM, perhaps reflecting maximal glycolysis with this combination of IFN- γ treatment and Mtb stimulation. These data indicate that IFN- γ increases ECAR in adult MDM while IL-4 decreases ECAR in both adult and cord MDM after Mtb stimulation.

4.2.3c IL-4 decreases the ECAR/OCR ratio in both adult and cord blood MDM after Mtb stimulation

The ECAR/OCR ratio was calculated for both the adult and cord blood MDM 150 minutes after Mtb stimulation for the untreated, IFN- γ and IL-4 treated MDM (Figure 4.18). In the adult MDM, IL-4 caused a significant decrease in the ECAR/OCR ratio compared with

untreated ($P < 0.05$) or IFN- γ treated MDM (Figure 4.18 A, $P < 0.05$). Cord blood MDM pre-treated with IL-4 also have a significantly decreased ECAR/OCR ratio compared with untreated ($P < 0.05$, Student's t-test) or IFN- γ treated MDM ($P < 0.01$; Figure 4.18 B). Directly comparing the ECAR/OCR ratios do not reveal any significant differences between adult and cord blood MDM (Figure 4.18 C).

4.2.3d IFN- γ augments glycolysis in adult MDM but not in cord blood MDM in response to stimulation with Mtb

Comparison of the adult and cord blood ECAR and OCR changes after Mtb stimulation show that there are different shifts in glycolysis after IFN- γ exposure (Figure 4.19). The differences seen between adult and cord blood MDM were not statistically significant for OCR (Figure 4.19A), ECAR (Figure 4.19 B), an OCR % change from untreated (Figure 4.19 C). The adult MDM treated with IFN- γ have a significantly increased ($P < 0.01$) rise in ECAR in response to Mtb (as reflected by the % change from unstimulated cells) compared with IFN- γ treated cord blood MDM (Figure 4.19 D). The % change in OCR from baseline was not significantly different between adult and cord blood MDM after Mtb stimulation (Figure 4.19 E). However, the % change in ECAR from baseline, indicative of the ability of the cells to undergo a glycolytic shift after Mtb stimulation, was significantly reduced in the cord blood MDM when compared to the adult ($P < 0.05$; Figure 4.19 F). These data illustrate the augmentation of glycolysis by IFN- γ in adult but not cord blood MDM.

4.2.3e IL-4 abrogates the decreased OCR observed in response to LPS stimulation in adult MDM

Figure 4.20 illustrates the time course graphs of the OCR response of both adult and cord blood MDM in real-time response to LPS stimulation after 24 hours of treatment with IFN- γ or IL-4. The OCR graph in adult MDM shows the increase in OCR caused by IFN- γ and the small decrease caused by IL-4 (Figure 4.20 A). The drop in OCR in response to LPS occurs in both the untreated and IFN- γ treated MDM but the IL-4 OCR remain unchanged. In the cord blood MDM the IFN- γ treated MDM OCR remains above the untreated but the IL-4 treated MDM start at the same point as the untreated MDM but increase above the untreated MDM after LPS stimulation (Figure 4.20 B). The time course graph of the % change from the untreated in adult MDM shows that the IFN- γ treated MDM have elevated OCR whereas the IL-4 treated MDM have an OCR less than the untreated prior to LPS stimulation that rises above the untreated after LPS stimulation (Figure 4.20 C). No obvious differences are seen in the cord blood MDM time course graph normalised to % OCR change from the untreated, in either IFN- γ or IL-4 treated cells (Figure 4.20 D). The % change in OCR from baseline in the adult MDM after LPS stimulation show that the IFN- γ treated and untreated MDM decrease OCR from baseline (recapitulating the Warburg effect observed in chapter 3 in adults in response to stimulation) but that IL-4 treated MDM slightly increase OCR and then do not drop below the baseline level OCR in response to stimulation with LPS (Figure 4.20 E). The cord blood shows no change in the the IFN- γ treated and untreated MDM in % OCR from baseline and the IL-4 treated MDM have a slight increase in OCR from baseline (Figure 4.20 F).

In order to quantify these changes over time, analyses of the changes were carried out 150 minutes post stimulation, as above. The OCR in adult MDM shows no significant differences in IFN- γ or IL-4 treated MDM after LPS stimulation compared with untreated controls (Figure 4.21 A). There is a significant increase in OCR in cord blood MDM after LPS stimulation when cells were pre-treated with IL-4 (Figure 4.21 B, $P < 0.05$, Student's t-test). The % change in OCR from unstimulated adult MDM also showed no significant differences across the groups (Figure 4.21 C) but the cord blood MDM showed a significant increase in the OCR % change from unstimulated MDM in the presence of IL-4 (Figure 4.21 D). The % change in OCR from baseline in adult MDM showed a significant difference between untreated and IL-4 treated MDM after LPS stimulation (Figure 4.21 E), indicative of the ability of IL-4 to block the Warburg effect seen in adult MDM. No significant differences were seen in the % change in OCR in cord blood MDM (Figure 4.21 F).

4.2.3f IL-4 decreases ECAR in adult MDM after LPS stimulation

The shift in ECAR after LPS stimulation of the adult and cord blood MDM 24 hours after treatment with IFN- γ or IL-4 is shown in the time course graphs in Figure 4.22. The differences in ECAR between IFN- γ , IL-4 and untreated adult MDM before LPS stimulation is clear (Figure 4.22 A). LPS induces a rapid increase in glycolysis in all 3 conditions with the untreated MDM approaching the high ECAR observed in the IFN- γ treated MDM as the ECAR reaches its peak. Cord blood MDM also increase ECAR after LPS stimulation, with a different starting point for each condition but the ECAR of the untreated MDM almost matches the ECAR of the IFN- γ treated MDM, similar to the adult MDM (Figure 4.22 B). Analysis of the % change in ECAR from unstimulated MDM

show similar patterns in adult (Figure 4.22 C) and cord blood (Figure 4.22 D) to the raw ECAR values. The % change from baseline ECAR in the adult (Figure 4.22 E) and cord blood MDM (Figure 4.22 F) showed that both the untreated and IL-4 treated cells exhibit a similar response and upregulate ECAR compared with their baseline, however, this analysis highlights that IFN- γ treated MDM have an attenuated ability to ramp up glycolysis compared to their own baseline (because the ECAR is already increased pre-stimulation). These data suggest that IFN- γ treated MDM may have already maxed out their capacity to shift to glycolysis resulting in a reduced capacity to upregulate the ECAR in response to stimulation with LPS.

Analysis of these responses at the time point indicated (150 minutes post stimulation) was undertaken and is shown in Figure 4.23. The ECAR of adult MDM after LPS stimulation is significantly reduced by IL-4 pre-treatment ($P < 0.05$) (Figure 4.23 A) but no differences are seen in the cord blood MDM (Figure 4.23 B). The % change from unstimulated MDM also shows a significant reduction in IL-4 pre-treated adult MDM ($P < 0.05$, Student's t-test) (Figure 4.23 C) but no difference in cord blood MDM (Figure 4.23 D). There is a statistically significant decrease in the % change of ECAR from baseline after LPS stimulation in both adult (Figure 4.23 E) and cord blood MDM (Figure 4.23 F) pre-treated with IFN- γ ($P < 0.05$ Student's t-test for both). These data indicate that the increase in ECAR after IFN- γ treatment blunts the subsequent glycolytic shift seen after LPS stimulation, likely representing a maximal glycolytic rate achieved by these two potent macrophage activators in combination.

4.2.3g IL-4 decreases the ECAR/OCR ratio in both adult and cord blood MDM after LPS stimulation

The ECAR/OCR ratio was calculated for both the adult and cord blood MDM after LPS stimulation at the time point indicated on the time course graphs; 150 minutes post stimulation. In adult MDM, IL-4 caused a significant decrease in the ECAR/OCR ratio when compared with untreated or IFN- γ treated MDM (Figure 4.24 A, $P < 0.01$). In cord blood MDM, IL-4 caused a significant decrease in the ECAR/OCR ratio compared with untreated MDM was noted ($P < 0.05$) (Figure 4.24 B). Comparison of the adult and cord blood ECAR/OCR ratios do not show any significant differences (Figure 4.24 C).

4.2.3h Direct comparison of LPS responses between adult and cord blood MDM after IFN- γ or IL-4

Comparison of the adult and cord blood metabolic changes after LPS stimulation are shown in Figure 4.25. No significant differences were seen in OCR (Figure 4.25 A), ECAR (Figure 4.25 B), % change from unstimulated in OCR (Figure 4.25 C) or ECAR (Figure 4.25 D), nor % change in baseline in OCR (Figure 4.25 E) or ECAR (Figure 4.25 F) between the adult and cord blood MDM.

Cumulatively, these data indicate that there are differences in the way that the cytokines IFN- γ and IL-4 effect adult and cord blood MDM metabolic responses to Mtb and LPS stimulation. Inflammatory Warburg occurs in adult MDM but does not occur in cord blood MDM as demonstrated in Chapter 3, however, IL-4 blocks the reduction in OCR in adult MDM after Mtb or LPS stimulation. IL-4 decreases ECAR in Mtb or LPS stimulated adult and cord blood MDM. IFN- γ increases ECAR in adult MDM stimulated

with Mtb, compared with their untreated controls, but not in LPS stimulated adult MDM or cord blood MDM.

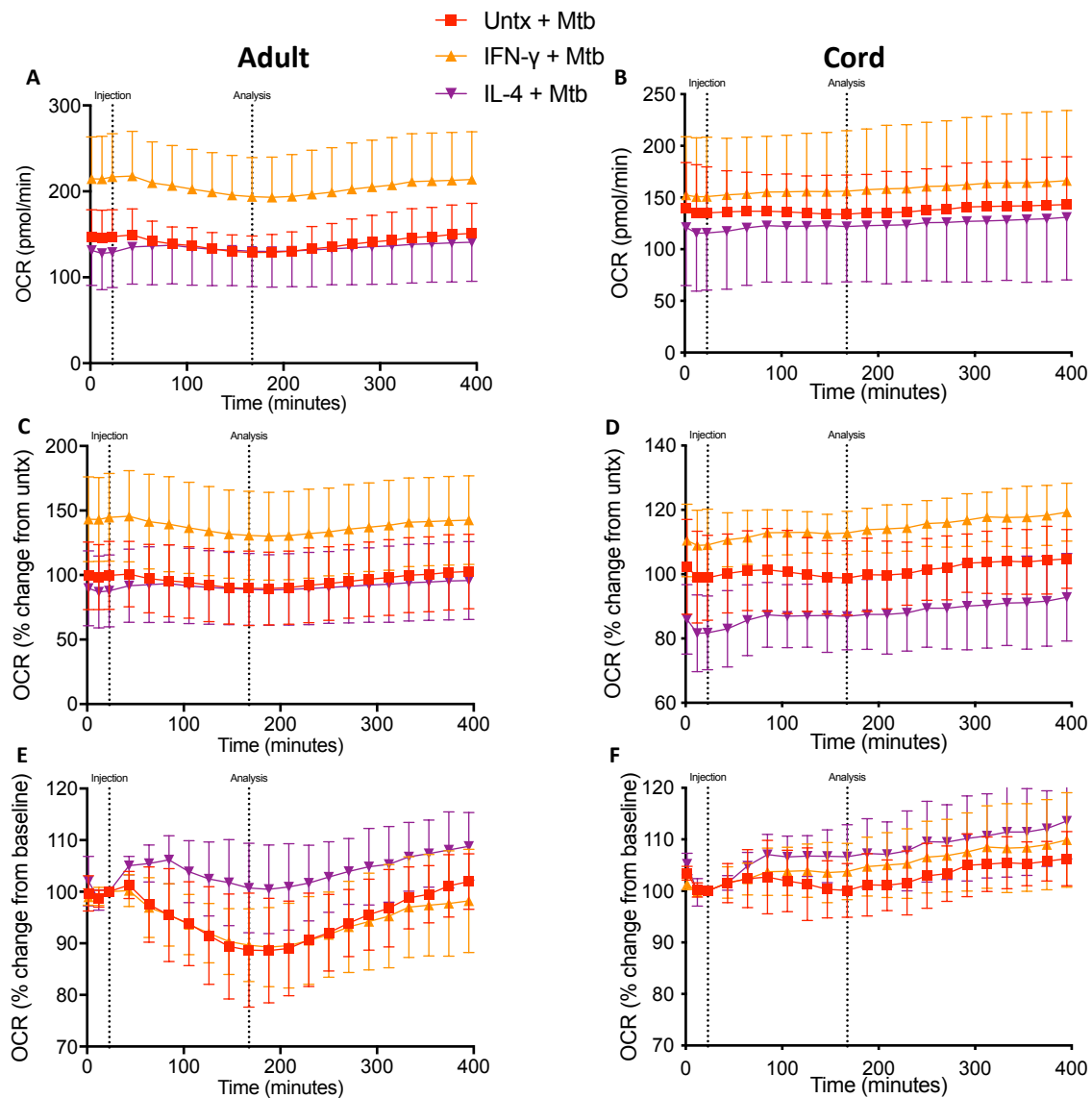


Figure 4.14 IL-4 inhibits the drop in OCR seen after Mtb stimulation in adult MDM. PBMC were isolated from buffy coats or from umbilical cord blood samples taken immediately following delivery. Adult or cord blood MDM were adherence purified for 7 days in 10% human serum. MDM were washed and detached from the plates by cooling and gently scraped, counted and re-seeded on Seahorse culture plates prior to analysis in the Seahorse XFe24 Analyzer. IFN- γ (10ng/ml) or IL-4 (10ng/ml) was added 24 hours prior to analysis. Mtb (iH37Rv; MOI 1-10) was added to the MDM in the Seahorse Analyzer. The OCR was recorded approximately every 20 minutes. The third Seahorse reading was taken as the baseline in order to calculate the % change from baseline. The third reading of the untreated MDM, prior to Mtb stimulation, was used as the comparison for the % change from unstimulated MDM. The time-course graphs illustrate the OCR of adult (A,C,E n=6) or cord blood MDM (B,D,F n=3) in real time in response to stimulation with Mtb, 24 hours after stimulation with IFN- γ or IL-4.

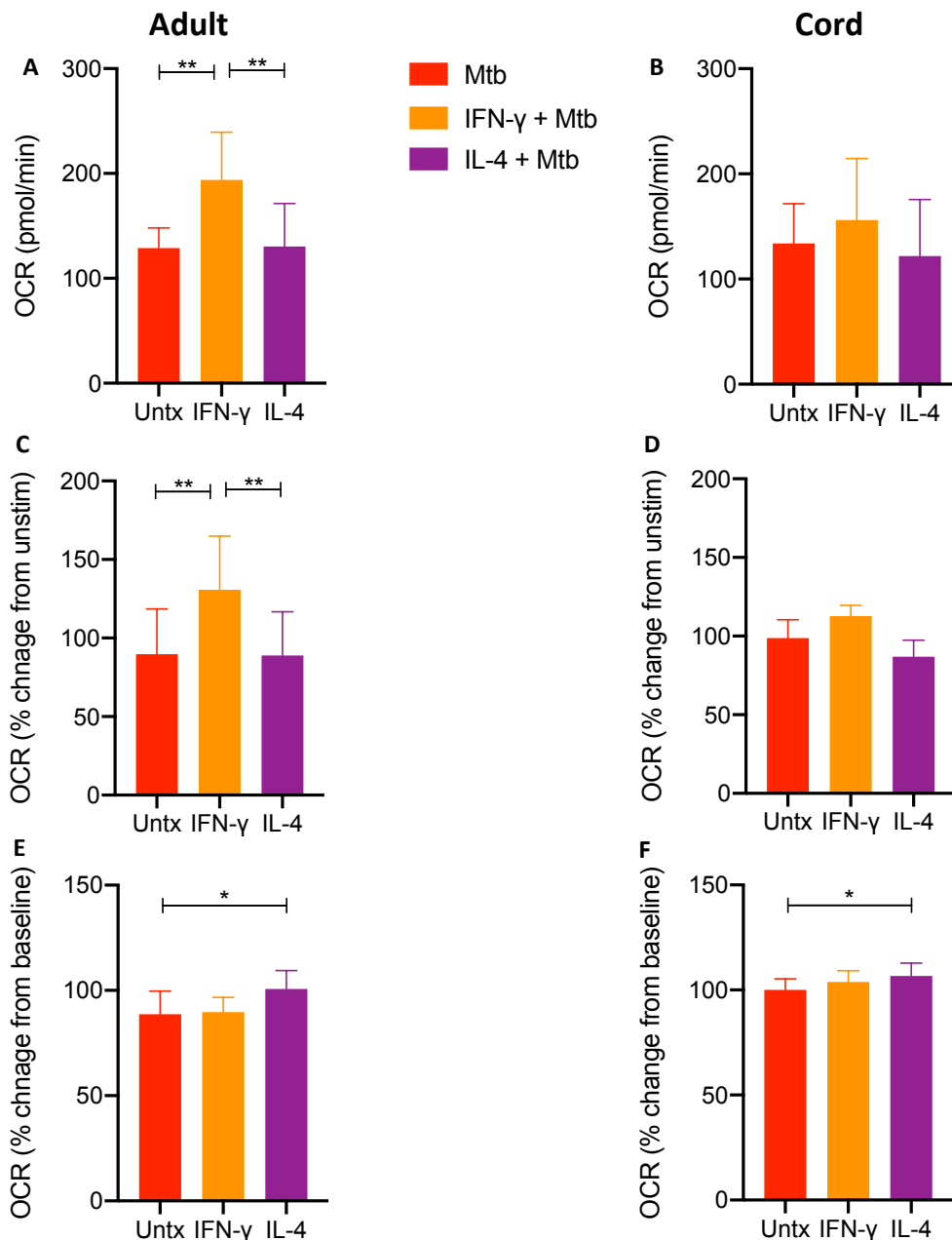


Figure 4.15 Analysis of OCR in IFN- γ and IL-4 treated adult and cord blood MDM after Mtb stimulation.

PBMC were isolated from buffy coats or from umbilical cord blood samples taken immediately following delivery. Adult or cord blood MDM were adherence purified for 7 days in 10% human serum. MDM were washed and detached from the plates by cooling and gently scraped, counted and re-seeded on Seahorse culture plates prior to analysis in the Seahorse XFe24 Analyzer. IFN- γ (10ng/ml) or IL-4 (10ng/ml) was added 24 hours prior to analysis. Mtb (iH37Rv; MOI 1-10) was added to the MDM in the Seahorse Analyzer. The OCR was recorded approximately every 20 minutes. The third reading was taken as the baseline in order to calculate the % change from baseline. The third reading of the unstimulated MDM, prior to Mtb stimulation, was used as the comparison for the % change from unstimulated MDM. 150 minutes after stimulation, the OCR was analysed for Mtb stimulated cells for the adult (A,C,E n=6) and cord blood MDM (B,D,F n=3). Statistical significance was determined using one-way ANOVA with Tukey's multiple comparison test; * P<0.05, **P<0.01.

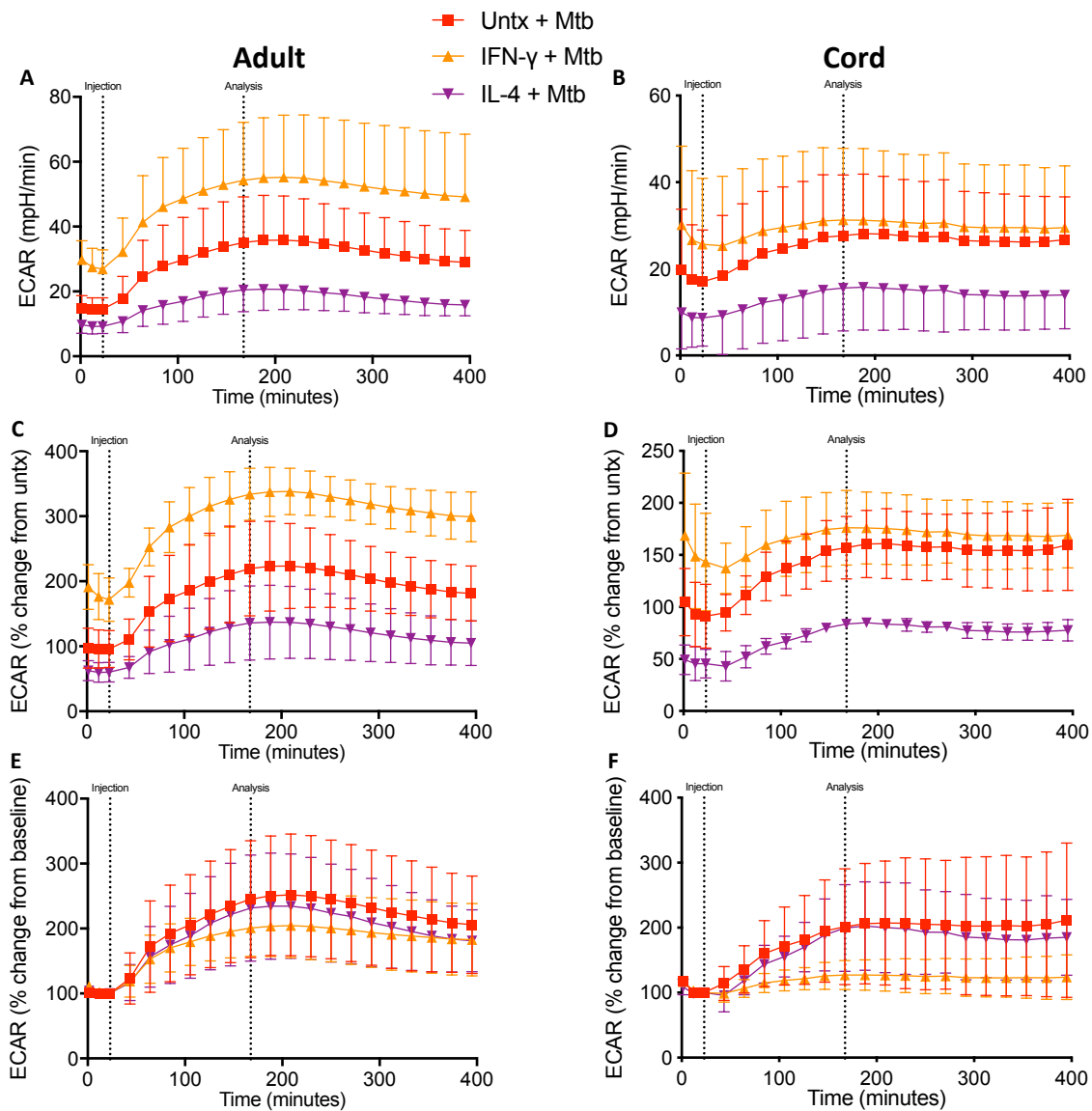


Figure 4.16 IFN- γ increases ECAR in adult MDM while IL-4 decreases ECAR in both adult and cord MDM after Mtb stimulation.

PBMC were isolated from buffy coats or from umbilical cord blood samples taken immediately following delivery. Adult or cord blood MDM were adherence purified for 7 days in 10% human serum. MDM were washed and detached from the plates by cooling and gently scraped, counted and re-seeded on Seahorse culture plates prior to analysis in the Seahorse XFe24 Analyzer. IFN- γ (10ng/ml) or IL-4 (10ng/ml) was added 24 hours prior to analysis. Mtb (iH37Rv; MOI 1-10) was added to the MDM in the Seahorse Analyzer. The ECAR was recorded approximately every 20 minutes. The third Seahorse reading was taken as the baseline in order to calculate the % change from baseline. The third reading of the untreated MDM, prior to Mtb stimulation, was used as the comparison for the % change from unstimulated MDM. The time-course graphs illustrate the ECAR of adult (A,C,E n=6) or cord blood MDM (B,D,F n=3) in real time in response to stimulation with Mtb, 24 hours after stimulation with IFN- γ or IL-4.

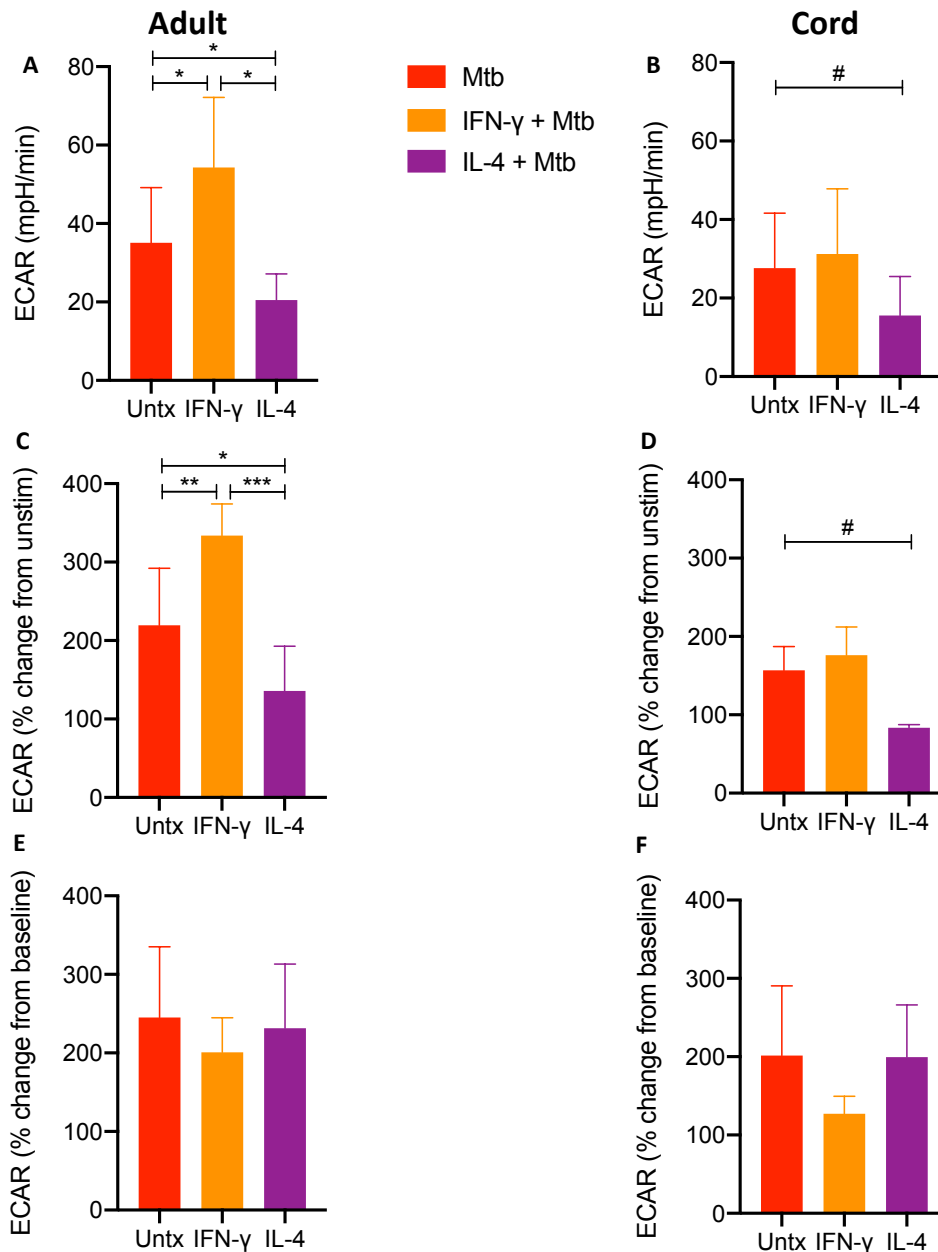


Figure 4.17 Analysis of ECAR in IFN- γ and IL-4 treated adult and cord blood MDM after Mtb stimulation.

PBMC were isolated from buffy coats or from umbilical cord blood samples taken immediately following delivery. Adult or cord blood MDM were adherence purified for 7 days in 10% human serum. MDM were washed and detached from the plates by cooling and gently scraped, counted and re-seeded on Seahorse culture plates prior to analysis in the Seahorse XFe24 Analyzer. IFN- γ (10ng/ml) or IL-4 (10ng/ml) was added 24 hours prior to analysis. Mtb (iH37Rv; MOI 1-10) was added to the MDM in the Seahorse Analyzer. The ECAR was recorded approximately every 20 minutes. The third reading was taken as the baseline in order to calculate the % change from baseline. The third reading of the unstimulated MDM, prior to Mtb stimulation, was used as the comparison for the % change from unstimulated MDM. 150 minutes after stimulation, the ECAR was analysed for Mtb stimulated cells for the adult (A,C,E n=6) and cord blood MDM (B,D,F n=3). Statistical significance was determined using one-way ANOVA with Tukey's multiple comparison test; * P<0.05, **P<0.01; and a Student's t-test; # P<0.05.

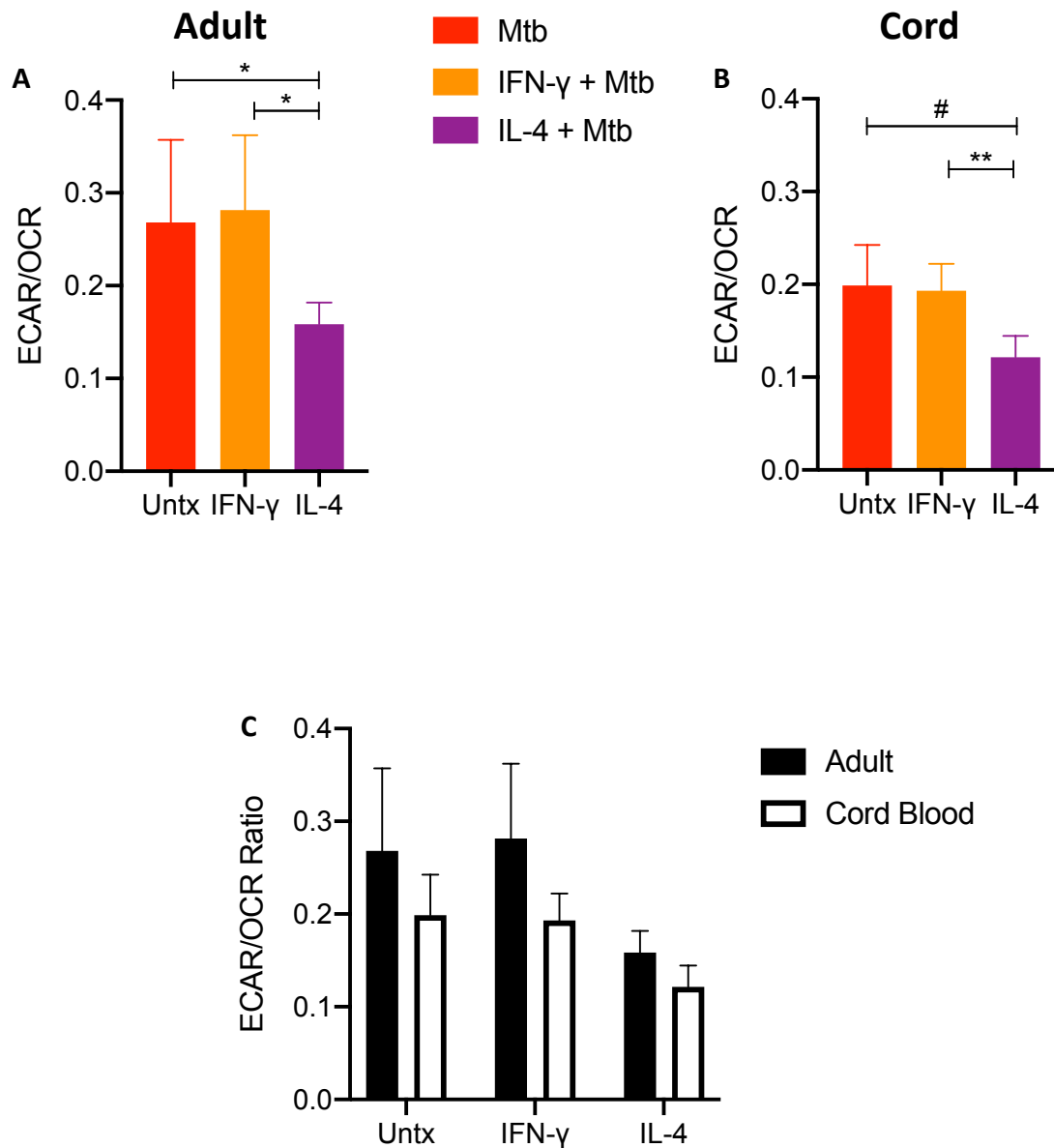


Figure 4.18 IL-4 decreases the ECAR/OCR ratio in both adult and cord blood MDM. Adult or cord blood MDM were adherence purified for 7 days in 10% human serum. MDM were washed and detached from the plates by cooling and gently scraped, counted and re-seeded on Seahorse culture plates prior to analysis in the Seahorse XFe24 Analyzer. IFN- γ (10ng/ml) or IL-4 (10ng/ml) was added 24 hours prior to analysis. Mtb (iH37Rv; MOI 1-10) was added to the MDM in the Seahorse Analyzer. The OCR and ECAR was recorded approximately every 20 minutes. At the time point indicated in Figure 4.16, 150 minutes after stimulation, the ECAR/OCR ratio was calculated for Mtb stimulated cells for the adult (A, n=6) and cord blood MDM (B, n=3). Comparative analysis between the adult and cord blood ECAR/OCR ratio is shown (C). Statistical significance was determined using one-way ANOVA with Tukey's multiple comparison test and two-way ANOVA using Sidak's multiple comparison test; * P<0.05, **P<0.01. Paired student t-tests were also performed; # P<0.05.

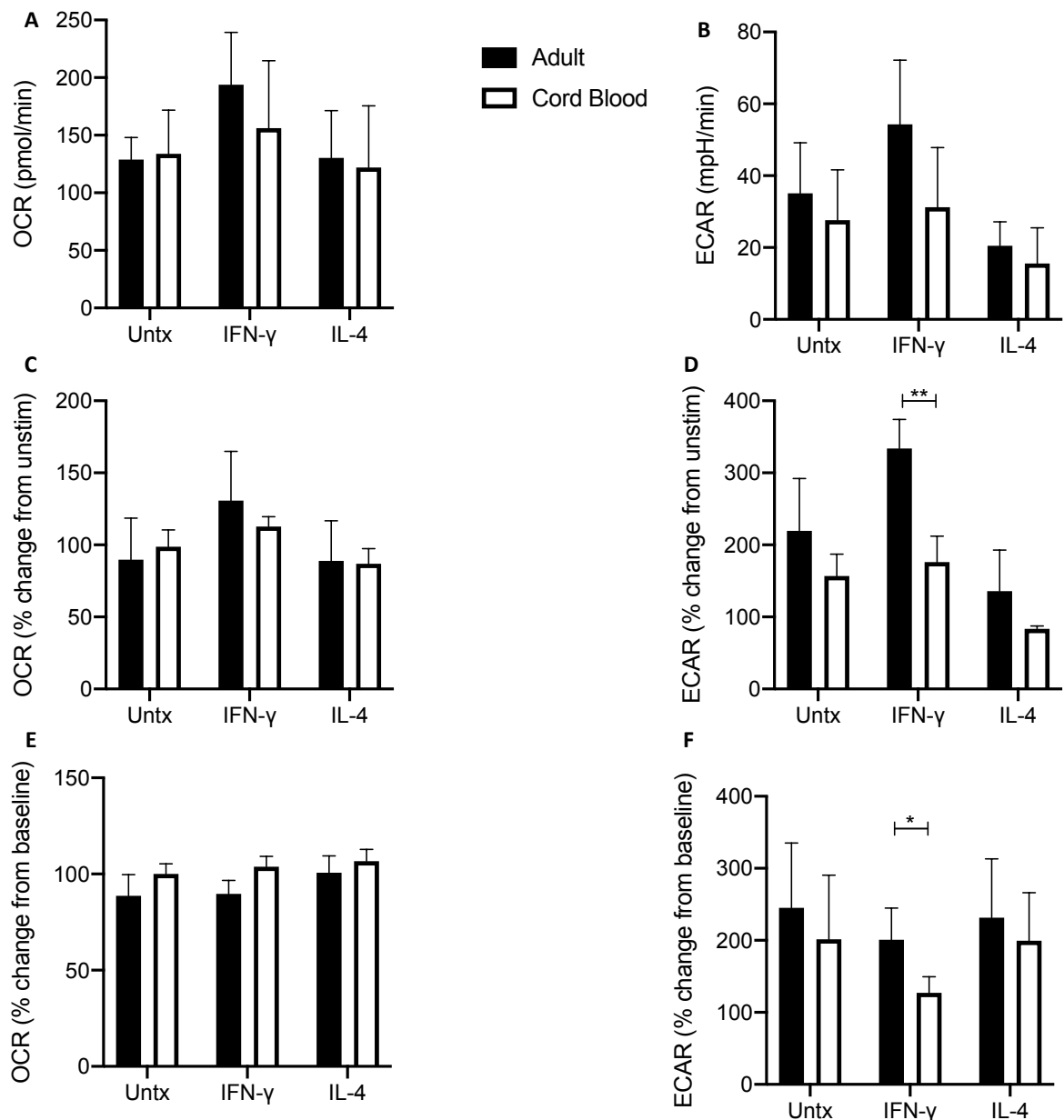


Figure 4.19 Comparison between adult and cord blood MDM metabolic responses after Mtb stimulation, 24 hours after IFN- γ or IL-4 treatment.

PBMC were isolated from buffy coats or from umbilical cord blood samples taken immediately following delivery. Adult or cord blood MDM were adherence purified for 7 days in 10% human serum. MDM were washed and detached from the plates by cooling and gently scraped, counted and re-seeded on Seahorse culture plates prior to analysis in the Seahorse XFe24 Analyzer. IFN- γ (10ng/ml) or IL-4 (10ng/ml) was added 24 hours prior to analysis in the Seahorse Analyzer. Mtb (iH37Rv; MOI 1-10) was added to the MDM in the Seahorse Analyzer. The OCR and ECAR was recorded approximately every 20 minutes. 150 minutes after stimulation, comparative analysis of the adult (A n=6) and cord blood MDM (B n=3) was performed. The third reading of the unstimulated MDM, prior to Mtb stimulation, was used as the comparison for the % change from unstimulated MDM (C,D). The third reading was taken as the baseline in order to calculate the % change from baseline (E,F). Statistically significant differences were determined using two-way ANOVA using Sidak's multiple comparison test; * P<0.05, ** P<0.01.

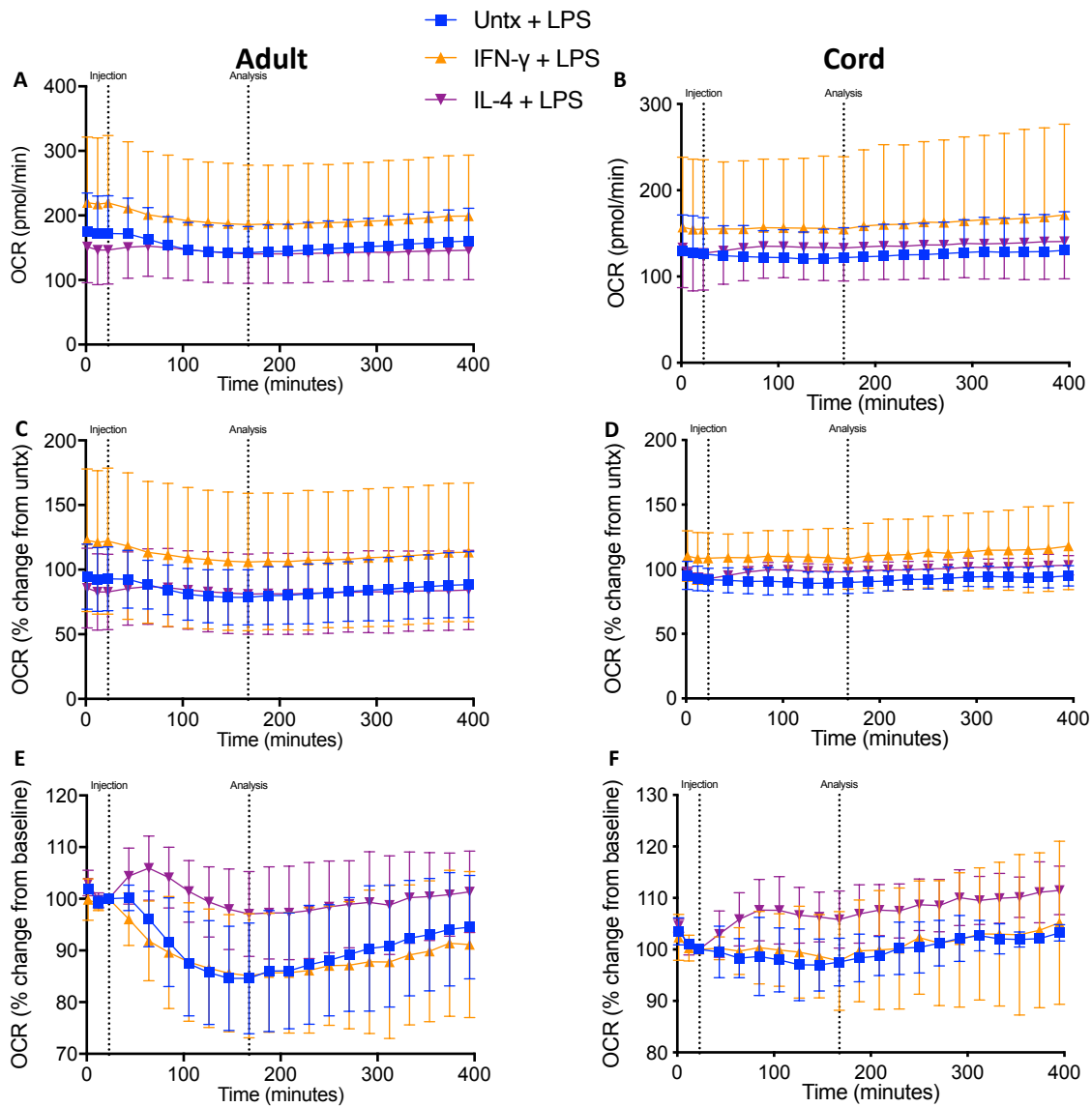


Figure 4.20 IL-4 inhibits the decrease in OCR seen after LPS stimulation in adult MDM. PBMC were isolated from buffy coats or from umbilical cord blood samples taken immediately following delivery. Adult or cord blood MDM were adherence purified for 7 days in 10% human serum. MDM were washed and detached from the plates by cooling and gently scraped, counted and re-seeded on Seahorse culture plates prior to analysis in the Seahorse XFe24 Analyzer. IFN- γ (10ng/ml) or IL-4 (10ng/ml) was added 24 hours prior to analysis. LPS (100 ng/ml) was added to the MDM in the Seahorse Analyzer. The OCR was recorded approximately every 20 minutes. The third Seahorse reading was taken as the baseline in order to calculate the % change from baseline. The third reading of the untreated MDM, prior to LPS stimulation, was used as the comparison for the % change from unstimulated MDM. The time-course graphs illustrate the OCR of adult (A,C,E n=5) or cord blood MDM (B,D,F n=3) in real time in response to stimulation with LPS, 24 hours after stimulation with IFN- γ or IL-4.

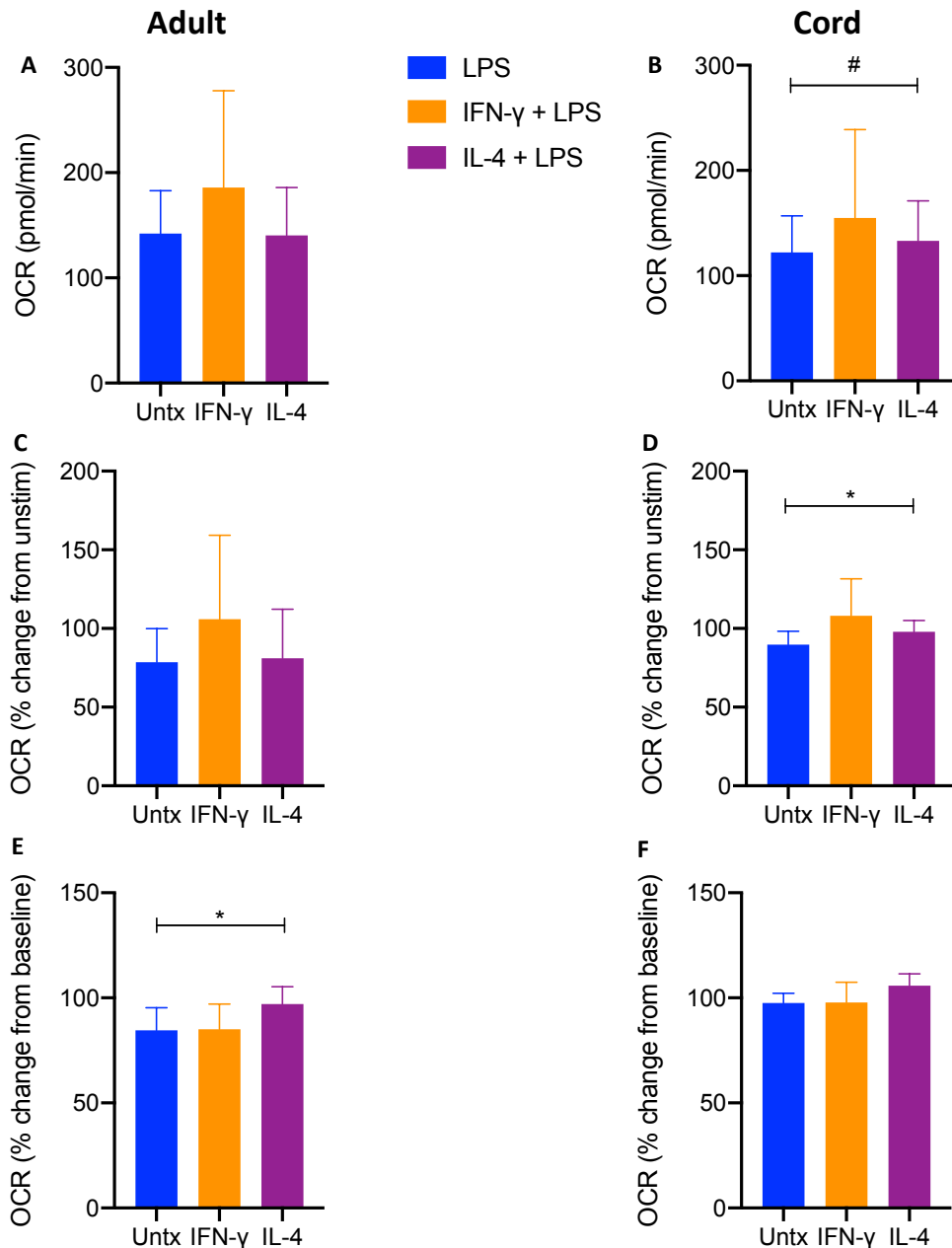


Figure 4.21 Analysis of OCR in IFN- γ and IL-4 treated adult and cord blood MDM after LPS stimulation.

PBMC were isolated from buffy coats or from umbilical cord blood samples taken immediately following delivery. Adult or cord blood MDM were adherence purified for 7 days in 10% human serum. MDM were washed and detached from the plates by cooling and gently scraped, counted and re-seeded on Seahorse culture plates prior to analysis in the Seahorse XFe24 Analyzer. IFN- γ (10ng/ml) or IL-4 (10ng/ml) was added 24 hours prior to analysis. LPS (100 ng/ml) was added to the MDM in the Seahorse Analyzer. 150 minutes after stimulation, analysis of the adult (A n=5) and cord blood MDM OCR (B n=3) was performed. The third reading of the unstimulated MDM, prior to LPS stimulation, was used as the comparison for the % change from unstimulated MDM (C,D). The third reading was taken as the baseline in order to calculate the % change from baseline (E,F). Statistical significance was determined using one-way ANOVA with Tukey's multiple comparison test; * P<0.05; and a Student's t-test; # P<0.05.

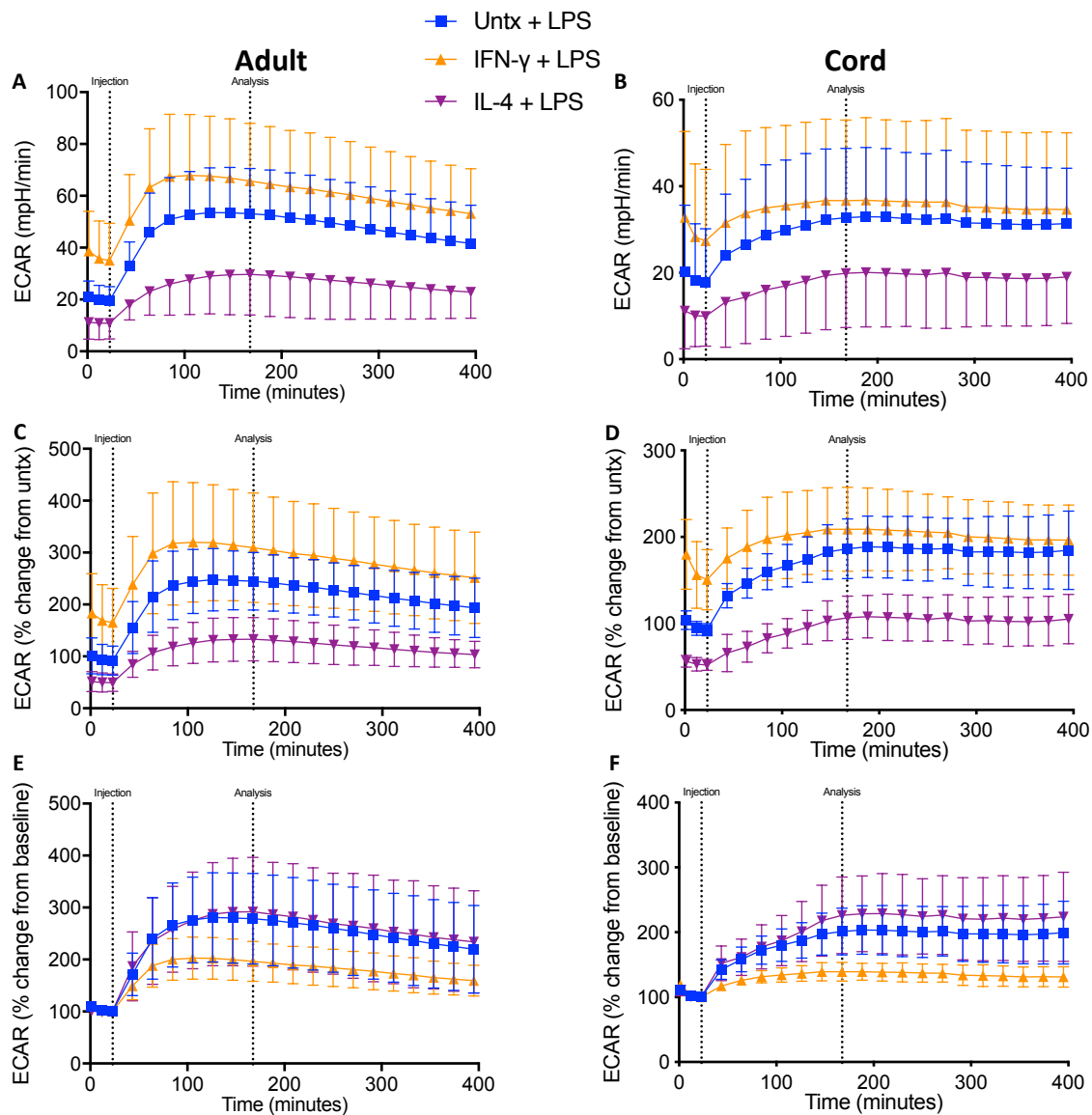


Figure 4.22 IL-4 decreases ECAR in adult MDM after LPS stimulation.

PBMC were isolated from buffy coats or from umbilical cord blood samples taken immediately following delivery. Adult or cord blood MDM were adherence purified for 7 days in 10% human serum. MDM were washed and detached from the plates by cooling and gently scraped, counted and re-seeded on Seahorse culture plates prior to analysis in the Seahorse XFe24 Analyzer. IFN- γ (10ng/ml) or IL-4 (10ng/ml) was added 24 hours prior to analysis. LPS (100 ng/ml) was added to the MDM in the Seahorse Analyzer. The third Seahorse reading was taken as the baseline in order to calculate the % change from baseline. The third reading of the untreated MDM, prior to LPS stimulation, was used as the comparison for the % change from unstimulated MDM. The time-course graphs illustrate the ECAR of adult (A,C,E n=5) or cord blood MDM (B,D,F n=3) in real time in response to stimulation with LPS, 24 hours after stimulation with IFN- γ or IL-4.

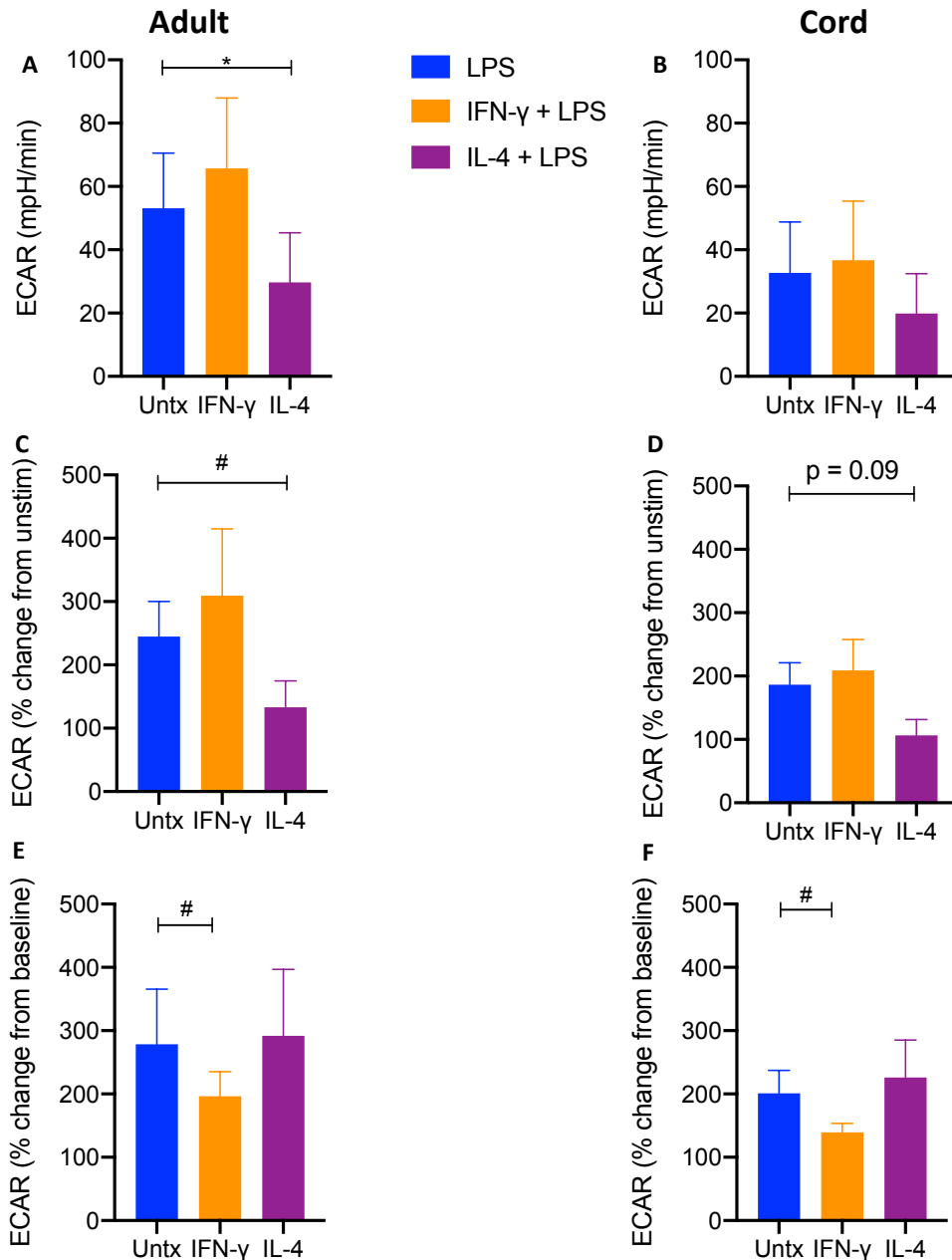


Figure 4.23 Analysis of ECAR in IFN- γ and IL-4 treated adult and cord blood MDM after LPS stimulation.

PBMC were isolated from buffy coats or from umbilical cord blood samples taken immediately following delivery. Adult or cord blood MDM were adherence purified for 7 days in 10% human serum. MDM were washed and detached from the plates by cooling and gently scraped, counted and re-seeded on Seahorse culture plates prior to analysis in the Seahorse XFe24 Analyzer. IFN- γ (10ng/ml) or IL-4 (10ng/ml) was added 24 hours prior to analysis. LPS (100 ng/ml) was added to the MDM in the Seahorse Analyzer. The third Seahorse reading was taken as the baseline in order to calculate the % change from baseline. The third reading of the untreated MDM, prior to LPS stimulation, was used as the comparison for the % change from unstimulated MDM. 150 minutes after stimulation, the ECAR was analysed for LPS stimulated cells for the adult (A,C,E n=5) or cord blood MDM (B,D,F n=3). Statistical significance was determined using one-way ANOVA with Tukey's multiple comparison test; * P<0.05; and a Student's t-test; # P<0.05.

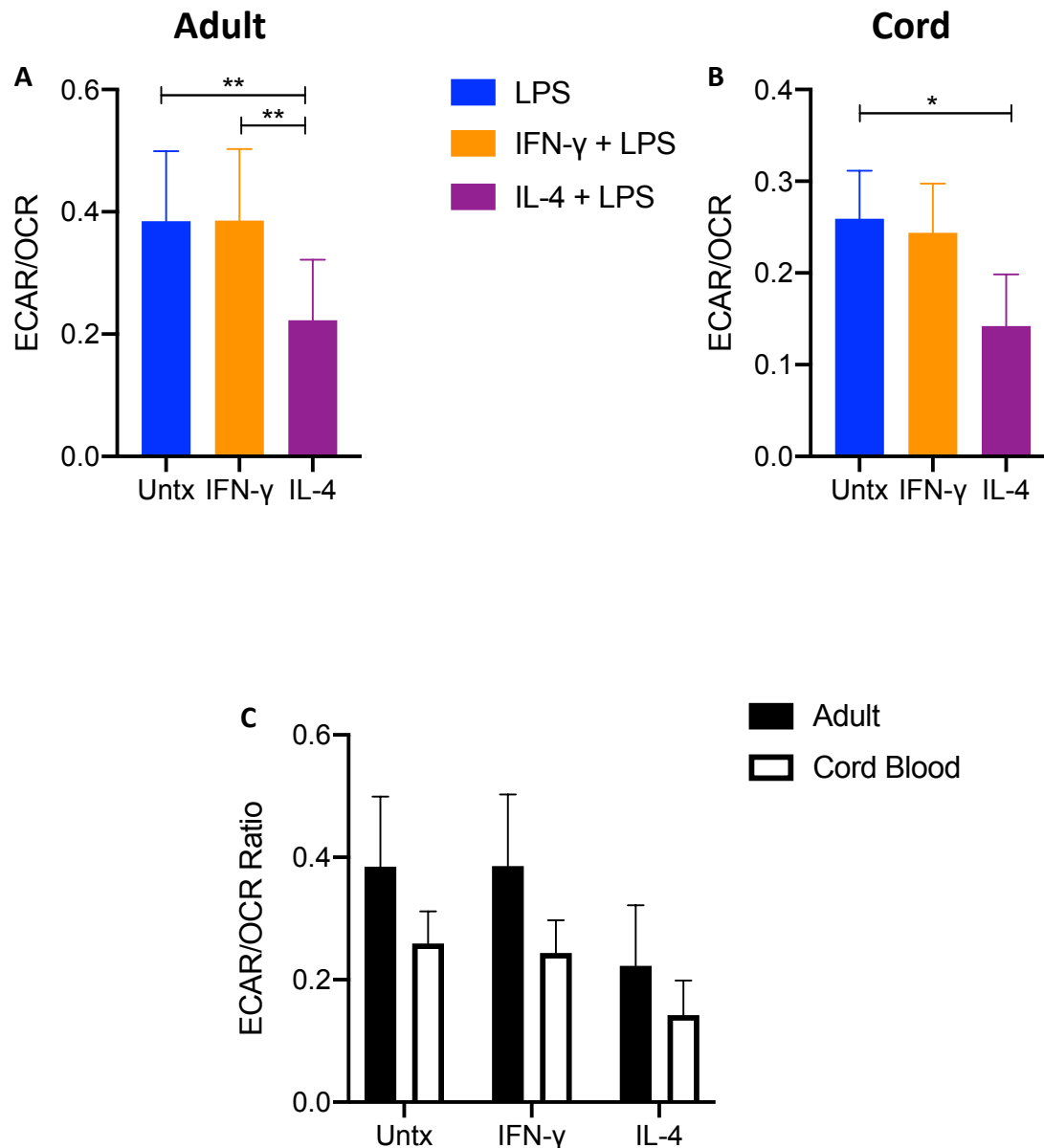


Figure 4.24 IL-4 decreases the ECAR/OCR ratio in both adult and cord blood MDM after LPS stimulation

Adult or cord blood MDM were adherence purified for 7 days in 10% human serum. MDM were washed and detached from the plates by cooling and gently scraped, counted and re-seeded on Seahorse culture plates prior to analysis in the Seahorse XFe24 Analyzer. IFN- γ (10ng/ml) or IL-4 (10ng/ml) was added 24 hours prior to analysis. LPS (100 ng/ml) was added to the MDM in the Seahorse Analyzer. The OCR and ECAR was recorded approximately every 20 minutes. 150 minutes after stimulation, the ECAR/OCR ratio was calculated for LPS stimulated cells for the adult (A, n=5) and cord blood MDM (B, n=3). Comparative analysis between the adult and cord blood ECAR/OCR ratio is shown (C). Statistical significance was determined using one-way ANOVA with Tukey's multiple comparison test and two-way ANOVA using Sidak's multiple comparison test; * P<0.05, **P<0.01.

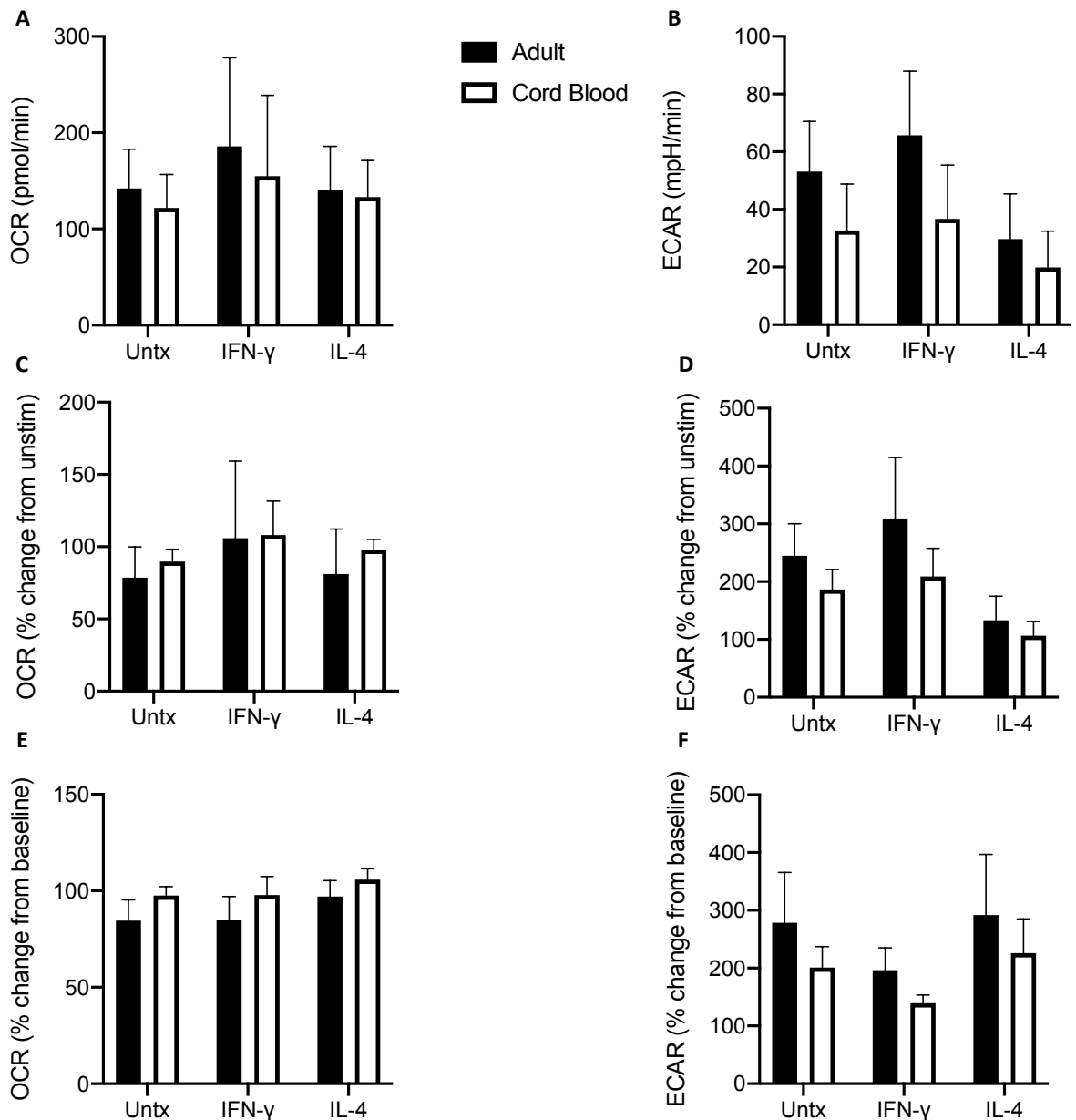


Figure 4.25 Comparison between adult and cord blood MDM metabolic responses after LPS stimulation, 24 hours after IFN- γ or IL-4 treatment.

PBMC were isolated from buffy coats or from umbilical cord blood samples taken immediately following delivery. Adult or cord blood MDM were adherence purified for 7 days in 10% human serum. MDM were washed and detached from the plates by cooling and gently scraped, counted and re-seeded on Seahorse culture plates prior to analysis in the Seahorse XFe24 Analyzer. IFN- γ (10ng/ml) or IL-4 (10ng/ml) was added 24 hours prior to analysis in the Seahorse Analyzer. LPS (100 ng/ml) was added to the MDM in the Seahorse Analyzer. The OCR and ECAR was recorded approximately every 20 minutes. 150 minutes after stimulation, comparative analysis of the adult (A n=5) and cord blood MDM (B n=3) was performed. The third reading of the unstimulated MDM, prior to Mtb stimulation, was used as the comparison for the % change from unstimulated MDM (C,D). The third reading was taken as the baseline in order to calculate the % change from baseline (E,F). Statistically significant differences were determined using two-way ANOVA using Sidak's multiple comparison test.

4.2.4 Expression of cell surface markers in IFN- γ or IL-4 treated adult and cord blood MDM after Mtb or LPS stimulation

In order to examine the cumulative effect of both cytokine treatment with IFN- γ or IL-4, and stimulation with Mtb or LPS on the cell surface expression of activation markers, flow cytometry analysis was performed on adult and cord blood MDM. PBMC were isolated from adult buffy coats or from umbilical cord blood which was collected immediately following delivery. MDM were adherence purified for 7 days in RPMI with 10% human serum and non-adherent cells were washed off on days 2 and 5. IFN- γ (10ng/ml) or IL-4 (10ng/ml) were added 24 hours prior to the addition of Mtb (iH37Rv; MOI 1-10) or LPS (100 ng/ml). After a further 24 hours, MDM were harvested by placing in ice-cold PBS at 4°C for 30 minutes prior to gentle scraping. Cells were Fc blocked and stained with Zombie NIR viability dye and fluorochrome-conjugated antibodies specific for CD68, CD14, CD40, CD80, HLA-DR, CD83 and CD206 (mannose receptor; MMR) prior to acquisition by flow cytometry. MDM were gated on the basis of forward and side scatter, doublets and dead cells were excluded, and macrophages were identified as CD68⁺ CD14⁺ described in the methods section **2.3** and shown in the accompanying gating strategy (Figure 2.7).

Expression of HLA-DR, an antigen presenting molecule, was determined by MFI and a representative adult donor histogram of untreated MDM and MDM treated with IFN- γ or IL-4, 24 hours after Mtb stimulation, is shown in Figure 4.26 A. Bar graphs illustrate collated data; pre-treatment with IFN- γ significantly increases expression of HLA-DR after both Mtb ($P < 0.001$) or LPS stimulation (Figure 4.26 B, $P < 0.01$). IL-4 pre-treatment did not significantly alter HLA-DR expression in adult MDM after Mtb or LPS stimulation

(Figure 4.26 C). A representative histogram from a cord blood donor after Mtb stimulation is also shown (Figure 4.26 D). IFN- γ significantly increases the expression of HLA-DR after Mtb or LPS stimulation (Figure 4.26 E, $P < 0.01$). In cord blood MDM, IL-4 significantly increased HLA-DR expression after Mtb ($P < 0.001$) or LPS ($P < 0.01$) stimulation (Figure 4.26 F). There was no significant difference in expression of HLA-DR between adult and cord blood MDM after Mtb or LPS stimulation when pre-treated with either IFN- γ (Figure 4.26 G) or IL-4 (Figure 4.26 H).

The expression of MMR from an adult donor, pre-treated with IFN- γ or IL-4, after Mtb stimulation is shown in Figure 4.27 A. Both IFN- γ (Figure 4.27 B, $P < 0.05$) and IL-4 (Figure 4.27 C, $P < 0.01$) pre-treatment resulted in significantly increased MMR after LPS stimulation but no difference was seen after Mtb stimulation. For the cord blood MDM, a representative histogram is also shown (Figure 4.27 D). Treatment with IFN- γ (Figure 4.27 E) or IL-4 (Figure 4.27 F) did not affect the subsequent expression of MMR after Mtb or LPS stimulation in cord blood MDM. There was no significant difference between adult and cord blood MDM expression of MMR after IFN- γ (Figure 4.27 G) or IL-4 (Figure 4.27 H).

CD40 is a key co-stimulatory molecule associated with macrophage activation and antigen presentation. Its expression in an Mtb stimulated adult donor pre-treated with IFN- γ or IL-4 is shown in a representative histogram (Figure 4.28 A). IFN- γ resulted in significantly increased CD40 expression after both Mtb and LPS stimulation ($P < 0.001$) in adult MDM (Figure 4.28 B). IL-4 did not cause any significant difference in CD40 expression after Mtb or LPS (Figure 4.28 C). A cord blood donor representative

histogram for CD40 expression after Mtb stimulation is shown in Figure 4.28 D. Treatment with IFN- γ caused a significant increase in CD40 expression after Mtb or LPS stimulation ($P < 0.01$) in cord blood MDM (Figure 4.28 E). IL-4 treatment resulted in a statistically significant increase in CD40 expression after Mtb stimulation ($P < 0.05$) but not after LPS stimulation (Figure 4.28 F). There was no significant difference in CD40 expression between adult and cord blood MDM after Mtb or LPS stimulation when cells were pre-treated with IFN- γ (Figure 4.28 G) or IL-4 (Figure 4.28 H).

A representative histogram of an adult donor showing the expression of CD83 after Mtb stimulation for MDM pretreated IFN- γ or IL-4 is illustrated in Figure 4.29 A. Pre-treatment with IFN- γ resulted in increased expression of CD83 in Mtb ($P < 0.01$) and LPS ($P < 0.001$) stimulated adult MDM (Figure 4.29 B). IL-4 caused a significant increase in LPS induced CD83 expression ($P < 0.05$) in adult MDM (Figure 4.29 C). CD83 expression in cord blood MDM after Mtb stimulation is shown in a representative histogram in Figure 4.29 D. IFN- γ treatment resulted in increased CD83 expression after both Mtb and LPS stimulation (Figure 4.29 E, $P < 0.01$). IL-4 caused an increase in CD83 expression in cord blood MDM stimulated with either Mtb or LPS (Figure 4.29 F, < 0.05). There was no significant difference between adult and cord blood MDM expression of CD83 after IFN- γ (Figure 4.29 G) or IL-4 treatment (Figure 4.29 H).

A histogram from one representative adult donor after Mtb stimulation is shown for the costimulatory molecule CD80 (Figure 4.30 A). IFN- γ treatment in adult MDM induced increased expression in CD80 after both Mtb and LPS stimulation (Figure 4.30 B, $P < 0.001$). IL-4 did not effect CD80 expression in adult MDM after stimulation with Mtb

or LPS (Figure 4.30 C). A representative cord blood donor histogram of CD80 expression is shown in Figure 4.30 D. IFN- γ increased CD80 expression in cord blood MDM stimulated with LPS ($P < 0.05$) but not Mtb (Figure 4.30 E). IL-4 did not impact CD80 expression in cord blood MDM after Mtb or LPS stimulation (Figure 4.30 F). There was no significant difference in expression of CD80 between adult and cord blood MDM after Mtb or LPS with either IFN- γ (Figure 4.30 G) or IL-4 pre-treatment (Figure 4.30 H).

The co-stimulatory molecule CD86 was also analysed. A representative histogram for CD86 expression for an IFN- γ or IL-4 pre-treated adult donor after Mtb stimulation is shown in Figure 4.31 A. IFN- γ increased CD86 expression after both Mtb or LPS stimulation ($P < 0.01$ for both) (Figure 4.31 B). IL-4 also increased CD86 expression after both Mtb or LPS stimulation ($P < 0.01$ for both) (Figure 4.31 C). A representative histogram from a cord blood donor is shown in Figure 4.31 D. IFN- γ treatment did not significantly alter CD86 expression in cord blood MDM stimulated with Mtb or LPS (Figure 4.31 E). IL-4 treatment significantly increased CD86 expression after Mtb ($P < 0.01$) or LPS (< 0.001) stimulation (Figure 4.31 F). There was no significant difference between adult and cord blood MDM expression of CD86 after Mtb or LPS stimulation when pre-treated with IFN- γ (Figure 4.31 G) or IL-4 (Figure 4.31 H).

In summary these data show that pre-treatment with IFN- γ increases expression of HLA-DR, CD40 and CD83 in both adult and cord blood MDM when subsequently stimulated with Mtb or LPS. IL-4 pre-treatment had the most significant impact on CD86 expression in MDM stimulated with Mtb or LPS. Pre-treatment with IFN- γ overcomes the deficit seen in cord blood MDM HLA-DR expression when treated with LPS.

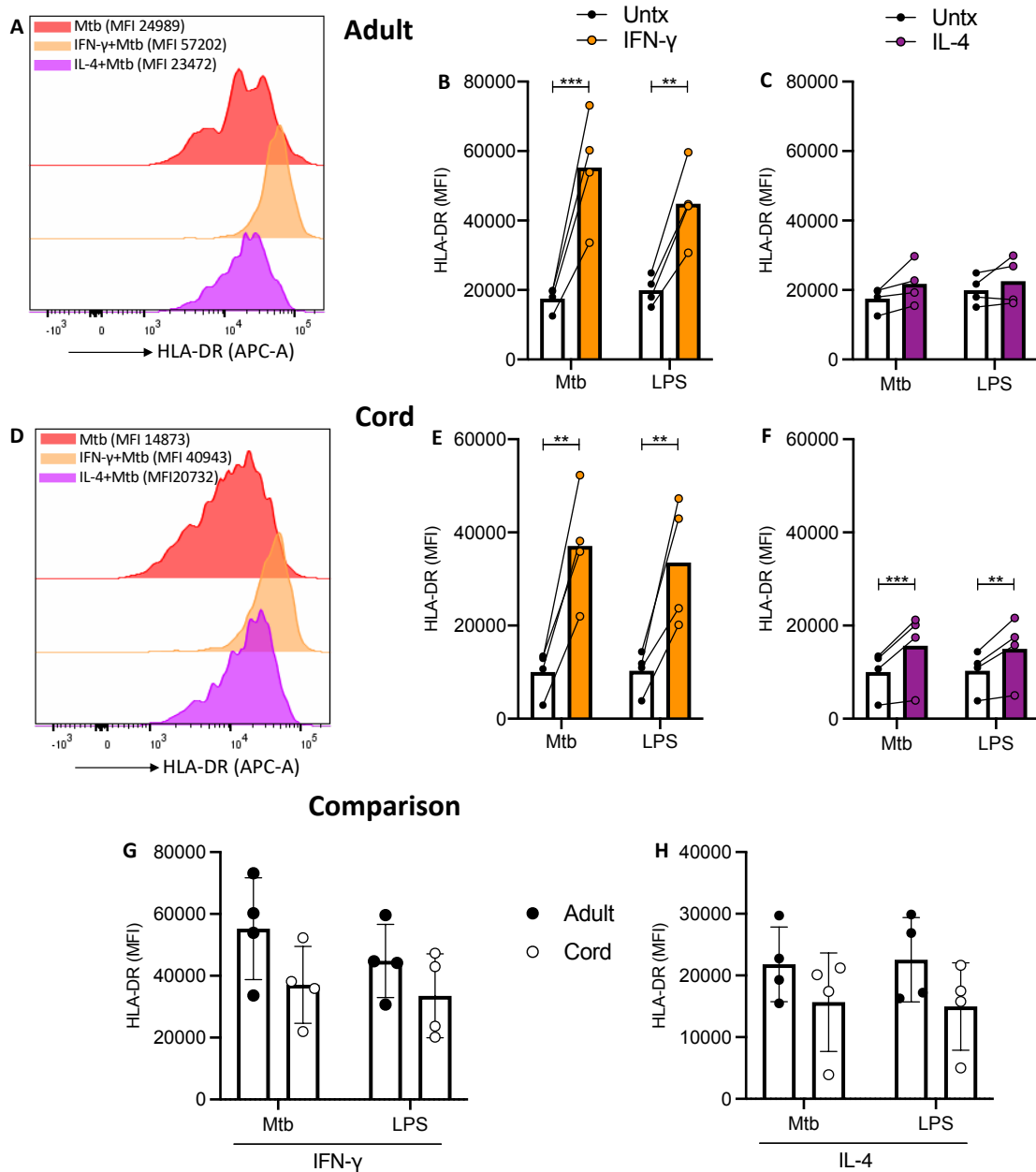


Figure 4.26 Expression of HLA-DR on adult and cord blood MDM 48 hours after IFN- γ or IL-4 treatment and 24 hours after Mtb or LPS stimulation.

PBMC were isolated from buffy coats or from umbilical cord blood samples taken immediately following delivery. Adult or cord blood MDM were adherence purified for 7 days in 10% human serum. 24 hours after treatment with IFN- γ (10ng/ml) or IL-4 (10ng/ml), MDM were stimulated with Mtb (iH37Rv; MOI 1-10) or LPS (100 ng/ml). MDM were washed and detached from the plates by cooling and gentle scraping 24 hours after stimulation with Mtb or LPS. Cells were Fc blocked, exposed to viability dye Zombie NIR and stained with fluorochrome-conjugated antibodies specific for CD14, CD68 and HLA-DR. Cells were analysed by flow cytometry. A representative histogram for one donor of adult (A) and cord (D) MDM stimulated with Mtb is shown. The MFI of HLA-DR for the adult (B,C n=4 \pm SD) and cord (n=4 \pm SD) MDM is shown. Comparison between the adult and cord blood values are shown (G,H). Statistical significance was determined by two-way ANOVA using Sidak's multiple comparison test **P<0.01, ***P<0.001.

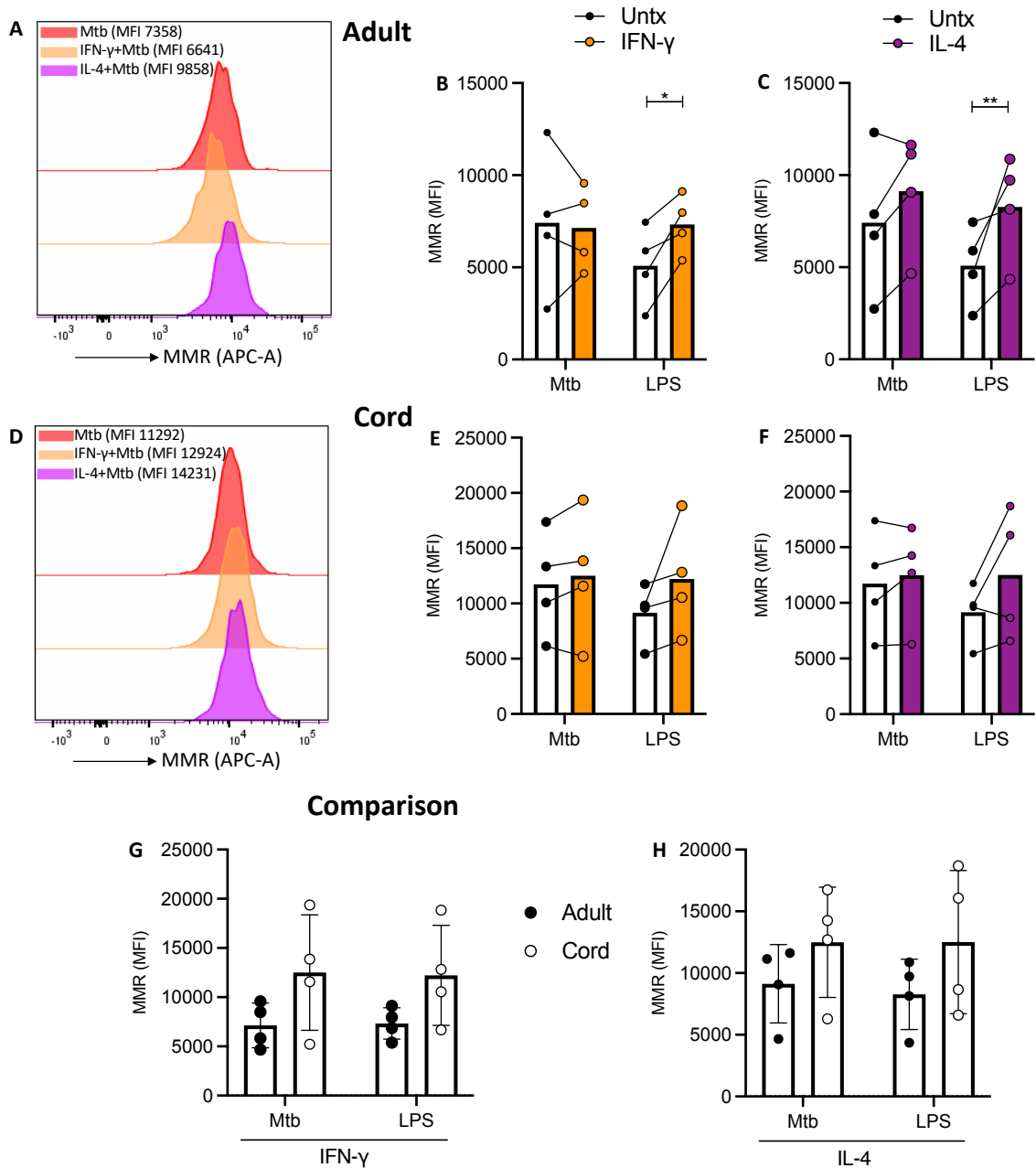


Figure 4.27 Expression of MMR on adult and cord blood MDM 48 hours after IFN- γ or IL-4 treatment and 24 hours after Mtb or LPS stimulation.

PBMC were isolated from buffy coats or from umbilical cord blood samples taken immediately following delivery. Adult or cord blood MDM were adherence purified for 7 days in 10% human serum. 24 hours after treatment with IFN- γ (10ng/ml) or IL-4 (10ng/ml), MDM were stimulated with Mtb (iH37Rv; MOI 1-10) or LPS (100 ng/ml). MDM were washed and detached from the plates by cooling and gentle scraping 24 hours after stimulation with Mtb or LPS. Cells were Fc blocked, exposed to viability dye Zombie NIR and stained with fluorochrome-conjugated antibodies specific for CD14, CD68 and MMR. Cells were analysed by flow cytometry. A representative histogram for one donor of adult (A) and cord (D) MDM stimulated with Mtb is shown. The MFI of MMR for the adult (B,C n=4 \pm SD) and cord (n=4 \pm SD) MDM is shown. Comparison between the adult and cord blood values are shown (G,H). Statistical significance was determined by two-way ANOVA using Sidak's multiple comparison test * P<0.05, **P<0.01.

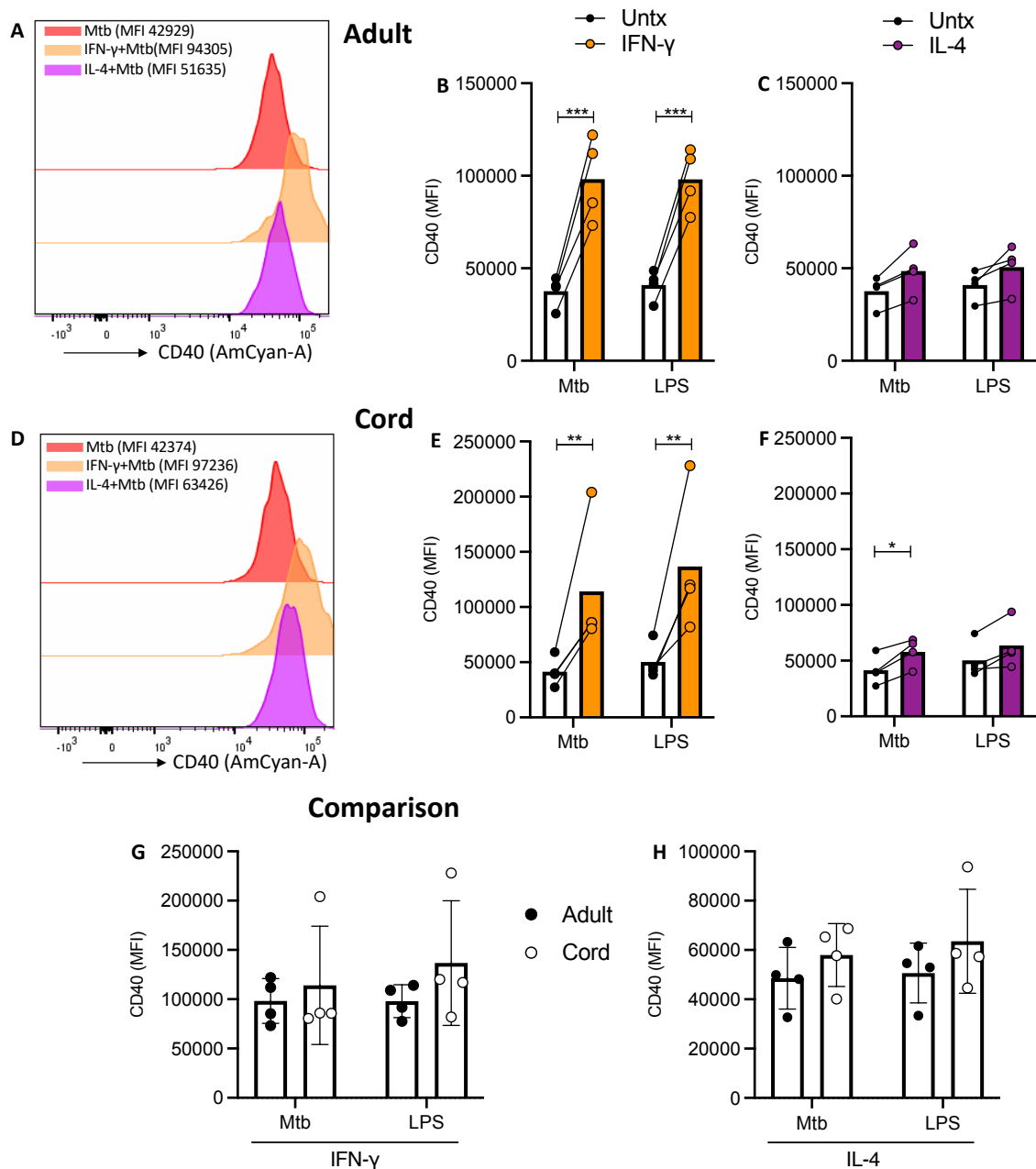


Figure 4.28 Expression of CD40 on adult and cord blood MDM 48 hours after IFN- γ or IL-4 treatment and 24 hours after Mtb or LPS stimulation.

PBMC were isolated from buffy coats or from umbilical cord blood samples taken immediately following delivery. Adult or cord blood MDM were adherence purified for 7 days in 10% human serum. 24 hours after treatment with IFN- γ (10ng/ml) or IL-4 (10ng/ml), MDM were stimulated with Mtb (iH37Rv; MOI 1-10) or LPS (100 ng/ml). MDM were washed and detached from the plates by cooling and gentle scraping 24 hours after stimulation with Mtb or LPS. Cells were Fc blocked, exposed to viability dye Zombie NIR and stained with fluorochrome-conjugated antibodies specific for CD14, CD68 and CD40. Cells were analysed by flow cytometry. A representative histogram for one donor of adult (A) and cord (D) MDM stimulated with Mtb is shown. The MFI of CD40 for the adult (B,C n=4 \pm SD) and cord (n=4 \pm SD) MDM is shown. Comparison between the adult and cord blood values are shown (G,H). Statistical significance was determined by two-way ANOVA using Sidak's multiple comparison test * P<0.05, **P<0.01, ***P<0.001.

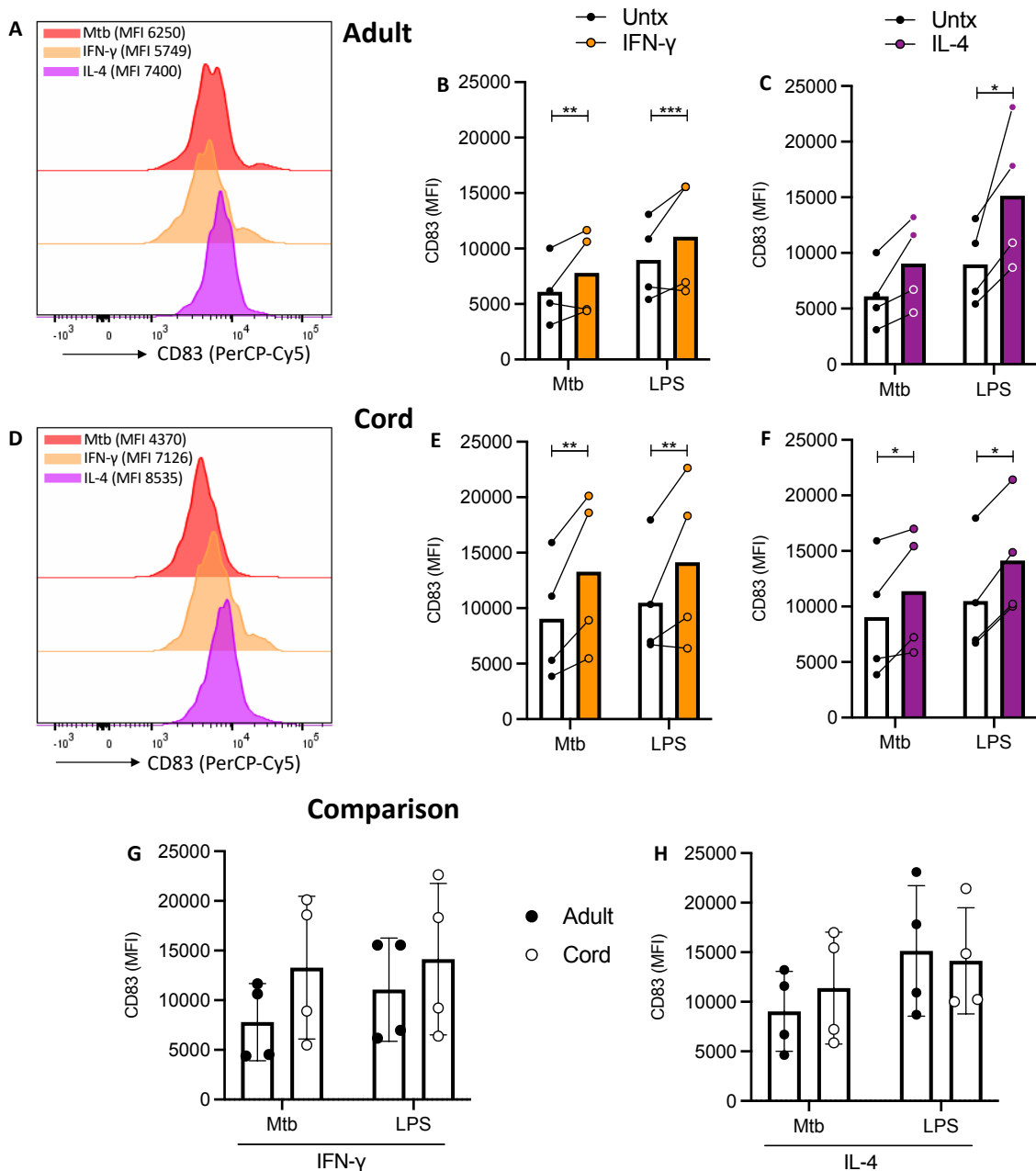


Figure 4.29 Expression of CD83 on adult and cord blood MDM 48 hours after IFN- γ or IL-4 treatment and 24 hours after Mtb or LPS stimulation.

PBMC were isolated from buffy coats or from umbilical cord blood samples taken immediately following delivery. Adult or cord blood MDM were adherence purified for 7 days in 10% human serum. 24 hours after treatment with IFN- γ (10ng/ml) or IL-4 (10ng/ml), MDM were stimulated with Mtb (iH37Rv; MOI 1-10) or LPS (100 ng/ml). MDM were washed and detached from the plates by cooling and gentle scraping 24 hours after stimulation with Mtb or LPS. Cells were Fc blocked, exposed to viability dye Zombie NIR and stained with fluorochrome-conjugated antibodies specific for CD14, CD68 and CD83. Cells were analysed by flow cytometry. A representative histogram for one donor of adult (A) and cord (D) MDM stimulated with Mtb is shown. The MFI of CD83 for the adult (B,C n=4 \pm SD) and cord (n=4 \pm SD) MDM is shown. Comparison between the adult and cord blood values are shown (G,H). Statistical significance was determined by two-way ANOVA using Sidak's multiple comparison test * P<0.05, **P<0.01, ***P<0.001.

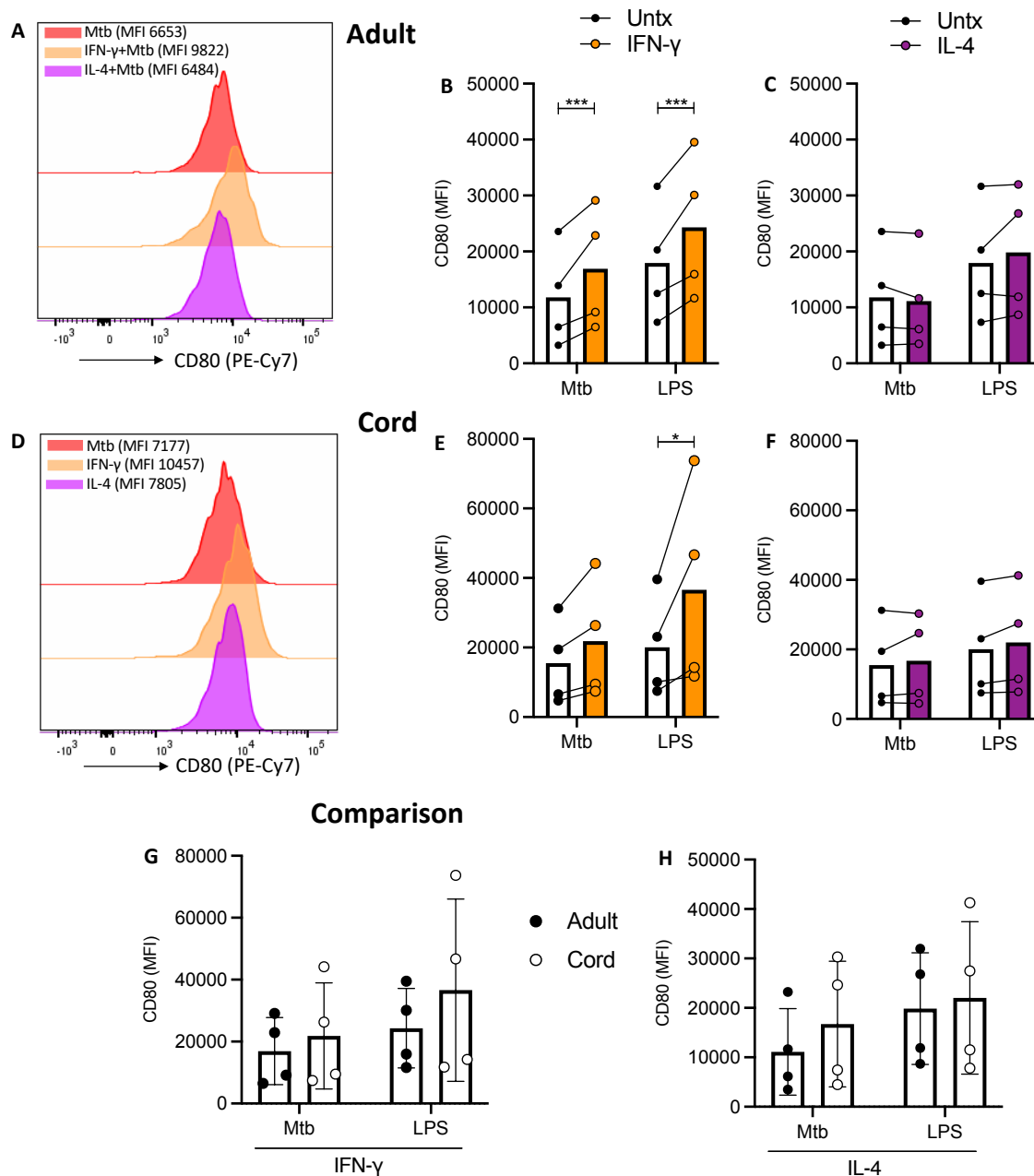


Figure 4.30 Expression of CD80 on adult and cord blood MDM 48 hours after IFN- γ or IL-4 treatment and 24 hours after Mtb or LPS stimulation.

PBMC were isolated from buffy coats or from umbilical cord blood samples taken immediately following delivery. Adult or cord blood MDM were adherence purified for 7 days in 10% human serum. 24 hours after treatment with IFN- γ (10ng/ml) or IL-4 (10ng/ml), MDM were stimulated with Mtb (iH37Rv; MOI 1-10) or LPS (100 ng/ml). MDM were washed and detached from the plates by cooling and gentle scraping 24 hours after stimulation with Mtb or LPS. Cells were Fc blocked, exposed to viability dye Zombie NIR and stained with fluorochrome-conjugated antibodies specific for CD14, CD68 and CD80. Cells were analysed by flow cytometry. A representative histogram for one donor of adult (A) and cord (D) MDM stimulated with Mtb is shown. The MFI of CD80 for the adult (B,C $n=4 \pm SD$) and cord ($n=4 \pm SD$) MDM is shown. Comparison between the adult and cord blood values are shown (G,H). Statistical significance was determined by two-way ANOVA using Sidak's multiple comparison test * $P<0.05$, *** $P<0.001$.

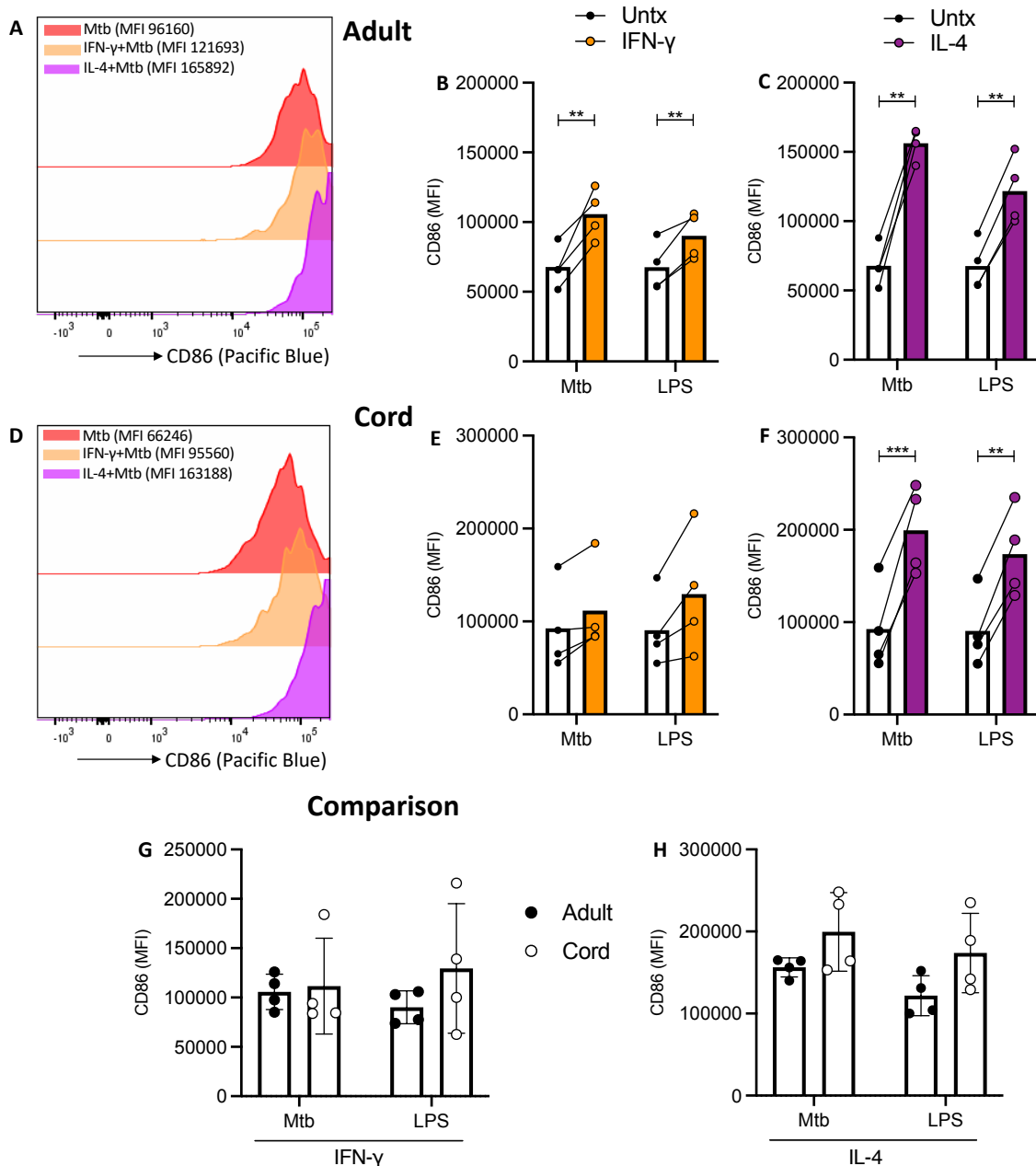


Figure 4.31 Expression of CD86 on adult and cord blood MDM 48 hours after IFN- γ or IL-4 treatment and 24 hours after Mtb or LPS stimulation.

PBMC were isolated from buffy coats or from umbilical cord blood samples taken immediately following delivery. Adult or cord blood MDM were adherence purified for 7 days in 10% human serum. 24 hours after treatment with IFN- γ (10ng/ml) or IL-4 (10ng/ml), MDM were stimulated with Mtb (iH37Rv; MOI 1-10) or LPS (100 ng/ml). MDM were washed and detached from the plates by cooling and gentle scraping 24 hours after stimulation with Mtb or LPS. Cells were Fc blocked, exposed to viability dye Zombie NIR and stained with fluorochrome-conjugated antibodies specific for CD14, CD68 and CD86. Cells were analysed by flow cytometry. A representative histogram for one donor of adult (A) and cord (D) MDM stimulated with Mtb is shown. The MFI of CD86 for the adult (B,C n=4 \pm SD) and cord (n=4 \pm SD) MDM is shown. Comparison between the adult and cord blood values are shown (G,H). Statistical significance was determined by two-way ANOVA using Sidak's multiple comparison test * P<0.05, **P<0.01.

4.2.5 The effect of pretreatment with IFN- γ or IL-4 on subsequent cytokine responses to Mtb or LPS

The effect of pretreating adult or cord blood MDM with IFN- γ or IL-4 on their ability to secrete cytokines in responses to Mtb or LPS was established. PBMC were isolated from adult buffy coats or from umbilical cord blood which was collected immediately following delivery. MDM were adherence purified for 7 days in RPMI with 10% human serum and non-adherent cells were washed off on days 2 and 5. IFN- γ (10ng/ml) or IL-4 (10ng/ml) were added 24 hours prior to the addition of Mtb (iH37Rv; MOI 1-10) or LPS (100 ng/ml). The concentrations of TNF, IL-1 β , IL-10 and IL-6 in supernatant were measured by Mesoscale Discovery assay 24 hours after stimulation with Mtb or LPS.

Pre-treatment with IFN- γ significantly increased Mtb induced IL-1 β production in adult MDM (Figure 4.32 A, $P < 0.05$) and IL-4 induced the opposite effect with by significantly reducing IL-1 β secretion (Figure 4.32 B, $P < 0.001$). IFN- γ did not cause any significant change in IL-1 β production from cord blood MDM (Figure 4.32 C) but IL-4 significantly reduced the production of IL-1 β following Mtb stimulation (Figure 4.32 D, $P < 0.001$). As expected, LPS did not induce IL-1 β production and there was no significant differences in adult or cord blood MDM production of IL-1 β after IFN- γ (Figure 4.32 E) or IL-4 treatment (Figure 4.32 F).

TNF was significantly increased in Mtb ($P < 0.0001$) and LPS ($P < 0.01$) stimulated adult MDM following IFN- γ treatment (Figure 4.33 A). IL-4 treatment did not have a significant impact on TNF production in adult MDM (Figure 4.33 B). Cord blood MDM produced significantly more TNF after Mtb stimulation when pre-treated with IFN- γ (Figure 4.33

C, $P < 0.01$) and significantly less TNF after LPS stimulation when pre-treated with IL-4 (Figure 4.33 D, ($P < 0.01$)). There was no significant differences in adult or cord blood MDM production of TNF after IFN- γ (Figure 4.33 E) or IL-4 treatment (Figure 4.33 F).

IFN- γ treatment significantly increased IL-6 production in both Mtb ($P < 0.001$) and LPS ($P < 0.01$) stimulated adult MDM (Figure 4.34 A). Although the changes seen after IL-4 treatment were not statistically significant, IL-6 production did trend downward, particularly in Mtb stimulated MDM (Figure 4.34 B, $P = 0.054$). In cord blood MDM, pre-treatment with IFN- γ caused a significant increase in IL-6 production after Mtb stimulation ($P < 0.01$) but not LPS stimulation (Figure 4.34 C). IL-4 did not significantly impact IL-6 production in cord blood MDM (Figure 4.34 D). There was no significant differences in adult or cord blood MDM production of IL-6 after IFN- γ (Figure 4.34 E) or IL-4 treatment (Figure 4.34 F).

IL-10 production was unaffected by pre-treatment with IFN- γ in adult MDM (Figure 4.35 A). IL-4 decreased production of IL-10 following Mtb stimulation ($P < 0.05$) but increased IL-10 following LPS stimulation ($P < 0.05$) in adult MDM (Figure 4.35 B). IFN- γ treatment did not alter IL-10 production in cord blood MDM (Figure 4.35 C). IL-4 caused a decrease in IL-10 production after Mtb ($P < 0.05$) but the concentrations of IL-10 after LPS stimulation were not significantly altered in the presence of IL-4 (Figure 4.35 D). There was no significant differences in adult or cord blood MDM production of IL-10 after IFN- γ (Figure 4.35 E) or IL-4 treatment (Figure 4.35 F).

These data show that pre-treatment with IL-4 causes a significant reduction in IL-1 β production in both adult and cord blood MDM stimulated with Mtb, in keeping with the reduction in glycolysis seen with IL-4 treatment. IFN- γ causes an increase in TNF production in adult and cord blood MDM stimulated with Mtb which corrects the deficient TNF production in cord blood MDM in response to Mtb observed in chapter 3.

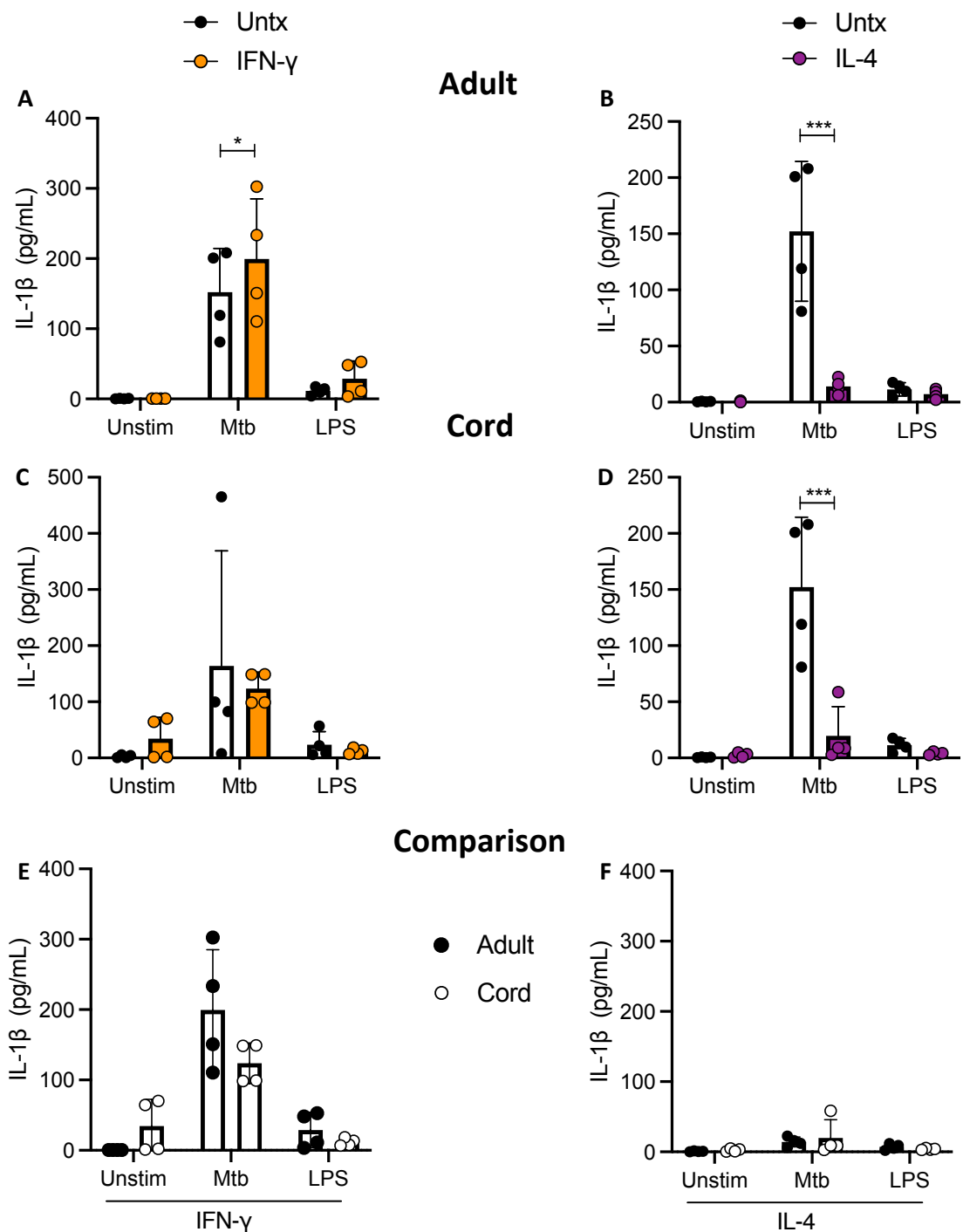


Figure 4.32 Mtb or LPS induced IL-1 β production after pre-treatment with IFN- γ or IL-4.

PBMC were isolated from buffy coats or from umbilical cord blood samples taken immediately following delivery. MDM were adherence purified for 7 days in 10% human serum. IFN- γ (10ng/ml) or IL-4 (10ng/ml) were added 24 hours prior to the addition of Mtb (iH37Rv; MOI 1-10) or LPS (100 ng/ml). The concentration of IL-1 β in supernatant was measured by Mesoscale Discovery assay 24 hours after stimulation with Mtb or LPS. Graphs illustrate collated data from adult (A,B) and cord (C,) MDM (n=4 \pm SD for both). Comparative analysis between adult and cord blood responses was performed (E,F). Statistical significance was determined using two-way ANOVA with Sidak's multiple comparison test; ** P<0.01, *** P<0.001.

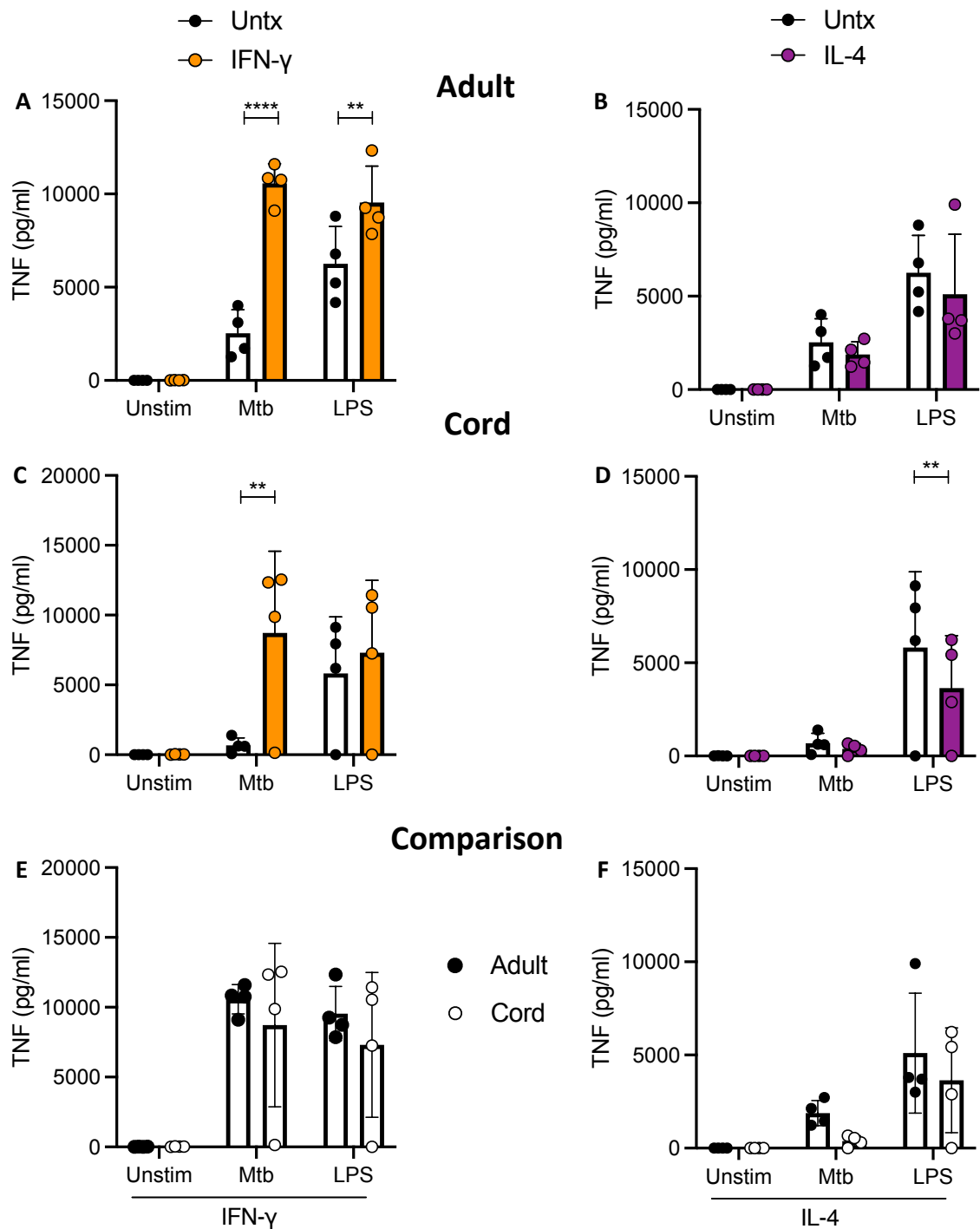


Figure 4.33 Mtb or LPS induced TNF production after pre-treatment with IFN- γ or IL-4.

PBMC were isolated from buffy coats or from umbilical cord blood samples taken immediately following delivery. MDM were adherence purified for 7 days in 10% human serum. IFN- γ (10ng/ml) or IL-4 (10ng/ml) were added 24 hours prior to the addition of Mtb (iH37Rv; MOI 1-10) or LPS (100 ng/ml). The concentration of TNF in supernatant was measured by Mesoscale Discovery assay 24 hours after stimulation with Mtb or LPS. Graphs illustrate collated data from adult (A,B) and cord (C,) MDM (n=4 \pm SD for both). Comparative analysis between adult and cord blood responses was performed (E,F). Statistical significance was determined using two-way ANOVA with Sidak's multiple comparison test; ** P<0.01, **** P<0.0001.

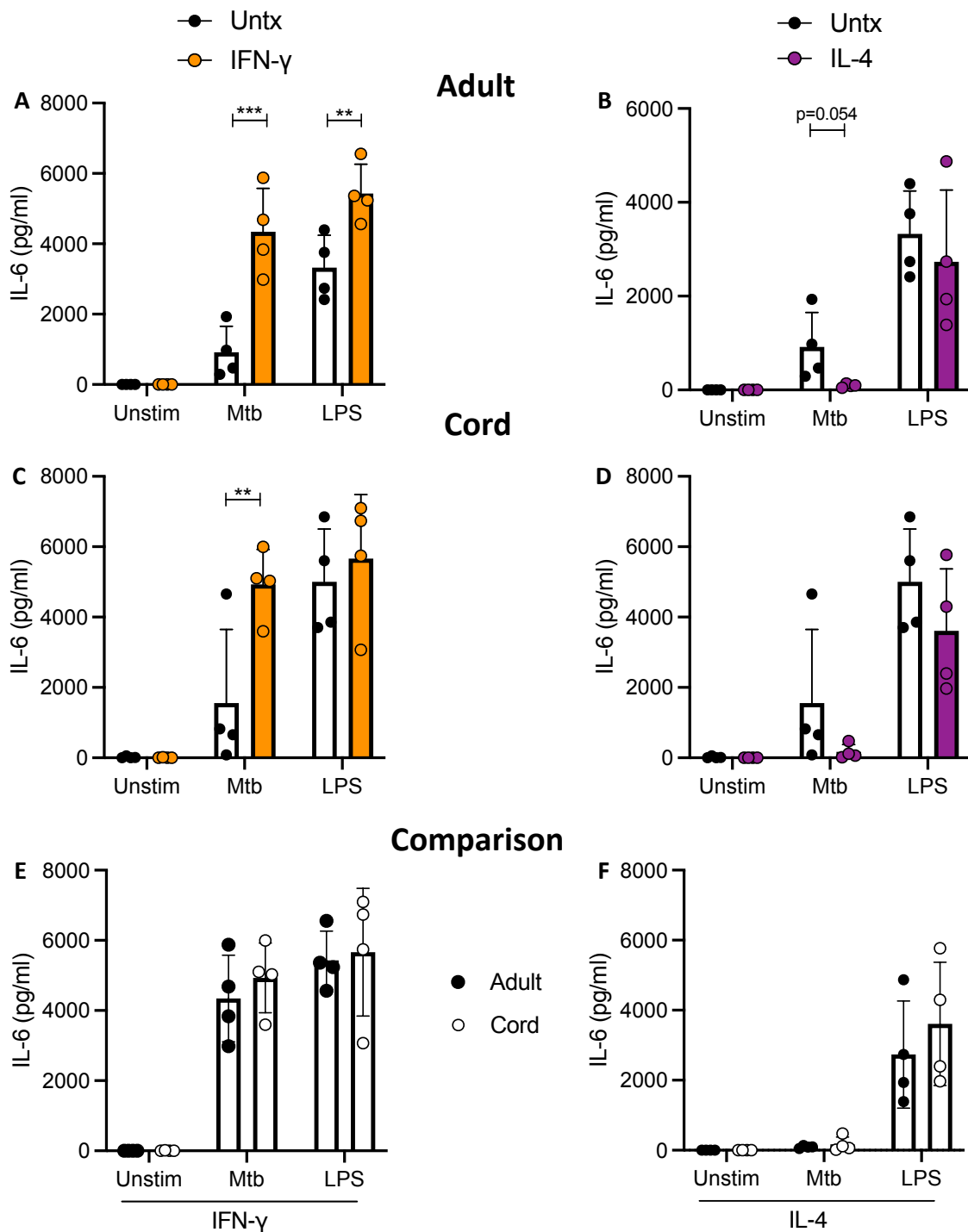


Figure 4.34 Mtb or LPS induced IL-6 production after pre-treatment with IFN- γ or IL-4. PBMC were isolated from buffy coats or from umbilical cord blood samples taken immediately following delivery. MDM were adherence purified for 7 days in 10% human serum. IFN- γ (10ng/ml) or IL-4 (10ng/ml) were added 24 hours prior to the addition of Mtb (iH37Rv; MOI 1-10) or LPS (100 ng/ml). The concentration of IL-6 in supernatant was measured by Mesoscale Discovery assay 24 hours after stimulation with Mtb or LPS. Graphs illustrate collated data from adult (A,B) and cord (C,) MDM (n=4 \pm SD for both). Comparative analysis between adult and cord blood responses was performed (E,F). Statistical significance was determined using two-way ANOVA with Sidak's multiple comparison test; ** P<0.01, *** P<0.001.

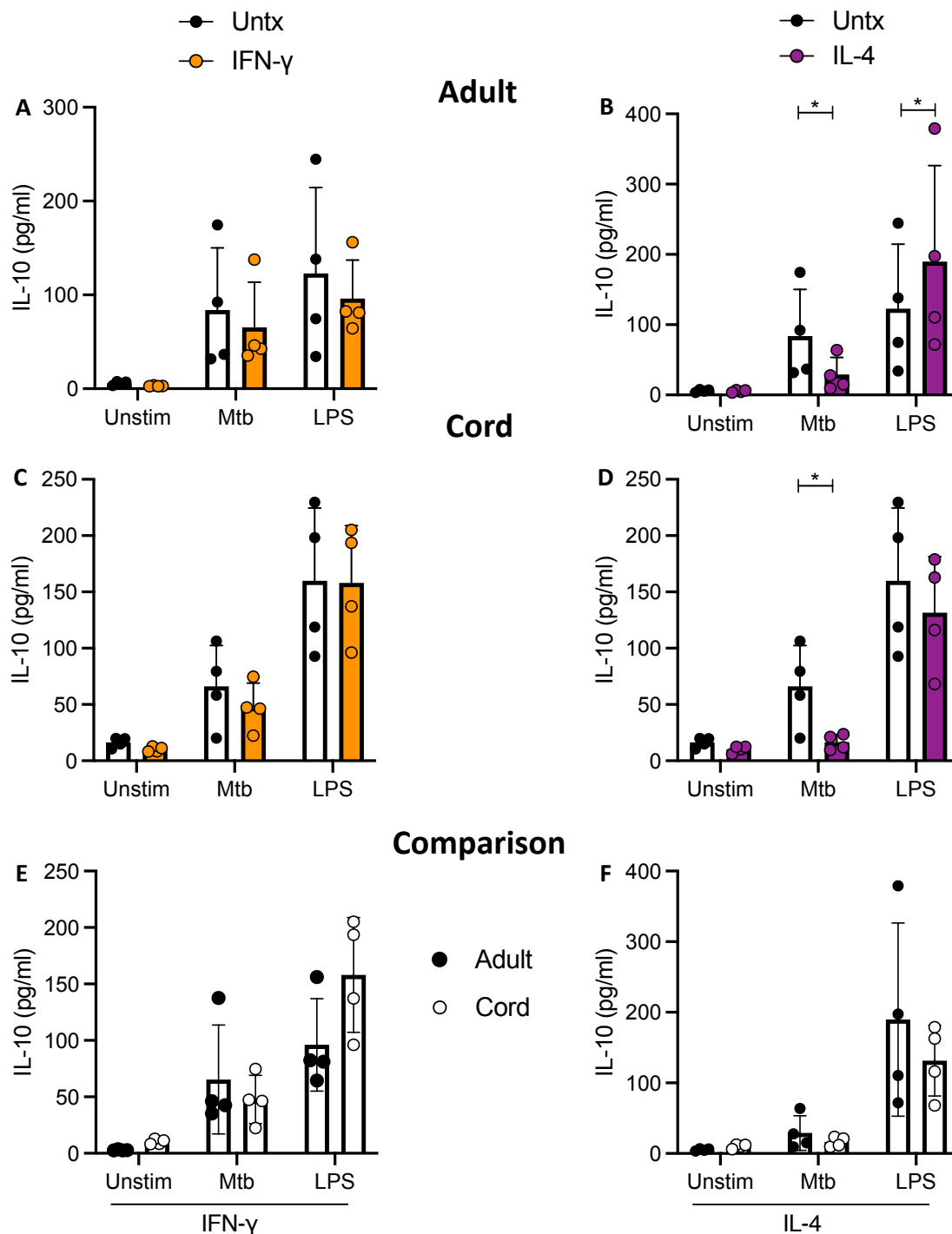


Figure 4.35 Mtb or LPS induced IL-10 production after pre-treatment with IFN- γ or IL-4.

PBMC were isolated from buffy coats or from umbilical cord blood samples taken immediately following delivery. MDM were adherence purified for 7 days in 10% human serum. IFN- γ (10ng/ml) or IL-4 (10ng/ml) were added 24 hours prior to the addition of Mtb (iH37Rv; MOI 1-10) or LPS (100 ng/ml). The concentration of IL-10 in supernatant was measured by Mesoscale Discovery assay 24 hours after stimulation with Mtb or LPS. Graphs illustrate collated data from adult (A,B) and cord (C,) MDM (n=4 \pm SD for both). Comparative analysis between adult and cord blood responses was performed (E,F). Statistical significance was determined using two-way ANOVA with Sidak's multiple comparison test; * P<0.05.

4.3 Discussion

The data generated in this chapter shows distinct metabolic and phenotypic changes in both adult and cord blood MDM after IFN- γ or IL-4 exposure. As mentioned previously, the heterogeneity in macrophage differentiation methodology makes interpretation of the cell surface markers difficult. A previous study in adult human macrophages showed similar patterns of increase in HLA-DR and CD86 with both IFN- γ or IL-4 and an increase in MMR with IL-4.¹⁶⁴ One of the few papers using human serum to differentiate macrophages polarised with IFN- γ in combination with LPS for an M1 phenotype and compared it with IL-4 treated macrophage which were not stimulated, therefore it is not fully comparable to these data set, but a similar increase in MMR after IL-4 was shown¹⁶². Despite differences in methodology the results of cell surface markers in adult MDM generated in this study appear to broadly correlate with the limited previously published human data²⁷⁷. The only significant difference seen between adult and cord blood MDM cell surface markers after polarisation was in the expression of CD40, which was significantly higher in cord blood MDM treated with IFN- γ (Figure 4.2). Published datasets are contradictory, with limited data using various methodologies^{173,179,230,278}.

The metabolic phenotype in murine BMDM following M1 polarisation is well described and has consistently been associated with increased glycolysis and decreased oxidative phosphorylation^{194,237,279,280}. Of note, Van der Bosh et al observed that IFN- γ did not increase glycolysis in BMDM but that LPS was required²⁷⁴. The findings in the current study therefore reveal a novel difference in human adult MDM responses to IFN- γ compared with their murine counterparts. Although the increase in glycolysis after LPS stimulation is seen in both human and murine macrophages, there is a concurrent

increase in OCR (Figure 4.9, Figure 4.11) in human MDM, the opposite of what is described in murine BMDM and similar to what is seen in LPS stimulated human MDM at 24 hours. These data again highlight the differences in murine and human immunometabolic responses.

Although this increase in ECAR was also seen in cord blood MDM treated with IFN- γ , the OCR was unchanged (Figure 4.9, Figure 4.11). OCR was also unchanged after Mtb or LPS stimulation in cord blood MDM. This raises the possibility of a common signaling mechanism for all 3 stimuli that may be defective in cord blood MDM. IFN- γ , Mtb and LPS all utilise STAT signaling and previous studies have shown defects in STAT signaling in cord blood MDM^{230,281}. The exploration of the possibility of a link between STAT signaling and OXPHOS was beyond the scope of the current study and the inability of cord blood MDM to alter OCR following stimulation may reflect a more intrinsic defect in regulation of OXPHOS. The cellular activation processes involved are likely multifactorial as although similar patterns were seen following activation by IFN- γ , Mtb or LPS, with increases in ECAR, there were significant differences in the immunophenotype, with no cytokine production following IFN- γ for example.

Alternative macrophage activation (or M2 polarisation) with IL4 in murine models is dependent on oxidative metabolism¹⁹⁴ and has been shown to increase ECAR^{238,275}. Small increases in both ECAR and OCR 24 hours after IL-4 in human MDM have been described but in MDM differentiated with M-CSF²⁸². A novel effect of IL-4 is described in this study in both adult and cord blood MDM with a significant reduction in ECAR in

adult MDM and approaching significance in the cord blood (Figure 2.9, P=0.06). No significant changes to OCR were noted in the absence of stimulation.

It has been long appreciated that macrophages can be “primed” by IFN- γ , augmenting subsequent responses to TLR stimulation, however, the majority of published work is in murine experimental models^{283,284}. The results described in this study reveal novel effects of IFN- γ on subsequent metabolic responses to Mtb and LPS stimulation in human MDM. Pre-treatment with IFN- γ increased the ECAR in adult MDM 150 minutes after Mtb but not LPS stimulus (Figure 4.16, Figure 4.22). The ECAR was not significantly increased in either Mtb or LPS stimulation in cord blood. The cumulative effect of IFN- γ and stimulation may have maximised the glycolytic response in the LPS stimulated adult MDM and the cord blood MDM. Despite the lack of significant increase in ECAR in LPS stimulated adult MDM after IFN- γ treatment, significant increases in HLA-DR, CD40, CD83, CD80 and CD86 were seen in both Mtb and LPS stimulated adult MDM. This was coupled with significant increases in TNF and IL-6 production in both Mtb and LPS stimulated MDM pre-treated with IFN- γ and in IL-1 β after Mtb. Cord blood MDM pre-treated with IFN- γ showed significant increases in HLA-DR, CD40, CD83, CD80 (LPS only) but not CD86. The IFN- γ induced increase in HLA-DR in cord blood MDM equalised the expression compared with adult MDM at baseline and reversed the defect observed in the ability of cord blood MDM to upregulate HLA-DR in response to LPS stimulation as described in Chapter 3. Pre-treatment of cord blood MDM with IFN- γ significantly increased IL-6 and TNF in Mtb stimulated cells, overcoming the defect in TNF production seen in untreated cord MDM in Chapter 3. These data indicate that although IFN- γ did not significantly increase the ECAR of LPS stimulated adult or cord blood MDM, it,

nevertheless, had an impact resulting in augmented cytokine production and expression of markers associated with APC function.

Pre-treatment with IL-4 resulted in a significant reduction of ECAR in both adult and cord blood MDM after Mtb and LPS (adult only, cord P=0.09) stimulation. The Warburg effect of a reduction in oxidative phosphorylation, seen in adult MDM, was inhibited by IL-4. Both of these factors resulted in significant alterations in the ECAR/OCR ratio for adult and cord blood MDM after both Mtb and LPS. IL-1 β production after IL-4 treatment was significantly reduced in both adult and cord blood MDM after Mtb stimulation. IL-1 β has previously been shown to be dependent on glycolysis^{188,189} and the reduction of ECAR caused by IL-4 may have impacted on IL-1 β production although definitive evidence linking this metabolic phenotype to the cytokine outputs remains elusive.

4.4 Conclusions

These data show that IFN- γ or IL-4 significantly alter metabolism in human MDM. This is a novel finding that is different to previously described murine metabolic shifts. Pre-treatment with IFN- γ significantly increased glycolysis in adult MDM stimulated with Mtb. IFN- γ increased the expression of cell surface markers and cytokine production, reversing the defect in TNF production seen in cord blood stimulated with Mtb in Chapter 3. IL-4 prevented the decrease in OCR seen in adult MDM following Mtb or LPS stimulation and significantly reduced ECAR. An associated decrease in IL-1 β production after Mtb stimulation was observed. Both IFN- γ and IL-4 have profound immunometabolic effects in human MDM, these findings allow greater understanding of

the many disease processes involving these cytokines and identify potential targets of immunometabolic manipulation.

Chapter 5 Lactate alters metabolism in human macrophages and improves their ability to kill *Mycobacterium tuberculosis*

5.1 Introduction

In the previous chapters, a shift towards aerobic glycolysis has been shown in human MDM after LPS or Mtb stimulation and after IFN- γ treatment. This shift has previously been demonstrated in human macrophages that are infected with Mtb^{41,188,228,229,235}, although the kinetics and extent of this metabolic alteration varies in different reports. This increased glycolytic flux is associated with the ability of the macrophage to effectively kill Mtb^{41,188,235}, as inhibition of glycolysis in macrophages results in increased growth of Mtb¹⁸⁸. Furthermore, Mtb can perturb host glycolytic metabolism to promote its own survival^{188,285}, which highlights the importance of the process of aerobic glycolysis in host defence against Mtb.

Lactate, the end-product of glycolysis (Figure 1.2), accumulates as a consequence of this altered metabolic function^{41,188,235,286}. In keeping with this finding, assays that measure extracellular lactate concentrations have been used to indicate that this metabolic shift has taken place in activated macrophages^{41,188,235,286}. Lactate, for decades regarded as an unwanted waste product, has now been shown to have numerous functions, including as a carbon source, signaling molecule, histone deacetylase inhibitor²⁸⁷ and, in the context of cancer, it influences cell growth and migration^{288–290}. Because many other types of immune cells also rely on this glycolytic switch for their activation, lactate is known to accumulate at sites of chronic inflammation and can propagate inappropriate inflammation via metabolic reprogramming²⁹¹. Clinically, elevated serum

lactate levels are associated with increased mortality in a diverse range of patients^{292,293}. Lactate levels predict mortality in patients with infection²⁹⁴ and sepsis²⁹⁵.

Lactate has been shown to inhibit glycolysis and cytokine production in human monocytes^{214,286} and murine macrophages stimulated with LPS²⁹⁶. While Mtb infected macrophages have been shown to alter the metabolic profiles of macrophages in their vicinity²⁹⁷, a knowledge gap exists around what effect lactate accumulation specifically has on bystander macrophages that subsequently become infected if the initially infected macrophage fails to control the infection and the bacteria escape back into the extracellular space.

5.1.1 Hypothesis and Aims

Hypothesis:

The glycolytic shift that is induced by macrophage activation results in increased lactate secretion and it was hypothesised that this molecule would have a direct immunometabolic effect on surrounding MDM.

Aims:

- Examine the effect of exogenous lactate on the immunometabolic profile of adult and cord blood macrophages using Seahorse XFe Analyzer technology.
- Elucidate how the presence of lactate alters the kinetics of immunometabolic changes in human macrophages stimulated with Mtb and LPS stimulation in real time.

- Examine the impact of lactate on cell surface markers associated with activation after Mtb or LPS stimulation.
- Examine the differential ability of adult or cord blood macrophages which have been pre-treated with lactate to produce key cytokines 24 hours after stimulation with Mtb or LPS.

5.2 Results

Physiological levels of lactate in human peripheral blood range between 0.5-2 mM, however, this increases in disease states such as sepsis and have been reported as high as 25 mM after strenuous exercise^{298,299}. Lactate is released from lung tissue in patients with sepsis and acute respiratory distress syndrome³⁰⁰. Local tissue concentrations of lactate during acute infections or in the context of chronic inflammation are largely unknown but concentrations of approximately 15 mM have been measured in the synovial joints of patients with rheumatoid arthritis³⁰¹. Furthermore, published work reports macrophages stimulated *in vitro* have varying concentrations of lactate in the supernatants, up to approximately 30 mM⁴¹. There has been contradictory evidence over the requirement for lactate to be acidified into its conjugate acid, lactic acid, in order for it to alter immune function²¹¹⁻²¹⁴. For the purpose of this study, sodium lactate at 25 mM was used throughout, unless where otherwise stated. The optimisation of lactate at this concentration is outlined in the material and methods section **2.8**.

5.2.1 Lactate alters human adult and cord blood MDM metabolism

Lactate has previously been shown to decrease the ECAR of human monocytes one hour after treatment²⁸⁶. In order to determine if exposure to exogenous lactate similarly

affects the metabolic function of resting human adult and cord blood MDM, a real time kinetic analysis of the metabolic effect of exogenous lactate (25 mM) was performed.

PBMC were isolated from buffy coats or from umbilical cord blood samples taken immediately following delivery. Adult or cord blood MDM were adherence purified for 6-8 days in 10% human serum. MDM were harvested by placing in ice-cold PBS at 4°C for 30 minutes prior to gentle scraping and seeded on Seahorse culture plates prior to analysis in the Seahorse XFe24 Analyzer.

5.2.1a Lactate immediately decreases ECAR and increases OCR in both adult and cord blood MDM

MDM were monitored for 30 minutes before lactate (25mM) or medium (untreated control) was injected into wells through the port in the Seahorse Analyzer. The ECAR and OCR readings were sampled every 9 minutes. Addition of lactate caused an immediate decrease in ECAR to adult (Figure 5.1 A) and cord blood (Figure 5.1 B) MDM. The third reading was taken as the baseline and the ECAR is expressed as percent (%) change from this baseline in order to correct for human variability and minor differences in cell seeding density on the Seahorse culture plate. The ECAR in both the adult (Figure 5.1 C) and cord blood (Figure 5.1 D) MDM, expressed as percent change from baseline, is decreased by the addition of lactate in the time course graph. Concurrently, an increase in the OCR is seen in both the adult and cord blood MDM (Figure 5.2A and B, respectively) and when these data are normalised to % change from baseline, the OCR remains elevated with the addition of lactate compared with control (Figure 5.2 C and D).

Analysis was undertaken at 70 mins (40 mins post treatment with lactate) as indicated on the time course graphs. This time point was chosen as the decrease in ECAR had plateaued as visualised on the time course graph. Collated data at the analysis timepoint illustrates that the decreases seen in both the ECAR raw values and % change from baseline were significant in the adult (Figure 5.3 A, $P < 0.05$, $P < 0.001$, respectively) and cord blood (Figure 5.3 B, $P < 0.05$, $P < 0.01$, respectively). The OCR expressed as % change from baseline were significantly increased in the adult (Figure 5.3 C, $P < 0.05$) and cord blood (Figure 5.3 D, $P < 0.05$), however; the OCR raw values were statistically significantly different. The ECAR/OCR ratio was calculated at this time point and it was significantly decreased in adult MDM (Figure 5.3 E, $P < 0.05$). The cord blood MDM decrease in ECAR/OCR ratio approached significance with a P value of 0.0547 (Figure 5.3 F).

5.2.1b NaCl has no effect on metabolism of adult MDM

In order to ensure that the changes on MDM metabolism observed in the presence of Na-L-Lactate were not due to the impact of the sodium ion or osmotic pressure, a live kinetic experiment was undertaken with equimolar concentrations of sodium chloride^{302,303} (NaCl). Due to limited cord blood donor availability these experiments were undertaken in adult MDM only. NaCl does not alter the OCR (Figure 5.4 A) or ECAR (Figure 5.4 B) in adult MDM. In addition, there were no differences in ECAR or OCR when the rates were normalised to the % change from baseline (Figure 5.4 C & D). In keeping, there was no difference in the ECAR/OCR ratio (Figure 5.4 E) after the administration of NaCl.

These data illustrate that exogenous lactate has an immediate effect on the metabolic function of resting macrophages, reducing ECAR and increasing OCR, the opposite of the Warburg effect seen with stimulation in Chapter 3.

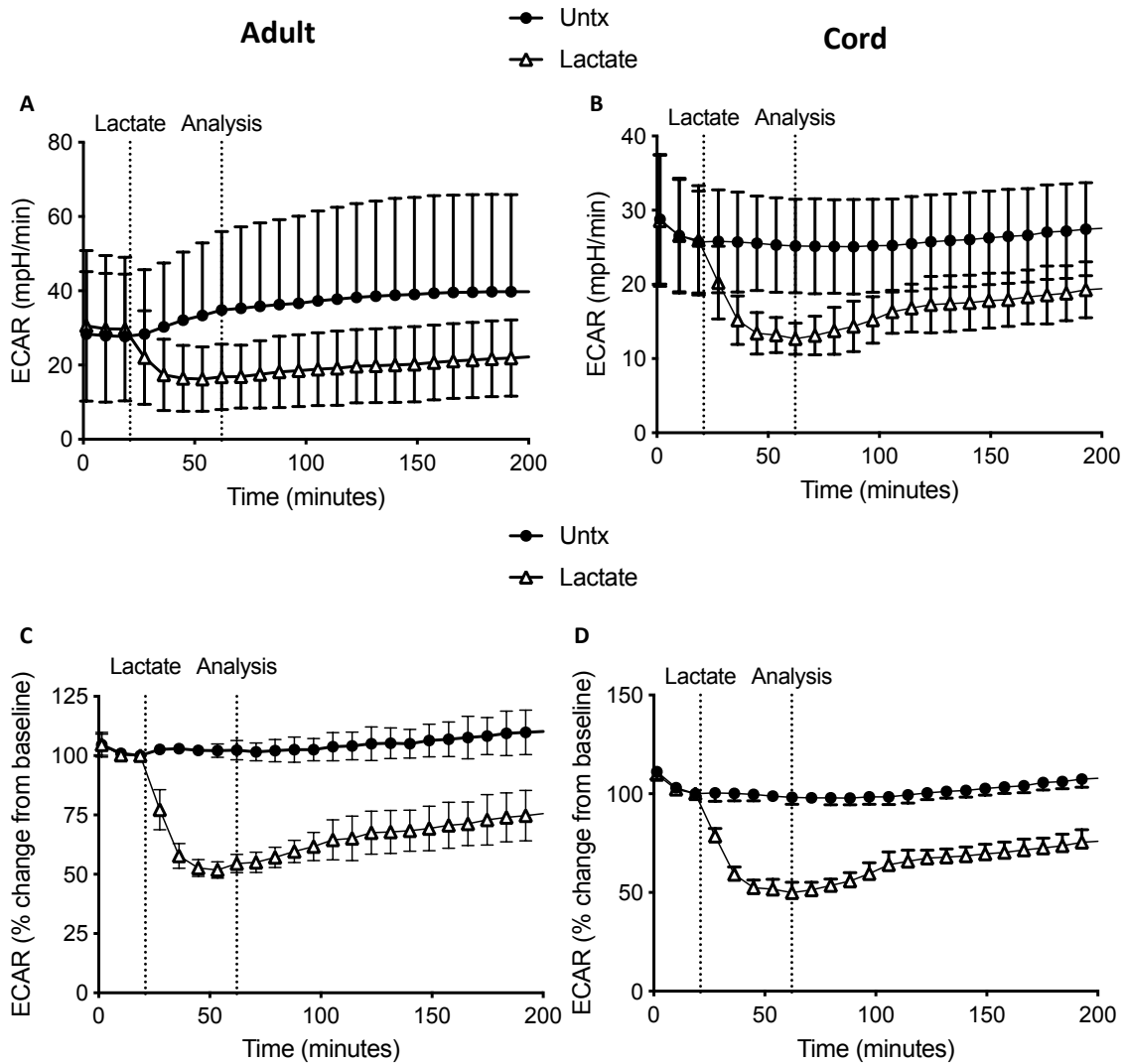


Figure 5.1 Lactate decreases ECAR in adult and cord blood MDM.

PBMC were isolated from buffy coats and MDM were adherence purified for 7 days in 10% human serum. MDM were gently scraped and seeded on Seahorse culture plates prior to analysis in the Seahorse XFe24 Analyzer. Lactate (25 mM) was added to the cells in the Seahorse Analyzer at the time point indicated. Correction for differences in cell density was achieved by % comparison to the OCR for the real-time analysis. The OCR was recorded approximately every 9 minutes. After 23 minutes, the SeahorseXFe24 Analyzer injected lactate or control medium (untreated; untx) into assigned wells. The OCR readings were then continually sampled in real time. The time-course graphs illustrate the OCR of human adult (n=5) and cord (n=3) MDM in response to treatment with lactate.

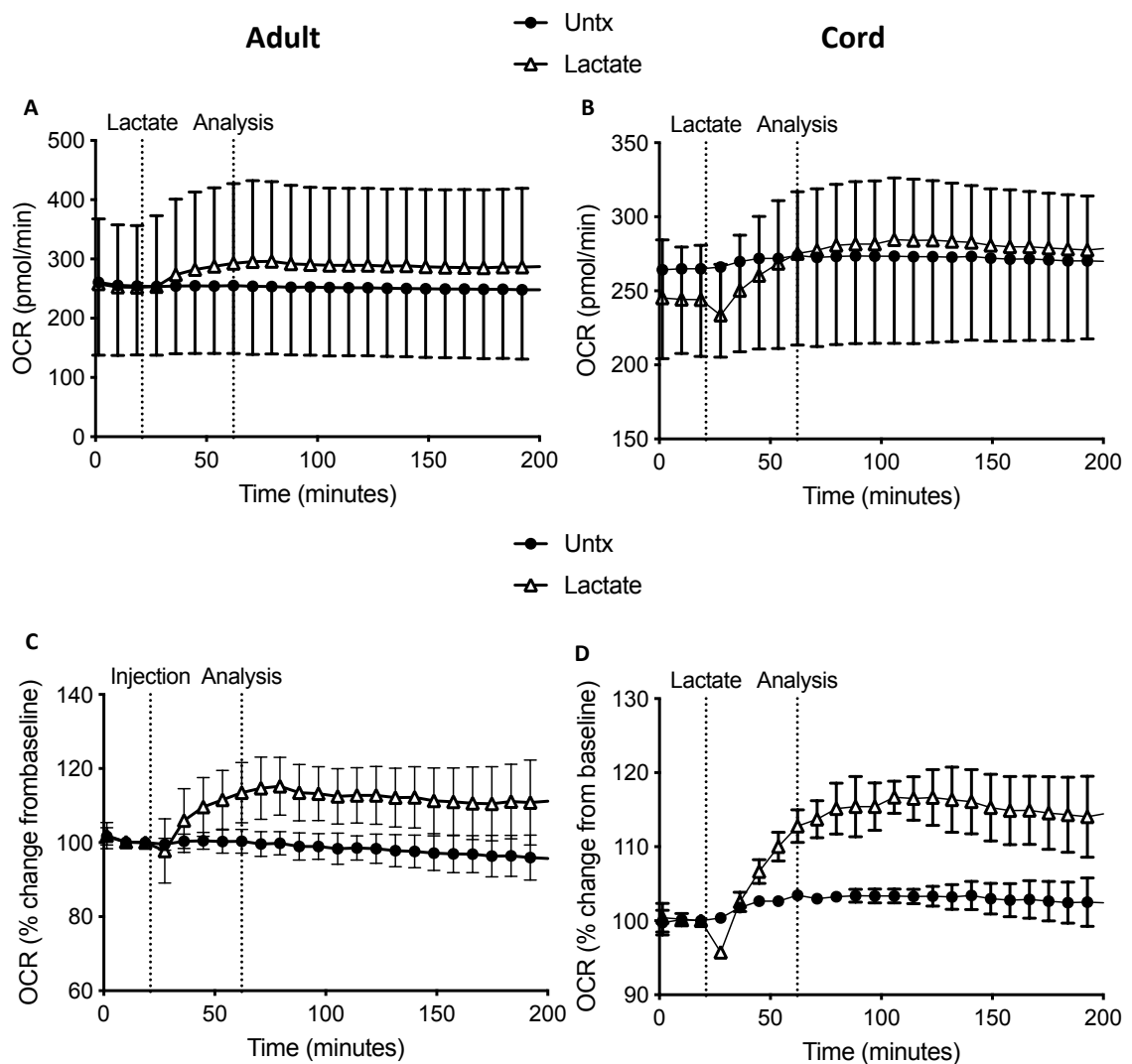


Figure 5.2 Lactate increases OCR in adult and cord blood MDM.

PBMC were isolated from buffy coats and MDM were adherence purified for 7 days in 10% human serum. MDM were gently scraped and seeded on Seahorse culture plates prior to analysis in the Seahorse XFe24 Analyzer. Lactate (25 mM) was added to the cells in the Seahorse Analyzer at the time point indicated. Correction for differences in cell density was achieved by % comparison to the ECAR for the real-time analysis. The ECAR was recorded approximately every 9 minutes. After 23 minutes, the SeahorseXFe24 Analyzer injected lactate or control medium (untreated; untx) into assigned wells. The ECAR readings were then continually sampled in real time. The time-course graphs illustrate the ECAR of human adult (n=5) and cord (n=3) MDM in response to treatment with lactate.

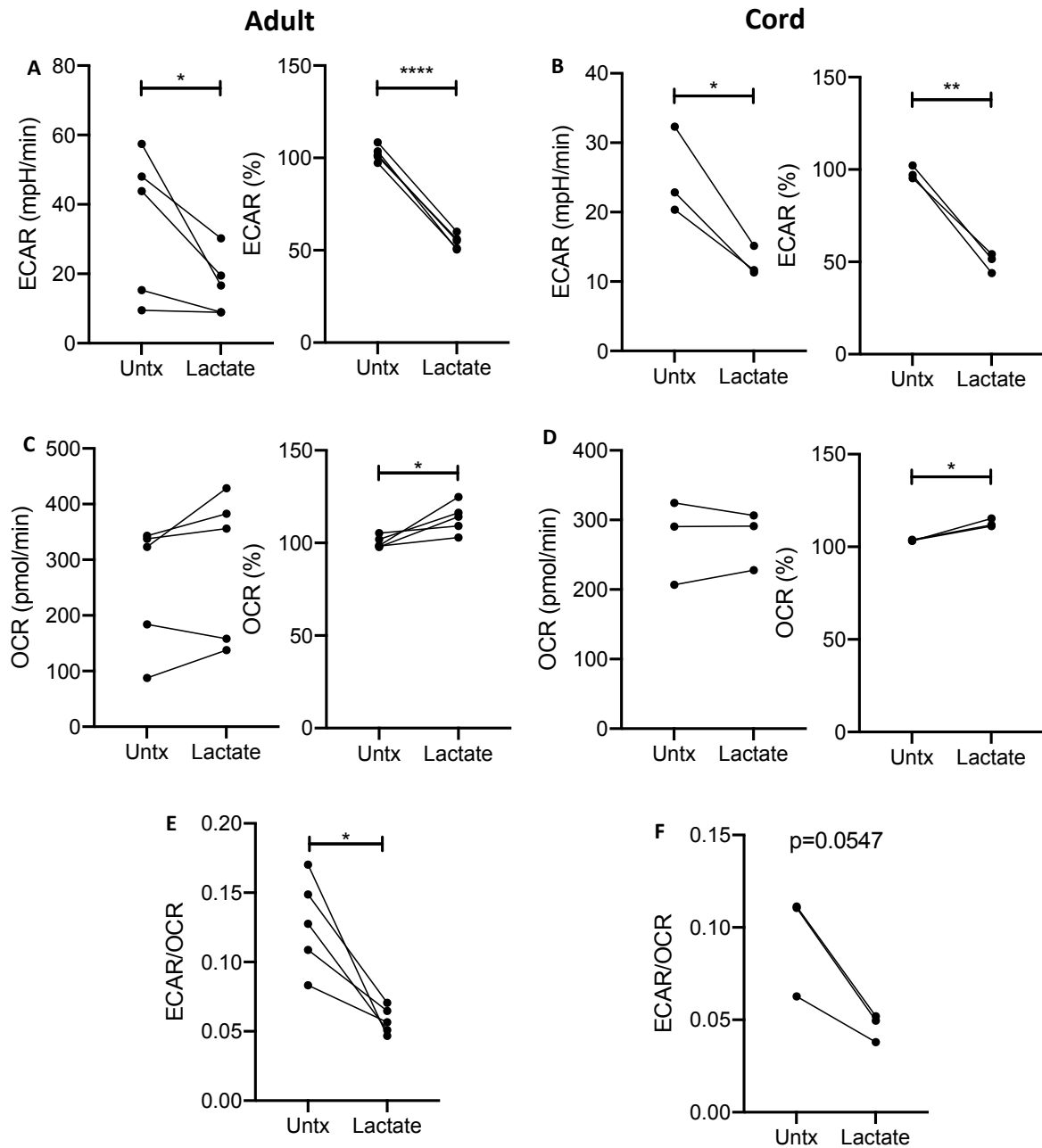


Figure 5.3 Analysis of the changes in ECAR and OCR in adult and cord blood MDM after lactate administration.

PBMC were isolated from buffy coats and MDM were adherence purified for 7 days in 10% human serum. MDM were gently scraped and seeded on Seahorse culture plates prior to analysis in the Seahorse XFe24 Analyzer. Lactate (25 mM) was added to the cells in the Seahorse Analyzer 40 minutes prior to analysis. Correction for differences in cell density was achieved by % comparison to the ECAR and OCR for the real-time analysis. Analysis of the ECAR raw and % change values for the adult (A, n=5) and cord blood (B, n=3) MDM are shown as well as the OCR raw and % change values for the adult (C) and cord blood (D). The ECAR/OCR ratio is calculated for the adult (E) and cord blood (F) MDM. Statistical significance was determined using a paired Student's t-test; *P<0.05, **P<0.01, ****P<0.0001.

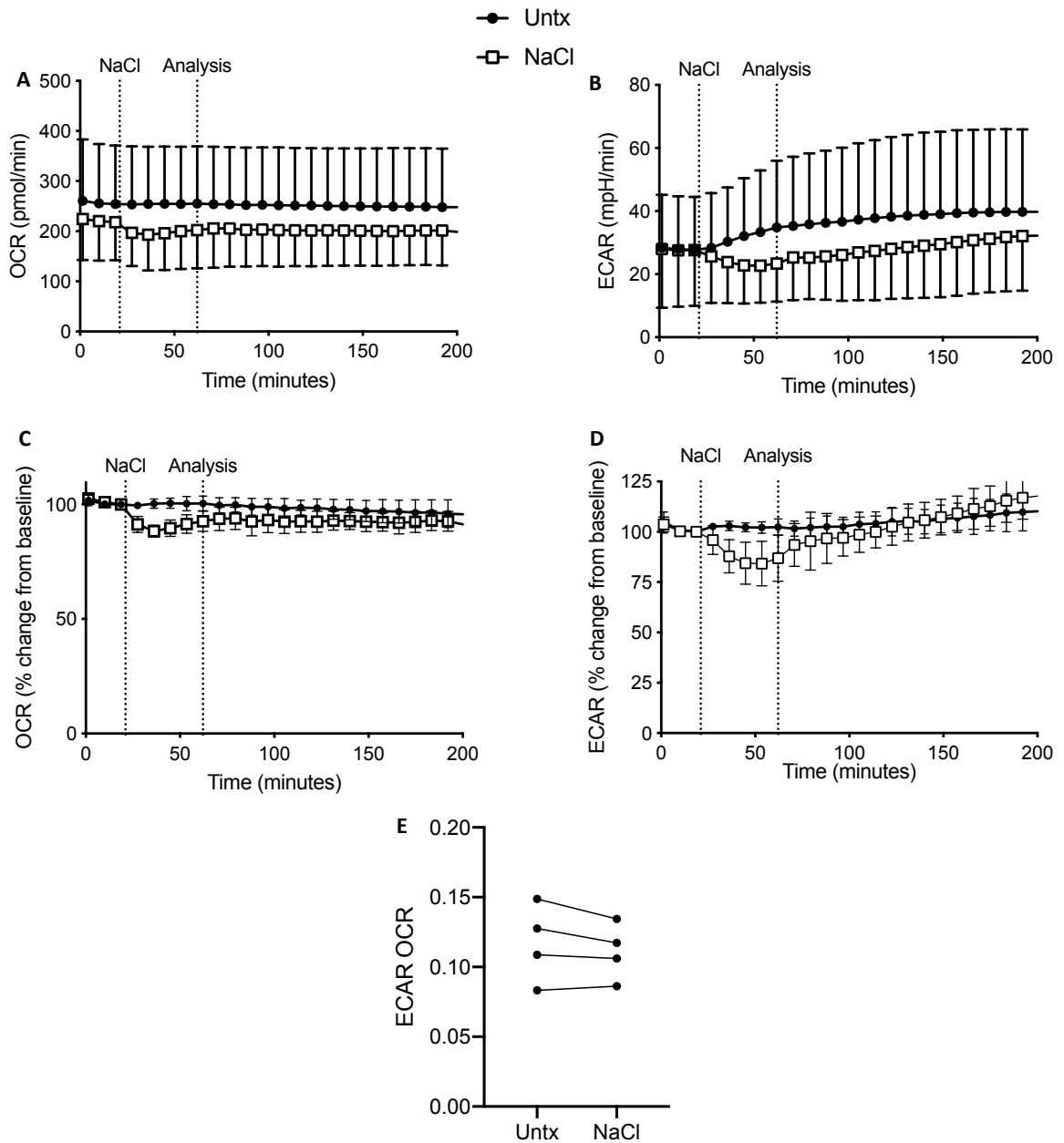


Figure 5.4 NaCl does induce metabolic changes in adult MDM.

PBMC were isolated from buffy coats and MDM were adherence purified for 7 days in 10% human serum. MDM were gently scraped and seeded on Seahorse culture plates prior to analysis in the Seahorse XFe24 Analyzer. NaCl (25 mM) was added to the cells in the Seahorse Analyzer at the time point indicated. The OCR (A) and ECAR (B) was recorded approximately every 9 minutes. Correction for differences in cell density was achieved by % comparison to the third reading of OCR (C) or ECAR (D) for the real-time analysis. After 23 minutes, the SeahorseXFe24 Analyzer injected NaCl or control medium (untreated; untx) into assigned wells. The ECAR and OCR readings were then continually sampled in real time. The time-course graphs illustrate the ECAR and OCR of adult (n=4) MDM in response to treatment with NaCl. Analysis was performed at the time point indicated to calculate the ECAR/OCR ratio (E) using a paired Student's t-test.

5.2.2 Lactate pretreatment alters MDM metabolic responses to Mtb or LPS

Having established that lactate alters the metabolism of resting MDM, the effect of lactate on the ability of MDM to shift towards glycolysis upon stimulation with Mtb or LPS was next determined. This scenario models the environmental milieu of early infection events, with bystander uninfected macrophages exposed to increasing levels of lactate produced by neighbouring infected cells that have increased glycolysis. If the infection overcomes the infected macrophage, the cells will die and release Mtb into the extracellular environment. This will result in bystander macrophages which were exposed to extracellular lactate from the increased glycolytic flux of neighbouring cells being subsequently infected by Mtb.

PBMC were isolated from buffy coats or from umbilical cord blood samples taken immediately following delivery. Adult or cord blood MDM were adherence purified for 7 days in 10% human serum. MDM were washed and detached from the plates by cooling and gentle scraping and then seeded on Seahorse culture plates prior to analysis in the Seahorse XFe24 Analyzer. Lactate was added via the Seahorse ports to adult and cord blood MDM as in Figure 5.1. Three hours after the addition of lactate, MDM were stimulated with Mtb (iH37Rv; MOI 1-10) or LPS (100 ng/ml) by injection through the ports of the SeahorseXFe24 Analyzer. The kinetics of the ensuing responses were monitored by analysing the ECAR and OCR in real time every 9 minutes for 10 hours.

5.2.2a Pre-treatment with lactate decreases ECAR after Mtb or LPS stimulation

The changes in ECAR were recorded in adult and cord blood MDM after Mtb (Figure 5.5) or LPS (Figure 5.6) stimulation. The time course graphs begin at approximately 200

minutes from the start of the experiment, 3 hours after the administration of lactate. These early events (up to 200 minutes post the addition of lactate to resting MDM) are shown previously in Figure 5.1. Stimulation with Mtb causes a rise in the raw values of ECAR for both the adult (Figure 5.5 A) and cord blood (Figure 5.5 B) MDM but the MDM that are pre-treated with lactate start from a lower baseline and peak at a lower value than the untreated MDM. The % change in ECAR is the % difference from the 3rd baseline reading, just prior to lactate administration (as previously described in 5.2.1 above). Following Mtb administration, the % change from ECAR baseline in the adult (Figure 5.5 C) and cord blood (Figure 5.5 D) MDM increases in both the lactate pre-treated and untreated MDM but the ECAR peak of the lactate treated MDM is lower than the untreated. Consistent with the stimulation of MDM with Mtb, LPS stimulation also resulted in a rise in the ECAR of the adult (Figure 5.6 A) and cord blood (Figure 5.6 B) MDM. Data normalised to the % change from baseline for both adult (Figure 5.6 C) and cord blood (Figure 5.6 D) MDM also demonstrates an increase in ECAR after stimulation with LPS but pre-treatment with lactate lowers the starting point and subsequent peak of ECAR. Analysis of the changes seen in ECAR after pre-treatment with lactate was undertaken at the time point indicated, 150 minutes after stimulation with Mtb or LPS, and is represented in Figure 5.7. The raw values of ECAR for the adult (Figure 5.7 A) and cord blood (Figure 5.7 B) stimulated with Mtb or LPS were not significantly altered. The % change in ECAR from baseline was significantly reduced in the adult MDM pre-treated with lactate after both Mtb ($P<0.05$) or LPS ($P<0.01$) stimulation (Figure 5.7 C). There was no significant differences in the ECAR % change from baseline in the cord blood MDM, although a trend downward was observed similar to the adult MDM (Figure 5.7 D).

5.2.2b Pre-treatment with lactate increases OCR after Mtb or LPS stimulation

The OCR for the adult and cord blood MDM stimulated with Mtb (Figure 5.8) or LPS (Figure 5.9) was concurrently measured with ECAR in the Seahorse XFe Analyzer. The time course graphs begin at approximately 200 minutes from the start of the experiment, 3 hours after the administration of lactate. Pre-treatment with lactate results in an increase in the OCR prior to stimulation. Stimulation with Mtb causes a decrease in the OCR in the untreated adult MDM but the lactate treated MDM did not have any change in the OCR (Figure 5.8 A). Consistent with the data in Chapter 3, stimulation with Mtb did not alter the OCR in the cord blood MDM in either the lactate treated or untreated cells, with the lactate treated MDM having a persistently raised OCR (Figure 5.8 B). Data normalised to the % difference from the 3rd baseline reading prior to lactate administration (% change in OCR), shows that following the addition of Mtb, lactate treated MDM did not alter their OCR, unlike the untreated MDM which decreased OCR (Figure 5.8 C), in keeping with the early Warburg effect observed in Chapter 3. The OCR in the cord blood MDM did not change after Mtb administration (Figure 5.8 D). Similarly, after LPS stimulation, there is an increase in the OCR of the adult (Figure 5.9 A) and cord blood (Figure 5.9 B) MDM treated with lactate prior to stimulation. Neither the adult or cord OCR in the lactate treated MDM decreases following LPS stimulation, a phenomenon that is observed in the adult untreated MDM. The normalised OCR in the lactate treated adult (Figure 5.9 C) and cord blood (Figure 5.9 D) MDM did not change after LPS stimulation. Figure 5.10 shows the analysis of the changes seen in OCR after pre-treatment with lactate, 150 minutes after stimulation with Mtb or LPS. The OCR for the adult MDM stimulated with Mtb or LPS are not significantly altered by the pre-treatment with lactate (Figure 5.10 A). A significant

increase in the OCR of the lactate treated cord blood MDM is observed with Mtb or LPS stimulation compared with untreated controls (Figure 5.10 B, $P < 0.05$). The % change in OCR of the MDM that were pre-treated with lactate was significantly increased ($P < 0.05$) from baseline after Mtb or LPS stimulation in both adult (Figure 5.10 C) and cord blood (Figure 5.10 D). The ECAR/OCR ratio was calculated at this time point. The adult MDM treated with lactate and then stimulated with LPS showed a significant decrease ($P < 0.05$) compared with the untreated MDM (Figure 5.10 E). The decrease seen in the adult Mtb stimulated MDM (Figure 5.10 E), and cord blood MDM stimulated with Mtb or LPS was not statistically significant (Figure 5.10 F) .

These data illustrate that lactate alters the metabolic response to Mtb or LPS stimulation in both adult and cord blood MDM. The glycolytic switch is not inhibited but the baseline ECAR is reduced resulting in a lower peak glycolysis after stimulation. Lactate increases the OCR at baseline in both adult and cord blood MDM. In addition lactate inhibited the decrease in oxygen consumption seen in the Warburg effect of adult MDM, resulting in an altered metabolic phenotype. This is highlighted in the phenogram of the adult MDM as shown in Figure 5.11. The phenogram plots ECAR (x-axis) against OCR (y-axis). Cells that have low levels of both ECAR and OCR are considered “Quiescent”, located in the lower left quadrant and cells with high levels of both are considered “Energetic”, in the right upper quadrant. When cells have a high ECAR and low OCR, they are considered “Glycolytic”, in the right lower quadrant. A high OCR and low ECAR is considered an “Oxidative” state. Plotted on the phenogram are the ECAR and OCR of adult MDM with and without treatment with lactate that are unstimulated or stimulated with Mtb (red arrow) or LPS (blue arrow). Pre-treatment

with lactate followed by stimulation with either Mtb or LPS, results in a metabolic switch that is more energetic compared with untreated MDM that exhibit a shift into the glycolytic quadrant upon stimulation.

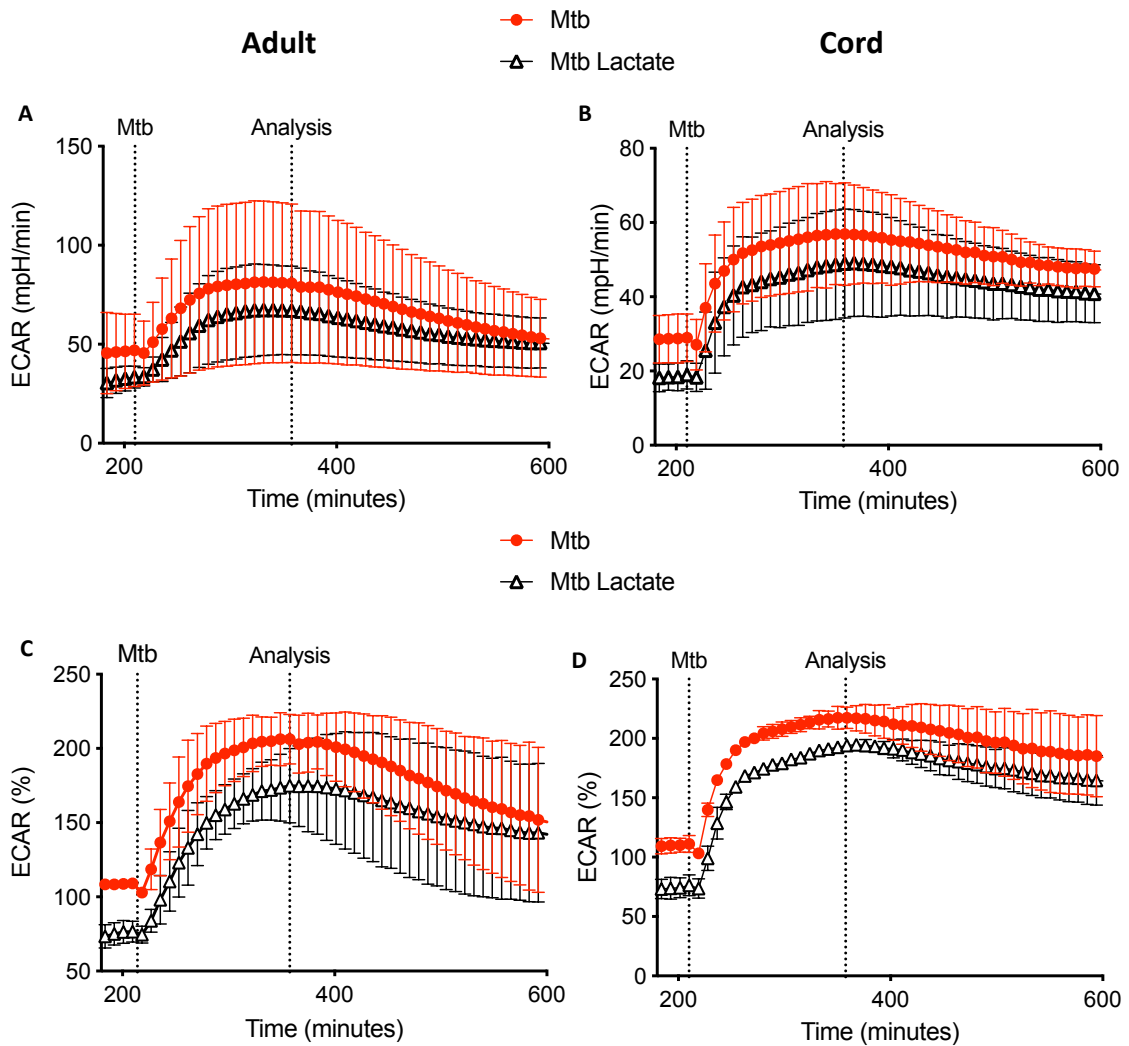


Figure 5.5 ECAR in adult and cord blood MDM pretreated with lactate after Mtb stimulation.

PBMC were isolated from buffy coats or from umbilical cord blood samples taken immediately following delivery. Adult or cord blood MDM were adherence purified for 7 days in 10% human serum. MDM were washed and detached from the plates by cooling and gently scraped, counted and re-seeded on Seahorse culture plates prior to analysis in the Seahorse XFe24 Analyzer. Lactate (25 mM) was added 3 hours prior to stimulation with Mtb (iH37Rv; MOI 1-10). The time-course graphs illustrate the ECAR of adult (A, $n=3 \pm SD$) and cord blood (B, $n=2 \pm SD$) MDM in real-time in response to stimulation with Mtb. Correction for differences in cell density was achieved by % comparison to the basal ECAR and the % change for the adult (C) and cord blood (D) are illustrated.

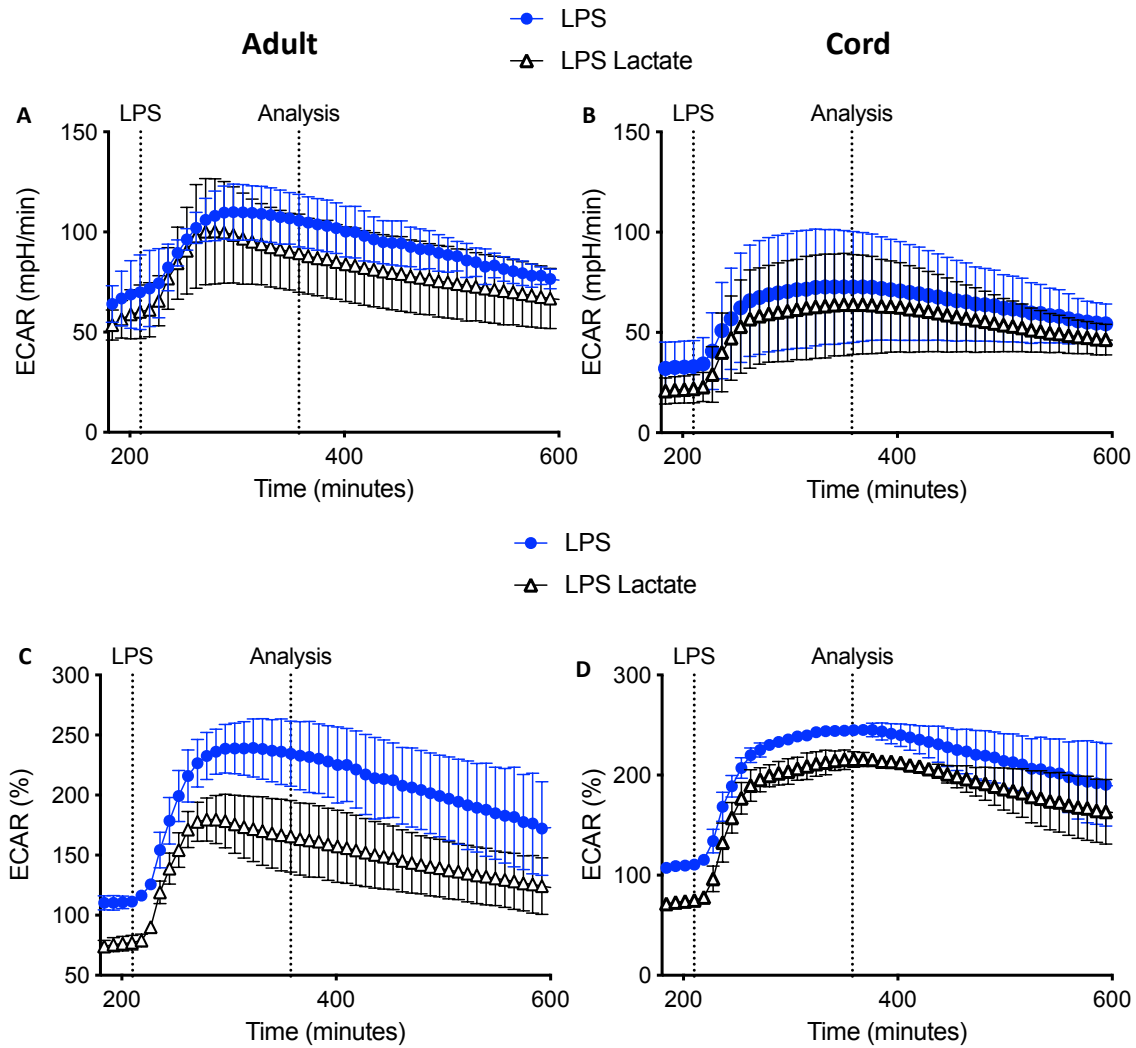


Figure 5.6 ECAR in adult and cord blood MDM pretreated with lactate after LPS stimulation.

PBMC were isolated from buffy coats or from umbilical cord blood samples taken immediately following delivery. Adult or cord blood MDM were adherence purified for 7 days in 10% human serum. MDM were washed and detached from the plates by cooling and gently scraped, counted and re-seeded on Seahorse culture plates prior to analysis in the Seahorse XFe24 Analyzer. Lactate (25 mM) was added 3 hours prior to stimulation with LPS (100 ng/ml). The time-course graphs illustrate the ECAR of adult (A, $n=3 \pm SD$) and cord blood (B, $n=2 \pm SD$) MDM in real-time in response to stimulation with LPS. Correction for differences in cell density was achieved by % comparison to the basal ECAR and the % change for the adult (C) and cord blood (D) are illustrated.

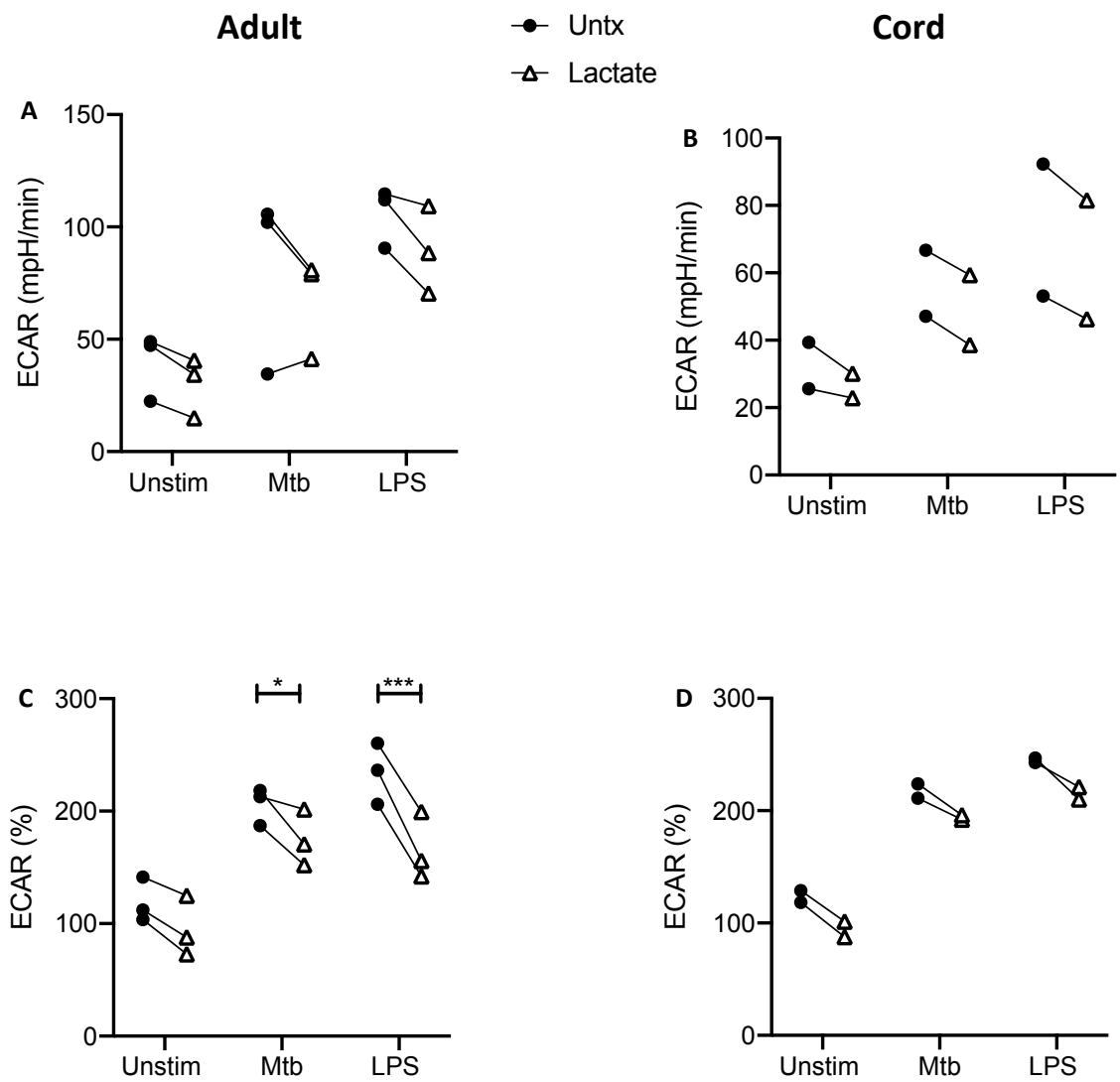


Figure 5.7 Analysis of the ECAR in adult and cord blood MDM pretreated with lactate after Mtb or LPS stimulation.

PBMC were isolated from buffy coats or from umbilical cord blood samples taken immediately following delivery. Adult or cord blood MDM were adherence purified for 7 days in 10% human serum. MDM were washed and detached from the plates by cooling and gently scraped, counted and re-seeded on Seahorse culture plates prior to analysis in the Seahorse XFe24 Analyzer. Lactate (25 mM) was added 3 hours prior to stimulation with Mtb (iH37Rv; MOI 1-10) or LPS (100 ng/ml). 150 minutes after stimulation, analysis was performed for the ECAR of the adult (A n=3) and cord blood (B n=2). Correction for differences in cell density was achieved by % comparison to the basal ECAR and the % change in ECAR for the adult (C) and cord blood (D) MDM are illustrated. Statistical significance was determined using two-way ANOVA with Sidak's multiple comparison test; * P<0.05, ** P< 0.01.

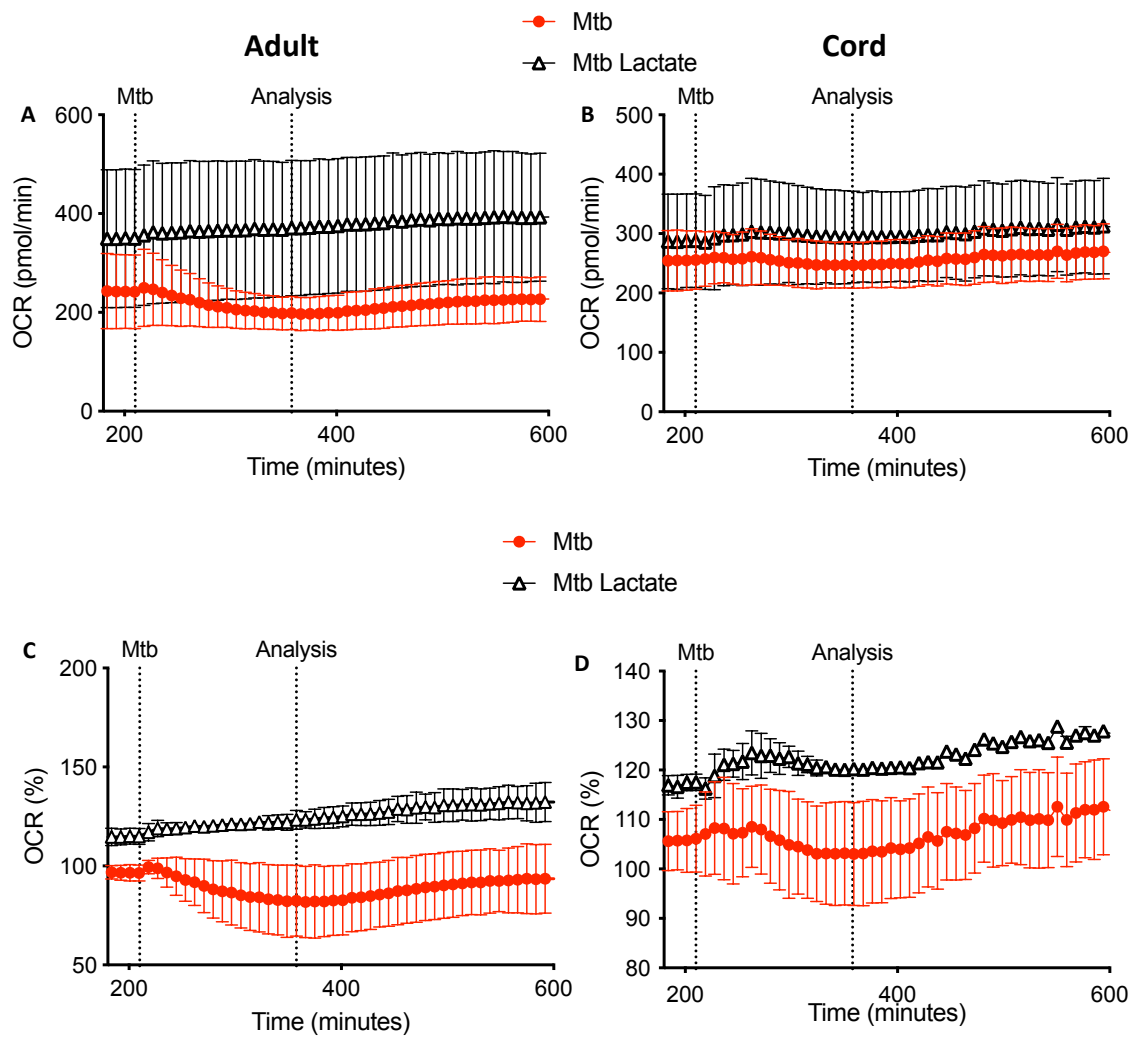


Figure 5.8 OCR in adult and cord blood MDM pretreated with lactate after Mtb stimulation.

PBMC were isolated from buffy coats or from umbilical cord blood samples taken immediately following delivery. Adult or cord blood MDM were adherence purified for 7 days in 10% human serum. MDM were washed and detached from the plates by cooling and gently scraped, counted and re-seeded on Seahorse culture plates prior to analysis in the Seahorse XFe24 Analyzer. Lactate (25 mM) was added 3 hours prior to stimulation with Mtb (iH37Rv; MOI 1-10). The time-course graphs illustrate the OCR of adult (A, $n=3 \pm SD$) and cord blood (B, $n=2 \pm SD$) MDM in real-time in response to stimulation with Mtb. Correction for differences in cell density was achieved by % comparison to the basal OCR and the % change for the adult (C) and cord blood (D) are illustrated.

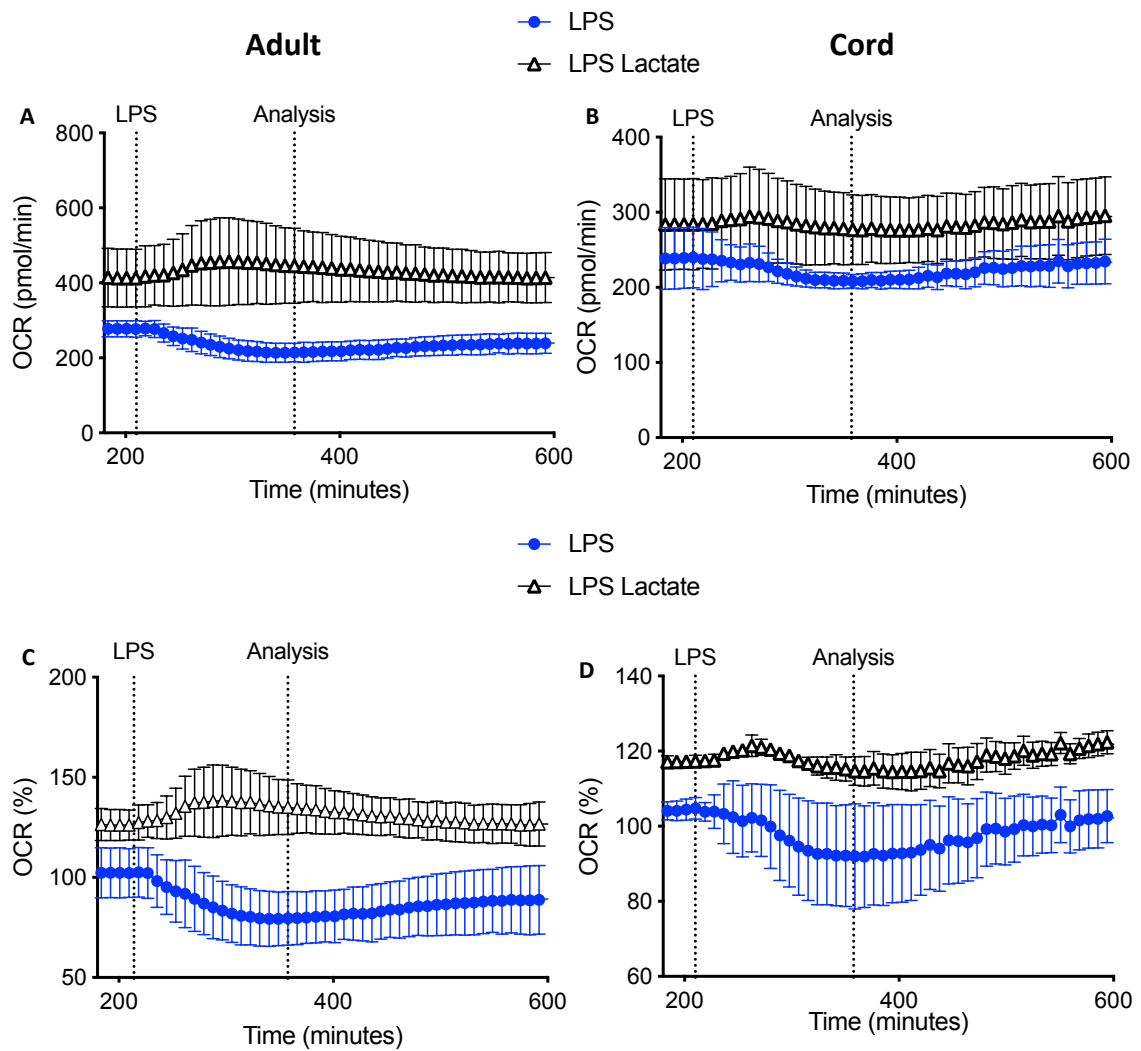


Figure 5.9 OCR in adult and cord blood MDM pretreated with lactate after LPS stimulation.

PBMC were isolated from buffy coats or from umbilical cord blood samples taken immediately following delivery. Adult or cord blood MDM were adherence purified for 7 days in 10% human serum. MDM were washed and detached from the plates by cooling and gently scraped, counted and re-seeded on Seahorse culture plates prior to analysis in the Seahorse XFe24 Analyzer. Lactate (25 mM) was added 3 hours prior to stimulation with LPS (100 ng/ml). The time-course graphs illustrate the OCR of adult (A, $n=3 \pm SD$) and cord blood (B, $n=2 \pm SD$) MDM in real-time in response to stimulation with LPS. Correction for differences in cell density was achieved by % comparison to the basal OCR and the % change for the adult (C) and cord blood (D) are illustrated.

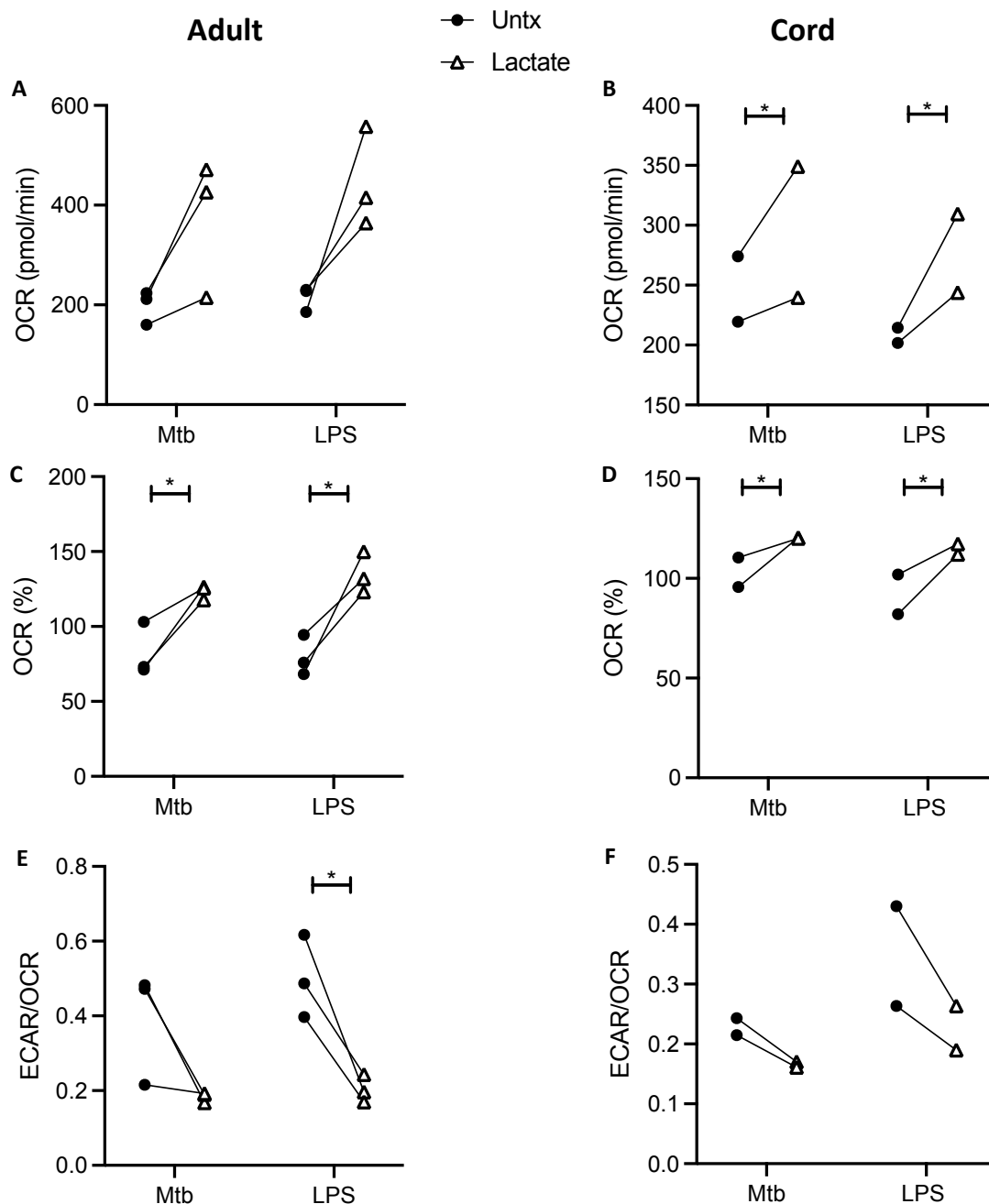


Figure 5.10 Analysis of the OCR and ECAR/OCR ratio in adult and cord blood MDM pretreated with lactate after Mtb or LPS stimulation.

PBMC were isolated from buffy coats or from umbilical cord blood samples taken immediately following delivery. Adult or cord blood MDM were adherence purified for 7 days in 10% human serum. MDM were washed and detached from the plates by cooling and gently scraped, counted and re-seeded on Seahorse culture plates prior to analysis in the Seahorse XFe24 Analyzer. Lactate (25 mM) was added 3 hours prior to stimulation with Mtb (iH37Rv; MOI 1-10) or LPS (100 ng/ml). 150 minutes after stimulation, as indicated in Figure 5.8, analysis was performed for the OCR of the adult (A n=3) and cord blood (B n=2). Correction for differences in cell density was achieved by % comparison to the basal ECAR and the % change in OCR for the adult (C) and cord blood (D) MDM are illustrated. The ECAR/OCR ratio was calculated at this time for the adult (E) and cord blood (F) at this time point. Statistical significance was determined using two-way ANOVA with Sidak's multiple comparison test; * P<0.05.

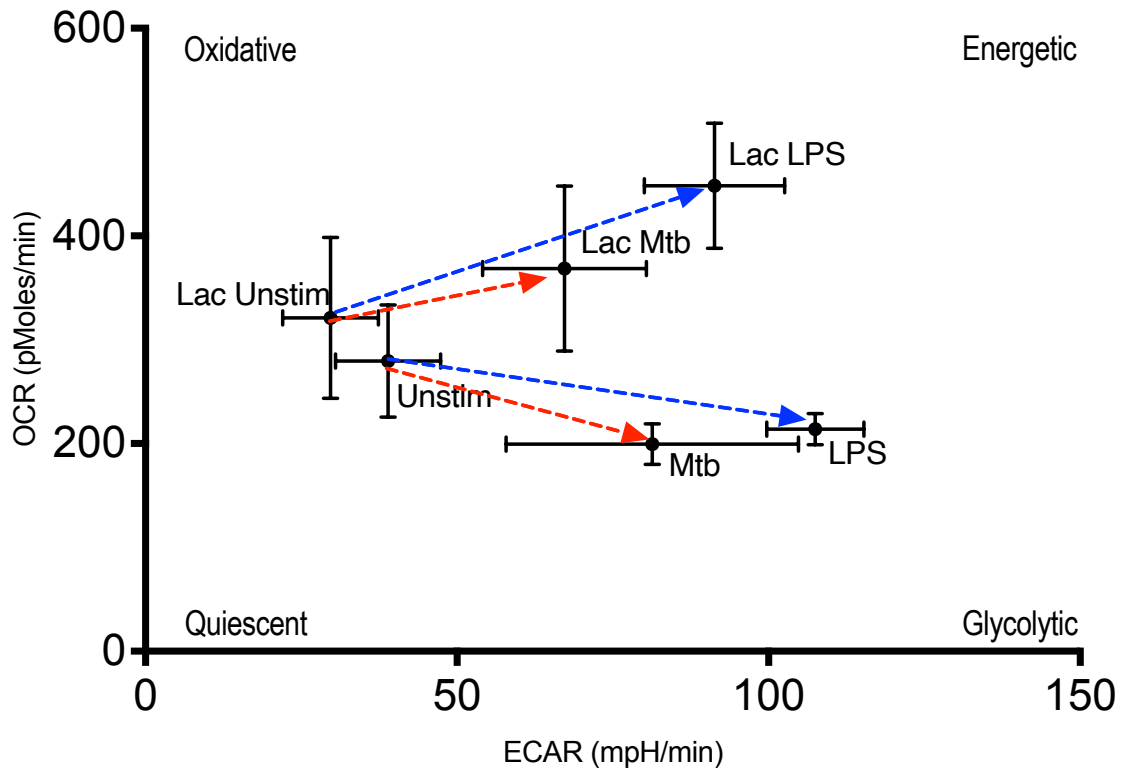


Figure 5.11 Phenogram of lactate treated adult MDM following Mtb or LPS stimulation.

PBMC were isolated from buffy coats and MDM were adherence purified for 7 days in 10% human serum. MDM were washed and detached from the plates by cooling and gently scraped, counted and re-seeded on Seahorse culture plates prior to analysis in the Seahorse XFe24 Analyzer. Lactate (25 mM) was added 3 hours prior to stimulation with Mtb (iH37Rv; MOI 1-10) or LPS (100 ng/ml). 150 minutes after stimulation analysis was performed on the ECAR and OCR. The phenograms illustrates the energetic profile of adult MDM by plotting ECAR versus OCR ($n=3 \pm \text{SEM}$).

5.2.3 The metabolic effect of pre-treatment with lactate 24 hours after Mtb or LPS stimulation.

The effect of exposure to lactate for 24 hours on cellular immunometabolism has been described in different studies to have both an anti²¹⁴ and pro-inflammatory³⁰⁴ effect. Lactate was shown to inhibit LPS activation of peritoneal macrophages in a murine model²⁹⁶ and to reduce LPS induced TNF production in human monocytes^{214,286}. Contrary to this, in a study using a human macrophage cell line, lactate was found to augment TLR-4 signaling activation³⁰⁴. In order to determine the impact of pre-treatment with lactate on cellular metabolism at a later timepoint, adult MDM were analysed 24 hours after stimulation with Mtb or LPS in the Seahorse XFe Analyzer and a mitochondrial stress test was performed. Due to limited cord blood donor availability, these experiments were only undertaken in adult MDM.

PBMC were isolated from buffy coats and MDM were adherence purified for 7 days in 10% human serum. MDM were harvested by placing in ice-cold PBS at 4°C for 30 minutes prior to gentle scraping and then seeded on Seahorse culture plates prior to analysis in the Seahorse XFe24 Analyzer. Three hours after the addition of lactate (25mM), MDM were stimulated with Mtb (iH37Rv; MOI 1-10) or LPS (100 ng/ml). 24 hours after Mtb or LPS stimulation the cells were placed in the Seahorse XFe24 Analyzer and a Mitochondrial Stress test was performed with the sequential administration of oligomycin (1 µM), FCCP (1 µM) and antimycin-A/rotenone (0.5 µM). Three baseline OCR and ECAR measurements were obtained prior to injection of oligomycin, FCCP, and antimycin-A/rotenone. Three subsequent OCR and ECAR measurements were also obtained over 15 min following injection with each of oligomycin, FCCP and antimycin-

A/rotenone. The ECAR and OCR graphs of the mitochondrial stress test are shown for the unstimulated (Figure 5.12 A), Mtb (Figure 5.12 B), or LPS (Figure 5.12 C) stimulated MDM with and without pre-treatment of lactate.

The third reading was taken as the baseline for ECAR and OCR as this allows time for the levels to reach steady state, and analysis was undertaken on this reading. The administration of lactate 3 hours prior to stimulation with Mtb significantly decreased the OCR 24 hours after stimulation when compared using a Student's t-test (Figure 5.13 A, $P < 0.05$). The OCR for the LPS stimulated MDM and the ECAR for any of the conditions (Figure 5.13 B) was not significantly altered by pre-treatment with lactate. The ECAR/OCR ratio was calculated, and the ratio was significantly increased in the Mtb stimulated MDM by pre-treatment with lactate (Figure 5.13 C) but not significantly changed in the unstimulated or LPS stimulated MDM.

The sequential addition of mitochondrial inhibitors during the Mitochondrial Stress Test allows for the analysis of several mitochondrial functions. ATP production was calculated by subtracting the OCR post oligomycin injection from baseline OCR prior to oligomycin addition (Figure 5.14A). This represents the portion of basal respiration that was being used to drive ATP production. A significant decrease was seen in the Mtb stimulated MDM that had been pre-treated by lactate compared with untreated, Mtb stimulated controls (Figure 5.14 A, $P < 0.05$, Student's t-test). No significant differences were seen between lactate treated and untreated cells in the unstimulated or LPS stimulated MDM. Maximal respiratory capacity is the maximum OCR post FCCP injection, which allows uninhibited electron flow through the electron transport chain,

and oxygen consumption by complex IV is maximised (Figure 5.14 B). Unstimulated MDM that had been pre-treated with lactate had a significant increase in maximal respiration ($P < 0.05$, Student's t-test) but lactate treatment did not induce significant differences in Mtb or LPS stimulated MDM (Figure 5.14 B). The Spare Respiratory Capacity (SRC) is the difference between the baseline OCR and the Maximal Respiration and represents the ability of the cell to respond to demand (Figure 5.14 C). Pre-treatment with lactate caused an increase in the SRC in the unstimulated MDM ($P < 0.05$, Student's t-test) but no significant differences in Mtb or LPS stimulated MDM were observed (Figure 5.14 C). Antimycin-A/rotenone inhibit Complex I and III, shutting down mitochondrial respiration. The OCR after Antimycin-A/rotenone is the non-mitochondrial oxygen consumption (NMOC) and the difference between the NMOC and the ATP production is the proton leak. Proton leak was significantly decreased in the Mtb stimulated MDM when pretreated with lactate, compared with untreated Mtb stimulated controls (Figure 5.14 D, $P < 0.05$) but was unchanged in the LPS stimulated or unstimulated MDM. Pre-treatment with lactate did not significantly alter the NMOC (Figure 5.14 E).

These data indicate that 24 hours after treatment with lactate and stimulation with Mtb or LPS, that lactate has continued to alter metabolism in adult MDM. The effect on glycolysis, seen immediately after lactate administration has resolved. However, lactate increased the maximal respiration and SRC of the unstimulated MDM. ATP linked respiration and proton leak were both significantly reduced in MDM stimulated with Mtb when pre-treated with lactate. No differences were seen in LPS stimulated MDM, highlighting the different immunometabolic responses with different stimuli.

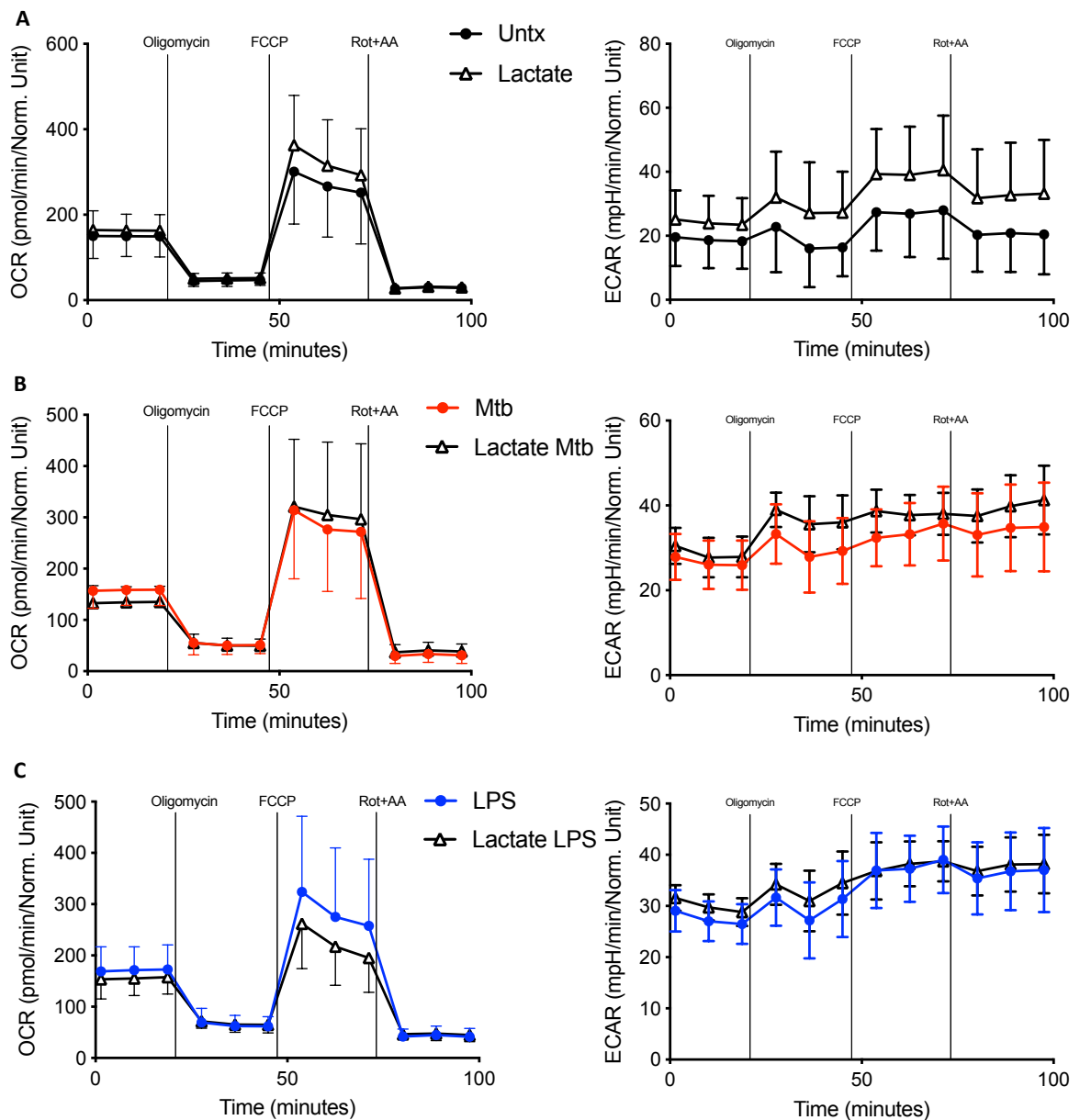


Figure 5.12 Mitochondrial stress test of lactate treated MDM 24 hours after Mtb or LPS stimulation.

PBMC were isolated from buffy coats and MDM were adherence purified for 7 days in 10% human serum. MDM were washed and detached from the plates by cooling and gently scraped, counted and re-seeded on Seahorse culture plates prior to analysis in the Seahorse XFe24 Analyzer. Lactate (25mM) was added 3 hours prior to stimulation with Mtb (iH37Rv; MOI 1-10) or LPS (100 ng/ml). 24 hours after stimulation, a mitochondrial stress test was performed with the sequential administration of oligomycin (1 μ M), FCCP (1 μ M) and antimycin-A/rotenone (0.5 μ M). Differences in cell density was corrected for by crystal violet normalization. The ECAR and OCR was recorded approximately every 9 minutes (n=4). Shown are the ECAR and OCR time graphs for the unstimulated MDM (A) and the MDM stimulated by Mtb (B) or LPS (C) with and without lactate.

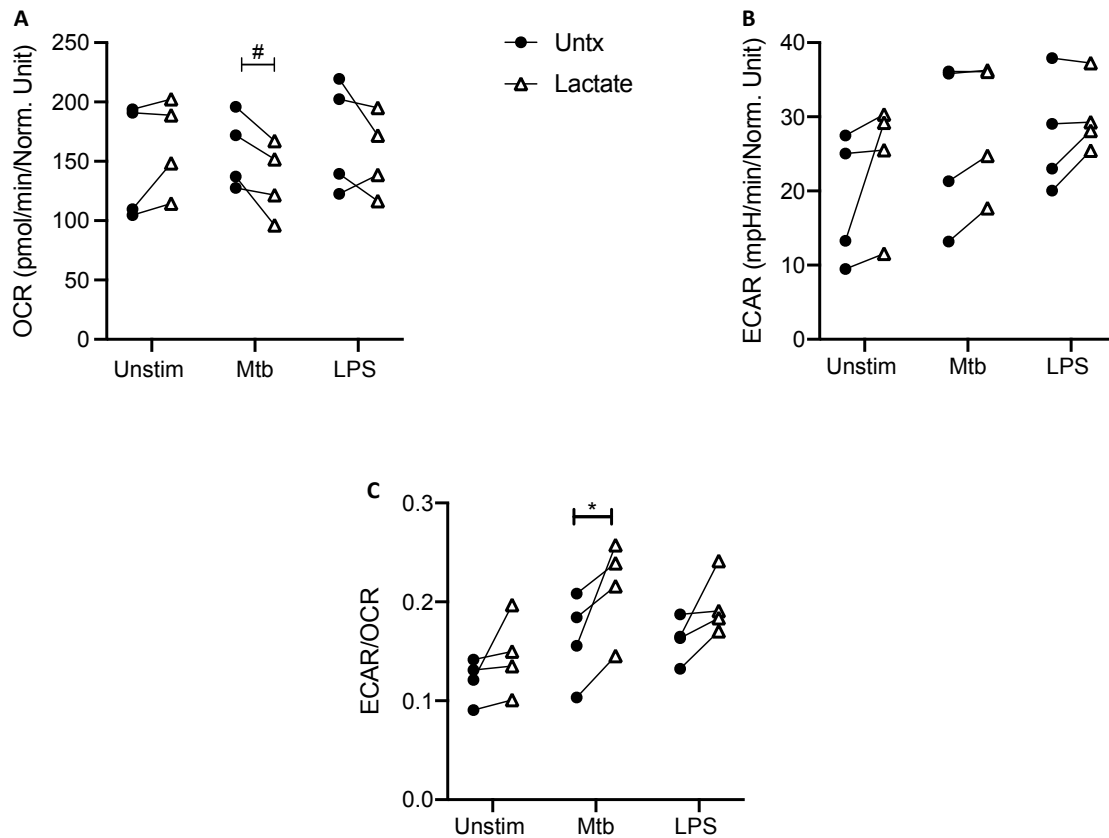


Figure 5.13 Analysis of the baseline OCR, ECAR and ECAR/OCR ratio of MDM pre-treated with lactate, 24 hours after stimulation with Mtb or LPS.

PBMC were isolated from buffy coats and MDM were adherence purified for 7 days in 10% human serum. MDM were washed and detached from the plates by cooling and gently scraped, counted and re-seeded on Seahorse culture plates. Lactate (25mM) was added 3 hours prior to stimulation with Mtb (iH37Rv; MOI 1-10) or LPS (100 ng/ml). 24 hours after stimulation the MDM analysed in the Seahorse XFe24 Analyzer. The 3rd reading was taken as the baseline reading and comparative analysis of the OCR (A) and ECAR (B) was performed. Statistical significance was determined using two-way ANOVA with Sidak's multiple comparison test; * P<0.05. A Student's t-test was also performed; # P<0.05.

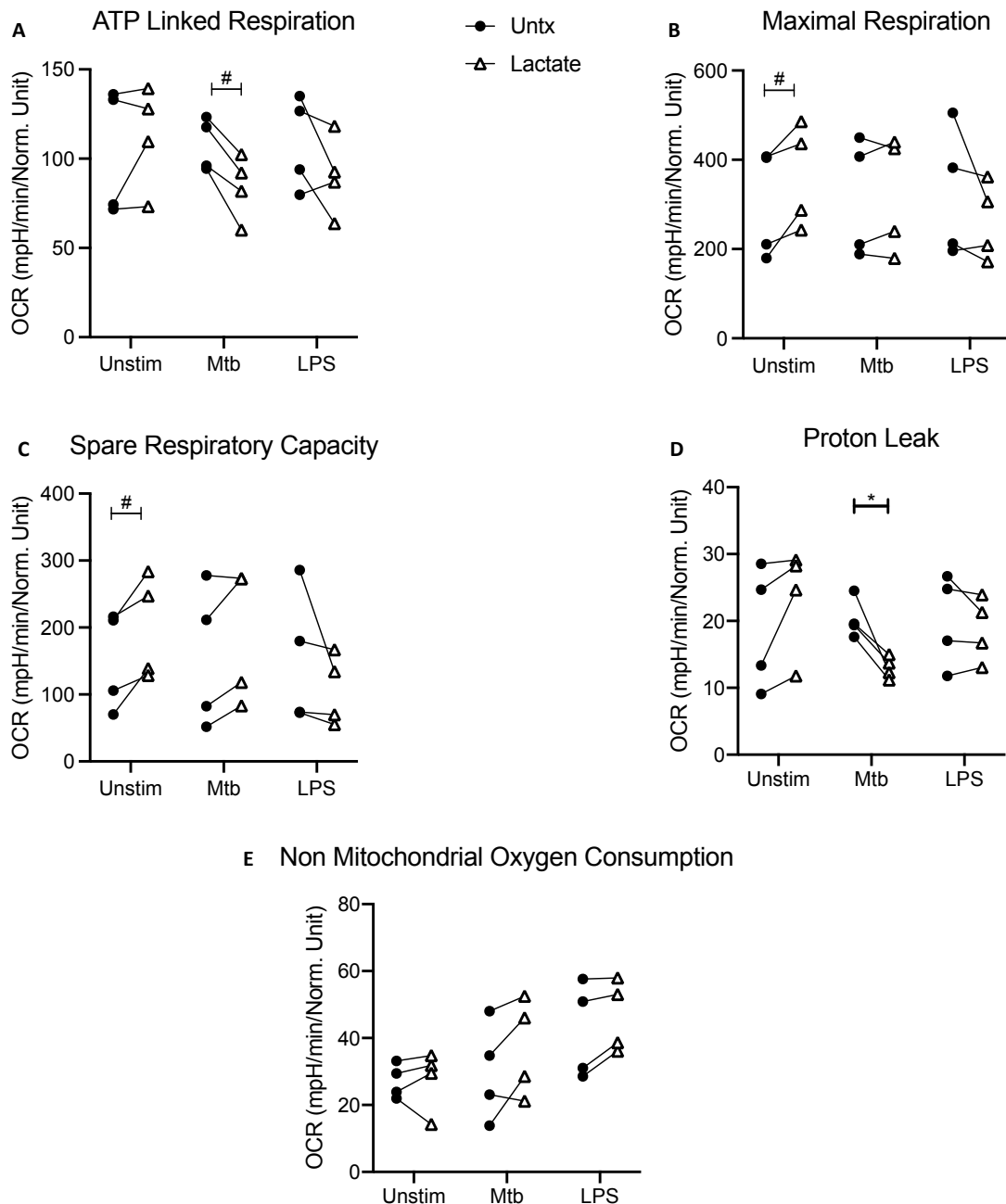


Figure 5.14 Mitochondrial stress test profile of MDM pre-treated with lactate 24 hours after Mtb or LPS stimulation.

PBMC were isolated from buffy coats and MDM were adherence purified for 7 days in 10% human serum. MDM were washed and detached from the plates by cooling and gently scraped, counted and re-seeded on Seahorse culture plates prior to analysis in the Seahorse XFe24 Analyzer. Lactate (25mM) was added 3 hours prior to stimulation with Mtb (iH37Rv; MOI 1-10) or LPS (100 ng/ml). 24 hours after stimulation, a mitochondrial stress test was performed with the sequential administration of oligomycin (1 μ M), FCCP (1 μ M) and antimycin-A/rotenone (0.5 μ M). Differences in cell density was corrected for by crystal violet normalization. The ATP linked respiration (A), Maximal respiration (B), Spare respiratory capacity (C), Proton leak (D) and Non mitochondrial oxygen consumption (E) were calculated and are illustrated. Statistical significance was determined using two-way ANOVA with Sidak's multiple comparison test; * P<0.05. A Student's t-test was also performed; # P<0.05.

5.2.4 Pre-treatment with lactate does not alter the expression of cell surface markers on adult and cord blood MDM after Mtb or LPS stimulation.

Lactate has previously been shown to induce a M2 like phenotype in a THP-1 cell line²⁹⁰. Having established that lactate downregulated the metabolic shift toward glycolysis, which is associated with a pro-inflammatory “M1-like” macrophage phenotype, this project next sought to determine the impact of lactate on the phenotypic profile of human adult and cord blood MDM. PBMC were isolated from adult buffy coats or from umbilical cord blood which was collected immediately following delivery. MDM were adherence purified for 7 days in RPMI with 10% human serum and non-adherent cells were washed off on days 2 and 5. On day 7, MDM were washed and treated with lactate (25mM) for 3 hours prior to stimulation with Mtb (iH37Rv; MOI 1-10) or LPS (100 ng/ml). 24 hours after Mtb or LPS stimulation the MDM were harvested by placing in ice-cold PBS at 4°C for 30 minutes prior to gentle scraping. Cells were Fc blocked and stained with Zombie NIR viability dye and fluorochrome-conjugated antibodies specific for CD68, CD14, CD40, CD80, HLA-DR, CD83 and CD206 (MMR) prior to acquisition by flow cytometry. MDM were gated on the basis of forward and side scatter, doublets and dead cells were excluded, and macrophages were identified as CD68+ CD14+ as described in the material and methods section **2.3** and shown in the accompanying gating strategy (Figure 2.7).

Cell surface expression of CD40, a key costimulatory molecule that is upregulated in macrophages upon activation, was determined by MFI. A representative histogram for the adult MDM shows the MFI for CD40 expression in MDM that are untreated, unstimulated (black), Mtb stimulated (red) and Mtb stimulated treated with lactate 3

hours prior to stimulation (white) (Figure 5.15 A). Collated data from n=4 adult donors show no significant differences in CD40 when pre-treated with lactate in the unstimulated MDM or in the changes that occur in CD40 expression after Mtb or LPS stimulation (Figure 5.15 B). The MFI for CD40 expression in Mtb stimulated cord blood MDM that have been pre-treated with lactate is shown in a representative histogram (Figure 5.15 C). Collated data from n=4 donors show that lactate does not influence CD40 expression in unstimulated MDM or the changes induced by Mtb or LPS (Figure 5.15 D).

A representative histogram for the cell surface expression of HLA-DR, an antigen presenting molecule, is shown in an adult donor in Figure 5.16 A. In adult MDM (n=4) there are no significant differences in HLA-DR expression when pre-treated with lactate in the unstimulated MDM or in the changes that occur in HLA-DR expression after Mtb or LPS stimulation (Figure 5.16 B). The MFI for HLA-DR expression in Mtb stimulated cord blood MDM that have been pre-treated with lactate is shown in a representative histogram (Figure 5.16 C). Collated data from n=4 donors show that lactate does not influence HLA-DR expression in unstimulated MDM, or the changes induced by Mtb or LPS (Figure 5.16 D).

The expression of the activation marker CD83 after lactate treatment is represented in the histogram from one adult donor in Figure 5.17 A. In adult MDM there are no significant differences in CD83 expression when cells were pre-treated with lactate in the unstimulated MDM or in the changes that occur in CD83 expression after Mtb or LPS stimulation (Figure 5.17 B). The MFI for CD83 expression in Mtb stimulated cord

blood MDM that have been pre-treated with lactate is shown in a representative histogram (Figure 5.17 C). Collated data from n=4 donors show that lactate does not influence CD83 expression in unstimulated MDM or the changes induced by Mtb or LPS (Figure 5.17 D).

A histogram from one representative adult donor is shown for the costimulatory molecule CD80 after lactate treatment and subsequent Mtb stimulation (Figure 5.18 A). In adult MDM (n=4) there are no significant differences in CD80 expression when pre-treated with lactate in the unstimulated MDM or in the changes that occur in CD80 expression after Mtb or LPS stimulation (Figure 5.18 B). The MFI for CD80 expression in Mtb stimulated cord blood MDM that have been pre-treated with lactate is shown in a representative histogram (Figure 5.18 C). Collated data from n=4 donors show that lactate does not influence HLA-DR expression in unstimulated MDM, or the changes induced by Mtb or LPS (Figure 5.18 D).

A representative histogram for the costimulatory molecule CD86, after Mtb stimulation with and without lactate pre-treatment, is shown in an adult donor in Figure 5.19 A. In adult MDM (n=4) there are no significant differences in CD86 expression when pre-treated with lactate in the unstimulated MDM or in the changes that occur in CD86 expression after Mtb or LPS stimulation (Figure 5.19 Figure 5.18 B). The MFI for CD86 expression in Mtb stimulated cord blood MDM that have been pre-treated with lactate is shown in a representative histogram (Figure 5.19 C). Collated data from n=4 donors show that lactate does not influence HLA-DR expression in unstimulated MDM, or the changes induced by Mtb or LPS (Figure 5.19 D).

MMR is a marker of M2 like activation and a representative histogram of its expression in an adult donor is shown in Figure 5.20 A. In adult MDM (n=4) there are no significant differences in MMR expression when pre-treated with lactate in the unstimulated MDM or in the changes that occur in MMR expression after Mtb or LPS stimulation (Figure 5.20 Figure 5.18 B). The MFI for MMR expression in Mtb stimulated cord blood MDM that have been pre-treated with lactate is shown in a representative histogram (Figure 5.20 C). Collated data from n=4 donors show that lactate does not influence HLA-DR expression in unstimulated MDM, or the changes induced by Mtb or LPS (Figure 5.20 D). These data indicate that pre-treatment with lactate does not alter cell surface marker expression in either adult or cord blood MDM whether stimulated with Mtb or LPS, or not.

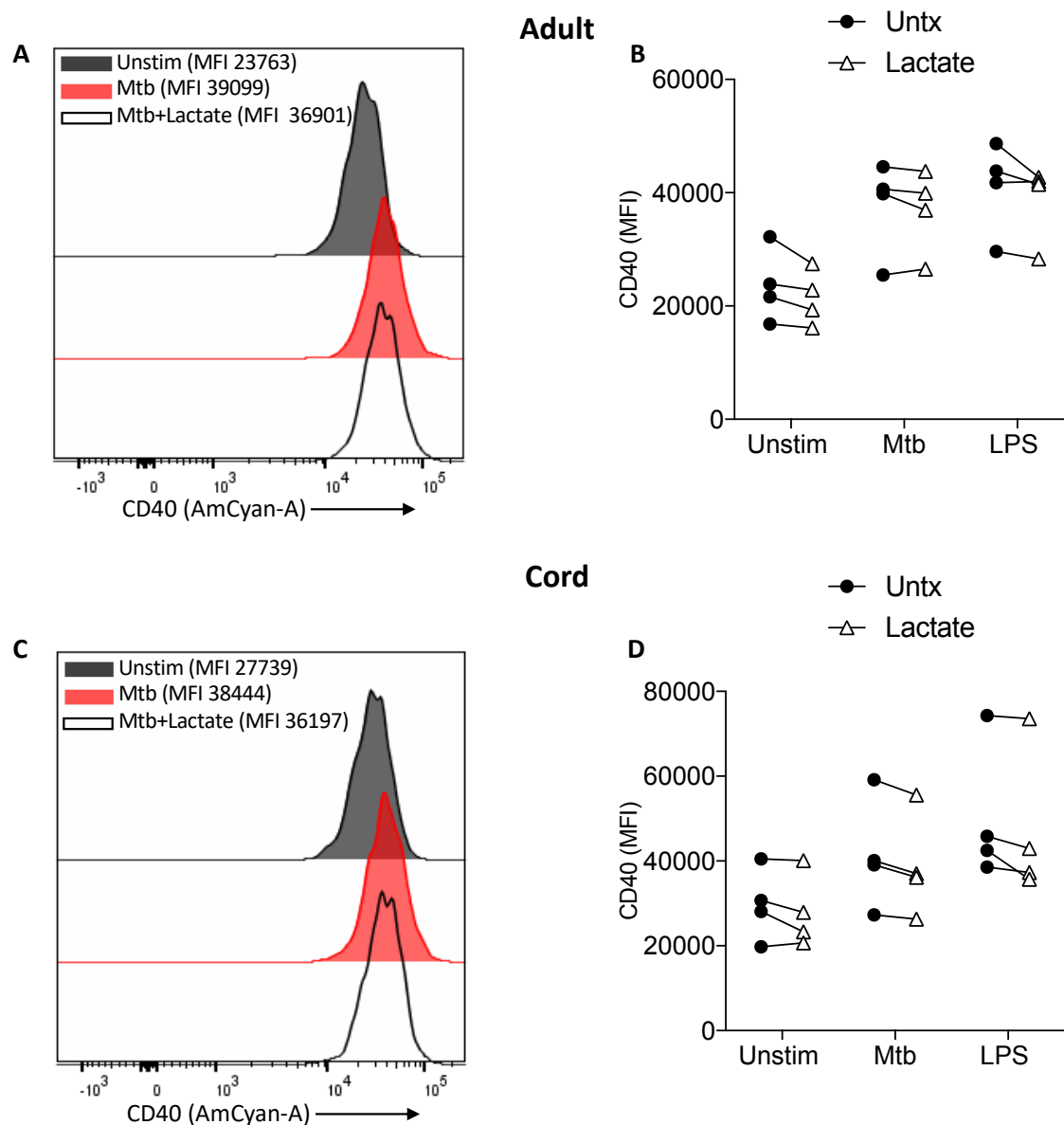


Figure 5.15 Expression of CD40 in lactate pre-treated adult and cord blood MDM 24 hours after Mtb or LPS stimulation.

PBMC were isolated from buffy coats or from umbilical cord blood samples taken immediately following delivery. Adult or cord blood MDM were adherence purified for 7 days in 10% human serum. Lactate (25mM) was added 3 hours prior to stimulation with Mtb (iH37Rv; MOI 1-10) or LPS (100 ng/ml). 24 hours after stimulation MDM were washed and detached from the plates by cooling and gently scraped and placed in flow cytometry tubes. Cells were Fc blocked, exposed to viability dye Zombie NIR and stained with fluorochrome-conjugated antibodies specific for CD14, CD68 and CD40. Cells were analysed by flow cytometry. A representative histogram for the adult (A) and cord (C) are shown. The mean fluorescent intensity (MFI) of the phenotypic markers for the adult (B; n=4 \pm SD) and cord (D; n=4 \pm SD) MDM is shown. Statistical significance was determined using two-way ANOVA using Sidak's multiple comparison test.

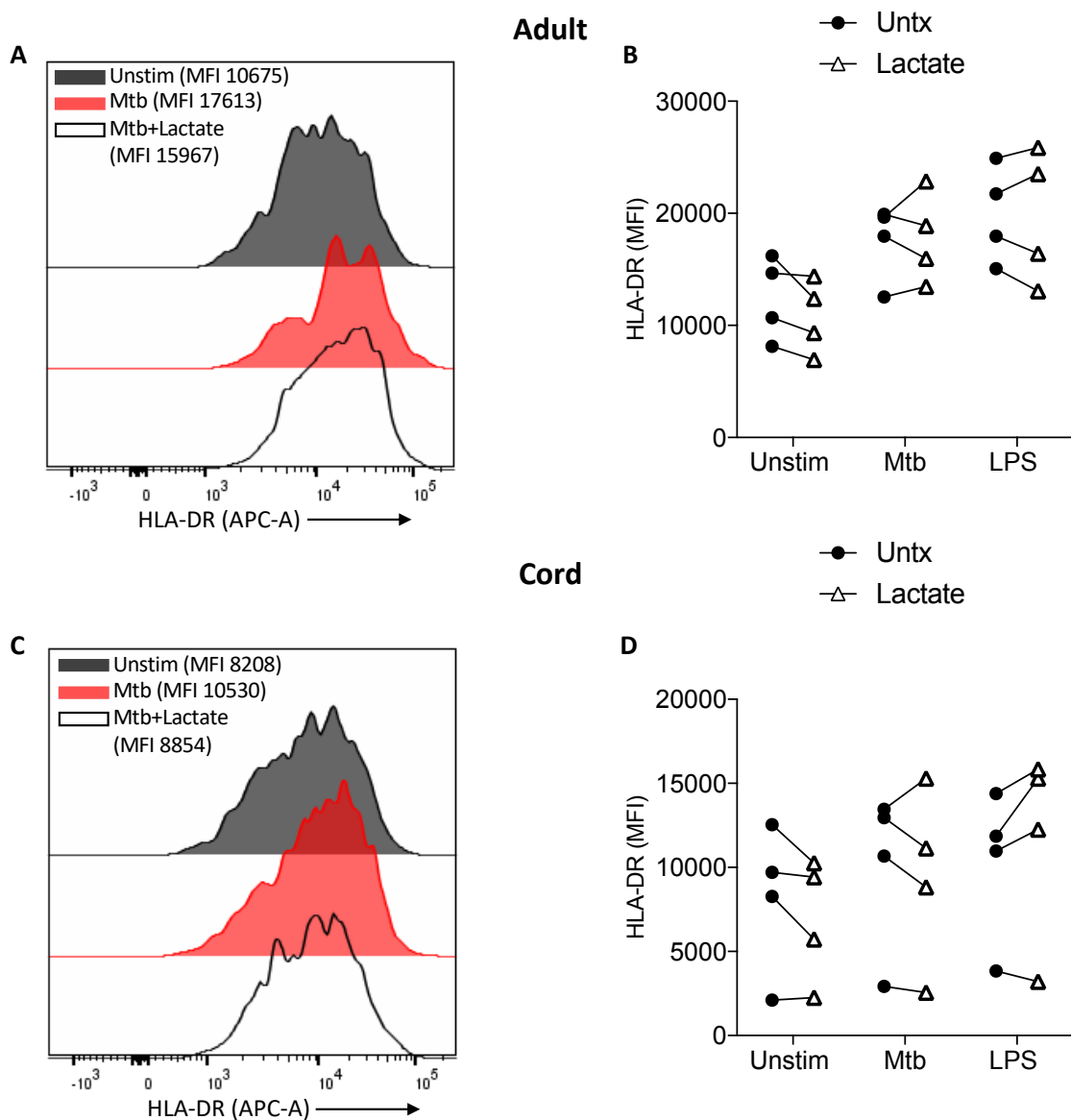


Figure 5.16 Expression of HLA-DR in lactate pre-treated adult and cord blood MDM 24 hours after Mtb or LPS stimulation.

PBMC were isolated from buffy coats or from umbilical cord blood samples taken immediately following delivery. Adult or cord blood MDM were adherence purified for 7 days in 10% human serum. Lactate (25mM) was added 3 hours prior to stimulation with Mtb (iH37Rv; MOI 1-10) or LPS (100 ng/ml). 24 hours after stimulation MDM were washed and detached from the plates by cooling and gently scraped and place in flow cytometry tubes. Cells were Fc blocked, exposed to viability dye Zombie NIR and stained with fluorochrome-conjugated antibodies specific for CD14, CD68 and HLA-DR. Cells were analysed by flow cytometry. A representative histogram for the adult (A) and cord (C) are shown. The mean fluorescent intensity (MFI) of the phenotypic markers for the adult (B; n=4 \pm SD) and cord (D; n=4 \pm SD) MDM is shown. Statistical significance was determined using two-way ANOVA using Sidak's multiple comparison test.

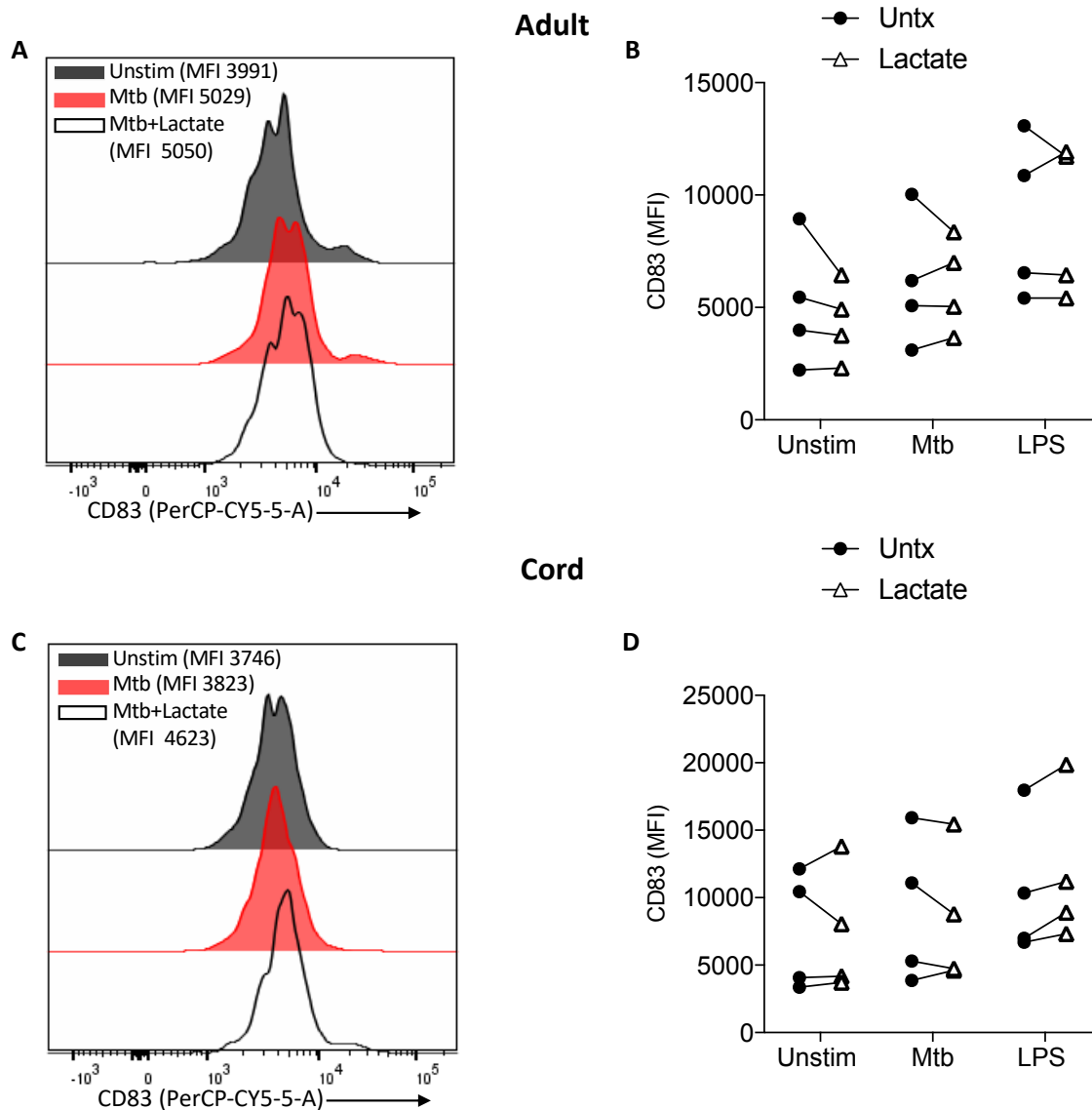


Figure 5.17 Expression of CD83 in lactate pre-treated adult and cord blood MDM 24 hours after Mtb or LPS stimulation.

PBMC were isolated from buffy coats or from umbilical cord blood samples taken immediately following delivery. Adult or cord blood MDM were adherence purified for 7 days in 10% human serum. Lactate (25mM) was added 3 hours prior to stimulation with Mtb (iH37Rv; MOI 1-10) or LPS (100 ng/ml). 24 hours after stimulation MDM were washed and detached from the plates by cooling and gently scraped and placed in flow cytometry tubes. Cells were Fc blocked, exposed to viability dye Zombie NIR and stained with fluorochrome-conjugated antibodies specific for CD14, CD68 and CD83. Cells were analysed by flow cytometry. A representative histogram for the adult (A) and cord (C) are shown. The mean fluorescent intensity (MFI) of the phenotypic markers for the adult (B; $n=4 \pm SD$) and cord (D; $n=4 \pm SD$) MDM is shown. Statistical significance was determined using two-way ANOVA using Sidak's multiple comparison test.

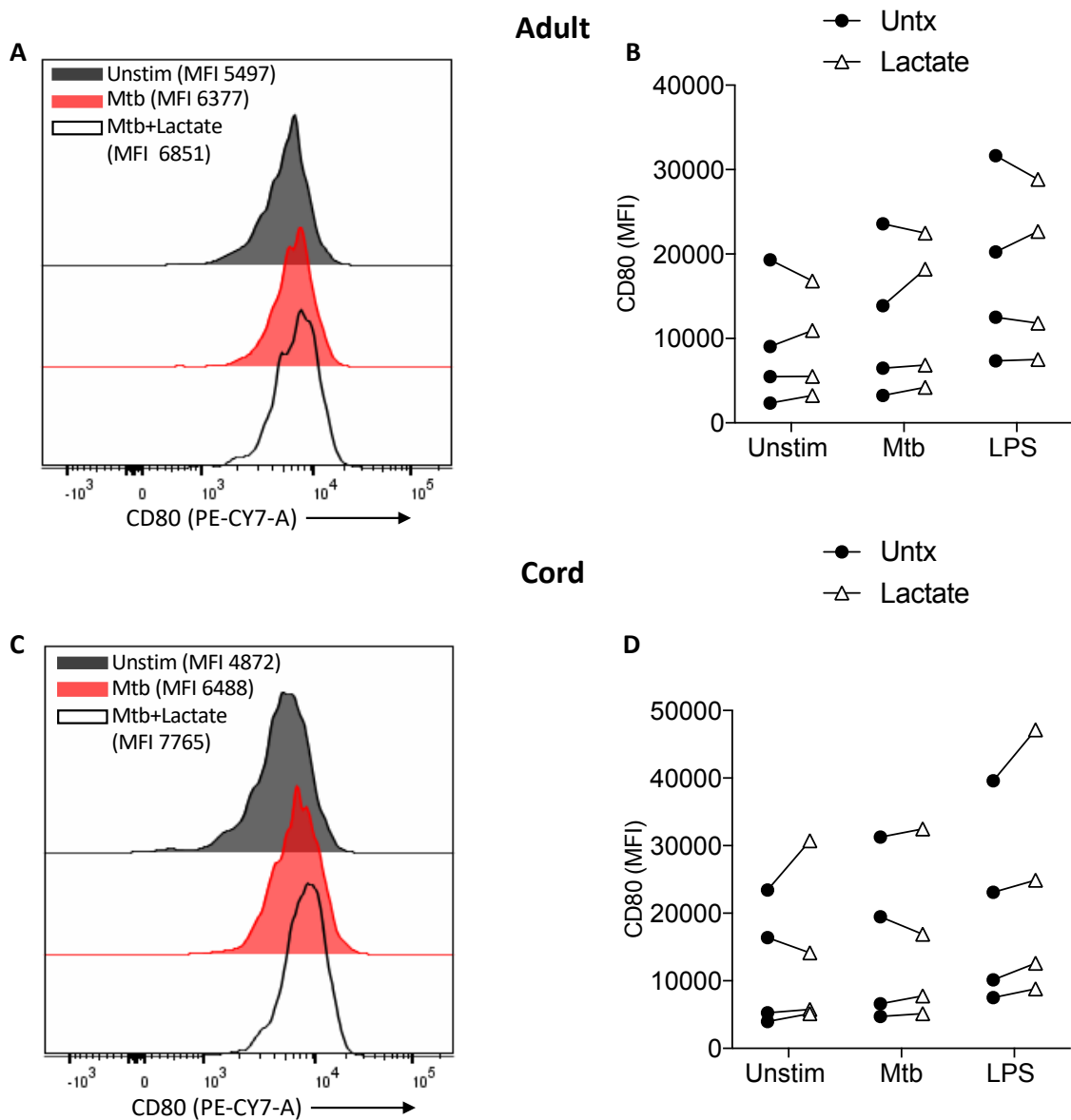


Figure 5.18 Expression of CD80 in lactate pre-treated adult and cord blood MDM 24 hours after Mtb or LPS stimulation.

PBMC were isolated from buffy coats or from umbilical cord blood samples taken immediately following delivery. Adult or cord blood MDM were adherence purified for 7 days in 10% human serum. Lactate (25mM) was added 3 hours prior to stimulation with Mtb (iH37Rv; MOI 1-10) or LPS (100 ng/ml). 24 hours after stimulation MDM were washed and detached from the plates by cooling and gently scraped and place in flow cytometry tubes. Cells were Fc blocked, exposed to viability dye Zombie NIR and stained with fluorochrome-conjugated antibodies specific for CD14, CD68 and CD80. Cells were analysed by flow cytometry. A representative histogram for the adult (A) and cord (C) are shown. The mean fluorescent intensity (MFI) of the phenotypic markers for the adult (B; n=4 \pm SD) and cord (D; n=4 \pm SD) MDM is shown. Statistical significance was determined using two-way ANOVA using Sidak's multiple comparison test.

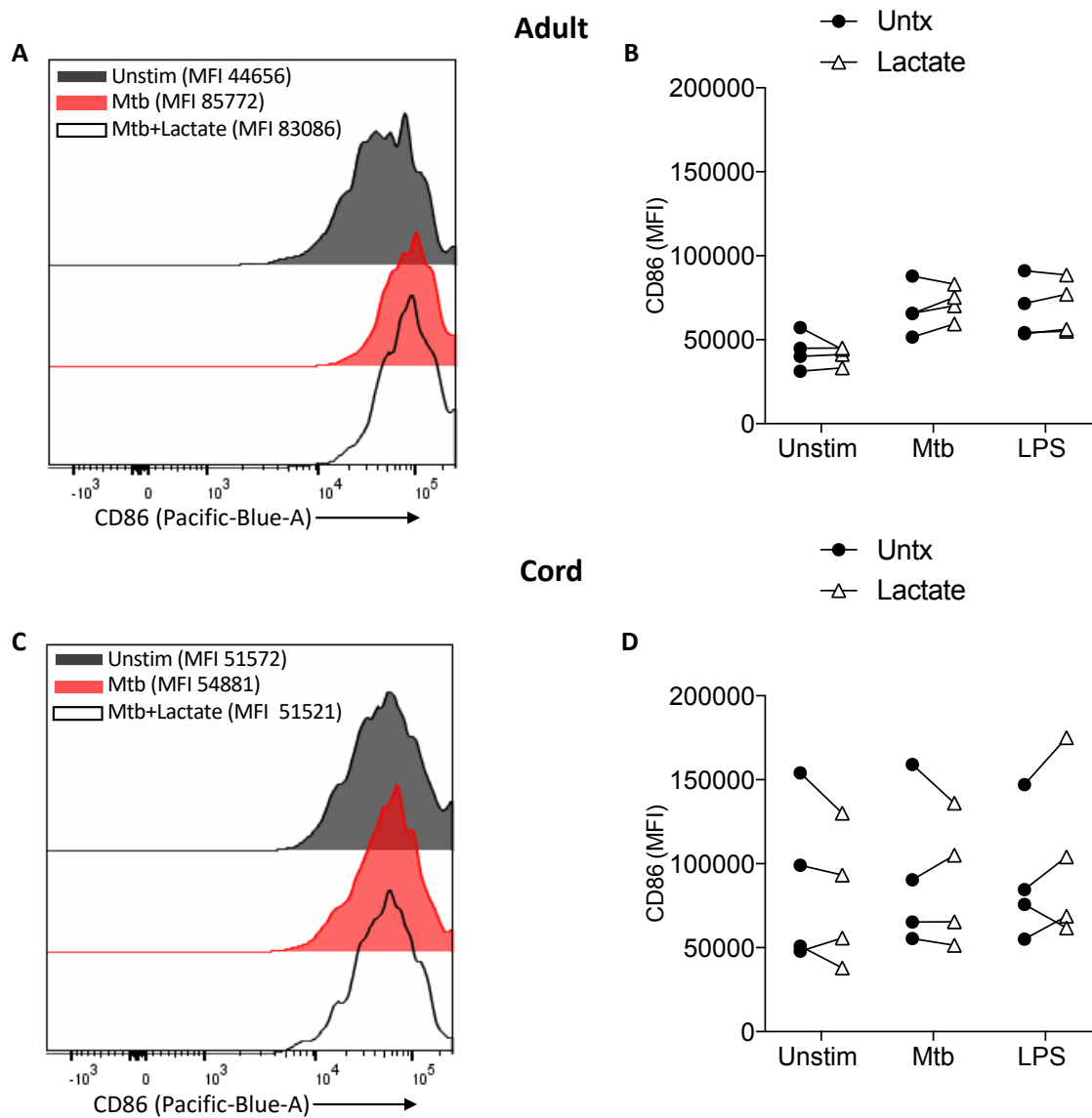


Figure 5.19 Expression of CD86 in lactate pre-treated adult and cord blood MDM 24 hours after Mtb or LPS stimulation.

PBMC were isolated from buffy coats or from umbilical cord blood samples taken immediately following delivery. Adult or cord blood MDM were adherence purified for 7 days in 10% human serum. Lactate (25mM) was added 3 hours prior to stimulation with Mtb (iH37Rv; MOI 1-10) or LPS (100 ng/ml). 24 hours after stimulation MDM were washed and detached from the plates by cooling and gently scraped and placed in flow cytometry tubes. Cells were Fc blocked, exposed to viability dye Zombie NIR and stained with fluorochrome-conjugated antibodies specific for CD14, CD68 and CD86. Cells were analysed by flow cytometry. A representative histogram for the adult (A) and cord (C) are shown. The mean fluorescent intensity (MFI) of the phenotypic markers for the adult (B; $n=4 \pm SD$) and cord (D; $n=4 \pm SD$) MDM is shown. Statistical significance was determined using two-way ANOVA using Sidak's multiple comparison test.

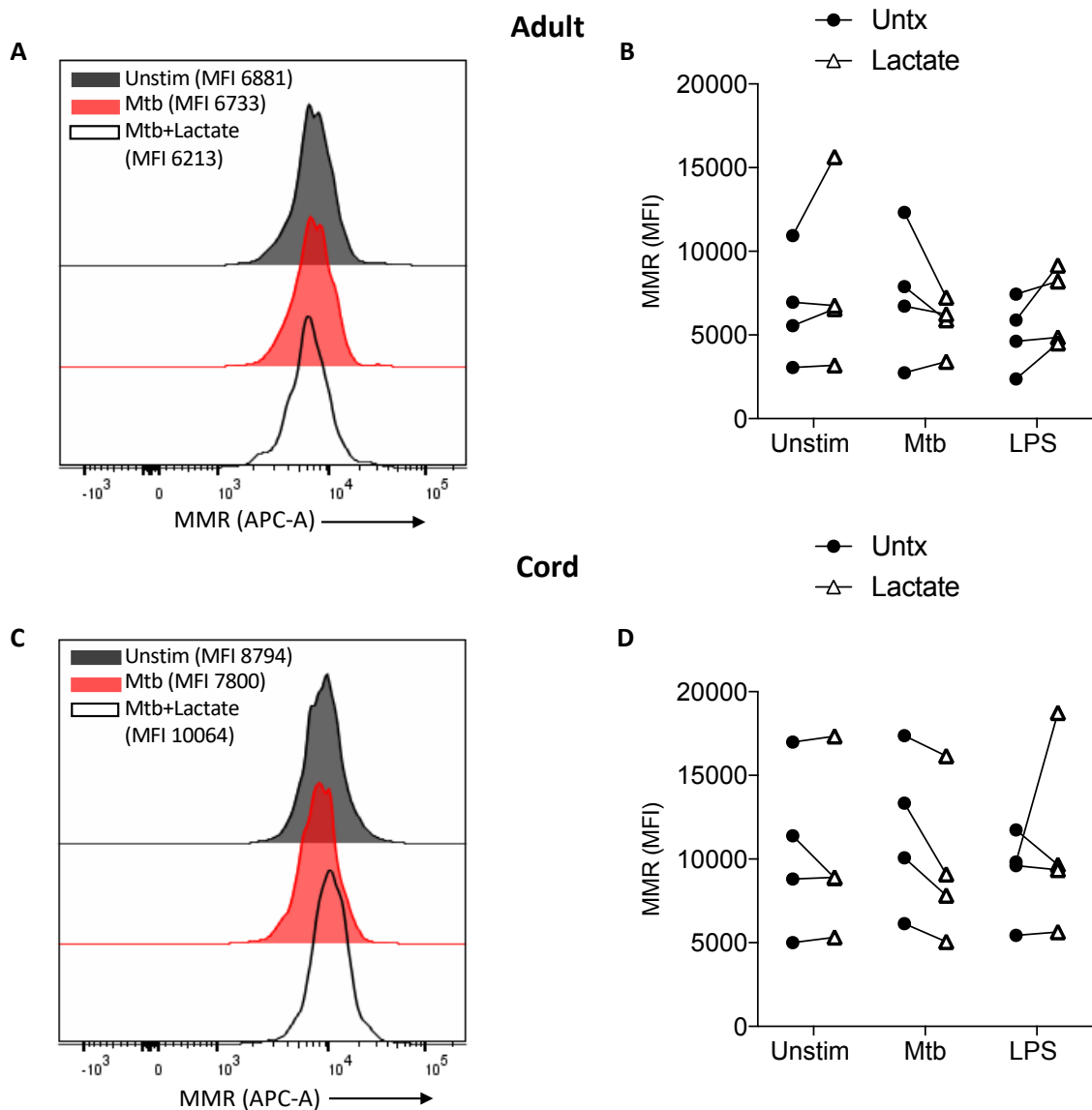


Figure 5.20 Expression of MMR in lactate pre-treated adult and cord blood MDM 24 hours after Mtb or LPS stimulation.

PBMC were isolated from buffy coats or from umbilical cord blood samples taken immediately following delivery. Adult or cord blood MDM were adherence purified for 7 days in 10% human serum. Lactate (25mM) was added 3 hours prior to stimulation with Mtb (iH37Rv; MOI 1-10) or LPS (100 ng/ml). 24 hours after stimulation MDM were washed and detached from the plates by cooling and gently scraped and place in flow cytometry tubes. Cells were Fc blocked, exposed to viability dye Zombie NIR and stained with fluorochrome-conjugated antibodies specific for CD14, CD68 and MMR. Cells were analysed by flow cytometry. A representative histogram for the adult (A) and cord (C) are shown. The mean fluorescent intensity (MFI) of the phenotypic markers for the adult (B; n=4 \pm SD) and cord (D; n=4 \pm SD) MDM is shown. Statistical significance was determined using two-way ANOVA using Sidak's multiple comparison test.

5.2.5 The effect of pre-treatment with lactate on cytokine secretion from adult and cord blood MDM after stimulation with Mtb or LPS.

The production of IL-1 β is closely associated with increased glycolysis and accompanying changes in cellular energetics in murine macrophages stimulated with LPS¹⁸⁷. In addition, increases in glycolysis in the context of Mtb infection is associated with increased IL-1 β production^{188,226,227,235}. TNF is a key proinflammatory cytokine produced by activated macrophages and is an important factor in the host response to Mtb^{29,73}. Lactate has previously been shown to modulate TNF production in human cells stimulated with LPS^{212,214,286}. It was next sought to determine if lactate modulated cytokine production in human macrophages. PBMC were isolated from adult buffy coats or from umbilical cord blood which was collected immediately following delivery. MDM were adherence purified for 7 days in RPMI with 10% human serum and non-adherent cells were washed off on days 2 and 5. MDM were treated with lactate (25mM) for 3 hours prior to stimulation with Mtb (iH37Rv; MOI 1-10) or LPS (100 ng/ml). 24 hours after Mtb or LPS stimulation, the concentrations of IL-1 β , TNF, IL-10 and IL-6 present in the supernatants were quantified by Meso Scale Discovery system ELISA.

In keeping with the observation that lactate attenuated glycolysis in macrophages stimulated with Mtb, pre-treatment with lactate significantly reduced concentrations of IL-1 β present in the supernatant of adult MDM 24 hours post stimulation with Mtb (P<0.01; Figure 5.21 A). Lactate significantly reduced TNF production in adult MDM stimulated with Mtb (P<0.05; Figure 5.21 B) but did not affect the concentrations of IL-6 (Figure 5.21 C) or IL-10 (Figure 5.21 D). In cord blood MDM pretreated with lactate and subsequently stimulated with Mtb, there was a downward trend but not a

statistically significant decrease in both IL-1 β (Figure 5.22 A) and TNF (Figure 5.22 B) production. There was no significant change in IL-6 (Figure 5.22 C) or IL-10 (Figure 5.22 D) production.

No differences were observed in IL-1 β production between lactate-treated and untreated adult MDM stimulated with LPS (Figure 5.23 A), as expected since there is no second signal to activate the inflammasome to produce mature IL-1 β . There was also no significant difference in TNF, IL-6 and IL-10 (Figure 5.23 B-D). In cord blood MDM pre-treated with lactate and stimulated with LPS, there was no significant alteration in IL-1 β , TNF or IL-6 (Figure 5.24 A-C). A small but statistically significant decrease in IL-10 was observed (Figure 5.24 D).

These data indicate that pre-treatment with lactate results in a reduction in secretion of pro-inflammatory cytokines TNF and IL-1 β following Mtb stimulation in adult MDM. A similar trend is seen in cord blood MDM, however, the decrease in TNF and IL-1 β production did not reach statistical significance.

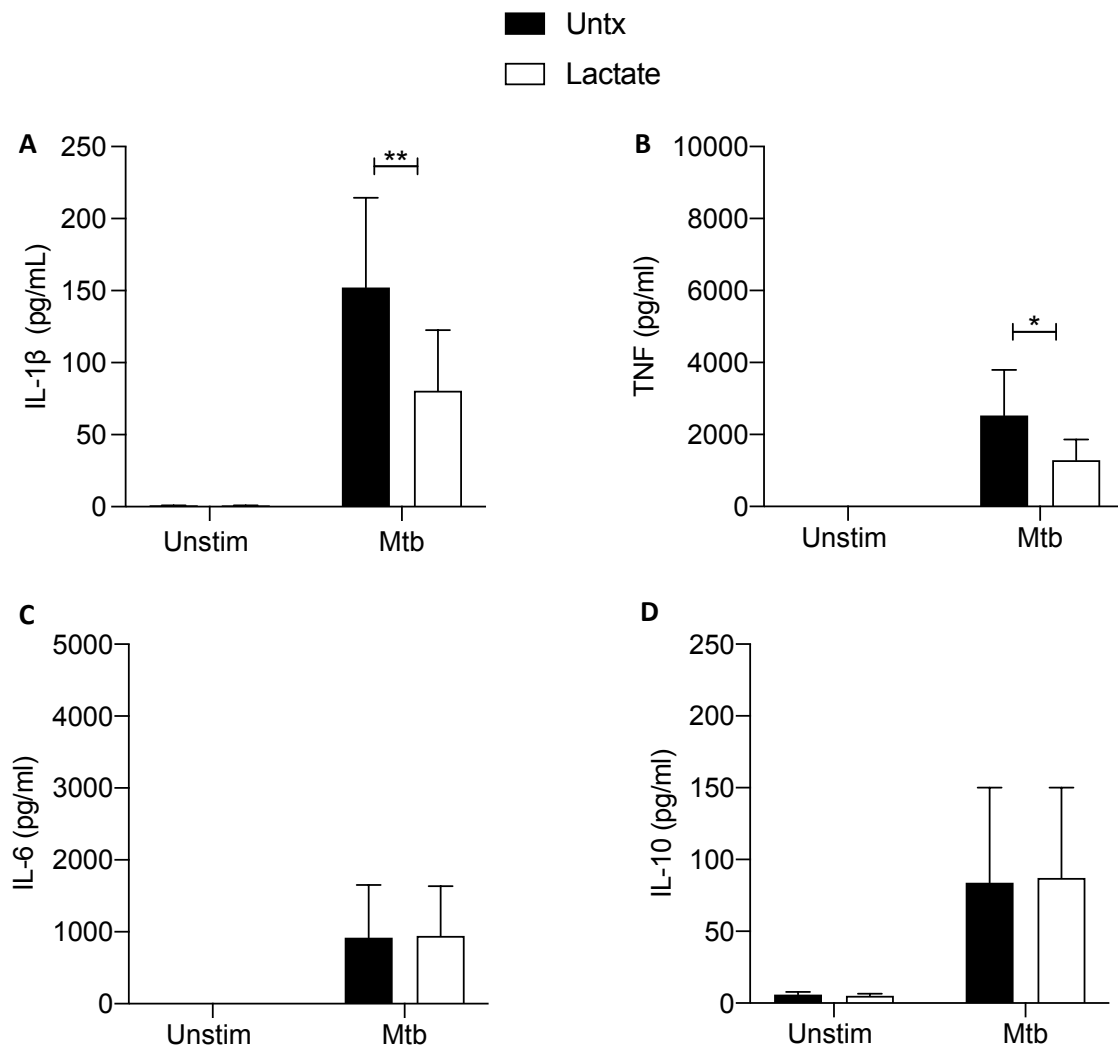


Figure 5.21 Cytokine production in adult MDM pre-treated with lactate 24 hours after Mtb stimulation.

PBMC were isolated from buffy coats and MDM were adherence purified for 7 days in 10% human serum. Lactate (25mM) was added 3 hours prior to stimulation with Mtb (iH37Rv; MOI 1-10). 24 hours after stimulation the concentration of IL-1 β (A), TNF (B), IL-6 (C) and IL-10 (D) in supernatant was measured by Mesoscale Discovery assay. Graphs illustrate collated data from adult MDM (n=4 \pm SD). Statistical significance was determined using two-way ANOVA with Sidak's multiple comparison test; ** P<0.01, *** P<0.001.

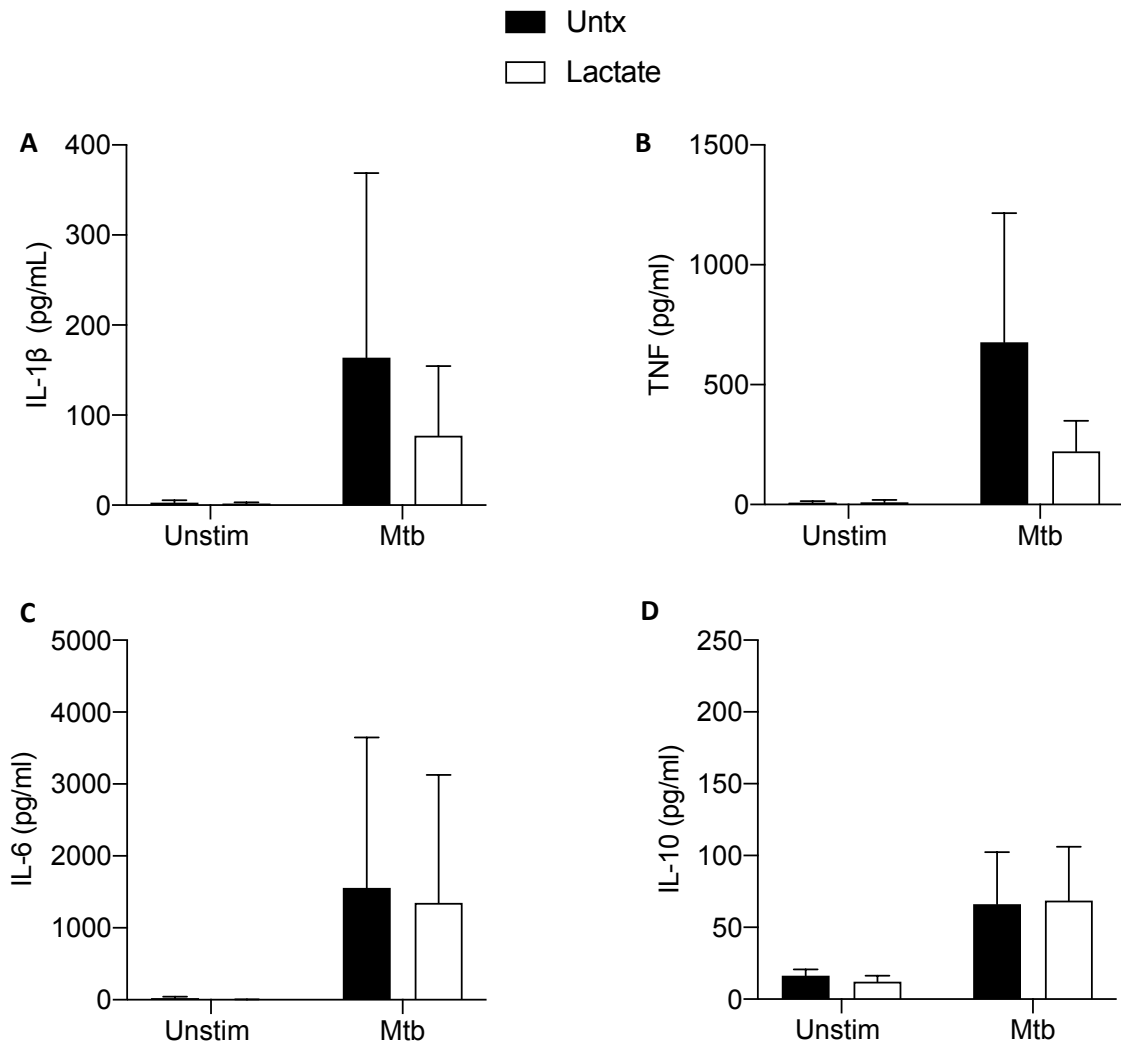


Figure 5.22 Cytokine production in cord blood MDM pre-treated with lactate 24 hours after Mtb stimulation.

PBMC were isolated from umbilical cord blood samples taken immediately following delivery and cord blood MDM was adherence purified for 7 days in 10% human serum. Lactate (25mM) was added 3 hours prior to stimulation with Mtb (iH37Rv; MOI 1-10). 24 hours after stimulation the concentration of IL-1 β (A), TNF (B), IL-6 (C) and IL-10 (D) in supernatant was measured by Mesoscale Discovery assay. Graphs illustrate collated data from adult MDM (n=4 \pm SD). Statistical significance was determined using two-way ANOVA with Sidak's multiple comparison test; ** P<0.01, *** P<0.001.

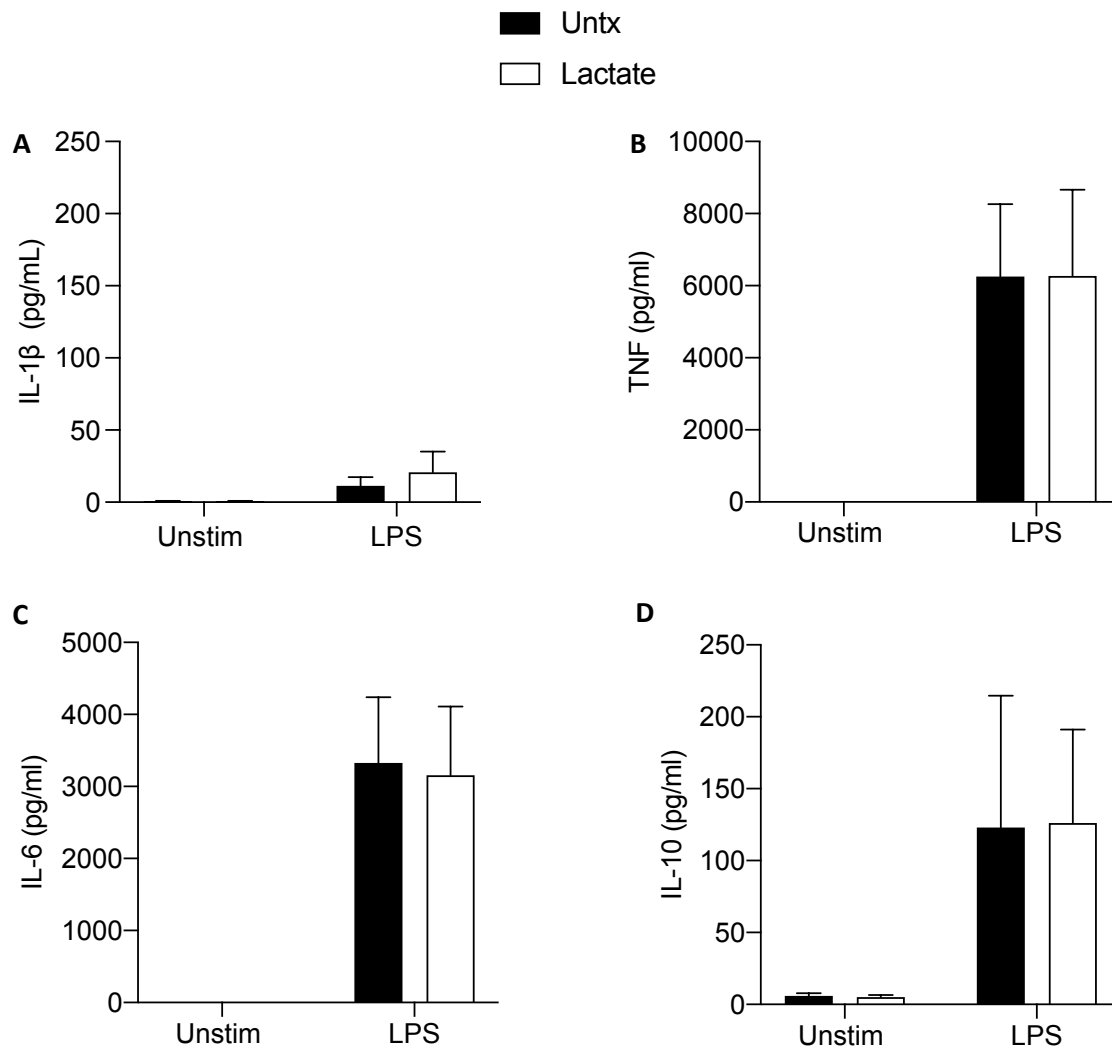


Figure 5.23 Cytokine production in adult MDM pre-treated with lactate 24 hours after LPS stimulation.

PBMC were isolated from buffy coats and MDM were adherence purified for 7 days in 10% human serum. Lactate (25mM) was added 3 hours prior to stimulation with LPS (100 ng/ml). 24 hours after stimulation the concentration of IL-1 β (A), TNF (B), IL-6 (C) and IL-10 (D) in supernatant was measured by Mesoscale Discovery assay. Graphs illustrate collated data from adult MDM (n=4 \pm SD). Statistical significance was determined using two-way ANOVA with Sidak's multiple comparison test.

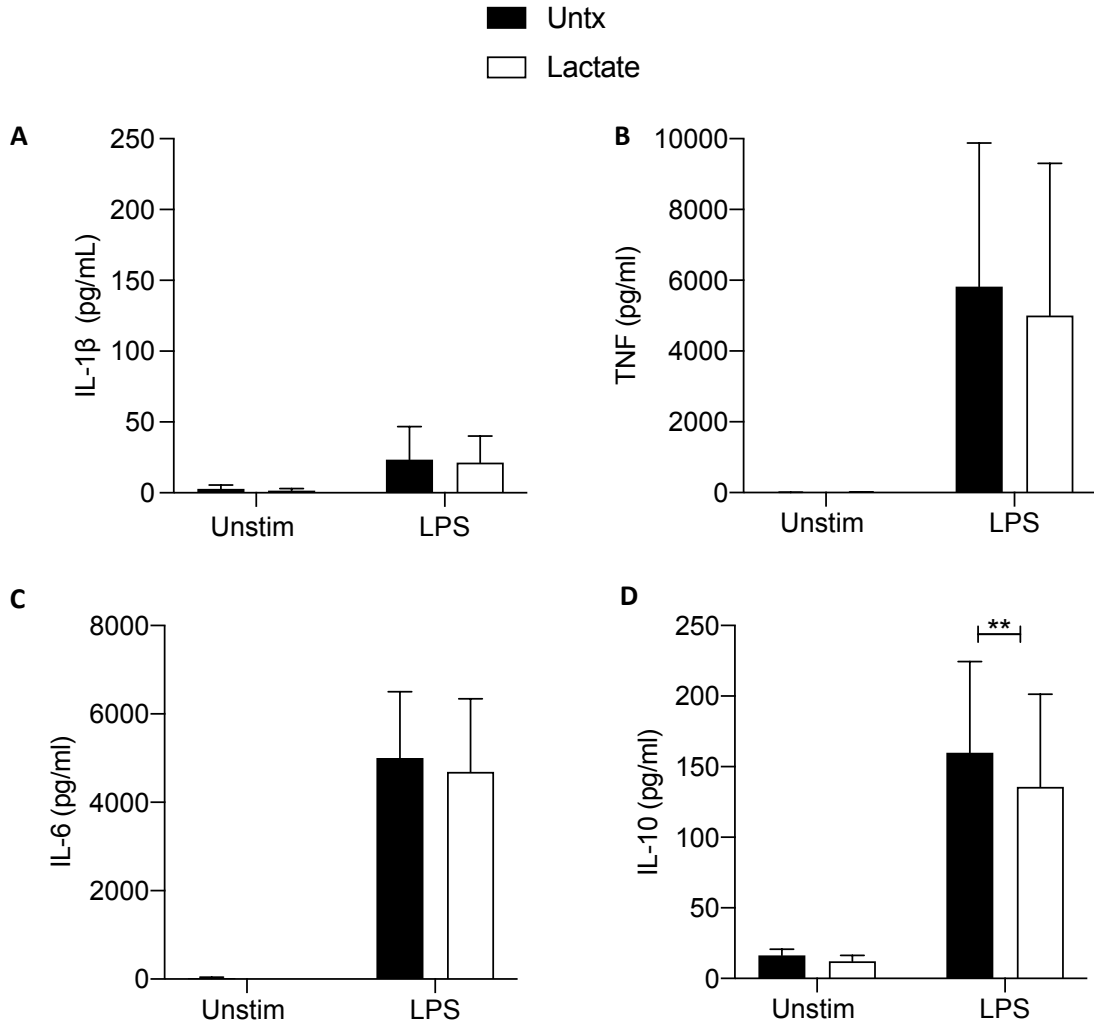


Figure 5.24 Cytokine production in cord blood MDM pre-treated with lactate 24 hours after LPS stimulation.

PBMC were isolated from umbilical cord blood samples taken immediately following delivery and cord blood MDM were adherence purified for 7 days in 10% human serum. Lactate (25mM) was added 3 hours prior to stimulation with LPS (100 ng/ml). 24 hours after stimulation the concentration of IL-1 β (A), TNF (B), IL-6 (C) and IL-10 (D) in supernatant was measured by Mesoscale Discovery assay. Graphs illustrate collated data from cord blood MDM (n=4 \pm SD). Statistical significance was determined using two-way ANOVA with Sidak's multiple comparison test; ** P<0.01.

5.2.6 Lactate improved ability of adult MDM to kill Mtb.

It has previously been reported that endogenous lactate production is increased in human MDM in response to infection with Mtb, indicative of increased flux through glycolysis^{188,235}. Moreover, this shift towards aerobic glycolysis, coupled with increased lactate, was associated with bacillary killing¹⁸⁸. This was attributed to the increased pro-inflammatory function of the macrophage, including increased production of IL-1 β . Having established herein that lactate exhibits a downregulatory effect on the ability of the cell to shift its metabolic function towards glycolysis and inhibits the early Warburg effect observed in human MDM stimulated with Mtb or LPS, the impact of lactate on bacillary clearance was next addressed. Since virulent Mtb is known to perturb host metabolism²⁸⁵, this project used live, attenuated, Mtb (H37Ra) to examine the effect of lactate on the ability of MDM to control an infection. Due to limited cord blood donor availability, these experiments were only undertaken in adult MDM. In order to control for the possible effect of sodium ion in the Na-L-Lactate compound, NaCl at equimolar concentrations were assayed in parallel as a control.

PBMC were isolated from buffy coats and MDM were adherence purified for 7 days in 10% human serum. MDM were left untreated or treated with 6.25, 12.5 or 25 mM of lactate or NaCl for three hours prior to infection with Mtb (H37Ra) at a MOI of 30-40% infectivity, 1-5 mycobacteria per cell (as defined by auramine O staining). After 3 hours of infection, cells were washed and lysed (day 0), diluted in Middlebrook medium and plated onto Middlebrook 7H10 agar (supplemented with OADC). On D2 and D5, supernatants were removed and extracellular bacteria was pelleted by centrifugation. Cells were lysed and lysates were pooled with the bacterial pellets from the

supernatants. Lysates were diluted in Middlebrook medium and plated onto Middlebrook 7H10 agar (supplemented with OADC). CFU were enumerated 21 days after plating. The lactate time course graph (Figure 5.25 A) shows the CFU results at day 0, 3 and 5 for each of the lactate concentrations. The differences in CFU growth for each concentration of lactate at the day 5 time point are graphed in Figure 5.25 B. Lactate caused a dose dependent reduction in CFU 5 days after infection, with a statistically significant decrease in CFU in MDM treated with 25 mM lactate compared with untreated controls (Figure 5.25 B, $P < 0.01$). No statistically significant differences in CFU growth were seen with NaCl at equivalent molar concentrations (Figure 5.25 C, D).

Lactate at 20mM has been previously been described to be optimal to support Mtb growth whereas growth was inhibited with 40mM lactate³⁰⁵. In this project, any extracellular Mtb is washed away three hours post infection. This reduces the likelihood that there would be any direct effects of lactate on Mtb growth early on. In order to assess the effect of lactate directly on Mtb growth, lactate was added to Mtb in axenic (cell-free) conditions and growth was determined using the BacT Alert automated microbial detection system. The concentration of Mtb was determined by adding equal volumes of Mtb corresponding to an MOI for an adult MDM infection for the CFU experiments, as described above. This volume of Mtb was added to 1 ml of Middlebrook 7H9 Broth (supplemented with ADC) in the presence of 0, 6.25, 12.5 and 25 mM of lactate. After three days of mycobacterial propagation, culture medium (20% dilution) was added to BacT bottles. Time to positivity, as measured by the BacT Alert Analyser and was recorded for each condition. The fold change from the time for the bottle with no lactate to become positive is illustrated in Figure 5.26. Lactate did not cause and

statistically significant change in time to positivity at any concentration. These data suggest that lactate promotes bacillary killing through cell-mediated mechanisms.

Autophagy is an essential protective strategy employed by the host, however, Mtb has been shown to disrupt autophagic flux³⁰⁶, although the impact of lactate on autophagy in human MDM is unknown. LC3 and p62 are cytosolic proteins that are recruited to the autophagosome upon initiation of autophagy and are degraded upon fusion of the autophagosome with the lysosome. Accumulation of LC3 and p62 after initiation of autophagy is indicative of a block in autophagic flux. 3-methyladenine (3MA) is a phosphoinositide 3-kinase (PI3K) inhibitor that has been shown to block autophagy³⁰⁷ and increase *Mycobacterium aurum* growth in a THP-1 cell line³⁰⁸.

In order to explore the hypothesis that induction of autophagy by lactate is the mechanism by which Mtb killing is increased, expression of LC3 and p62 in adult MDM infected with Mtb (H37Ra) in the presence or absence of lactate and in the presence or absence of 3MA (5mM, Sigma) was determined using Western blotting. As predicted, infection with Mtb increased the expression of p62 and LC3II, although the addition of lactate reversed this accumulation. The block in autophagy caused by 3MA was also reversed by lactate treatment. Shown is one representative donor (Figure 5.27 A).

In order to determine if lactate promoted intracellular killing of Mtb through increased autophagic flux, 3MA was used to block autophagy in the presence or absence of lactate. PBMC were isolated from buffy coats and MDM were adherence purified for 7 days in 10% human serum. MDM were left untreated or treated with 25 mM of lactate

for three hours prior to infection with Mtb (H37Ra) at a MOI of 30-40% infectivity, 1-5 mycobacteria per cell (as defined by Auramine O staining). One hour prior to infection 3MA (5mM) was added to the appropriate wells. After 3 hours of infection, cells were washed and lysed (day 0), diluted in Middlebrook medium and plated onto Middlebrook 7H10 agar (supplemented with OADC). On day 5, supernatants were removed and extracellular bacteria was pelleted by centrifugation. Cells were lysed and lysates were pooled with the bacterial pellets from the supernatants. Lysates were diluted in Middlebrook medium and plated onto Middlebrook 7H10 agar (supplemented with OADC). CFU were enumerated 21 days after plating and are graphed in Figure 5.27 B.

3MA caused a non-significant increase in CFU. The blocking of autophagy is the presumed mechanism of 3MA, thereby promoting Mtb survival. The addition of lactate prior to Mtb infection improved MDM ability to kill Mtb whether 3MA was present or not, suggesting that lactate was able to overcome the block in autophagic flux by 3MA. Taken together, the evidence indicating that lactate reduced p62 and LC3-II accumulation during Mtb infection and abrogated the inhibition of autophagy caused by 3MA suggests that lactate mediates its bactericidal effects, at least in part, through enhancing autophagic flux.

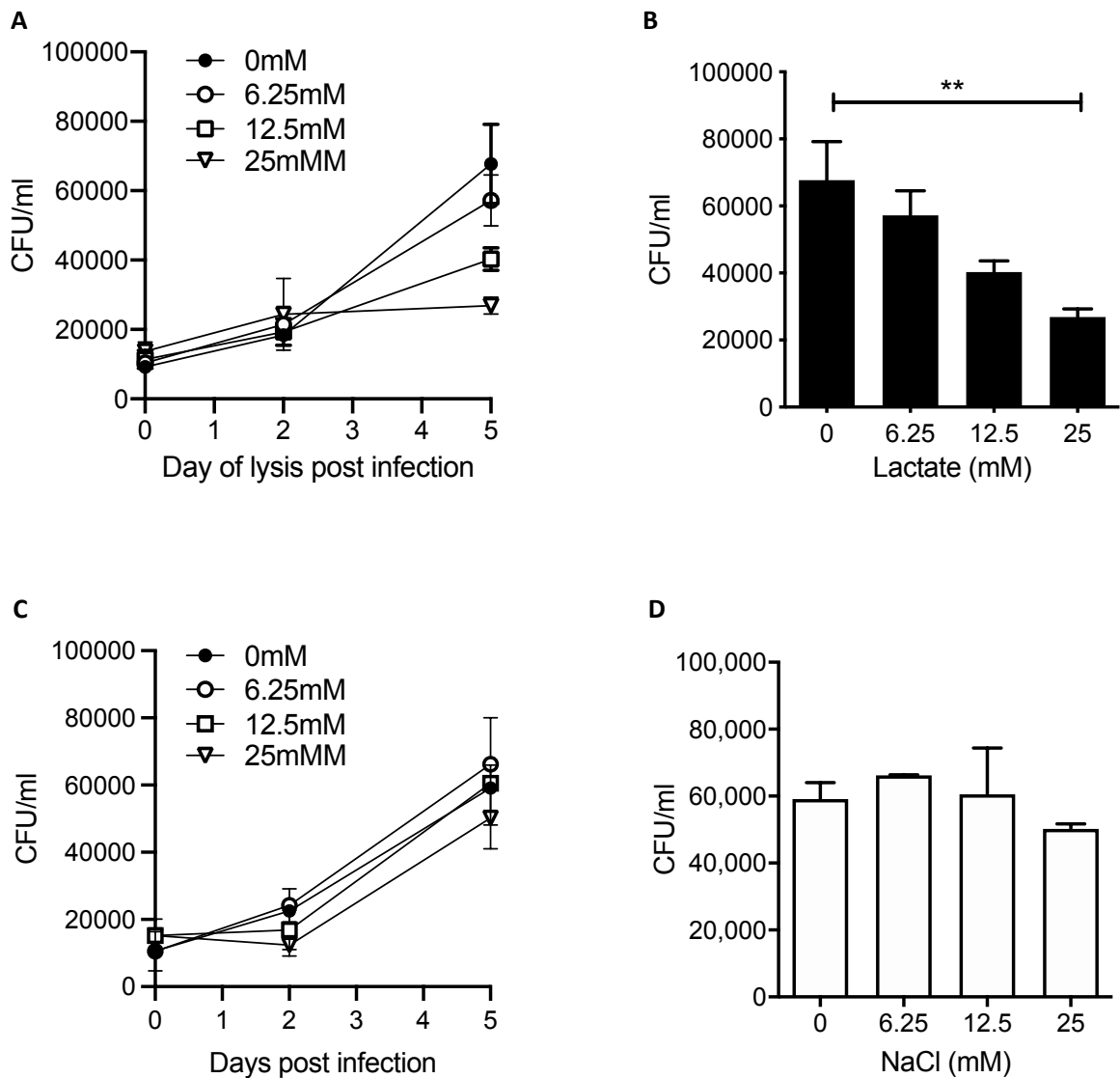


Figure 5.25 Lactate improved ability of adult MDM to kill Mtb.

PBMC were isolated from buffy coats and MDM were adherence purified for 7 days in 10% human serum. MDM were left untreated or treated with 6.25, 12.5 or 25 mM of lactate for three hours prior to infection with Mtb (H37Ra) at a MOI of 30-40% infectivity, 1-5 mycobacteria per cell (as defined by auramine O staining) and were then lysed on day 0 (3 hours post-infection), day 2 and day 5 and plated on Middlebrook 7H10 agar (+OADC). CFU were enumerated 21 days after plating. The time course graph (A) shows the CFU results at day 0, 3 and 5 for each of the lactate concentrations ($n=5 \pm SD$). The differences in CFU growth for each concentration of lactate at the day 5 time point are graphed in B ($n=5 \pm SD$). The NaCl time course graph (C) shows the CFU results at day 0, 3 and 5 for each of the NaCl concentrations ($n=3 \pm SD$). The differences in CFU growth for each concentration of NaCl at the day 5 time point are graphed in D ($n=5 \pm SD$). Statistical significance was determined using one-way ANOVA with Tukey's comparison test; ** $P < 0.01$.

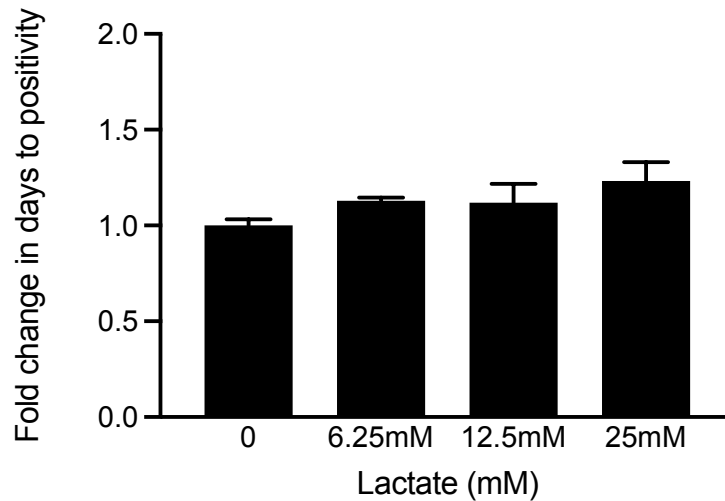


Figure 5.26 Lactate does not affect Mtb growth in axenic conditions.

A volume of Mtb (H37Ra) corresponding with the volume of Mtb required to elicit an MOI of 30-40% infectivity and 1-5 bacteria per cell in an adult MDM infection, was added to 1ml of Middlebrook 7H9 Broth (supplemented with ADC) in the presence of 0, 6.25, 12.5 and 25mM of sodium-lactate. After three days of mycobacterial propagation, a 20% dilution of each treatment condition was added to BacT bottles and placed in the BacT Alert Analyser. Time to positivity was recorded for each condition and the fold change was calculated by comparison with the time to positivity for the sample with no lactate ($n=2 \pm \text{SEM}$). Statistical significance was determined using one-way ANOVA with Tukey's comparison test.

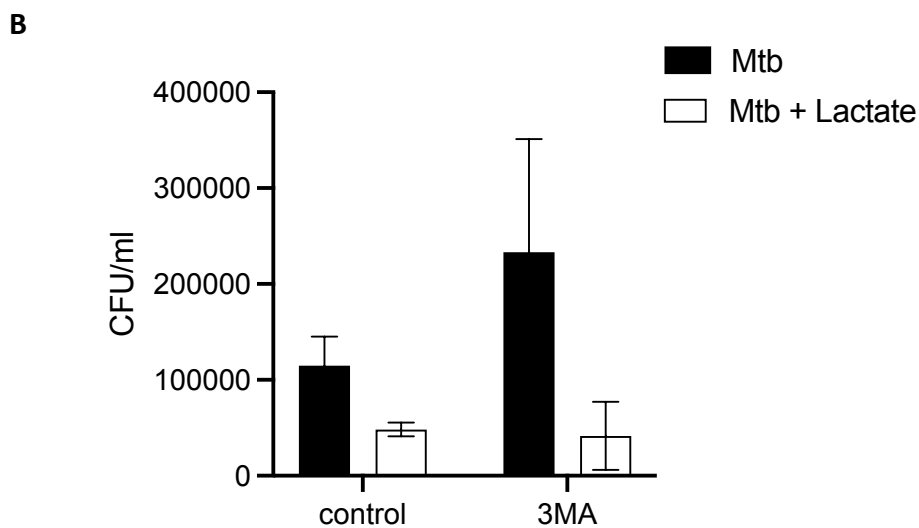
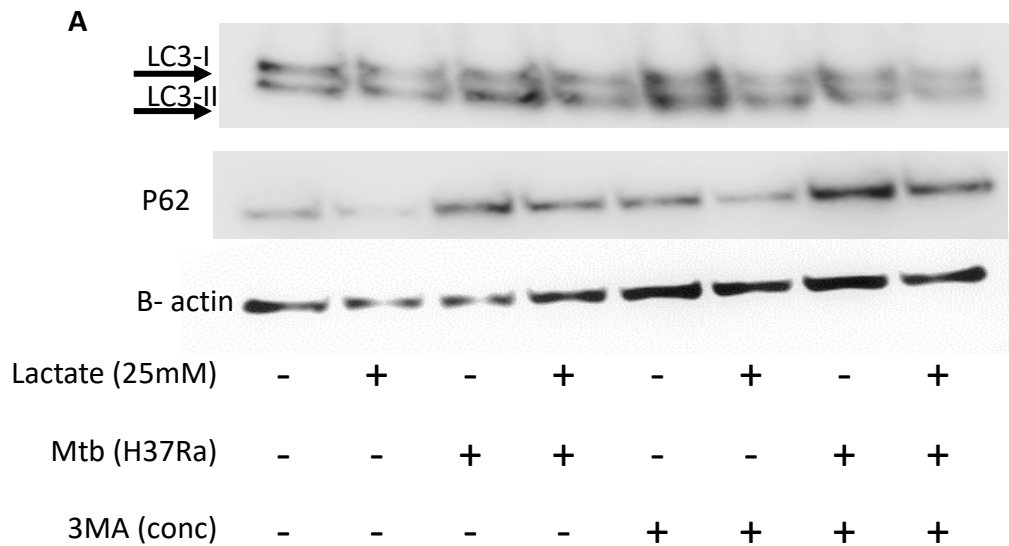


Figure 5.27 Lactate overcomes the autophagic block caused by Mtb and 3MA.

PBMC were isolated from buffy coats and MDM were adherence purified for 7 days in 10% human serum. MDM were left untreated or treated with 25 mM of lactate for three hours prior to infection with Mtb (H37Ra) at a MOI of 30-40% infectivity, 1-5 mycobacteria per cell (as defined by auramine O staining). One hour prior to infection 3MA (5mM) was added to the indicated wells. 24 hours after infection whole cell lysates were prepared and analysed for the presence of LC3II and p62 by immunoblotting (A). Shown is one representative donor. On day 5, infected cells were lysed and plated on Middlebrook 7H10 agar (+OADC). CFU were enumerated 21 days after plating and are graphed in B (n=2 ± SD).

5.3 Discussion

The data generated in this project shows that lactate has an immediate effect on human macrophage metabolism, reducing glycolysis and increasing oxidative phosphorylation, a reverse of the Warburg effect. Lactate also alters macrophage function by decreasing pro-inflammatory IL-1 β and TNF cytokine secretion following stimulation with either Mtb or LPS. Furthermore, lactate augments the ability of human macrophages to kill Mtb.

Previous studies have reported that lactate inhibits glycolysis in PBMC, monocytes and mast cells^{212,214,286,309}. These data are in keeping with published findings, showing that lactate causes a rapid and significant reduction in glycolysis in differentiated human macrophages but does not prevent the glycolytic shift following stimulation with Mtb or LPS. While lactate reduces the peak of glycolysis following stimulation, this is due to lactate reducing the glycolytic rate prior to stimulation. Interestingly, lactate increased oxidative phosphorylation in resting macrophages and blocked the reduction in oxygen consumption observed early after stimulation with Mtb or LPS. Taken together, lactate attenuated glycolytic metabolism, and concomitantly maintained oxygen consumption; in effect, blocking the early shift to Warburg metabolism observed in human macrophages immediately after stimulation. The data generated in Chapter 3 is the first to report that human macrophages undergo early Warburg metabolism in response to Mtb or LPS stimulation²⁷⁶ and the importance of this early metabolic switch in human immune cells is still poorly understood. These data indicate that lactate, the product of increased glycolysis, has a negative feedback effect on bystander macrophages; inhibiting further Warburg metabolism but maintaining the ability to shift towards

glycolytic metabolism, albeit attenuated, and more energetic than glycolytic as shown by the phenogram. This suggests that the early decrease in oxidative phosphorylation may be a critical regulatory node in the activation of proinflammatory macrophage responses.

In the context of an active ongoing infection, this negative feedback mechanism may have multiple purposes including downregulating inflammation to limit collateral tissue damage, promoting resolution and a return to homeostasis, or may be a mechanism by which bystander macrophage glucose consumption is restricted to support the nutrient needs of neighbouring infected macrophages that are producing the lactate. This is in keeping with published observations showing that the metabolic function of one immune cell can be regulated by increased demand on nutrients from another immune cell in the environment³¹⁰.

A previous study in human monocytes found that the metabolic effects of lactate were mostly short lived with only an increase in SRC noted²⁸⁶ at 24 hours. These data indicate that 24 hours after stimulation with Mtb, a reduction in OCR is seen when cells were pretreated with lactate. The effect on glycolysis, seen immediately after lactate administration had resolved. ATP linked respiration and proton leak were both significantly reduced in MDM stimulated with Mtb when pre-treated with lactate. Lactate also increased the maximal respiration and SRC of the unstimulated MDM. No differences were seen in LPS stimulated MDM at 24 hours, highlighting the different immunometabolic responses with different stimuli. At 24 hours, no difference in M1 or M2 associated cell surface activation markers were seen.

The production of mature IL-1 β is linked to Warburg metabolism in mice¹⁸⁷ and to the ability of human macrophages to increase glycolysis in response to infection with Mtb^{188,226,227,235}. Significantly reduced concentrations of IL-1 β in Mtb-stimulated adult MDM pre-treated with lactate compared with control was observed. This suggests that the maximal rate of glycolysis and not the degree of change, is an important factor in production of IL-1 β in human MDM. Significantly reduced concentrations of TNF in Mtb-stimulated adult MDM pre-treated with lactate compared with control was also observed. Studies with murine macrophages *in vitro* show that modulating glycolysis has no effect on TNF production^{187,311} but inhibiting glycolysis in an *in vivo* mouse model of Mtb infection results in reduced TNF production from macrophages¹⁴⁷. Promoting glycolysis in human macrophages during Mtb infection results in increased TNF production^{226,227}. Furthermore, the data from Chapter 3 shows that umbilical cord blood macrophages fail to reduce oxidative phosphorylation upon stimulation, and also produce less TNF specifically in response to Mtb infection but not LPS-stimulation compared with adult macrophages. Cumulatively, these findings suggesting that there may be a metabolic link to TNF production in macrophages in the context of Mtb infection that requires further elucidation. It is likely that metabolic shifts can influence TNF production but only as one part of a multi-factorial system, unlike in IL-1 β production which appears to be dependent on glycolysis.

Lactate bore a similar effect on the metabolic flux of macrophages stimulated with LPS compared to those stimulated with Mtb. In contrast, lactate did not reduce the concentrations of TNF produced by LPS stimulated macrophages. This is in keeping with published work showing that lactate did not reduce TNF production in LPS-stimulated

human monocytes²⁸⁶. These findings highlight stimulation-specific downstream effects of metabolic manipulation on macrophage effector function. Lactate may have a direct impact on Mtb stimulated cytokine pathways independent of metabolic shifts or LPS may have more redundancy in its activation pathway.

Lactate promoted Mtb killing in human MDM despite reducing IL-1 β and TNF production. This somewhat counterintuitive finding indicates that the metabolic switch that occurs in human macrophages upon stimulation causing increased flux through glycolysis promotes bacillary clearance (at least in part) via the production of lactate. Lactate can function as a carbon source for Mtb and thus promote bacterial growth but, at high concentrations, can inhibit growth in axenic conditions³¹². The data herein suggests that the effects of lactate on bacillary clearance are cell mediated because of the dose-dependent effect observed on bacterial growth and the evidence indicating that lactate promotes autophagy. In addition, the infection model protocol used in this project removes extracellular bacteria 3 hours post infection by thoroughly washing and no differences are observed in the number of live bacteria phagocytosed by MDM during this timeframe (as evidenced by CFU counts at day 0 and confirmed by Auramine O staining). Lactate may mediate bacillary clearance by increasing autophagic flux and this would be consistent with studies showing that lactate promotes autophagy in cancer cells³¹³. The possibility that lactate promotes autophagy may be independent of its effect on metabolic function, however these pathways are intrinsically linked because nutrient stress in the environment triggers autophagy and modulates metabolic function³¹⁴. Furthermore, both glycolysis and autophagy are regulated by mTOR signaling³¹⁵ indicating that these processes may be linked in macrophages³¹⁶.

5.4 Conclusions

Exogenous lactate causes an immediate decrease in glycolysis and increase in oxidative phosphorylation in resting human macrophages. The presence of lactate blocks the early Warburg effect in macrophages stimulated with Mtb or LPS. Furthermore, lactate reduced IL-1 β and TNF production and increased bacillary killing in human macrophages infected with Mtb.

Put in the context of Mtb infection *in vivo*, an accumulation of lactate in the extracellular milieu, caused by infected macrophages, has an immediate negative feedback effect on bystander unstimulated macrophages; causing them to downregulate glycolysis and upregulate oxidative phosphorylation. The reasons for this could be to limit inappropriate pathological inflammation and promote resolution or it may also serve to prevent resting macrophages competing for glucose resources when in the presence of other highly glycolytic cells. Since this anti-inflammatory effect is also, somewhat counterintuitively, associated with increased ability to kill the bacteria, it is postulated that the previously described association between glycolysis and bacillary clearance may, at least in part, be mediated by the effects of lactate, the end-product of glycolysis^{41,188,235}.

Chapter 6 General Discussion and Future Work

6.1 General Discussion

The field of immunometabolism is rapidly expanding as the importance of underlying metabolic pathways for appropriate immune function is realised^{182,246,317,318}. The aim of this research was to define the immunometabolic response of human macrophages to pathogenic stimuli and to polarising cytokines, to explore if underlying metabolic differences underpinned the differences in adult and neonatal immune responses, and to examine the effect of lactate on macrophage immunometabolism.

The paucity of immunometabolic research in human macrophages is well recognised, with the majority of work to date performed in murine models^{153,196}. This study provides evidence for the first time that the Warburg effect, with increasing glycolysis and decreased OXPHOS, occurs in human macrophages²⁷⁶ following stimulation with LPS or Mtb. The data highlights the importance of timing when looking at immunometabolic responses. As predicted, based on observations in peak metabolite levels after stimulation in other studies²¹⁹, the metabolic response occurs rapidly in human MDM. In a study examining polarisation of murine BMDM¹⁹³, a similar live analysis experiment is undertaken as is demonstrated here in human MDM. LPS induces a rapid change in glycolysis as measured by a 50% increase in ECAR with a slower decrease in OCR, which is decreased by approximately 20% after 4 hours. This is in stark contrast to the data presented in this study, with a peak ECAR increase of approximately 250%, 150 minutes after LPS stimulation. A similar decrease of 20% is seen in OCR but this has resolved by 4 hours. The established murine metabolic phenotype shows an increase in glycolysis and a decrease in OXPHOS 24 hours after LPS stimulation. In contrast, the findings

presented in this study show an increase in both glycolysis and OXPHOS at this later time point in human MDM. These kinetic differences may offer insight into the differential production of nitric oxide (NO) in human MDM and mouse BMDM; there is controversy over whether or not human macrophages can produce NO as there is a general lack of evidence showing NO production in humans^{190,319}. From these findings in humans demonstrating that OXPHOS rapidly decreases in response to stimulation then resolves, it may be reasonable to postulate that NO production could follow similar kinetics; potentially being rapidly produced but short lived in humans. The decrease in OXPHOS in murine models after LPS stimulation has been associated with increased succinate, citrate and itaconate levels in murine BMDM^{187,273,288,320,321}. In murine models, these metabolites are shown to have downstream impact on immune function. Succinate stabilises HIF-1 α , increasing expression of glycolytic enzymes; citrate fuels fatty acid synthesis and itaconate has anti-inflammatory properties by acting through NRF-2 and even has bactericidal properties at high concentrations^{249,320}. Whether the short lived OXPHOS decrease seen in human MDM after LPS stimulation results in similar accumulation of these metabolites, and determining if the subsequent increase in OXPHOS further alters their concentrations, will require time specific metabolomic experiments to be undertaken and further highlight differences in murine and human macrophage immunology.

Understanding the role of OXPHOS in human MDM immune responses is also required in order to expand on a novel finding in umbilical cord blood MDM that is revealed in this work. The OXPHOS in umbilical cord MDM neither decreases at the early time point, nor increases at 24 hours when compared to adult MDM after LPS stimulation. Whether

the differences in oxygen consumption seen in adult and cord blood MDM relates directly to differences in immunologically active substrates such as itaconate and succinate is an area for future study. In addition, the benefit of this stabilised OXPHOS in neonatal macrophages may help to shed light on the process of immune development in these early days and weeks.

Human variation in cellular immunology is common and evident in these assays. For example, a variety of responses are seen between individual donors during the live stimulation of human MDM in the Seahorse XFe Analyzer. Although the decrease in OCR in adult MDM is statistically significant 2.5 hours post stimulation, 2 of the 7 donors do not alter their OXPHOS. In the cord blood MDM, 2 out of 6 donors slightly decrease OXPHOS, but there are no significant changes seen in the collated data. Whether or not changes in OXPHOS are associated with potential immune vulnerability seen more commonly in umbilical cord blood MDM than adult remains to be determined. Evidence to causally link differential metabolic function in cord blood and adult macrophages to infection outcomes, such as the intracellular growth of Mtb, are unexplored but this work supports the hypothesis that differences in immunometabolic function may leave infants uniquely susceptible to TB.

The importance of the decrease in OXPHOS observed in adult MDM post stimulation is further highlighted by the changes induced by IL-4 or lactate treatment, which are newly described in this research. Pre-treatment with either IL-4 or lactate prevents the decrease in OXPHOS seen following Mtb or LPS stimulation, however the increase in OXPHOS at baseline seen with lactate treatment was not seen with IL-4. Lactate has previously been shown to induce a M2 like phenotype in a THP-1 cell line²⁹⁰. While a

similar abrogation in glycolysis was seen after lactate treatment as with IL-4, it did not alter any of the cell surface markers in contrast to IL-4 treatment. This suggests that whilst lactate shifted MDM towards a more anti-inflammatory phenotype, this phenotype did not exactly replicate the M2 macrophage seen by polarising with IL-4. This adds further evidence that macrophage function and phenotype represents a spectrum of cell functions and behaviours rather than the simplified M1/M2 dichotomy.

Pre-treatment with lactate or IL-4 also decreased production of IL-1 β after Mtb stimulation, which has previously been linked to glycolysis. Studies in both human MDM and murine BMDM have shown that blocking glycolysis with 2DG decreases IL-1 β production^{187,188}. Interestingly, pre-treatment with IL-4 or lactate resulted in a decrease in the baseline ECAR but the glycolytic switch remained intact, with the ECAR having a similar fold change to the untreated MDM following Mtb or LPS stimulation. The subsequent decrease in Mtb induced IL-1 β production seen after lactate or IL-4 treatment is perhaps a reflection of the decreased maximal rate of glycolysis, a novel finding that will require further exploration. The fact that pre-treatment with IFN- γ increases maximal glycolysis in Mtb stimulated adult MDM but not cord blood MDM, with a subsequent increase in IL-1 β production in adult but not cord blood MDM, lends further credence to this theory. When adult and umbilical cord blood MDM are pre-treated with IFN- γ , the ECAR % increase from baseline after LPS stimulation is significantly reduced. This may indicate that the MDM have a maximal glycolytic capacity whose threshold is reached by the combined action of these pro-inflammatory stimuli. The significance of this glycolytic ceiling in perhaps acting as a checkpoint and

limiting pro-inflammatory signaling from activated macrophages will require further exploration.

This observation, that IFN- γ and LPS are individually significant drivers of metabolic shifts, raises the issue of combining these powerful immunomodulatory agents to polarise human MDM. IFN- γ was initially used to create a M1 phenotype but the addition of LPS appears to now be a standard methodology in human MDM work, carried over from murine BMDM research^{150,157}. The data presented in this project illustrate 5 distinct M1 phenotypes with IFN- γ , Mtb or LPS alone, and IFN- γ combined with Mtb or LPS. These data also highlight the differential immunometabolic phenotype following Mtb or LPS stimulation, underscoring that findings based on TLR agonists are not generalisable to all infectious disease states. The published literature on human macrophage polarisation is inconsistent. This is in part due to the various methodologies utilised to differentiate macrophages from monocytes. GM-CSF and MCSF partially polarise towards M1 or M2 phenotype respectively and are commonly used in macrophage differentiation¹⁶². The method in this project, of differentiating macrophages in the presence of human serum results in a high purity of a neutral macrophage phenotype, as evidenced by the resting phenotype which can easily be shifted depending on the signals it receives. This work could act as a benchmark for future research as it systematically describes distinct immunometabolic phenotypes across the spectrum of macrophage activation and polarisation. These data are highlighted in Figure 6.1.

The published data on the umbilical cord blood MDM phenotype are equally incoherent. Previous studies have been contradictory with most published work describing relatively similar expression of cell surface markers between adult and cord blood MDM, except for HLA-DR, which is replicated herein^{259,322,323}. A novel finding of decreased TNF production in umbilical cord blood MDM compared to adult MDM following Mtb stimulation is described²⁷⁶. IFN- γ increases baseline ECAR in both adult and umbilical cord blood MDM. In contrast to one previous published study, which showed that umbilical cord blood MDM did not undergo glycolysis during a glycolysis stress test after IFN- γ , these data illustrate that cord blood MDM respond to both LPS and Mtb by increasing glycolysis even after the pre-treatment with IFN- γ or IL-4. Interestingly, the addition of IFN- γ enhanced TNF production and HLA-DR expression in umbilical cord blood, thereby overcoming the 'defects' seen in cord blood MDM immune responses. It is well recognised that IFN- γ concentration is reduced in cord blood and it has been postulated as a cause of reduced TNF production^{126,132,281}. However, the underlying defect in production of TNF in this research is apparent in the absence of IFN- γ , indicating an inherent defect in TNF production in umbilical cord MDM which occurs specifically in the context of stimulation with Mtb, and not LPS. The changes in OXPHOS seen in adult MDM, with a decrease seen early in response to stimulation, resulting in an inflammatory Warburg effect followed by a return to baseline and then an increase in OXPHOS at 24 hours after LPS stimulation or IFN- γ treatment, is not replicated in cord blood MDM. This may reflect an inherent inability of umbilical cord blood MDM to alter OXPHOS. Whether these metabolic differences are linked to the functional defects seen in umbilical cord MDM will require further mechanistic research.

A distinct immunometabolic phenotype has been described herein for cord blood MDM despite the fact that both adult and cord MDM are allowed to differentiate using the same methodology in the presence of adult human serum for one week. This system negates the impact of any potential immunological mediators present in cord blood such as adenosine¹³⁷. These findings need to be taken in the context of the ontogeny of immunity in early life. Neonates are more prone to intra and extra cellular infections due to impaired Th1 and Th17 responses respectively³²⁴. The immunometabolism of neonates has been linked to their susceptibility to sepsis³²⁵, although detailed work on metabolic differences in individual cell types in neonates is lacking. Most of the vulnerability to infection has resolved after the first 5 years of life^{326,327}. Whether this immune maturation, resulting in better immune defence from infancy into childhood, is associated with alterations in the immunometabolic phenotype as the infant ages is a key knowledge gap that will be of great interest to both the scientific and clinical community. The nuances of the effects of differential metabolic responses on functional outcomes requires further work in different age groups to appropriately answer these questions. This work may also inform research into immunosenescence, where metabolic defects are linked to immune vulnerabilities in the elderly³²⁸. In order to fully appreciate the importance of metabolic shifts throughout the human life span, mapping of the immunometabolic responses from birth to old age is required.

The data in chapters 3 and 4 illustrate the glycolytic shift in human macrophage activation and the subsequent increase in lactate production. The importance of lactate as a carbohydrate shuttle and immune modulator is increasingly being realised^{329,330}.

The data presented herein corroborate previously published literature in monocytes demonstrating that lactate has an immunosuppressive effect^{214,286}. As with all *in vitro* work, the environment in which the experiment is undertaken does not replicate the *in vivo* milieu. The acidification of the extracellular environment by increased lactic acid production is not addressed in this work. However, the fact that sodium lactate at physiological pH induces these changes makes it a more viable therapeutic candidate. The prospect of using inhalable, aerosolised sodium lactate in the scenario of active pulmonary TB disease, where there is both ongoing mycobacterial replication and destruction of pulmonary tissue due to an unchecked pro-inflammatory response is of great appeal. Lactate may also play a role in early disease clearance where the improvement in mycobacterial clearance would be of benefit, however, the abrogation of IL-1 β and TNF may not be of benefit to the host at this stage of the disease. Mtb blocks autophagic flux as a method of subverting host defence^{331,332} and preliminary work has been shown to indicate that induction of autophagy may be the mechanism by which lactate promotes Mtb killing in MDM. Autophagy also plays a role in a wide range of other disease states such as Crohn's disease, cancer and heart disease³³³, indicating that lactate may hold therapeutic potential in many disease settings.

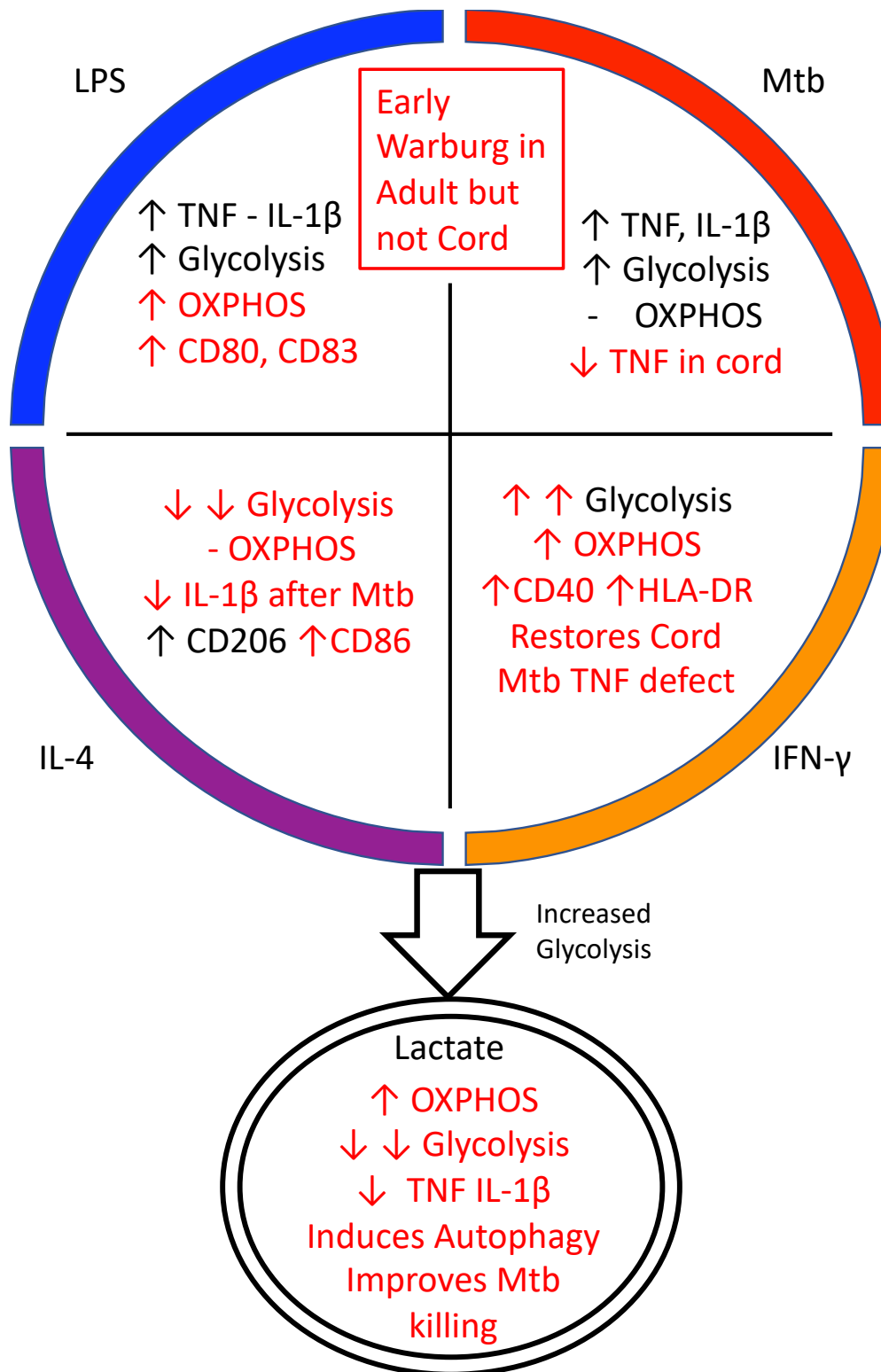


Figure 6.1 Macrophage activation states in human MDM.

This schematic represents the different macrophage activation states in human MDM 24 hours after stimulation with LPS (100 ng/ml) or Mtb (iH37Rv; MOI 1-10) or treatment with IFN- γ (10ng/ml), IL-4 (10ng/ml) or Lactate (25mM) as determined by cytokine analysis with MSD, flow cytometry for cell surface markers, SeahorseXFe24 Analyzer for metabolic flux analysis, Western blotting for protein analysis and CFU for mycobacterial killing. Novel discoveries described in this thesis are highlighted in red.

6.2 Study limitations and newly identified research gaps

Although human macrophages undergo early Warburg metabolism, the importance of this mechanism in a human system is yet to be fully understood. Inhibition of glycolysis is known to inhibit IL-1 β production, but the downstream effect of the decreased oxidative phosphorylation on macrophage activation remains elusive. This work has shown that both increased glycolysis and concomitantly decreased OXPHOS occurs early in adult macrophages stimulated with Mtb whereas cord blood macrophages have stable rates of OXPHOS. This has uncovered a key knowledge gap and raises the research questions of how changes to OXPHOS may contribute to control of bacterial growth or macrophage effector function. Future research targeting OXPHOS in infant macrophages to replicate the adult metabolic response may reveal the purpose of this metabolic shift, particularly if this intervention also aligns the infant immune response to the adult phenotype and would then hold potential as a host directed therapy.

Numerous mechanisms for metabolic activation following immune stimuli have been described including the stabilisation of HIF-1 α by succinate, upregulation of glycolytic enzymes and alteration of mitochondrial potential^{216,237,249}. The immediate metabolic response to Mtb or LPS stimulation suggests other mechanisms that may be triggered by PRRs. Glucose transport through monocarboxylate transporters have the potential to be rapidly switched on and may upregulate glycolysis. Alternatively, enzymatic control of glycolysis may be rapidly manipulated causing an influx of glucose. The dynamic processes of early metabolic shifts in human cells and their importance on subsequent immune responses will require further research.

The data generated in this research on the impact of lactate on MDM metabolism and potentially on autophagy open many avenues of research. A cell surface receptor for lactate called GPR81 has been found to have multiple roles including in angiogenesis and lipolysis, but the data are primarily generated in mice^{334,335}. The effect of GPR81 activation on autophagy has yet to be explored. GPR81 antagonists are being developed which will assist in answering this question³³⁶. The addition of exogenous lactate used in this experimental model causes a rapid reduction in ECAR and an increase in OCR. Lactate may act in a negative feedback loop on LDH, preventing the transition of pyruvate to lactate. LDH inhibitors have been shown to increase Mtb killing in human macrophages³³⁷. Exogenous lactate may alter glucose uptake, subsequently leading to less activity of glycolysis and reduction in ECAR. Glycolysis and pyruvate production may continue unchanged however, with lactate signaling causing a shift in glucose utilisation to OXPHOS. Carbon labelling experiments will be key in determining the impact of exogeneous lactate on glucose fate.

These data focus solely on MDM, therefore the effects observed need to be recapitulated in cellular systems encompassing multiple cells types or *in vivo* in humans. Since cytokines in the microenvironment, produced by T cells for example, can impact the polarisation status of macrophages, further work is required to establish a more robust picture of the metabolic function of human macrophages in different contexts, including on other metabolic pathways, such as fatty acid oxidation and the pentose phosphate pathway.

In order to fully explore the impact of immunometabolism in the context of Mtb, infection with live, replicating mycobacteria will be required. This model focuses on the host response to infection, which live Mtb has been shown to subvert. For this reason, irradiated H37Rv was used to assess the metabolic response of the host independent of bacterial evasion strategies. However, since different strains of live Mtb have been shown to differentially manipulate immunometabolic responses⁴¹, future translational research will need to take this into account. It is also recognised that while neonatal immune responses to Mtb may be insufficient and therefore result in disseminated disease with increased severity and mortality, strategies to boost immune responses may be detrimental in certain context of active TB disease where pathology may be immune mediated.

Neonatal and paediatric research is limited by small blood donation volumes, so using umbilical cord blood overcomes this issue. However, a knowledge gap exists around how closely cord blood recapitulates neonatal immune responses in early life. Furthermore, the mode of delivery can impact the immune responsiveness of cord blood³³⁸. By using umbilical cord blood from planned Caesarean sections only and by differentiating the monocytes *in vitro* with the same adult human serum used to differentiate adult MDM for 7 days, some of the confounding unknowns in this model are overcome and this increases the comparability of MDM from adult and cord blood.

6.3 Conclusions

The goal of improving the understanding of the human immunometabolic response to Mtb infection is to identify potential targets for host directed therapy. The majority of people exposed to Mtb do not get active disease. By identifying and targeting the immunometabolic vulnerabilities of those who succumb to the mycobacteria, improvements could be made to disease outcomes or in preventing active disease following exposure. The data presented in this study increases our fundamental understanding of human MDM immunometabolism, both in adults and neonates, highlighting the differences between the established murine model of macrophage metabolism and builds a platform for future research in TB and other disease states. This new paradigm of human MDM immunometabolic phenotype after LPS or Mtb stimulation or treatment with IFN- γ or IL-4 is summarised in Figure 6.1. Lactate has been identified as a potential host-directed therapy as it both decreases the potentially damaging pro-inflammatory cytokine response and it improves the ability of human MDM to kill Mtb. The first steps in identifying autophagy as the potential mechanism for this exciting treatment opportunity have been taken.

Appendix



3rd October, 2017.

Ospidéal an Rotunda
Cearnóg Parnell, Baile Átha Cliath 1, Éire.
The Rotunda Hospital
Parnell Square, Dublin 1, Ireland.
T: +353 1 817 1700 / F: +353 1 872 6523
www.rotunda.ie

Dr. Cilian O'Maoldomhnaigh
Tuberculosis Immunology Research Group
Office 0.50
Department of Clinical Medicine
Trinity Translational Medicine Institute, St. James's Hospital
Trinity College Dublin,
Dublin 8.

Our ref: REC-2017-024 (*please quote this reference on all correspondence*)
Re: Paediatric macrophage immuno-metabolism during
mycobacterial infection

Dear Cilian,

Many thanks for the amended documentation received in relation to the above research. One minor alteration is requested: the title used on the PIL differs from that on the consent form. Please use the version on the PIL for both. With the exception above, I am pleased to advise that the requirements set out by the Committee in respect of your study have now been met. This being the case, ethical approval for the research is granted and it may now commence.

You are requested to submit a progress report to the Committee in twelve months, and annually thereafter as applicable. We would also like to know when and where you publish or present your results. Please be aware of your responsibilities with respect to the Hospital's good research practice policies and guidelines.

Yours sincerely,

Professor Michael Geary,
Chairman,
Research Ethics Committee.

cc Professor Naomi McCallion, Consultant Neonatologist, Rotunda Hospital, Dublin 1.





Trinity College Dublin

Coláiste na Tríonóide, Baile Átha Cliath

The University of Dublin

Trinity Translational Medicine Institute

Institiúid Míochaine Aistritheach Choláiste na Tríonóide

Patient Information Leaflet

Study Title:

**Looking at newborn babies immune systems and how infection affects it
(Paediatric macrophage immunometabolism during mycobacterial infection)**

You are being invited to take part in a research study. This information sheet will help you understand why we are undertaking the research and what we would like you to do. Please ask us if there is anything that is not clear to you or if you would like more information. Thank you for reading this.

Purpose of the Research Study

The purpose of this study is to examine how a baby's immune system works. We know that small babies are more prone to certain types of infection. We can look at a baby's immune system by doing experiments on the umbilical cord blood that is left behind after the baby is born. We hope to identify ways of improving newborn's response to infection or to vaccination.

Why as a Participant/Respondent have I been asked to take part in this study?

You have been asked to take part because you are about to have a baby and we need to use samples taken immediately after birth.

What does the research involve for me and my child?

We will take a blood sample from the placental umbilical cord after the baby is born, the placenta is delivered and the umbilical cord is cut. Sometimes a blood sample from the placenta is required for routine care; if so we will only take research samples after this has been completed. Neither you nor the baby will undergo any procedures as part of this study. We will also collect some anonymised data about you and the baby.

Do I have to take part?

Institiúid Míochaine Aistritheach Choláiste na Tríonóide,
Ionad Choláiste na Tríonóide do na hEolaíochtaí Sláinte,
Coláiste na Tríonóide, Baile Átha Cliath, Ollscoil Átha Cliath,
Ospidéal San Séamas
Baile Átha Cliath 8, Éire.

Trinity Translational Medicine Institute,
Trinity Centre for Health Sciences,
Trinity College Dublin, the University of Dublin,
St. James's Hospital,
Dublin 8,
Ireland.

T: +353 1 896 3268
E: ttmi@tcd.ie

W: www.tcd.ie/ttmi



Trinity College Dublin

Coláiste na Tríonóide, Baile Átha Cliath
The University of Dublin

Trinity Translational Medicine Institute

Institiúid Míochaine Aistritheach Choláiste na Tríonóide

No. It is entirely up to you to decide whether or not to take part. If you do decide to take part, you will be given this information sheet to keep and we will ask you to sign a consent form. If you do decide to take part you are still free to withdraw at any time and without giving a reason. A decision not to take part or to withdraw at any time will in no way affect the standard of clinical care you receive.

Will my taking part in this study be kept confidential?

Yes. All information collected about you or your child during the research will be anonymised and strictly confidential. The samples will be analysed in the Trinity Translational Medicine Institute on St James campus.

What will happen to the results of the study?

We plan to publish our results in an international scientific journal and in international meetings.

Who is organising and funding the research?

The research is being organised as part of a PhD study by Dr Cilian Ó Maoldomhnaigh who is a paediatrician. The research is being funded by the National Children's Research Centre.

Is there any payment for taking part?

No, we are not paying patients to take part in the study.

Who has reviewed this study?

The Rotunda Hospital Ethics and Research committee has reviewed and approved this study.

Who should I contact about enquiries or complaints?

Please contact Dr Cilian Ó Maoldomhnaigh omaoldoc@tcd.ie if you have any questions or concerns regarding the study.

Institiúid Míochaine Aistritheach Choláiste na Tríonóide,
Ionad Choláiste na Tríonóide do na hEolaíochtaí Sláinte,
Coláiste na Tríonóide, Baile Átha Cliath, Ollscoil Átha Cliath,
Ospidéal San Séamas
Baile Átha Cliath 8, Éire.

Trinity Translational Medicine Institute,
Trinity Centre for Health Sciences,
Trinity College Dublin, the University of Dublin,
St. James's Hospital,
Dublin 8,
Ireland.

T: +353 1 896 3268
E: ttmi@tcd.ie
W: www.tcd.ie/ttmi



Trinity College Dublin

Coláiste na Tríonóide, Baile Átha Cliath

The University of Dublin

Trinity Translational Medicine Institute

Institiúid Míochaine Aistritheach Choláiste na Tríonóide

CONSENT FORM

Looking at newborn babies immune systems and how tuberculosis infection affects it - (Paediatric macrophage immunometabolism during mycobacterial infection)

Researcher: Dr. Cillian Ó Maoldomhnaigh Tel: 0868398601 Email: omaoldoc@tcd.ie

DECLARATION by participant: Please tick (✓) and provide your initials

1. I have read the information leaflet for this research study and I understand the contents. Yes [] No [] initials []
2. I have had the opportunity to ask questions and all my questions have been answered to my satisfaction. Yes [] No [] initials []
3. I fully understand that my/my babies' participation is completely voluntary and that I am free to withdraw from the study at any time (prior to anonymisation/publication) without giving a reason and that this will not affect my care/my babies care in any way. Yes [] No [] initials []
4. I agree to an umbilical cord blood sample being taken and used for research as part of this study Yes [] No [] initials []
5. I understand that the researchers undertaking this research will hold in confidence and securely all collected data and other relevant information. Yes [] No [] initials []
6. I freely and voluntarily consent to participating/allowing my baby participate in this research study. Yes [] No [] initials []

Institiúid Míochaine Aistritheach Choláiste na Tríonóide,
Ionad Choláiste na Tríonóide do na hEolaíochtaí Sláinte,
Coláiste na Tríonóide, Baile Átha Cliath, Ollscoil Átha Cliath,
Ospidéal San Séamas
Baile Átha Cliath 8, Éire.

Trinity Translational Medicine Institute,
Trinity Centre for Health Sciences,
Trinity College Dublin, the University of Dublin,
St. James's Hospital,
Dublin 8,
Ireland.

T: +353 1 896 3268
E: ttmi@tcd.ie

W: www.tcd.ie/ttmi



Trinity College Dublin
 Coláiste na Tríonóide, Baile Átha Cliath
 The University of Dublin

Trinity Translational Medicine Institute
 Institiúid Míochaine Aistritheach Choláiste na Tríonóide

PARTICIPANT'S NAME

Contact Address

.....

Phone number: **Email:**

Participant's signature: **Date:**

Name of person taking consent: **Signature:** **Date:**

Researcher: **Signature:** **Date:**

Institiúid Míochaine Aistritheach Choláiste na Tríonóide,
 Ionad Choláiste na Tríonóide do na hEolaíochtaí Sláinte,
 Coláiste na Tríonóide, Baile Átha Cliath, Ollscoil Átha Cliath,
 Ospidéal San Séamas
 Baile Átha Cliath 8, Éire.

Trinity Translational Medicine Institute,
 Trinity Centre for Health Sciences,
 Trinity College Dublin, the University of Dublin,
 St. James's Hospital,
 Dublin 8,
 Ireland.

T: +353 1 896 3268
 E: ttmi@tcd.ie
 W: www.tcd.ie/ttmi

References

1. Barberis I, Bragazzi NL, Galluzzo L, Martini M. The history of tuberculosis: From the first historical records to the isolation of Koch's bacillus. *J Prev Med Hyg.* 2017;58(1):E9-E12. doi:10.15167/2421-4248/jpmh2017.58.1.728
2. World Health Organization. *Global Tuberculosis Report 2020.* Geneva: World Health Organization; 2020.; 2020.
3. Visca D, Ong CWM, Tiberi S, et al. Tuberculosis and COVID-19 interaction: A review of biological, clinical and public health effects. *Pulmonology.* 2021;27(2):151-165. doi:10.1016/j.pulmoe.2020.12.012
4. Aznar ML, Espinosa-Pereiro J, Saborit N, et al. Impact of the COVID-19 pandemic on tuberculosis management in Spain. *Int J Infect Dis.* 2021;(January). doi:10.1016/j.ijid.2021.04.075
5. Hani C, Academic B, Mother RM, et al. Trends in paediatric tuberculosis diagnoses in two South African hospitals early in the COVID-19 pandemic. *South African Med J.* 2020;110(12):1149-1150.
6. Zumla A, Chakaya J, Khan M, et al. World Tuberculosis Day 2021 Theme — 'The Clock is Ticking' — and the world is running out of time to deliver the United Nations General Assembly commitments to End TB due to the COVID-19 pandemic. *Int J Infect Dis.* 2021;(xxxx). doi:10.1016/j.ijid.2021.03.046
7. Chakaya J, Khan M, Ntoumi F, et al. Global Tuberculosis Report 2020 — Reflections on the Global TB burden, treatment and prevention efforts. *Int J Infect Dis.* 2021;(xxxx):4-9. doi:10.1016/j.ijid.2021.02.107
8. Marshall G. Early Diagnosis of Pulmonary Tuberculosis. *BMJ.* 1937;2(4013):1103-1104. doi:10.1136/bmj.2.4013.1103
9. Ravimohan S, Kornfeld H, Weissman D, Bisson GP. Tuberculosis and lung damage: from epidemiology to pathophysiology. *Eur Respir Rev.* 2018;27(147):170077. doi:10.1183/16000617.0077-2017
10. Elkington PT, D'Armiento JM, Friedland JS. Tuberculosis Immunopathology: The Neglected Role of Extracellular Matrix Destruction. *Sci Transl Med.* 2011;3(71):71ps6-71ps6. doi:10.1126/scitranslmed.3001847
11. Ong CWMM, Elkington PT, Friedland JS. Tuberculosis, pulmonary cavitation, and matrix metalloproteinases. *Am J Respir Crit Care Med.* 2014;190(1):9-18. doi:10.1164/rccm.201311-2106PP
12. de Oliveira MCB, Sant'Anna CC, Raggio RL, Kritski AL. Tuberculosis among children and adolescents in Rio de Janeiro, Brazil — Focus on extrapulmonary disease. *Int J Infect Dis.* 2021;105:105-112. doi:10.1016/j.ijid.2021.02.023
13. Heron GA. Koch's Researches on Tuberculosis. *Glasgow Med J.* 1883;19(2):94-104.
14. Churchyard G, Kim P, Shah NS, et al. What We Know about Tuberculosis Transmission: An Overview. *J Infect Dis.* 2017;216(Suppl 6):S629-S635. doi:10.1093/infdis/jix362
15. Chai Q, Lu Z, Liu CH. Host defense mechanisms against Mycobacterium tuberculosis. *Cell Mol Life Sci.* 2020;77(10):1859-1878. doi:10.1007/s00018-019-03353-5
16. Furin J, Cox H, Pai M. Tuberculosis. *Lancet.* 2019;393(10181):1642-1656. doi:10.1016/S0140-6736(19)30308-3

17. Russell DG, Cardona P-JJ, Kim M-JJ, Allain S, Altare F. Foamy macrophages and the progression of the human tuberculosis granuloma. *Nat Immunol.* 2009;10(9):943-948. doi:10.1038/ni.1781
18. Flynn JL, Chan J, Lin PL. Macrophages and control of granulomatous inflammation in tuberculosis. *Mucosal Immunol.* 2011;4(3):271-278. doi:10.1038/mi.2011.14
19. Fox GJ, Orlova M, Schurr E. Tuberculosis in Newborns: The Lessons of the “Lübeck Disaster” (1929–1933). *PLoS Pathog.* 2016;12(1):1-10. doi:10.1371/journal.ppat.1005271
20. Houben RMGJ, Dodd PJ. The Global Burden of Latent Tuberculosis Infection: A Re-estimation Using Mathematical Modelling. *PLoS Med.* 2016;13(10):1-13. doi:10.1371/journal.pmed.1002152
21. Fox GJ, Nguyen TA, Coleman M, Trajman A, Velen K, Marais BJ. Implementing tuberculosis preventive treatment in high-prevalence settings. *Int J Infect Dis.* 2021;(xxxx):92-94. doi:10.1016/j.ijid.2021.02.094
22. Khan N, Divangahi M. Mycobacterium tuberculosis and HIV Coinfection Brings Fire and Fury to Macrophages. *J Infect Dis.* Published online 2018. doi:10.1093/infdis/jix626
23. Narasimhan P, Wood J, Macintyre CR, Mathai D. Risk factors for tuberculosis. *Pulm Med.* 2013;(February). doi:10.1155/2013/828939
24. Jick SS, Lieberman ES, Rahman MU, Choi HK. Glucocorticoid Use , Other Associated Factors , and the Risk of Tuberculosis. 2006;55(1):19-26. doi:10.1002/art.21705
25. O’Leary SM, Coleman MM, Chew WM, et al. Cigarette smoking impairs human pulmonary immunity to mycobacterium tuberculosis. *Am J Respir Crit Care Med.* 2014;190(12):1430-1436. doi:10.1164/rccm.201407-1385OC
26. Gleeson LE, O’Leary SM, Ryan D, McLaughlin AM, Sheedy FJ, Keane J. Cigarette smoking impairs the bioenergetic immune response to mycobacterium tuberculosis infection. *Am J Respir Cell Mol Biol.* Published online 2018. doi:10.1165/rcmb.2018-0162OC
27. Reed GW, Choi H, Lee SY, et al. Impact of Diabetes and Smoking on Mortality in Tuberculosis. *PLoS One.* 2013;8(2). doi:10.1371/journal.pone.0058044
28. Martinez N, Kornfeld H. Diabetes and immunity to tuberculosis. *Eur J Immunol.* 2014;44(3):617-626. doi:10.1002/eji.201344301
29. Keane J, Gershon S, Wise RP, et al. Tuberculosis Associated with Infliximab, a Tumor Necrosis Factor α -Neutralizing Agent. *N Engl J Med.* 2001;345(15):1098-1104. doi:10.1056/nejmoa011110
30. Fujita K, Terashima T, Mio T. Anti-PD1 Antibody Treatment and the Development of Acute Pulmonary Tuberculosis. *J Thorac Oncol.* 2016;11(12):7-9. doi:10.1016/j.jtho.2016.07.006
31. Schaaf HS, Collins A, Bekker A, Davies PDO. Tuberculosis at extremes of age. *Respirology.* 2010;15(5):747-763. doi:10.1111/j.1440-1843.2010.01784.x
32. Stead WW. Epidemiologic basis of tuberculosis eradication. *Ann Intern Med.* 1970;73(1):135-136. doi:10.7326/0003-4819-73-1-135
33. Committee TCT. Various Combinations of Isoniazid with Streptomycin or with P.A.S. in the Treatment of Pulmonary Tuberculosis: Seventh Report to the Medical Research Council. *BMJ.* 1955;1(4911):435-445.

- doi:10.1136/bmj.1.4911.435
34. Crofton J. The MRC randomized trial of streptomycin and its legacy: a view from the clinical front line. *J R Soc Med*. 2006;99(10):531-534.
doi:10.1258/jrsm.99.10.531
 35. Nahid P, Dorman SE, Alipanah N, et al. Official American Thoracic Society/Centers for Disease Control and Prevention/Infectious Diseases Society of America Clinical Practice Guidelines: Treatment of Drug-Susceptible Tuberculosis. *Clin Infect Dis*. 2016;63(7):e147-e195. doi:10.1093/cid/ciw376
 36. Ahmed A, Rakshit S, Adiga V, et al. A century of BCG: Impact on tuberculosis control and beyond*. *Immunol Rev*. 2021;(March):98-121.
doi:10.1111/imr.12968
 37. Roy P, Vekemans J, Clark A, Sanderson C, Harris RC, White RG. Potential effect of age of BCG vaccination on global paediatric tuberculosis mortality: a modelling study. *Lancet Glob Heal*. 2019;7(12):e1655-e1663.
doi:10.1016/S2214-109X(19)30444-9
 38. Roy A, Eisenhut M, Harris RJ, et al. Effect of BCG vaccination against Mycobacterium tuberculosis infection in children: Systematic review and meta-analysis. *BMJ*. 2014;349(August):1-11. doi:10.1136/bmj.g4643
 39. Migliori GB, Tiberi S, Zumla A, et al. MDR/XDR-TB management of patients and contacts: Challenges facing the new decade. The 2020 clinical update by the Global Tuberculosis Network. *Int J Infect Dis*. 2020;92:S15-S25.
doi:10.1016/j.ijid.2020.01.042
 40. Pang Y, Lu J, Huo F, et al. Prevalence and treatment outcome of extensively drug-resistant tuberculosis plus additional drug resistance from the National Clinical Center for Tuberculosis in China: a five-year review. *J Infect*. Published online 2017. doi:10.1016/j.jinf.2017.08.005
 41. Howard NC, Marin ND, Ahmed M, et al. Mycobacterium tuberculosis carrying a rifampicin drug resistance mutation reprograms macrophage metabolism through cell wall lipid changes. *Nat Microbiol*. Published online 2018.
doi:10.1038/s41564-018-0245-0
 42. Marie A, Laughlin M, Donnell RAO, et al. Extensively Drug-Resistant Tuberculosis (XDR-TB) - A Potential Threat in Ireland. 2007;353(1):7-9.
 43. Kendall EA. Tuberculosis in children: under-counted and under-treated. *Lancet Glob Heal*. 2017;5(9):e845-e846. doi:10.1016/S2214-109X(17)30305-4
 44. Dodd PJ, Yuen CM, Sismanidis C, Seddon JA, Jenkins HE. The global burden of tuberculosis mortality in children: a mathematical modelling study. *Lancet Glob Heal*. 2017;5(9):e898-e906. doi:10.1016/S2214-109X(17)30289-9
 45. Piccini P, Chiappini E, Tortoli E, de Martino M, Galli L. Clinical peculiarities of tuberculosis. *BMC Infect Dis*. 2014;14(Suppl 1):S4. doi:10.1186/1471-2334-14-S1-S4
 46. Jenkins HE, Yuen CM, Rodriguez CA, et al. Mortality in children diagnosed with tuberculosis: a systematic review and meta-analysis. *Lancet Infect Dis*. 2017;17(3):285-295. doi:10.1016/S1473-3099(16)30474-1
 47. Jones C, Whittaker E, Bamford A, Kampmann B. Immunology and pathogenesis of childhood TB. *Paediatr Respir Rev*. 2011;12(1):3-8.
doi:10.1016/j.prrv.2010.09.006
 48. Ki HP, Shingadia D. Tuberculosis in children. *Paediatr Child Heal (United*

- Kingdom*). 2017;27(3):109-115. doi:10.1016/j.paed.2016.12.004
49. Basu Roy R, Whittaker E, Seddon JA, Kampmann B. Tuberculosis susceptibility and protection in children. *Lancet Infect Dis*. 2019;19(3):e96-e108. doi:10.1016/S1473-3099(18)30157-9
 50. Donald PR, Beyers N. The natural history of childhood intra-thoracic tuberculosis : a critical review of literature from the pre-chemotherapy era. *New York*. 2004;8(4):392-402.
 51. Vanden Driessche K, Persson A, Marais BJ, Fink PJ, Urdahl KB. Immune vulnerability of infants to tuberculosis. *Clin Dev Immunol*. 2013;2013. doi:10.1155/2013/781320
 52. Phelan JJ, Basdeo SA, Tazoll SC, McGivern S, Saborido JR, Keane J. Modulating iron for metabolic support of TB host defense. *Front Immunol*. 2018;9(OCT):1-18. doi:10.3389/fimmu.2018.02296
 53. Kolloli A, Subbian S. Host-Directed Therapeutic Strategies for Tuberculosis. *Front Med*. 2017;4(October). doi:10.3389/fmed.2017.00171
 54. Wallis RS, Hafner R. Advancing host-directed therapy for tuberculosis. *Nat Rev Immunol*. 2015;15(4):255-263. doi:10.1038/nri3813\rnri3813 [pii]
 55. Kleinnijenhuis J, Oosting M, Joosten LAB, Netea MG, Van Crevel R. Innate Immune Recognition of *Mycobacterium tuberculosis*. *Clin Dev Immunol*. 2011;2011:1-12. doi:10.1155/2011/405310
 56. Reuschl AK, Edwards MR, Parker R, et al. Innate activation of human primary epithelial cells broadens the host response to *Mycobacterium tuberculosis* in the airways. *PLoS Pathog*. 2017;13(9):1-26. doi:10.1371/journal.ppat.1006577
 57. Vu A, Calzadilla A, Gidfar S, Calderon-Candelario R, Mirsaeidi M. Toll-like receptors in mycobacterial infection. *Eur J Pharmacol*. 2017;808(October 2016):1-7. doi:10.1016/j.ejphar.2016.10.018
 58. Means TK, Wang S, Lien E, Yoshimura A, Golenbock DT, Fenton MJ. Human toll-like receptors mediate cellular activation by *Mycobacterium tuberculosis*. *J Immunol*. 1999;163(7):3920-3927. <http://www.ncbi.nlm.nih.gov/pubmed/10490993>
 59. Faridgozar M, Nikoueinejad H. New findings of Toll-like receptors involved in *Mycobacterium tuberculosis* infection. *Pathog Glob Health*. 2017;111(5):256-264. doi:10.1080/20477724.2017.1351080
 60. Bulut Y, Michelsen KS, Hayrapetian L, et al. *Mycobacterium tuberculosis* heat shock proteins use diverse toll-like receptor pathways to activate pro-inflammatory signals. *J Biol Chem*. 2005;280(22):20961-20967. doi:10.1074/jbc.M411379200
 61. Verrall AJ, G. Netea M, Alisjahbana B, Hill PC, van Crevel R. Early clearance of *Mycobacterium tuberculosis*: A new frontier in prevention. *Immunology*. 2014;141(4):506-513. doi:10.1111/imm.12223
 62. Schurz H, Daya M, Möller M, Hoal EG, Salie M. TLR1, 2, 4, 6 and 9 variants associated with tuberculosis susceptibility: A systematic review and meta-analysis. *PLoS One*. 2015;10(10). doi:10.1371/journal.pone.0139711
 63. Lai YF, Lin TM, Wang CH, et al. Functional polymorphisms of the TLR7 and TLR8 genes contribute to *Mycobacterium tuberculosis* infection. *Tuberculosis*. 2016;98:125-131. doi:10.1016/j.tube.2016.03.008
 64. Ní Cheallaigh C, Sheedy FJ, Harris J, et al. A Common Variant in the Adaptor Mal

- Regulates Interferon Gamma Signaling. *Immunity*. 2016;44(2):368-379. doi:10.1016/j.immuni.2016.01.019
65. Goletti D, Petruccioli E, Romagnoli A, Piacentini M, Fimia GM. Autophagy in Mycobacterium tuberculosis infection: A passepartout to flush the intruder out? *Cytokine Growth Factor Rev*. 2013;24(4):335-343. doi:10.1016/j.cytogfr.2013.01.002
 66. Goyal S, Klassert TE, Slevogt H. C-type lectin receptors in tuberculosis: what we know. *Med Microbiol Immunol*. 2016;205(6):513-535. doi:10.1007/s00430-016-0470-1
 67. Juárez E, Carranza C, Hernández-Sánchez F, et al. NOD2 enhances the innate response of alveolar macrophages to Mycobacterium tuberculosis in humans. *Eur J Immunol*. 2012;42(4):880-889. doi:10.1002/eji.201142105
 68. Ferwerda G, Girardin SE, Kullberg BJ, et al. NOD2 and toll-like receptors are nonredundant recognition systems of Mycobacterium tuberculosis. *PLoS Pathog*. 2005;1(3):0279-0285. doi:10.1371/journal.ppat.0010034
 69. Kleinnijenhuis J, Joosten LAB, van de Veerdonk FL, et al. Transcriptional and inflammasome-mediated pathways for the induction of IL-1 β production by Mycobacterium tuberculosis. *Eur J Immunol*. 2009;39(7):1914-1922. doi:10.1002/eji.200839115
 70. Tsao TCY, Hong J, Huang C, Yang P, Liao SK, Chang KSS. Increased TNF- α , IL-1 β and IL-6 levels in the bronchoalveolar lavage fluid with the upregulation of their mRNA in macrophages lavaged from patients with active pulmonary tuberculosis. *Tuber Lung Dis*. 1999;79(5):279-285. doi:10.1054/tuld.1999.0215
 71. Berner R, Welter P, Brandis M. Cytokine expression of cord and adult blood mononuclear cells in response to Streptococcus agalactiae. *Pediatr Res*. 2002;51(3):304-309. doi:10.1203/00006450-200203000-00007
 72. Su WL, Perng WC, Huang CH, Yang CY, Wu CP, Chen JH. Association of reduced tumor necrosis factor alpha, gamma interferon, and interleukin-1 β (IL-1 β) but increased IL-10 expression with improved chest radiography in patients with pulmonary tuberculosis. *Clin Vaccine Immunol*. 2010;17(2):223-231. doi:10.1128/CVI.00381-09
 73. Bourigault M-L, Segueni N, Rose S, et al. Relative contribution of IL-1 α , IL-1 β and TNF to the host response to Mycobacterium tuberculosis and attenuated M. bovis BCG. *Immunity, Inflamm Dis*. 2013;1(1):47-62. doi:10.1002/iid3.9
 74. Joshi L, Ponnana M, Sivangala R, et al. Evaluation of TNF- α , il-10 and il-6 cytokine production and their correlation with genotype variants amongst tuberculosis patients and their household contacts. *PLoS One*. 2015;10(9):1-15. doi:10.1371/journal.pone.0137727
 75. Carswell EA, Old LJ, Kassel RL, Green S, Fiore N, Williamson B. An endotoxin induced serum factor that causes necrosis of tumors. *Proc Natl Acad Sci U S A*. 1975;72(9):3666-3670. doi:10.1073/pnas.72.9.3666
 76. Pennica D, Nedwin GE, Hayflick JS, et al. Human tumour necrosis factor: Precursor structure, expression and homology to lymphotoxin. *Nature*. 1984;312(5996):724-729. doi:10.1038/312724a0
 77. Mootoo A, Stylianou E, Arias MA, Reljic R. TNF- α in tuberculosis: A cytokine with a split personality. *Inflamm Allergy - Drug Targets*. 2009;8(1):53-62. doi:10.2174/187152809787582543

78. Cohen J, Vincent JL, Adhikari NKJ, et al. Sepsis: A roadmap for future research. *Lancet Infect Dis*. 2015;15(5):581-614. doi:10.1016/S1473-3099(15)70112-X
79. Roca FJ, Ramakrishnan L. TNF dually mediates resistance and susceptibility to mycobacteria via mitochondrial reactive oxygen species. *Cell*. 2013;153(3):521-534. doi:10.1016/j.cell.2013.03.022
80. Xu G, Wang J, Gao GF, Liu CH. Insights into battles between Mycobacterium tuberculosis and macrophages. *Protein Cell*. 2014;5(10):728-736. doi:10.1007/s13238-014-0077-5
81. Weiss G, Schaible UE. Macrophage defense mechanisms against intracellular bacteria. *Immunol Rev*. 2015;264(1):182-203. doi:10.1111/imr.12266
82. Fratazzi C, Arbeit RD, Carini C, et al. Macrophage apoptosis in mycobacterial infections. *J Leukoc Biol*. 1999;66(5):763-764. doi:10.1002/jlb.66.5.763
83. Robinson N, Ganesan R, Hegedűs C, Kovács K, Kufer TA, Virág L. Programmed necrotic cell death of macrophages: Focus on pyroptosis, necroptosis, and parthanatos. *Redox Biol*. 2019;26(June). doi:10.1016/j.redox.2019.101239
84. Keane J, Balcewicz-Sablinska MK, Remold HG, et al. Infection by Mycobacterium tuberculosis promotes human alveolar macrophage apoptosis. *Infect Immun*. 1997;65(1):298-304. doi:8975927
85. Algood HMS, Lin PL, Flynn JAL. Tumor necrosis factor and chemokine interactions in the formation and maintenance of granulomas in tuberculosis. *Clin Infect Dis*. 2005;41(3 SUPPL.):189-193. doi:10.1086/429994
86. Mayer-Barber KD, Barber DL, Shenderov K, et al. Cutting Edge: Caspase-1 Independent IL-1 β Production Is Critical for Host Resistance to Mycobacterium tuberculosis and Does Not Require TLR Signaling In Vivo . *J Immunol*. 2010;184(7):3326-3330. doi:10.4049/jimmunol.0904189
87. Sugawara I, Yamada H, Hua S, Mizuno S. Role of interleukin (IL)-1 type 1 receptor in mycobacterial infection. *Microbiol Immunol*. 2001;45(11):743-750. doi:10.1111/j.1348-0421.2001.tb01310.x
88. Yamada H, Mizuno S, Horai R, Iwakura Y, Sugawara I. Protective role of interleukin-1 in mycobacterial infection in IL-1 α/β double-knockout mice. *Lab Invest*. 2000;80(5):759-767. doi:10.1038/labinvest.3780079
89. Fremont CM, Togbe D, Doz E, et al. IL-1 Receptor-Mediated Signal Is an Essential Component of MyD88-Dependent Innate Response to Mycobacterium tuberculosis Infection . *J Immunol*. 2007;179(2):1178-1189. doi:10.4049/jimmunol.179.2.1178
90. Briken V, Ahlbrand SE, Shah S. Mycobacterium tuberculosis and the host cell inflammasome: a complex relationship. *Front Cell Infect Microbiol*. 2013;3(October):62. doi:10.3389/fcimb.2013.00062
91. Ma J, Zhao S, Gao X, et al. The roles of inflammasomes in host defense against mycobacterium tuberculosis. *Pathogens*. 2021;10(2):1-15. doi:10.3390/pathogens10020120
92. He Y, Hara H, Núñez G. Mechanism and Regulation of NLRP3 Inflammasome Activation. *Trends Biochem Sci*. 2016;41(12):1012-1021. doi:10.1016/j.tibs.2016.09.002
93. Netea MG, Nold-Petry CA, Nold MF, et al. Differential requirement for the activation of the inflammasome for processing and release of IL-1 β in monocytes and macrophages. *Blood*. 2009;113(10):2324-2335.

- doi:10.1182/blood-2008-03-146720
94. Dinarello CA. Biologic basis for interleukin-1 in disease. *Blood*. 1996;87(6):2095-2147. doi:10.1182/blood.v87.6.2095.bloodjournal8762095
 95. Marin ND, París SC, Vélez VM, Rojas CA, Rojas M, García LF. Regulatory T cell frequency and modulation of IFN-gamma and IL-17 in active and latent tuberculosis. *Tuberculosis*. 2010;90(4):252-261. doi:10.1016/j.tube.2010.05.003
 96. Hirano T, Yasukawa K, Harada H, et al. Complementary DNA for a novel human interleukin (BSF-2) that induces B lymphocytes to produce immunoglobulin. *Nature*. 1986;324(6092):73-76. doi:10.1038/324073a0
 97. Tanaka T, Narazaki M, Kishimoto T. IL-6 in inflammation, Immunity, And disease. *Cold Spring Harb Perspect Biol*. 2014;6(10):1-16. doi:10.1101/cshperspect.a016295
 98. Heinrich PC, Castell J V., Andus T. Interleukin-6 and the acute phase response. *Biochem J*. 1990;265(3):621-636. doi:10.1042/bj2650621
 99. Korn T, Bettelli E, Oukka M, Kuchroo VK. IL-17 and Th17 cells. *Annu Rev Immunol*. 2009;27:485-517. doi:10.1146/annurev.immunol.021908.132710
 100. Poli V, Balena R, Fattori E, et al. Interleukin-6 deficient mice are protected from bone loss caused by estrogen depletion. *EMBO J*. 1994;13(5):1189-1196. doi:10.1002/j.1460-2075.1994.tb06368.x
 101. Nakahara H, Song J, Sugimoto M, et al. Anti-interleukin-6 receptor antibody therapy reduces vascular endothelial growth factor production in rheumatoid arthritis. *Arthritis Rheum*. 2003;48(6):1521-1529. doi:10.1002/art.11143
 102. Ladel CH, Blum C, Dreher A, Reifenberg K, Kopf M, Kaufmann SHE. Lethal tuberculosis in interleukin-6-deficient mutant mice. *Infect Immun*. 1997;65(11):4843-4849. doi:10.1128/iai.65.11.4843-4849.1997
 103. Saunders BM, Frank AA, Orme IM, Cooper AM. Interleukin-6 induces early gamma interferon production in the infected lung but is not required for generation of specific immunity to Mycobacterium tuberculosis infection. *Infect Immun*. 2000;68(6):3322-3326. doi:10.1128/IAI.68.6.3322-3326.2000
 104. Dutta RK, Kathania M, Raje M, Majumdar S. IL-6 inhibits IFN- γ induced autophagy in Mycobacterium tuberculosis H37Rv infected macrophages. *Int J Biochem Cell Biol*. 2012;44(6):942-954. doi:10.1016/j.biocel.2012.02.021
 105. Barnes PF, Lu S, Abrams JS, Wang E, Yamamura M, Modlin RL. Cytokine production at the site of disease in human tuberculosis. *Infect Immun*. 1993;61(8):3482-3489. doi:10.1128/iai.61.8.3482-3489.1993
 106. Bonecini-Almeida MG, Ho JL, Boéchat N, et al. Down-Modulation of Lung Immune Responses by Interleukin-10 and Transforming Growth Factor β (TGF- β) and Analysis of TGF- β Receptors I and II in Active Tuberculosis. *Infect Immun*. 2004;72(5):2628-2634. doi:10.1128/IAI.72.5.2628-2634.2004
 107. Almeida AS, Lago PM, Boechat N, et al. Tuberculosis Is Associated with a Down-Modulatory Lung Immune Response That Impairs Th1-Type Immunity. *J Immunol*. 2009;183(1):718-731. doi:10.4049/jimmunol.0801212
 108. Mosmann VR, Cherwinski H, Bond MW, Giedlin MA, Coffman RL. Two types of murine helper T cell clone. I. Definition according to profiles of lymphokine activities and secreted proteins. *J Immunol*. 1986;136(7):2348-2357. doi:10.1103/PhysRevB.89.054105
 109. Ouyang W, Rutz S, Crellin NK, Valdez PA, Hymowitz SG. Regulation and

- functions of the IL-10 family of cytokines in inflammation and disease. *Annu Rev Immunol*. 2011;29:71-109. doi:10.1146/annurev-immunol-031210-101312
110. Mege JL, Meghari S, Honstetter A, Capo C, Raoult D. The two faces of interleukin 10 in human infectious diseases. *Lancet Infect Dis*. 2006;6(9):557-569. doi:10.1016/S1473-3099(06)70577-1
 111. O’Leary S, O’Sullivan MP, Keane J. IL-10 blocks phagosome maturation in Mycobacterium tuberculosis-infected human macrophages. *Am J Respir Cell Mol Biol*. 2011;45(1):172-180. doi:10.1165/rcmb.2010-0319OC
 112. McNab F, Mayer-Barber K, Sher A, Wack A, O’Garra A. Type I interferons in infectious disease. *Nat Rev Immunol*. 2015;15(2):87-103. doi:10.1038/nri3787
 113. O’Garra A, Redford PS, McNab FW, Bloom CI, Wilkinson RJ, Berry MPR. *The Immune Response in Tuberculosis*. Vol 31.; 2013. doi:10.1146/annurev-immunol-032712-095939
 114. Gold MC, Cerri S, Smyk-Pearson S, et al. Human mucosal associated invariant T cells detect bacterially infected cells. *PLoS Biol*. 2010;8(6):1-14. doi:10.1371/journal.pbio.1000407
 115. Cooper AM, Mayer-Barber KD, Sher A. Role of innate cytokines in mycobacterial infection. *Mucosal Immunol*. 2011;4(3):252-260. doi:10.1038/mi.2011.13
 116. Flynn JAL, Chan J, Triebold KJ, Dalton DK, Stewart TA, Bloom BR. An essential role for interferon γ in resistance to mycobacterium tuberculosis infection. *J Exp Med*. 1993;178(6):2249-2254. doi:10.1084/jem.178.6.2249
 117. Cooper AM, Dalton DK, Stewart TA, Griffin JP, Russell DG, Orme IM. Disseminated tuberculosis in interferon gamma gene-disrupted mice. *JExpMed*. 1993;178(December):2243-2247.
 118. Kerner G, Rosain J, Guérin A, et al. Inherited human IFN- γ deficiency underlies mycobacterial disease. *J Clin Invest*. 2020;130(6):3158-3171. doi:10.1172/JCI135460
 119. Rosain J, Kong X, Martinez-Barricarte R, et al. Mendelian susceptibility to mycobacterial disease: 2014–2018 update. *Immunol Cell Biol*. 2019;97(4):360-367. doi:10.1111/imcb.12210
 120. Mihret A. The role of dendritic cells in Mycobacterium tuberculosis infection. *Virulence*. 2012;3(7):654-659. doi:10.4161/viru.22586
 121. Caruso AM, Serbina N, Klein E, Triebold K, Bloom BR, Flynn JL. Mice deficient in CD4 T cells have only transiently diminished levels of IFN-gamma, yet succumb to tuberculosis. *J Immunol*. 1999;162(9):5407-5416. <http://www.ncbi.nlm.nih.gov/pubmed/10228018>
 122. Sia JK, Georgieva M, Rengarajan J. Innate Immune Defenses in Human Tuberculosis: An Overview of the Interactions between Mycobacterium tuberculosis and Innate Immune Cells. *J Immunol Res*. 2015;2015. doi:10.1155/2015/747543
 123. Winslow GM, Cooper A, Reiley W, Chatterjee M, Woodland DL. Early T-cell responses in tuberculosis immunity. *Immunol Rev*. 2008;225(1):284-299. doi:10.1111/j.1600-065X.2008.00693.x
 124. Hmama Z, Peña-Díaz S, Joseph S, Av-Gay Y. Immuno-evasion and immunosuppression of the macrophage by Mycobacterium tuberculosis. *Immunol Rev*. 2015;264(1):220-232. doi:10.1111/imr.12268
 125. Basu Roy R, Whittaker E, Kampmann B. Current understanding of the immune

- response to tuberculosis in children. *Curr Opin Infect Dis.* 2012;25(3):250-257. doi:10.1097/QCO.0b013e3283529af9
126. Corbett NP, Blimkie D, Ho KC, et al. Ontogeny of toll-like receptor mediated cytokine responses of human blood mononuclear cells. *PLoS One.* 2010;5(11). doi:10.1371/journal.pone.0015041
 127. Levy O, Zarembek KA, Roy RM, Cywes C, Godowski PJ, Wessels MR. Selective Impairment of TLR-Mediated Innate Immunity in Human Newborns: Neonatal Blood Plasma Reduces Monocyte TNF- Induction by Bacterial Lipopeptides, Lipopolysaccharide, and Imiquimod, but Preserves the Response to R-848. *J Immunol.* 2004;173(7):4627-4634. doi:10.4049/jimmunol.173.7.4627
 128. Angelone DF, Wessels MR, Coughlin M, et al. Innate immunity of the human newborn is polarized toward a high ratio of IL-6/TNF- α production in vitro and in vivo. *Pediatr Res.* 2006;60(2):205-209. doi:10.1203/01.pdr.0000228319.10481.ea
 129. Kollmann TR, Levy O, Montgomery RR, Goriely S. Innate Immune Function by Toll-like Receptors: Distinct Responses in Newborns and the Elderly. *Immunity.* 2012;37(5):771-783. doi:10.1016/j.immuni.2012.10.014
 130. Shey MS, Nemes E, Whatney W, et al. Maturation of Innate Responses to Mycobacteria over the First Nine Months of Life. *J Immunol.* 2014;192(10):4833-4843. doi:10.4049/jimmunol.1400062
 131. Taylor S, Bryson YJ. Impaired production of gamma-interferon by newborn cells in vitro is due to a functionally immature macrophage. *J Immunol.* 1985;134(3):1493-1497. <http://www.ncbi.nlm.nih.gov/pubmed/3918100>
 132. Maródi L. Deficient interferon- γ receptor-mediated signaling in neonatal macrophages. In: *Acta Paediatrica, International Journal of Paediatrics, Supplement.* ; 2002.
 133. Maródi L, Káposzta R, Campbell DE, Polin RA, Csongor J, Johnston RB. Candidacidal mechanisms in the human neonate. Impaired IFN-gamma activation of macrophages in newborn infants. *J Immunol.* 1994;153:5643-5649.
 134. Goenka A, Prise IE, Connolly E, et al. Infant Alveolar Macrophages Are Unable to Effectively Contain Mycobacterium tuberculosis. *Front Immunol.* 2020;11(March):1-12. doi:10.3389/fimmu.2020.00486
 135. Dowling DJ, Levy O. Ontogeny of early life immunity. *Trends Immunol.* Published online 2014. doi:10.1016/j.it.2014.04.007
 136. Zhang X, Zhivaki D, Lo-Man R. Unique aspects of the perinatal immune system. *Nat Rev Immunol.* Published online 2017. doi:10.1038/nri.2017.54
 137. Ofer Levy^{2,*},†, Melissa Coughlin*, Bruce N. Cronstein‡, Rene M. Roy*, Avani Desai‡ and MRW. The Adenosine System Selectively Inhibits TLR-Mediated TNF- α Production in the Human Newborn. *J Immunol.* 2006;95(4):1295-1301.e1. <http://linkinghub.elsevier.com/retrieve/pii/S0015028210025471>
 138. Crane DC, Shui G, Bendt AK, et al. The synthesis of mycolic acids. *J Biol Chem.* 2005;280(3):1-88.
 139. Elahi S, Ertelt JM, Kinder JM, et al. Immunosuppressive CD71+ erythroid cells compromise neonatal host defence against infection. *Nature.* 2013;504(7478):158-162. doi:10.1038/nature12675
 140. Namdar A, Koleva P, Shahbaz S, Strom S, Gerdtts V, Elahi S. CD71+ erythroid suppressor cells impair adaptive immunity against Bordetella pertussis. *Sci Rep.*

- 2017;7(1):7728. doi:10.1038/s41598-017-07938-7
141. Kaufmann SHE. Immunology's foundation: The 100-year anniversary of the Nobel Prize to Paul Ehrlich and Elie Metchnikoff. *Nat Immunol*. 2008;9(7):705-712. doi:10.1038/ni0708-705
 142. Gordon S. Elie Metchnikoff: Father of natural immunity. *Eur J Immunol*. 2008;38(12):3257-3264. doi:10.1002/eji.200838855
 143. van Furth R. Origin and Kinetics of Mononuclear Phagocytes. *Ann N Y Acad Sci*. 1976;278(1):161-175. doi:10.1111/j.1749-6632.1976.tb47027.x
 144. Sreejit G, Fleetwood AJ, Murphy AJ, Nagareddy PR. Origins and diversity of macrophages in health and disease. *Clin Transl Immunol*. 2020;9(12):1-19. doi:10.1002/cti2.1222
 145. Hoeffel G, Ginhoux F. Ontogeny of tissue-resident macrophages. *Front Immunol*. 2015;6(SEP). doi:10.3389/fimmu.2015.00486
 146. Srivastava S, Ernst JD, Desvignes L. Beyond macrophages: the diversity of mononuclear cells in tuberculosis. *Immunol Rev*. 2014;262(1):179-192. doi:10.1111/imr.12217
 147. Huang L, Nazarova E V., Tan S, Liu Y, Russell DG. Growth of Mycobacterium tuberculosis in vivo segregates with host macrophage metabolism and ontogeny. *J Exp Med*. 2018;215(4):1135-1152. doi:10.1084/jem.20172020
 148. Cassetta L, Cassol E, Poli G. Macrophage polarization in health and disease. *ScientificWorldJournal*. 2011;11:2391-2402. doi:10.1100/2011/213962
 149. Mackaness GB. Cellular Resistance to Infection. *J Exp Med*. 1962;116(3):381-406. doi:10.1084/jem.116.3.381
 150. Nathan CF, Murray HW, Wlebe IE, Rubin BY. Identification of interferon- γ , as the lymphokine that activates human macrophage oxidative metabolism and antimicrobial activity. *J Exp Med*. 1983;158(3):670-689. doi:10.1084/jem.158.3.670
 151. Stein M, Keshav S, Harris N, Gordon S. Interleukin 4 Potently Enhances Murine Macrophage Mannose Receptor Activity: A Marker of Alternative Immunologic Macrophage Activation By Michael Stein, Satish Keshav, Neil Harris,* and Siamon Gordon. *J Exp Med*. 1992;176(July):287-292.
 152. Mills CD, Kincaid K, Alt JM, Heilman MJ, Hill AM. M-1/M-2 Macrophages and the Th1/Th2 Paradigm. *J Immunol*. 2000;164(12):6166-6173. doi:10.4049/jimmunol.164.12.6166
 153. Murray PJ, Allen JE, Biswas SK, et al. Macrophage Activation and Polarization: Nomenclature and Experimental Guidelines. *Immunity*. 2014;41(1):14-20. doi:10.1016/j.immuni.2014.06.008
 154. Becker M, De Bastiani MA, Parisi MM, et al. Integrated Transcriptomics Establish Macrophage Polarization Signatures and have Potential Applications for Clinical Health and Disease. *Sci Rep*. 2015;5(August):1-12. doi:10.1038/srep13351
 155. Tarique AA, Logan J, Thomas E, Holt PG, Sly PD, Fantino E. Phenotypic, functional, and plasticity features of classical and alternatively activated human macrophages. *Am J Respir Cell Mol Biol*. 2015;53(5):676-688. doi:10.1165/rcmb.2015-0012OC
 156. Huang Z, Luo Q, Guo Y, et al. Mycobacterium tuberculosis-induced polarization of human macrophage orchestrates the formation and development of

- tuberculous granulomas in vitro. *PLoS One*. 2015;10(6).
doi:10.1371/journal.pone.0129744
157. Martinez FO, Gordon S. The M1 and M2 paradigm of macrophage activation: time for reassessment. *F1000Prime Rep*. 2014;6(March):13. doi:10.12703/P6-13
 158. Martinez FO, Gordon S, Locati M, Mantovani A. Transcriptional Profiling of the Human Monocyte-to-Macrophage Differentiation and Polarization: New Molecules and Patterns of Gene Expression. *J Immunol*. 2006;177(10):7303-7311. doi:10.4049/jimmunol.177.10.7303
 159. Mestas J, Hughes CCW. Of Mice and Not Men: Differences between Mouse and Human Immunology. *J Immunol*. 2004;172(5):2731-2738. doi:10.4049/jimmunol.172.5.2731
 160. Murray PJ, Wynn TA. Obstacles and opportunities for understanding macrophage polarization. *J Leukoc Biol*. 2011;89(4):557-563. doi:10.1189/jlb.0710409
 161. Nielsen MC, Andersen MN, Møller HJ. Monocyte isolation techniques significantly impact the phenotype of both isolated monocytes and derived macrophages in vitro. *Immunology*. 2020;159(1):63-74. doi:10.1111/imm.13125
 162. Vogel DYS, Glim JE, Stavenuiter AWD, et al. Human macrophage polarization in vitro: Maturation and activation methods compared. *Immunobiology*. 2014;219(9):695-703. doi:10.1016/j.imbio.2014.05.002
 163. Trus E, Basta S, Gee K. Who's in charge here? Macrophage colony stimulating factor and granulocyte macrophage colony stimulating factor: Competing factors in macrophage polarization. *Cytokine*. 2020;127(June 2019):154939. doi:10.1016/j.cyto.2019.154939
 164. Ambarus CA, Krausz S, van Eijk M, et al. Systematic validation of specific phenotypic markers for in vitro polarized human macrophages. *J Immunol Methods*. 2012;375(1-2):196-206. doi:10.1016/j.jim.2011.10.013
 165. Sudan B, Wacker MA, Wilson ME, Graff JW. A systematic approach to identify markers of distinctly activated human macrophages. *Front Immunol*. 2015;6(MAY):1-18. doi:10.3389/fimmu.2015.00253
 166. Micklem K, Rigney E, Cordell J, et al. A human macrophage-associated antigen (CD68) detected by six different monoclonal antibodies. *Br J Haematol*. 1989;73(1):6-11. doi:10.1111/j.1365-2141.1989.tb00210.x
 167. Wu Z, Zhang Z, Lei Z, Lei P. CD14: Biology and role in the pathogenesis of disease. *Cytokine Growth Factor Rev*. 2019;48(June):24-31. doi:10.1016/j.cytogfr.2019.06.003
 168. Suttles J, Stout RD. Macrophage CD40 signaling: A pivotal regulator of disease protection and pathogenesis. *Semin Immunol*. 2009;21(5):257-264. doi:10.1016/j.smim.2009.05.011
 169. Khan N, Pahari S, Vidarthi A, Aqdas M, Agrewala JN. Stimulation through CD40 and TLR-4 Is an effective host directed therapy against Mycobacterium tuberculosis. *Front Immunol*. 2016;7(SEP):1-16. doi:10.3389/fimmu.2016.00386
 170. Drohan L, Harding JJ, Holm B, et al. Selective developmental defects of cord blood antigen-presenting cell subsets. *Hum Immunol*. 2004;65(11):1356-1369. doi:10.1016/j.humimm.2004.09.011
 171. Petro TM, Chen SSA, Panther RB. Effect of CD80 and CD86 on t cell cytokine production. *Immunol Invest*. 1995;24(6):965-976.

- doi:10.3109/08820139509060721
172. Nolan A, Kobayashi H, Naveed B, et al. Differential role for CD80 and CD86 in the regulation of the innate immune response in murine polymicrobial sepsis. *PLoS One*. 2009;4(8):2-9. doi:10.1371/journal.pone.0006600
 173. Orlikowsky TW, Spring B, Dannecker GE, Niethammer D, Poets CF, Hoffmann MK. Expression and regulation of B7 family molecules on macrophages (M Φ) in preterm and term neonatal cord blood and peripheral blood of adults. *Cytometry*. 2003;53B(1):40-47. doi:10.1002/cyto.b.10033
 174. Dubaniewicz A, Lewko B, Moszkowska G, Zamorska B, Stepinski J. Molecular subtypes of the HLA-DR antigens in pulmonary tuberculosis. *Int J Infect Dis*. 2000;4(3):129-133. doi:10.1016/S1201-9712(00)90073-0
 175. Grosche L, Knippertz I, König C, et al. The CD83 Molecule – An Important Immune Checkpoint. *Front Immunol*. 2020;11(April):1-16. doi:10.3389/fimmu.2020.00721
 176. Li Z, Ju X, Silveira PA, et al. CD83: Activation marker for antigen presenting cells and its therapeutic potential. *Front Immunol*. 2019;10(JUN):1-9. doi:10.3389/fimmu.2019.01312
 177. Liu E, Law HKW, Lau YL. BCG promotes cord blood monocyte-derived dendritic cell maturation with nuclear Rel-B up-regulation and cytosolic I κ B α and β degradation. *Pediatr Res*. Published online 2003. doi:10.1203/01.PDR.0000069703.58586.8B
 178. Azad AK, Rajaram MVS, Schlesinger LS. Exploitation of the Macrophage Mannose Receptor (CD206) in Infectious Disease Diagnostics and Therapeutics. *J Cytol Mol Biol*. 2014;1(1):1-10. doi:10.13188/2325-4653.1000003
 179. Schneider A, Weier M, Herderschee J, et al. IRF5 Is a key regulator of macrophage response to lipopolysaccharide in newborns. *Front Immunol*. 2018;9(JUL):1-13. doi:10.3389/fimmu.2018.01597
 180. O'Neill LAJJ, Kishton RJ, Rathmell J. A guide to immunometabolism for immunologists. *Nat Rev Immunol*. 2016;16(9):553-565. doi:10.1038/nri.2016.70
 181. Diskin C, Pålsson-mcdermott EM. Metabolic modulation in macrophage effector function. *Front Immunol*. 2018;9(FEB):1-17. doi:10.3389/fimmu.2018.00270
 182. O'Neill LAJ, Artyomov MN. Itaconate: the poster child of metabolic reprogramming in macrophage function. *Nat Rev Immunol*. 2019;1840. doi:10.1038/s41577-019-0128-5
 183. Ferguson BS, Rogatzki MJ, Goodwin ML, Kane DA, Rightmire Z, Gladden LB. *Lactate Metabolism: Historical Context, Prior Misinterpretations, and Current Understanding*. Vol 118. Springer Berlin Heidelberg; 2018. doi:10.1007/s00421-017-3795-6
 184. Warburg O. The metabolism of carcinoma cells 1. *J Cancer Res*. Published online 1925. doi:10.1158/jcr.1925.148
 185. OREN R, FARNHAM AE, SAITO K, MILOFSKY E, KARNOVSKY ML. Metabolic patterns in three types of phagocytizing cells. *J Cell Biol*. 1963;17:487-501. doi:10.1083/jcb.17.3.487
 186. Ardawi MSM. Metabolism of glucose, glutamine, long-chain fatty acids and ketone bodies by lungs of the rat. *Biochimie*. 1991;73(5):557-562. doi:10.1016/0300-9084(91)90023-T
 187. Tannahill G, Curtis A, Adamik J, et al. Succinate is a danger signal that induces IL-

- 1 β via HIF-1 α . *Nature*. 2013;496(7444):238-242.
doi:10.1038/nature11986.Succinate
188. Gleeson LE, Sheedy FJ, Palsson-McDermott EM, et al. Cutting Edge: Mycobacterium tuberculosis Induces Aerobic Glycolysis in Human Alveolar Macrophages That Is Required for Control of Intracellular Bacillary Replication. *J Immunol*. 2016;196(6):2444-2449. doi:10.4049/jimmunol.1501612
 189. Palsson-Mcdermott EM, Curtis AM, Goel G, et al. Pyruvate kinase M2 regulates hif-1 α activity and il-1 β induction and is a critical determinant of the warburg effect in LPS-activated macrophages. *Cell Metab*. 2015;21(1):65-80. doi:10.1016/j.cmet.2014.12.005
 190. Artyomov MN, Sergushichev A, Schilling JD. Integrating immunometabolism and macrophage diversity. *Semin Immunol*. 2016;28(5):417-424. doi:10.1016/j.smim.2016.10.004
 191. Williams NC, O'Neill LAJ. A role for the krebs cycle intermediate citrate in metabolic reprogramming in innate immunity and inflammation. *Front Immunol*. 2018;9(FEB):1-11. doi:10.3389/fimmu.2018.00141
 192. Jessop F, Buntyn R, Schwarz B, Wehrly T, Scott D, Bosio CM. Interferon gamma reprograms host mitochondrial metabolism through inhibition of complex II to control intracellular bacterial replication. *Infect Immun*. 2020;88(2):1-18. doi:10.1128/IAI.00744-19
 193. Haschemi A, Kosma P, Gille L, et al. The sedoheptulose kinase CARKL directs macrophage polarization through control of glucose metabolism. *Cell Metab*. 2012;15(6):813-826. doi:10.1016/j.cmet.2012.04.023
 194. Vats D, Mukundan L, Odegaard JI, et al. Oxidative metabolism and PGC-1 β attenuate macrophage-mediated inflammation. *Cell Metab*. 2006;4(1):13-24. doi:10.1016/j.cmet.2006.05.011
 195. Namgaladze D, Brüne B. Fatty acid oxidation is dispensable for human macrophage IL-4-induced polarization. *Biochim Biophys Acta - Mol Cell Biol Lipids*. 2014;1841(9):1329-1335. doi:10.1016/j.bbalip.2014.06.007
 196. Van den Bossche J, O'Neill LA, Menon D. Macrophage Immunometabolism: Where Are We (Going)? *Trends Immunol*. 2017;38(6):395-406. doi:10.1016/j.it.2017.03.001
 197. Vijayan V, Pradhan P, Braud L, et al. Human and murine macrophages exhibit differential metabolic responses to lipopolysaccharide - A divergent role for glycolysis. *Redox Biol*. 2019;22(February):101147. doi:10.1016/j.redox.2019.101147
 198. Thomas AC, Mattila JT. "Of mice and men": Arginine metabolism in macrophages. *Front Immunol*. 2014;5(OCT):3389. doi:10.3389/fimmu.2014.00479
 199. Reales-Calderón JA, Aguilera-Montilla N, Corbí ÁL, Molero G, Gil C. Proteomic characterization of human proinflammatory M1 and anti-inflammatory M2 macrophages and their response to Candida albicans. *Proteomics*. 2014;14(12):1503-1518. doi:10.1002/pmic.201300508
 200. Su X, Yu Y, Zhong Y, et al. Interferon- γ regulates cellular metabolism and mRNA translation to potentiate macrophage activation. *Nat Immunol*. 2015;16(8):838-849. doi:10.1038/ni.3205
 201. Lachmandas E, Boutens L, Ratter JM, et al. Microbial stimulation of different

- Toll-like receptor signaling pathways induces diverse metabolic programmes in human monocytes. *Nat Microbiol.* 2016;2(December 2016). doi:10.1038/nmicrobiol.2016.246
202. Dreschers S, Ohl K, Lehrke M, et al. Impaired cellular energy metabolism in cord blood macrophages contributes to abortive response toward inflammatory threats. *Nat Commun.* 2019;10(1). doi:10.1038/s41467-019-09359-8
 203. Shi L, Eugenin EA, Subbian S. Immunometabolism in tuberculosis. *Front Immunol.* 2016;7(APR):1-15. doi:10.3389/fimmu.2016.00150
 204. Shi L, Salamon H, Eugenin EA, Pine R, Cooper A, Gennaro ML. Infection with Mycobacterium tuberculosis induces the Warburg effect in mouse lungs. *Nat Publ Gr.* 2015;(July):1-13. doi:10.1038/srep18176
 205. Shin JH, Yang JY, Jeon BY, et al. H NMR-based Metabolomic Profiling in Mice Infected with Mycobacterium tuberculosis. *J Proteome Res.* 2011;10(5):2238-2247. doi:10.1021/pr101054m
 206. Subbian S, Tsenova L, Yang G, et al. Chronic pulmonary cavitary tuberculosis in rabbits: A failed host immune response. *Open Biol.* 2011;1(DECEMBER). doi:10.1098/rsob.110016
 207. Böhme J, Martinez N, Li S, et al. Metformin enhances anti-mycobacterial responses by educating CD8+ T-cell immunometabolic circuits. *Nat Commun.* 2020;11(1). doi:10.1038/s41467-020-19095-z
 208. Naicker N, Sigal A, Naidoo K. Metformin as Host-Directed Therapy for TB Treatment : Scoping Review. 2020;11(April):1-11. doi:10.3389/fmicb.2020.00435
 209. Kim JS, Kim YR, Yang CS. Host-Directed Therapy in Tuberculosis: Targeting Host Metabolism. *Front Immunol.* 2020;11(August):1-12. doi:10.3389/fimmu.2020.01790
 210. Cumming BM, Pacl HT, Steyn AJC. Relevance of the Warburg Effect in Tuberculosis for Host-Directed Therapy. *Front Cell Infect Microbiol.* 2020;10(September):1-13. doi:10.3389/fcimb.2020.576596
 211. Abeyayehu D, Spence AJ, Qayum AA, et al. Lactic Acid Suppresses IL-33-Mediated Mast Cell Inflammatory Responses via Hypoxia-Inducible Factor-1 - Dependent miR-155 Suppression. *J Immunol.* 2016;197(7):2909-2917. doi:10.4049/jimmunol.1600651
 212. Peter K, Rehli M, Singer K, Renner-Sattler K, Kreutz M. Lactic acid delays the inflammatory response of human monocytes. *Biochem Biophys Res Commun.* 2015;457(3):412-418. doi:10.1016/j.bbrc.2015.01.005
 213. Robergs RA, McNulty CR, Minett GM, Holland J, Trajano G. Lactate, not lactic acid, is produced by cellular cytosolic energy catabolism. *Physiology.* 2018;33(1):10-12. doi:10.1152/physiol.00033.2017
 214. Dietl K, Renner K, Dettmer K, et al. Lactic acid and acidification inhibit TNF secretion and glycolysis of human monocytes. *J Immunol.* 2010;184(3):1200-1209. doi:10.4049/jimmunol.0902584
 215. Van den Bossche J, Baardman J, Otto NA, et al. Mitochondrial Dysfunction Prevents Repolarization of Inflammatory Macrophages. *Cell Rep.* 2016;17(3):684-696. doi:10.1016/j.celrep.2016.09.008
 216. O'Neill LAJ. A Broken Krebs Cycle in Macrophages. *Immunity.* 2015;42(3):393-394. doi:10.1016/j.immuni.2015.02.017

217. Ogawa M, Yoshida SI, Mizuguchi Y. 2-Deoxy-D-glucose inhibits intracellular multiplication and promotes intracellular killing of *Legionella pneumophila* in A/J mouse macrophages. *Infect Immun*. 1994;62(1):266-270. doi:10.1128/iai.62.1.266-270.1994
218. Munford RS. Murine responses to endotoxin: Another dirty little secret? *J Infect Dis*. Published online 2010. doi:10.1086/649558
219. Michelucci A, Cordes T, Ghel J, et al. Immune-responsive gene 1 protein links metabolism to immunity by catalyzing itaconic acid production. *Proc Natl Acad Sci*. 2013;110(19):7820-7825. doi:10.1073/pnas.1218599110
220. Mills EL, Ryan DG, Prag HA, et al. Itaconate is an anti-inflammatory metabolite that activates Nrf2 via alkylation of KEAP1. *Nature*. Published online 2018. doi:10.1038/nature25986
221. Fei F, Lee KM, McCarry BE, Bowdish DME. Age-associated metabolic dysregulation in bone marrow-derived macrophages stimulated with lipopolysaccharide. *Sci Rep*. 2016;6(March):1-12. doi:10.1038/srep22637
222. Lissner MM, Thomas BJ, Wee K, Tong AJ, Kollmann TR, Smale ST. Age-related gene expression differences in monocytes from Human Neonates, Young Adults, and Older Adults. *PLoS One*. 2015;10(7):1-18. doi:10.1371/journal.pone.0132061
223. Yarbro JR, Pence BD. Classical monocytes from older adults maintain capacity for metabolic compensation during glucose deprivation and lipopolysaccharide stimulation. *Mech Ageing Dev*. Published online 2019. doi:10.1016/j.mad.2019.111146
224. Kumar SKM, Bhat BV. Distinct mechanisms of the newborn innate immunity. *Immunol Lett*. 2016;173:42-54. doi:10.1016/j.imlet.2016.03.009
225. Dowling DJ, Levy O. Ontogeny of early life immunity. *Trends Immunol*. 2014;35(7):299-310. doi:10.1016/j.it.2014.04.007
226. Cox DJ, Coleman AM, Gogan KM, et al. Inhibiting Histone Deacetylases in Human Macrophages Promotes Glycolysis, IL-1 β , and T Helper Cell Responses to *Mycobacterium tuberculosis*. *Front Immunol*. 2020;11(July):1-15. doi:10.3389/fimmu.2020.01609
227. Phelan JJ, McQuaid K, Kenny C, et al. Desferrioxamine Supports Metabolic Function in Primary Human Macrophages Infected With *Mycobacterium tuberculosis*. 2020;11(May):1-18. doi:10.3389/fimmu.2020.00836
228. Osada-Oka M, Goda N, Saiga H, et al. Metabolic adaptation to glycolysis is a basic defense mechanism of macrophages for *Mycobacterium tuberculosis* infection. *Int Immunol*. 2019;31(12):781-793. doi:10.1093/intimm/dxz048
229. Kumar R, Singh P, Kolloli A, et al. Immunometabolism of Phagocytes During *Mycobacterium tuberculosis* Infection. *Front Mol Biosci*. 2019;6(October):1-20. doi:10.3389/fmolb.2019.00105
230. Dreschers S, Ohl K, Schulte N, Tenbrock K, Orlikowsky TW. Impaired functional capacity of polarised neonatal macrophages. *Sci Rep*. 2020;10(1):1-12. doi:10.1038/s41598-019-56928-4
231. Sohlberg E, Saghafian-Hedengren S, Bremme K, Sverremark-Ekström E. Cord blood monocyte subsets are similar to adult and show potent peptidoglycan-stimulated cytokine responses. *Immunology*. 2011;133(1):41-50. doi:10.1111/j.1365-2567.2011.03407.x

232. Ho W-Z, Liyo J, Song L, Cutilli JR, Polin RA, Douglas ' SD. Infection of Cord Blood Monocyte-Derived Macrophages with Human Immunodeficiency Virus Type 1. *J Virol.* 1992;66(1):573-579.
233. Speer CP, Ambruso DR, Grimsley J, Johnston RB. Oxidative Metabolism in Cord Blood Monocytes and Monocyte- Derived Macrophages. *Infect Immun.* Published online 1985:919-921.
234. Coleman MM, Basdeo SA, Coleman AM, et al. All-trans retinoic acid augments autophagy during intracellular bacterial infection. *Am J Respir Cell Mol Biol.* 2018;59(5):548-556. doi:10.1165/rcmb.2017-0382OC
235. Hackett EE, Charles-Messance H, O'Leary SM, et al. Mycobacterium tuberculosis Limits Host Glycolysis and IL-1 β by Restriction of PFK-M via MicroRNA-21. *Cell Rep.* 2020;30(1):124-136.e4. doi:10.1016/j.celrep.2019.12.015
236. Cumming BM, Addicott KW, Adamson JH, Steyn AJ. Mycobacterium tuberculosis induces decelerated bioenergetic metabolism in human macrophages. *Elife.* 2018;7:1-28. doi:10.7554/eLife.39169
237. Galván-Peña S, O'Neill LAJ. Metabolic reprogramming in macrophage polarization. *Front Immunol.* 2014;5(AUG):1-6. doi:10.3389/fimmu.2014.00420
238. Jha AK, Huang SCC, Sergushichev A, et al. Network integration of parallel metabolic and transcriptional data reveals metabolic modules that regulate macrophage polarization. *Immunity.* 2015;42(3):419-430. doi:10.1016/j.immuni.2015.02.005
239. Basha S, Surendran N, Pichichero M. Immune responses in neonates. *Expert Rev Clin Immunol.* Published online 2014. doi:10.1586/1744666X.2014.942288
240. Li YP, Yu SL, Huang ZJ, et al. An Impaired Inflammatory Cytokine Response to Gram-Negative LPS in Human Neonates is Associated with the Defective TLR-Mediated Signaling Pathway. *J Clin Immunol.* 2015;35(2):218-226. doi:10.1007/s10875-015-0128-6
241. Brennan K, O'Leary BD, Mc Laughlin D, et al. Type 1 IFN Induction by Cytosolic Nucleic Acid Is Intact in Neonatal Mononuclear Cells, Contrasting Starkly with Neonatal Hyporesponsiveness to TLR Ligation Due to Independence from Endosome-Mediated IRF3 Activation. *J Immunol.* Published online 2018;ji1700956. doi:10.4049/jimmunol.1700956
242. Burl S, Townend J, Njie-Jobe J, et al. Age-dependent maturation of toll-like receptor-mediated cytokine responses in gambian infants. *PLoS One.* 2011;6(4). doi:10.1371/journal.pone.0018185
243. Angelone DF, Wessels MR, Coughlin M, et al. Innate immunity of the human newborn is polarized toward a high ratio of IL-6/TNF- α production in vitro and in vivo. *Pediatr Res.* 2006;60(2):205-209. doi:10.1203/01.pdr.0000228319.10481.ea
244. Pedraza-Sánchez S, Hise AG, Ramachandra L, Arechavaleta-Velasco F, King CL. Reduced frequency of a CD14+ CD16+ monocyte subset with high toll-like receptor 4 expression in cord blood compared to adult blood contributes to lipopolysaccharide hyporesponsiveness in newborns. *Clin Vaccine Immunol.* Published online 2013. doi:10.1128/CVI.00609-12
245. Redford PS, Boonstra A, Read S, et al. Enhanced protection to Mycobacterium tuberculosis infection in IL-10-deficient mice is accompanied by early and enhanced Th1 responses in the lung. *Eur J Immunol.* Published online 2010.

- doi:10.1002/eji.201040433
246. Gleeson LE, Sheedy FJ. Metabolic reprogramming & inflammation: Fuelling the host response to pathogens. *Semin Immunol*. 2016;28(5):450-468. doi:10.1016/j.smim.2016.10.007
 247. Tan Z, Xie N, Banerjee S, et al. The monocarboxylate transporter 4 is required for glycolytic reprogramming and inflammatory response in macrophages. *J Biol Chem*. 2015;290(1):46-55. doi:10.1074/jbc.M114.603589
 248. Halestrap AP. The monocarboxylate transporter family-Structure and functional characterization. *IUBMB Life*. 2012;64(1):1-9. doi:10.1002/iub.573
 249. Corcoran SE, O'Neill LA. HIF1alpha and metabolic reprogramming in inflammation. *J Clin Invest*. 2016;126(10):3699-3707. doi:10.1172/JCI84431
 250. Mohareer K, Medikonda J, Vadankula GR, Banerjee S. Mycobacterial Control of Host Mitochondria: Bioenergetic and Metabolic Changes Shaping Cell Fate and Infection Outcome. *Front Cell Infect Microbiol*. 2020;10(September). doi:10.3389/fcimb.2020.00457
 251. de Martino M, Lodi L, Galli L, Chiappini E. Immune Response to Mycobacterium tuberculosis: A Narrative Review. *Front Pediatr*. 2019;7(August):1-8. doi:10.3389/fped.2019.00350
 252. López MC, Palmer BE, Lawrence DA. Naïve T cells, unconventional NK and NKT cells, and highly responsive monocyte-derived macrophages characterize human cord blood. *Immunobiology*. Published online 2014. doi:10.1016/j.imbio.2014.06.001
 253. Kollmann TR, Crabtree J, Rein-Weston A, et al. Neonatal Innate TLR-Mediated Responses Are Distinct from Those of Adults. *J Immunol*. 2009;183(11):7150-7160. doi:10.4049/jimmunol.0901481
 254. Gille C, Spring B, Tewes L, Poets CF, Orlikowsky T. A new method to quantify phagocytosis and intracellular degradation using green fluorescent protein-labeled Escherichia coli: Comparison of cord blood macrophages and peripheral blood macrophages of healthy adults. *Cytom Part A*. 2006;69(3):152-154. doi:10.1002/cyto.a.20222
 255. Speer CP, Gahr M, Wieland M, Eber S. Phagocytosis-associated functions in neonatal monocyte-derived macrophages. *Pediatr Res*. 1988;24(2):213-216. doi:10.1203/00006450-198808000-00015
 256. Lekkou A, Karakantza M, Mouzaki A, Kalfarentzos F, Gogos CA. Cytokine Production and Monocyte HLA-DR Expression as Predictors of Outcome for Patients with Community-Acquired Severe Infections. *Clin Diagn Lab Immunol*. 2004;11(1):161-167. doi:10.1128/CDLI.11.1.161-167.2004
 257. Winkler MS, Rissiek A, Priefler M, et al. Human leucocyte antigen (HLA-DR) gene expression is reduced in sepsis and correlates with impaired TNF α response: A diagnostic tool for immunosuppression? *PLoS One*. 2017;12(8):1-14. doi:10.1371/journal.pone.0182427
 258. Juskewitch JE, Abraham RS, League SC, et al. Monocyte HLA-DR expression and neutrophil CD64 expression as biomarkers of infection in critically ill neonates and infants. *Pediatr Res*. 2015;78(6):683-690. doi:10.1038/pr.2015.164
 259. Schefold JC, Porz L, Uebe B, et al. Diminished HLA-DR expression on monocyte and dendritic cell subsets indicating impairment of cellular immunity in pre-term neonates: A prospective observational analysis. *J Perinat Med*.

- 2015;43(5):609-618. doi:10.1515/jpm-2014-0226
260. Grigg J, Riedler J, Robertson CF, Boyle W, Uren S. Alveolar macrophage immaturity in infants and young children. *Eur Respir J*. 1999;14(5):1198-1205. doi:10.1183/09031936.99.14511989
 261. Gaidt MM, Ebert TS, Chauhan D, et al. Human Monocytes Engage an Alternative Inflammasome Pathway. *Immunity*. 2016;44(4):833-846. doi:10.1016/j.immuni.2016.01.012
 262. Vrieling F, Kostidis S, Spaink HP, et al. Analyzing the impact of Mycobacterium tuberculosis infection on primary human macrophages by combined exploratory and targeted metabolomics. *Sci Rep*. 2020;10(1):1-13. doi:10.1038/s41598-020-62911-1
 263. Atri C, Guerfali FZ, Laouini D. Role of human macrophage polarization in inflammation during infectious diseases. *Int J Mol Sci*. 2018;19(6). doi:10.3390/ijms19061801
 264. Wang F, Zhang S, Jeon R, et al. Interferon Gamma Induces Reversible Metabolic Reprogramming of M1 Macrophages to Sustain Cell Viability and Pro-Inflammatory Activity. *EBioMedicine*. 2018;30:303-316. doi:10.1016/j.ebiom.2018.02.009
 265. Nibbering PH, Pos O. Interferon- γ -activated human granulocytes kill ingested. Published online 1990:869-873.
 266. Condos R, Rom WN, Schluger NW. Treatment of multidrug-resistant pulmonary tuberculosis with interferon- γ via aerosol. *Lancet*. 1997;349(9064):1513-1515. doi:10.1016/S0140-6736(96)12273-X
 267. Khan TA, Mazhar H, Saleha S, Tipu HN, Muhammad N, Abbas MN. Interferon-Gamma Improves Macrophages Function against *M. tuberculosis* in Multidrug-Resistant Tuberculosis Patients. *Chemother Res Pract*. 2016;2016:1-6. doi:10.1155/2016/7295390
 268. Bellete B, Coberly J, Barnes GL, et al. Evaluation of a whole-blood interferon- γ release assay for the detection of Mycobacterium tuberculosis infection in 2 study populations. *Clin Infect Dis*. 2002;34(11):1449-1456. doi:10.1086/340397
 269. Silberer J, Ihorst G, Kopp MV. Cytokine levels in supernatants of whole blood and mononuclear cell cultures in adults and neonates reveal significant differences with respect to interleukin-13 and interferon-gamma. *Pediatr Allergy Immunol*. 2008;19(2):140-147. doi:10.1111/j.1399-3038.2007.00605.x
 270. Rook GAW, Hernandez-Pando R, Dheda K, Teng Seah G. IL-4 in tuberculosis: Implications for vaccine design. *Trends Immunol*. 2004;25(9):483-488. doi:10.1016/j.it.2004.06.005
 271. Kuchroo VK, Prabhu Das M, Brown JA, et al. B7-1 and B7-2 costimulatory molecules activate differentially the Th1/Th2 developmental pathways: Application to autoimmune disease therapy. *Cell*. 1995;80(5):707-718. doi:10.1016/0092-8674(95)90349-6
 272. Deszo EL, Brake DK, Kelley KW, Freund GG. IL-4-dependent CD86 expression requires JAK/STAT6 activation and is negatively regulated by PKC δ . *Cell Signal*. 2004;16(2):271-280. doi:10.1016/S0898-6568(03)00137-2
 273. Viola A, Munari F, Sánchez-Rodríguez R, Scolaro T, Castegna A. The metabolic signature of macrophage responses. *Front Immunol*. 2019;10(JULY):1-16. doi:10.3389/fimmu.2019.01462

274. Van den Bossche J, Baardman J, de Winther MPJ. Metabolic characterization of polarized M1 and M2 bone marrow-derived macrophages using real-time extracellular flux analysis. *J Vis Exp*. 2015;2015(105):1-7. doi:10.3791/53424
275. Zhao Q, Chu Z, Zhu L, et al. 2-Deoxy-d-glucose treatment decreases anti-inflammatory M2 macrophage polarization in mice with tumor and allergic airway inflammation. *Front Immunol*. 2017;8(JUN). doi:10.3389/fimmu.2017.00637
276. Ó Maoldomhnaigh C, Cox DJ, Phelan JJ, Malone FD, Keane J, Basdeo SA. The Warburg Effect Occurs Rapidly in Stimulated Human Adult but Not Umbilical Cord Blood Derived Macrophages. *Front Immunol*. 2021;12(April):1-13. doi:10.3389/fimmu.2021.657261
277. Raggi F, Pelassa S, Pierobon D, et al. Regulation of human Macrophage M1-M2 Polarization Balance by hypoxia and the Triggering receptor expressed on Myeloid cells-1. *Front Immunol*. 2017;8(SEP):1-18. doi:10.3389/fimmu.2017.01097
278. Kraft JD, Horzempa J, Davis C, et al. Neonatal macrophages express elevated levels of interleukin-27 that oppose immune responses. *Immunology*. Published online 2013:484-493. doi:10.1111/imm.12095
279. Rodríguez-Prados J-C, Través PG, Cuenca J, et al. Substrate Fate in Activated Macrophages: A Comparison between Innate, Classic, and Alternative Activation. *J Immunol*. 2010;185(1):605-614. doi:10.4049/jimmunol.0901698
280. Liu Y, Xu R, Gu H, et al. Metabolic reprogramming in macrophage responses. *Biomark Res*. 2021;9(1):1-17. doi:10.1186/s40364-020-00251-y
281. Maródi L, Goda K, Palicz A, Szabó G. Cytokine receptor signaling in neonatal macrophage: Defective STAT-1 phosphorylation in response to stimulation with ifn- γ . *Clin Exp Immunol*. 2001;126(3):456-460. doi:10.1046/j.1365-2249.2001.01693.x
282. Namgaladze D, Brüne B. Fatty acid oxidation is dispensable for human macrophage IL-4-induced polarization. *Biochim Biophys Acta - Mol Cell Biol Lipids*. 2014;1841(9):1329-1335. doi:10.1016/j.bbalip.2014.06.007
283. Hu X, Ivashkiv LB. Cross-regulation of Signaling and Immune Responses by IFN- γ and STAT1. *Immunity*. 2009;31(4):539-550. doi:10.1016/j.immuni.2009.09.002.Cross-regulation
284. Schroder K, Sweet MJ, Hume DA. Signal integration between IFN γ and TLR signaling pathways in macrophages. *Immunobiology*. 2006;211(6-8):511-524. doi:10.1016/j.imbio.2006.05.007
285. Howard NC, Khader SA. Immunometabolism during Mycobacterium tuberculosis Infection. *Trends Microbiol*. 2020;28(10):832-850. doi:10.1016/j.tim.2020.04.010
286. Ratter JM, Rooijackers HMM, Hooiveld GJ, et al. In vitro and in vivo Effects of Lactate on Metabolism and Cytokine Production of Human Primary PBMCs and Monocytes. *Front Immunol*. 2018;9(November):2564. doi:10.3389/fimmu.2018.02564
287. Latham T, MacKay L, Sproul D, et al. Lactate, a product of glycolytic metabolism, inhibits histone deacetylase activity and promotes changes in gene expression. *Nucleic Acids Res*. 2012;40(11):4794-4803. doi:10.1093/nar/gks066
288. Haas R, Cucchi D, Smith J, Pucino V, Macdougall CE, Mauro C. Intermediates of

- Metabolism: From Bystanders to Signaling Molecules. *Trends Biochem Sci.* 2016;41(5):460-471. doi:10.1016/j.tibs.2016.02.003
289. Hui S, Ghergurovich JM, Morscher RJ, et al. Glucose feeds the TCA cycle via circulating lactate. *Nat Publ Gr.* Published online 2017. doi:10.1038/nature24057
 290. Lin S, Sun L, Lyu X, et al. Lactate-activated macrophages induced aerobic glycolysis and epithelial-mesenchymal transition in breast cancer by regulation of CCL5-CCR5 axis: A positive metabolic feedback loop. *Oncotarget.* 2017;8(66):110426-110443. doi:10.18632/oncotarget.22786
 291. Pucino V, Certo M, Bulusu V, et al. Lactate Buildup at the Site of Chronic Inflammation Promotes Disease by Inducing CD4+ T Cell Metabolic Rewiring. *Cell Metab.* 2019;30(6):1055-1074.e8. doi:10.1016/j.cmet.2019.10.004
 292. Bou Chebl R, El Khuri C, Shami A, et al. Serum lactate is an independent predictor of hospital mortality in critically ill patients in the emergency department: A retrospective study. *Scand J Trauma Resusc Emerg Med.* Published online 2017. doi:10.1186/s13049-017-0415-8
 293. Villar J, Short JH, Lighthall G. Lactate Predicts Both Short- and Long-Term Mortality in Patients With and Without Sepsis. *Infect Dis Res Treat.* Published online 2019. doi:10.1177/1178633719862776
 294. Trzeciak S, Dellinger RP, Chansky ME, et al. Serum lactate as a predictor of mortality in patients with infection. *Intensive Care Med.* Published online 2007. doi:10.1007/s00134-007-0563-9
 295. Liu Z, Meng Z, Li Y, et al. Prognostic accuracy of the serum lactate level, the SOFA score and the qSOFA score for mortality among adults with Sepsis. *Scand J Trauma Resusc Emerg Med.* Published online 2019. doi:10.1186/s13049-019-0609-3
 296. Errea A, Cayet D, Marchetti P, et al. Lactate inhibits the pro-inflammatory response and metabolic reprogramming in Murine macrophages in a GPR81-independent manner. *PLoS One.* 2016;11(11):1-11. doi:10.1371/journal.pone.0164098
 297. Leisching G, Keane J. Bystander macrophage metabolic shift after mycobacterium tuberculosis infection. *Am J Respir Cell Mol Biol.* Published online 2020. doi:10.1165/rcmb.2020-0200LE
 298. Goodwin ML, Harris JE, Hernández A, Gladden LB. Blood lactate measurements and analysis during exercise: A guide for clinicians. *J Diabetes Sci Technol.* 2007;1(4):558-569. doi:10.1177/193229680700100414
 299. Garcia-Alvarez M, Marik P, Bellomo R. Sepsis-associated hyperlactatemia. *Crit Care.* 2014;18(5):1-11. doi:10.1186/s13054-014-0503-3
 300. Brown SD, Clark C, Gutierrez G. Pulmonary lactate release in patients with sepsis and the adult respiratory distress syndrome. *J Crit Care.* 1996;11(1):2-8. doi:10.1016/S0883-9441(96)90014-3
 301. Haas R, Smith J, Rocher-Ros V, et al. Lactate regulates metabolic and proinflammatory circuits in control of T cell migration and effector functions. *PLoS Biol.* 2015;13(7):1-24. doi:10.1371/journal.pbio.1002202
 302. Neubert P, Weichselbaum A, Reitinger C, et al. HIF1A and NFAT5 coordinate Na⁺-boosted antibacterial defense via enhanced autophagy and autolysosomal targeting. *Autophagy.* 2019;0(0):1-18. doi:10.1080/15548627.2019.1596483

303. Amara S, Whalen M, Tiriveedhi V. High salt induces anti-inflammatory MΦ2-like phenotype in peripheral macrophages. *Biochem Biophys Reports*. 2016;7:1-9. doi:10.1016/j.bbrep.2016.05.009
304. Samuvel DJ, Sundararaj KP, Nareika A, Lopes-Virella MF, Huang Y. Lactate boosts TLR4 signaling and NF-kappaB pathway-mediated gene transcription in macrophages via monocarboxylate transporters and MD-2 up-regulation. *J Immunol (Baltimore, Md 1950)*. 2009;182(4):2476-2484. doi:10.4049/jimmunol.0802059
305. Billig S, Schneefeld M, Huber C, Grassl GA, Eisenreich W, Bange FC. Lactate oxidation facilitates growth of Mycobacterium tuberculosis in human macrophages. *Sci Rep*. 2017;7(1):1-12. doi:10.1038/s41598-017-05916-7
306. Deretic V. Autophagy, an immunologic magic bullet: Mycobacterium tuberculosis phagosome maturation block and how to bypass it. *Future Microbiol*. 2008;3(5):517-524. doi:10.2217/17460913.3.5.517
307. Wu YT, Tan HL, Shui G, et al. Dual role of 3-methyladenine in modulation of autophagy via different temporal patterns of inhibition on class I and III phosphoinositide 3-kinase. *J Biol Chem*. 2010;285(14):10850-10861. doi:10.1074/jbc.M109.080796
308. Lu L, Arranz-Trullén J, Prats-Ejarque G, Pulido D, Bhakta S, Boix E. Human antimicrobial RNases inhibit intracellular bacterial growth and induce autophagy in mycobacteria-infected macrophages. *Front Immunol*. 2019;10(JUL). doi:10.3389/fimmu.2019.01500
309. Caslin HL, Abebayehu D, Abdul Qayum A, et al. Lactic Acid Inhibits Lipopolysaccharide-Induced Mast Cell Function by Limiting Glycolysis and ATP Availability. *J Immunol*. Published online 2019. doi:10.4049/jimmunol.1801005
310. Lawless SJ, Kedia-Mehta N, Walls JF, et al. Glucose represses dendritic cell-induced T cell responses. *Nat Commun*. Published online 2017. doi:10.1038/ncomms15620
311. Mills EL, Kelly B, Logan A, et al. Succinate Dehydrogenase Supports Metabolic Repurposing of Mitochondria to Drive Inflammatory Macrophages. *Cell*. 2016;167(2):457-470.e13. doi:10.1016/j.cell.2016.08.064
312. Billig S, Schneefeld M, Huber C, Grassl GA, Eisenreich W, Bange FC. Lactate oxidation facilitates growth of Mycobacterium tuberculosis in human macrophages. *Sci Rep*. 2017;7(1):1-12. doi:10.1038/s41598-017-05916-7
313. Brisson L, Bański P, Sboarina M, et al. Lactate Dehydrogenase B Controls Lysosome Activity and Autophagy in Cancer. *Cancer Cell*. 2016;30(3):418-431. doi:10.1016/j.ccell.2016.08.005
314. Tanida I. Autophagy basics. *Microbiol Immunol*. 2011;55(1):1-11. doi:10.1111/j.1348-0421.2010.00271.x
315. Shi D, Zhao D, Niu P, Zhu Y, Zhou J, Chen H. Glycolysis inhibition via mTOR suppression is a key step in cardamonin-induced autophagy in SKOV3 cells 06 Biological Sciences 0601 Biochemistry and Cell Biology. *BMC Complement Altern Med*. Published online 2018. doi:10.1186/s12906-018-2380-9
316. Martinez J, Verbist K, Wang R, Green DR. The Relationship between Metabolism and the Autophagy Machinery during the Innate Immune Response. *Cell Metab*. 2013;17(6):895-900. doi:10.1016/j.cmet.2013.05.012
317. Palsson-Mcdermott EM, O'Neill LAJ. The Warburg effect then and now: From

- cancer to inflammatory diseases. *BioEssays*. 2013;35(11):965-973. doi:10.1002/bies.201300084
318. Sheedy FJ, Divangahi M. Targeting immunometabolism in host defence against Mycobacterium tuberculosis. *Immunology*. 2021;162(2):145-159. doi:10.1111/imm.13276
 319. Palmieri EM, McGinity C, Wink DA, McVicar DW. Nitric oxide in macrophage immunometabolism: Hiding in plain sight. *Metabolites*. 2020;10(11):1-34. doi:10.3390/metabo10110429
 320. Ryan DG, O'Neill LAJ. Krebs cycle rewired for macrophage and dendritic cell effector functions. *FEBS Lett*. 2017;591:2992-3006. doi:10.1002/1873-3468.12744
 321. Cordes T, Wallace M, Michelucci A, et al. Immunoresponsive gene 1 and itaconate inhibit succinate dehydrogenase to modulate intracellular succinate levels. *J Biol Chem*. 2016;291(27):14274-14284. doi:10.1074/jbc.M115.685792
 322. Selkov SA, Selutin A V., Pavlova OM, Khromov-Borisov NN, Pavlov O V. Comparative phenotypic characterization of human cord blood monocytes and placental macrophages at term. *Placenta*. Published online 2013. doi:10.1016/j.placenta.2013.05.007
 323. Korb DS, Schneider BE, Schaible UE. Innate immunity in tuberculosis: myths and truth. *Microbes Infect*. 2008;10(9):995-1004. doi:10.1016/j.micinf.2008.07.039
 324. Dowling DJ, Levy O. Ontogeny of early life immunity. *Trends Immunol*. 2014;35(7):299-310. doi:10.1016/j.it.2014.04.007
 325. Conti MG, Angelidou A, Diray-Arce J, et al. Immunometabolic approaches to prevent, detect, and treat neonatal sepsis. *Pediatr Res*. 2020;87(2):399-405. doi:10.1038/s41390-019-0647-6
 326. Goenka A, Kollmann TR. Development of immunity in early life. *J Infect*. 2015;71(S1):S112-S120. doi:10.1016/j.jinf.2015.04.027
 327. Georgountzou A, Papadopoulos NG. Postnatal innate immune development: From birth to adulthood. *Front Immunol*. Published online 2017. doi:10.3389/fimmu.2017.00957
 328. Panda A, Arjona A, Sapey E, et al. Human innate immunosenescence: causes and consequences for immunity in old age. *Trends Immunol*. 2009;30(7):325-333. doi:10.1016/j.it.2009.05.004
 329. Adeva-Andany M, López-Ojén M, Funcasta-Calderón R, et al. Comprehensive review on lactate metabolism in human health. *Mitochondrion*. 2014;17:76-100. doi:10.1016/j.mito.2014.05.007
 330. Pucino V, Bombardieri M, Pitzalis C, Mauro C. Lactate at the crossroads of metabolism, inflammation, and autoimmunity. *Eur J Immunol*. 2017;47(1):14-21. doi:10.1002/eji.201646477
 331. Upadhyay S, Mittal E, Philips JA. Tuberculosis and the art of macrophage manipulation. *Pathog Dis*. 2018;76(4):1-12. doi:10.1093/femspd/fty037
 332. Liang M, Habib Z, Sakamoto K, Chen X, Cao G. Mycobacteria and autophagy: Many questions and few answers. *Curr Issues Mol Biol*. 2017;21:63. doi:10.21775/cimb.021.063
 333. Beth Levine, Guido Kroemer. Autophagy in the Pathogenesis of Disease. *Cell*. 2008;132(1):27-42. doi:10.1016/j.cell.2007.12.018. Autophagy

334. Hu J, Cai M, Liu Y, et al. The roles of GRP81 as a metabolic sensor and inflammatory mediator. *J Cell Physiol.* 2020;235(12):8938-8950. doi:10.1002/jcp.29739
335. Baltazar F, Afonso J, Costa M, Granja S. Lactate Beyond a Waste Metabolite: Metabolic Affairs and Signaling in Malignancy. *Front Oncol.* 2020;10(March):1-10. doi:10.3389/fonc.2020.00231
336. Shen Z, Jiang L, Yuan Y, et al. Inhibition of G Protein-Coupled Receptor 81 (GPR81) Protects Against Ischemic Brain Injury. *CNS Neurosci Ther.* 2015;21(3):271-279. doi:10.1111/cns.12362
337. Krishnamoorthy G, Kaiser P, Abed UA, et al. FX11 limits Mycobacterium tuberculosis growth and potentiates bactericidal activity of isoniazid through host-directed activity. 2020;13(3):32034005. doi:10.1242/dmm.041954
338. Molloy EJ, O'Neill AJ, Grantham JJ, et al. Labor promotes neonatal neutrophil survival and lipopolysaccharide responsiveness. *Pediatr Res.* Published online 2004. doi:10.1203/01.PDR.0000130473.30874.B6